A NEW DESIGN FRAMEWORK FOR FLEXIBLE LONG-LIFE PAVEMENTS

By

Mahdi Ghazavi

A DISSERTATION

Submitted to
Michigan State University
in partial fulfillment of the requirements
for the degree of

Civil Engineering – Doctor of Philosophy

2023

ABSTRACT

Long-life pavements are designed and built to last for over 50 years without needing major structural rehabilitation or reconstruction. Reported benefits of such pavements include low life-cycle cost, less frequent repair and/or rehabilitation, lower user-delay costs and lower environmental impact. Several approaches exist to design long-life pavements, all of which are based on mechanistic-empirical principles. While designing long-life pavements, deep structural distresses (e.g., bottom-up cracking) are designed to never develop, by limiting the maximum critical stresses and strains. Only surficial distresses (e.g., top-down cracking, rutting etc.) are allowed to occur, but they are managed via periodic maintenances (e.g., mill and overlay). Several states in the US have built long-life pavements by enhancing structural design methods, using better materials, improving specifications and construction practices. In Michigan, four pilot long-life pavement sections were constructed between 2017 and 2019; two rigid and two flexible pavements. Each pilot project included a long-life and an accompanying standard (control) section constructed on the same highway. Modifications to standard designs and materials were made to extend their service life. The focus of this dissertation is on evaluation of the two flexible pavement projects. The scope of the study included as-built analysis of these pilot long-life projects to determine their potential for meeting the intended design and service lives. MDOT performed numerous field tests and collected material samples from these projects. Extensive analysis of the field data and numerous laboratory tests were conducted to characterize the material properties. As-constructed material properties were used in different mechanistic-empirical (ME) design software to estimate the expected performance of all the pilot projects. Based on the detailed laboratory and field testing and the mechanistic-empirical performance predictions, recommendations were made in structural design, material selection, construction,

and quality control and quality assurance procedures. The main objective of this study is to perform a thorough analysis of the pilot flexible long-life projects which were designed based on state-of-the-practice methods and enhance the mechanistic-empirical design of these pavements and propose alternative design approach for long life pavements to potentially reduce life cycle cost and improve performance

This dissertation is dedicated to my dear parents and lovely siblings
Afsaneh and Masoud and my dear nephew, Iliya.
Thanks for always being there for me.

ACKNOWLEDGEMENTS

I would like to express my sincere gratitude to the Michigan Department of Transportation for their generous support and assistance throughout the course of my doctoral studies. Their funding provided invaluable resources that enabled me to conduct extensive research on long-life pavements and contributed significantly to the quality of this dissertation.

TABLE OF CONTENTS

LIST OF ABBREVIATIONS

3PBC	3 Point Bending Circular
AADTT	Average Annual Daily Truck Traffic
AASHTO	The American Association of State Highways and Transportation Officials
AC	Asphalt Concrete
AMPT	Asphalt Mixture Performance Tester
APA	Asphalt Pavement Alliance
BBF	Bending Beam Fatigue
BC	Base Course
CBR	California Bearing Ratio
CMS	Climatic-Materials-Structural
COV	Coefficient of Variation
D-LWR	Downwelling Longwave Radiation
D-SWR	Downwelling Shortwave Radiation
DCP	Dynamic Cone Penetrometer
DSR	Dynamic Shear Rheometer
ESAL	Equivalent Single Axle Load
FEL	Fatigue Endurance Limit
FWD	Falling Weight Deflectometer
GGSP	Gap-Graded SuperPave
HMA	Hot Mix Asphalt
HTV	High Traffic Volume

IDT	Indirect Tensile Test
IL	Inner lane
IRI	International Roughness Index
JMF	Job Mix Formula
LC	Levelling Course
LTV	Low Traffic Volume
LWD	Light Weight Deflectometer
MDOT	Michigan Department of Transportation
ME	Mechanistic Empirical
MEAPA	Mechanistic Empirical Asphalt Pavement Analysis
MEPDG	Mechanistic Empirical Pavement Design Guide
MSCR	Multiple Stress Creep and Recovery
MSU	Michigan State University
MTV	Medium Traffic Volume
NAPA	National Asphalt Pavement Association
NB	North Bound
NCAT	National Center for Asphalt Technology
NCHRP	National Cooperative Highway Research Program
NMAS	Nominal Maximum Aggregate Size
OGFC	Open Graded Friction Course
OL	Outer Lane
PG	Performance Grade

PPP	Public-Private Partnership
PWL	Percent Within Limits
QC/QA	Quality Control/Quality Assurance
RAP	Recycled Asphalt Pavement
RAS	Recycled Asphalt Shingles
RITF	Road Innovations Task Force
RLPD	Repeated Load Permanent Deformation
RP	Rest Period
RTFO	Rolling Thin-Film Oven
SAPA	State Asphalt Pavement Association
SB	South Bound
SMA	Stone Matrix Asphalt
SR	Stiffness Ratio
TS	Test Section
U-LWR	Upwelling Longwave Radiation
VECD	Viscoelastic Continuum Damage
VFA	Voids Filled with Asphalt
VMA	Voids in Mineral Aggregates
WC	Wearing Course
WOF	Work of Fracture

1 INTRODUCTION

The concept of perpetual or long-life pavements has been introduced in the USA and Europe in the last few decades (1–4). Such roadways are defined as a flexible or rigid pavement designed and built to last longer than 50 years without needing major structural rehabilitation or reconstruction and requiring only periodic surface renewal in response to distresses that are confined to the top surface. It is also recognized that many well-built, thick pavements that were categorized as either full-depth or deep-strength pavements had been in service for decades with only minor periodic surface rehabilitation to remove defects and improve ride quality. Therefore, it is a practical reality to consider long-life pavement concept. The primary advantages of such pavements include (4–8): (i) low life-cycle cost by avoiding deep pavement repairs or reconstruction, (ii) less frequent repair and rehabilitation and contribute to highway safety and congestion mitigation, (iii) low user-delay costs since minor surface rehabilitation of pavements only require short work windows that can avoid peak traffic hours, (iv) low environmental impact by reducing the construction materials amount over the pavement's life, (v) more relevance to a public-private partnership (PPP) because the longtime commitment typically involved favors the use of materials, design features, and construction techniques that result in long life and low maintenance.

A somewhat unified approach to designing long-life flexible pavements has been adopted by many experts (9, 10) based on mechanistic-empirical analysis and design concepts. The premise of this approach is that pavement distresses with deep pavement layer structure and appropriate materials can be avoided or delayed if pavement responses—stresses, strains, and deflections, are kept below critical values at the locations where the distresses initiate to occur.

Thus, pavement can be designed for an indefinite structural life for heavy vehicle loads and repetitions without being too conservative.

Several states in the US have built long-life pavements by incorporating enhancements in (i) structural design methods, (ii) materials evaluation and specification procedures, (iii) construction practices and (iv) maintenance practices (5, 8, 11–14).

In Michigan, four long-life pavement sections were constructed as a result of Public Act 175 (2015) and the Roads Innovation Task Force (RITF) Report (15) (i) 30- year HMA on US-131 in the Grand Region (constructed in 2017), (ii) 30-year concrete on I-69 in the Bay Region (constructed in 2018), (iii) 50-year concrete on US-131 in the Grand Region (constructed in 2018) and (iv) 50-year HMA on I-475 in the Bay Region (construction in 2019-2020). Locations of these long-life pilot projects are illustrated in Figure 1. As part of each project, several 'test sections' were identified for sampling and testing, which are listed in Table 1. The focus of this study is on the two flexible projects I-475 with 50-year design life for the long-life sections and 20-year design life for the standard sections and US-131 with 30-year design life for the long-life sections and 20-year design life for the standard sections. While designing these pilot projects, modifications were made to standard designs and materials to extend the design life via (i) increased layer thicknesses, (ii) improved materials, (iii) enhanced construction practices and specifications, and (iv) upgraded design aspects (e.g., increased drainage freeboard). It is essential to assess these pilot projects before further long-life projects are planned in Michigan. As-built evaluation of these long-life pavements will assist Michigan Department of Transportation (MDOT) in determining the potential of the four pilot projects for meeting their intended design and services lives (50 and 75 years). MDOT has collected material samples from the pilot projects for testing various engineering properties and characterizing the material used

in these pilot projects, which will be used to compare the performance predictions between the standard and the long-life pavement designs and cross-sections.

Table 1 List of MDOT's long-life pilot projects and standard and long-life test sections

Pavement type	Project	Test section	Location (Station)		Direction	Design life (years)
HMA	US-131	Test section 1	1090+00	1100+00	NB	30
		Test section 2	1127+52	1137+81	NB	30
		Test section 3	1170+00	1180+00	NB	30
		Test section 4	1210+10	1220+00	NB	20
	I-475	Test section 1	0650+00	0660+00	NB	50
		Test section 2	0745+00	0755+00	NB	50
		Test section 3	0770+00	0780+00	NB	50
		Test section 1	0650+00	0660+00	SB	20
		Test section 2	0745+00	0755+00	SB	20
		Test section 3	0770+00	0780+00	SB	20
JPCP (concrete)	I-69	Test section 1	0340+00	0350+00	EB	20
		Test section 2	0367+00	0377+00	EB	20
		Test section 3	0340+00	0350+00	WB	30
		Test section 4	0396+00	0406+00	WB	30
	US-131	Test section 1	0852+00	0862+00	NB	50
		Test section 2	0885+00	0895+00	NB	50
		Test section 3	0970+00	0980+00	NB	50
		Test section 1	0850+00	0860+00	SB	20
		Test section 2	0895+00	0905+00	SB	20
		Test section 3	0977+00	0987+00	SB	20

Evaluation of all aspects (design, construction, materials, etc.) of the as-constructed condition of the MDOT's long-life pilot projects will produce valuable information. This information will lead to adjustments to engineering design aspects and specifications that will improve the overall performance of the standard pavement designs.

2 OBJECTIVES

The main goal of this dissertation is to perform a thorough analysis of the pilot long life projects which were designed based on state-of-the-practice methods and propose alternative design frameworks for long life pavements to reduce life cycle cost and improve performance. Specific objectives include:

- Gather data on original pavement design and testing performed during construction to assess as-designed and as-built characteristics of the pilot long life projects
- Perform testing in the laboratory to compare material characteristics of layers in terms of modulus (stiffness), resistance to fatigue cracking, rutting and low temperature cracking. Use laboratory and field data to calibrate mechanistic-empirical pavement models to predict the long-term performances of the pavement sections
- Develop enhanced analysis and design methods for long life pavements

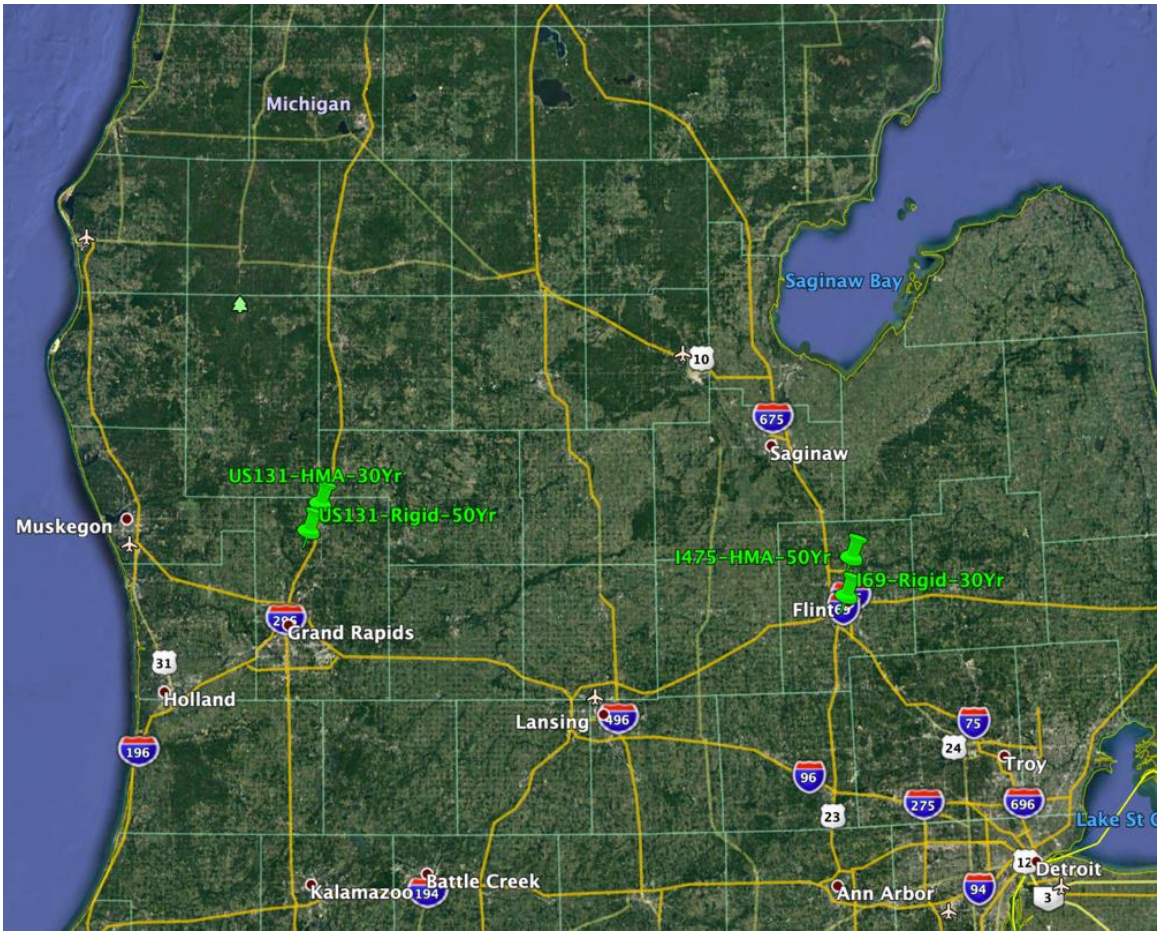

Figure 1 Locations of the four long life pilot projects

3 LITERATURE REVIEW

In this chapter, the focus is on providing a review of the current methodologies for structural design, material selection, construction best practices, and QC/QA specifications for long-life pavements.

The concept of perpetual pavements or long-life pavement has been used by pavement engineers in the past few decades. Long-life pavements are pavements that typically last longer than 50 years with no major structural rehabilitation. In these pavements, only periodic surface renewal is needed to remove or mitigate top surface distresses or improve the ride quality. Southern Cross Drive in Australia, using full-depth or deep strength pavements concept, can be mentioned as one of first long-life pavements which has been in service since 1960s with very little maintenance. In the United States, many States like Michigan, California, Texas and Washington have designed and constructed long-life pavements.

Although the main idea behind long-life pavements is to increase the thickness of the pavement to avoid bottom-up cracking at the bottom of the HMA layer and limit the rutting on top of the subgrade, several enhancements should be incorporated to reach the desired longer life as compared to conventional pavements. These enhancements can be categorized to:

- Structural design methods
- Materials characteristics and selection methods
- Construction practices
- Quality control and quality assurance specifications
- Maintenance practices

Cost-related aspects should be fully taken into consideration to evaluate the economic benefits of using long-life pavements by life cycle cost assessment or cost-benefit analysis. Some of these aspects are as follows:

- Initial construction costs
- Costs relates to periodic maintenance and traffic management at road works
- Road user costs
- Costs related to accidents for both road users and construction workers
- Environmental impacts of road construction and maintenance

Apparent higher initial cost for the construction of long-life pavements is a disadvantage. Based on the information provided by Michigan Department of Transportation (MDOT), there is a range of 41% to 59% increase in the cost (of materials only) per lane mile for the long-life sections as compared to the standard 20-year designs. However, when the entire construction cost is considered (including the overhead costs that are the same in standard and long-life pavements), the difference is about 15-20%. On the other hand, lower maintenance-related costs could result in a lower life cycle cost for long-life pavements. Proper determination and quantification of the factors affecting the life-cycle cost should be performed to be able to compare conventional pavements with long-life pavements. Although lowering the life cycle cost is probably the most important benefit of increasing the design life, it is not always feasible to fund higher initial costs because of budget limitations. MDOT currently applies a “mix of fixes” and most of the reconstruction projects are designed to the current 20-year standard design to optimize pavement condition across the entire network. Based on the Roads Innovation Task Force (RITF) Report (*15*), a summary of estimated funding projections required to meet and maintain the 90 percent good/fair pavement goal (approved by the State Transportation

Commission) using current design standards compared to 20, 30 and 50-year design lives and elimination of poor pavements on the state network within 10 years is presented in Table 2.

Table 2 Estimated Funding Projections

Funding Impacts	Investments Needed First 10 Years	Average Investments Needed Next 40 Years
Current Standards 20-Year Design Life with Mix of Fixes	$15 billion	$3.9 billion/year
20-Year Design Standards Reconstruct	$60 billion	$9 billion/year
30-Year Design Standards Reconstruct	$111 billion	$450 million/year
50-Year Design Standards Reconstruct	$140 billion	$560 million/year

The structural design of long-life pavement is mostly based on the concept of 'fatigue endurance limit'(FEL). In order to design a long-life pavement, it is necessary to provide enough stiffness in the upper HMA layers to avoid rutting and enough total HMA thickness and flexibility in the lowest HMA layer to avoid fatigue cracking at the bottom of the HMA layer. Different researchers have proposed that there seems to be a strain level below which there is no fatigue damage to HMA. At this level, increasing the pavement thickness is no more beneficial for avoiding fatigue cracking in the structure(16). Von Quintus (17) has defined the endurance limit for flexible pavements as: "the horizontal asymptote of the relationship between the applied stress or strain and the number of load repetitions, such that a lower stress or strain will result in an infinite number of load repetitions". The FEL concept is schematically shown in Figure 2.

During the evolution of fatigue endurance limit concept, different values have been proposed by researchers as FEL typically ranging from 60 με to 125 με. Monismith has suggested that the limiting tensile strain at the bottom of the asphalt layers should not be higher than 60 με, and that at the top of the subgrade the vertical strain should be limited to 200 με (*18*). Carpenter et al. (2003) conducted research to validate fatigue endurance limit theory. They

performed four-point bending test on asphalt specimens using a 10-Hz haversine load at 20ºC at different strain levels. Typical strain levels for this test ranges from 250 to 1000 με. The horizontal strain is calculated based on the vertical deflection at the center of the beam. Failure is defined as the number of loading cycles requires to reduce the initial stiffness of the specimen to a fraction of the initial stiffness. This fraction for typical mixes is assumed to be half of the initial stiffness. Due to large number of loading repetitions required to fail the specimen in low strain levels, the testing was conducted at strain levels from 250 to 1000 με and the strain level vs loading cycles relationships were extrapolated for strain levels below 250 με.

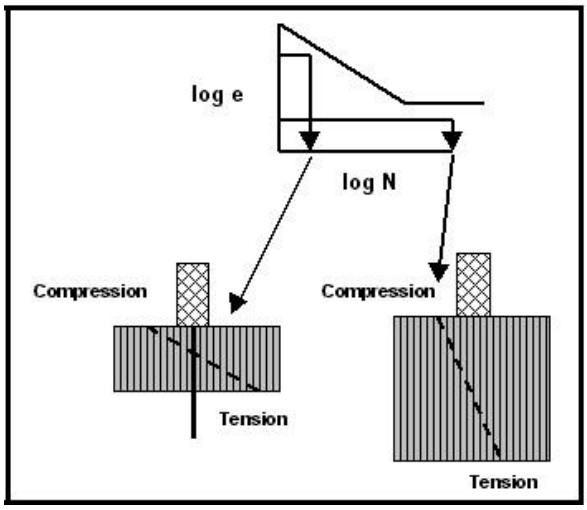

Figure 2 Tensile strain with pavement thickness (log e = log of strain; log N = log of number of cycles to failure) (*14*)

The extrapolated data showed that an asymptote occurred at a strain level of approximately 70 με. Similar testing was conducted by Asphalt institute in 2004 using the same test but at the strain level of 70 με. This test did not result in failure (50% of the initial stiffness) after 4,000,000 cycles (19). Dissipated energy model has also been used by Carpenter et al. and Peterson et al. to develop fatigue endurance limit. This model relates the rate of change in dissipated energy to fatigue failure by quantifying accumulation of the damage in the specimen

from one cycle to the next(16). Both researchers found similar values of 70 to 100 με depend on the type of mix. Some of the mixes could bear 100 με without reaching the failure.

3.1 Design Methodologies for Long-life Pavements

The main idea behind different approaches to designing perpetual pavements based on mechanistic-empirical concepts is to avoid deep structural distresses by keeping pavement responses below a certain limit. Using empirical methods like AASHTO 1993 method for designing perpetual pavements leads to ever-increasing the thickness of the pavement, although it has been shown that there is a limit beyond which increasing the thickness does not add to the structural capacity of the pavement anymore. This thickness limit heavily depends on the material used for different layers, load levels and load spectra (heaviest loads are of significant importance) and climatic condition of the area where the pavement is constructed. Additionally, in mechanistic-empirical methods, pavements can be analyzed for the heaviest loads and keeping the responses of the pavement under a certain limit to avoid the distresses that initiate at the critical locations of the pavement. This concept has been shown in Figure 3.

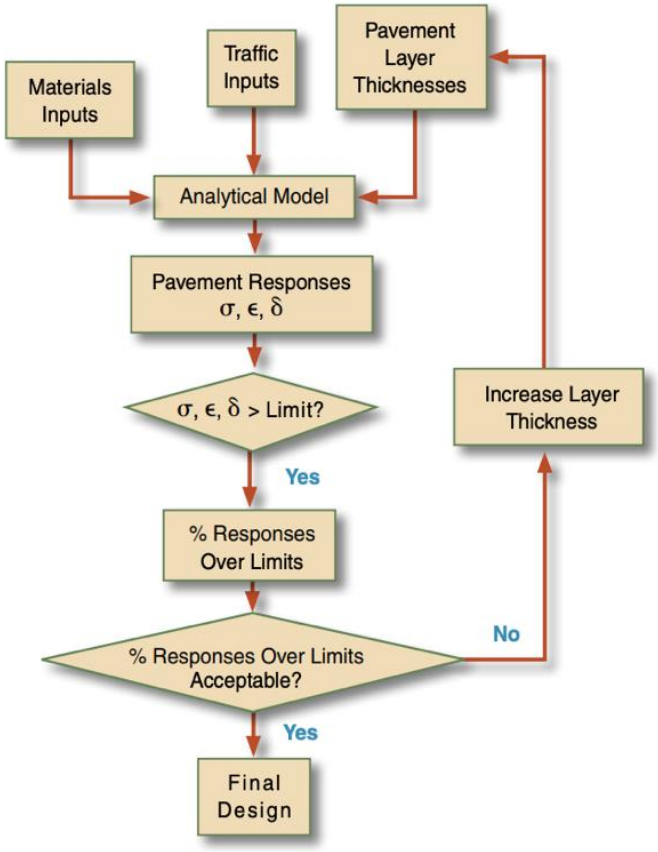

Figure 3 Simplified flowchart for perpetual pavement design (*1*)

The general concept of perpetual pavements design is shown in Figure 4. It should be emphasized that reaching to a longer life heavily depends on proper design, material selection, construction practices and maintenance activities. In perpetual pavements design process, it is necessary to define a limit for critical pavement responses below which structural damage does not accumulate. This concept will be discussed in detail in chapter 4. If all or the majority of or the loads experienced by the pavement are below that limit, the pavement can be considered as a perpetual pavement. Most approaches to long-life design for flexible pavements consider pavement responses for bottom-up cracking and rutting.

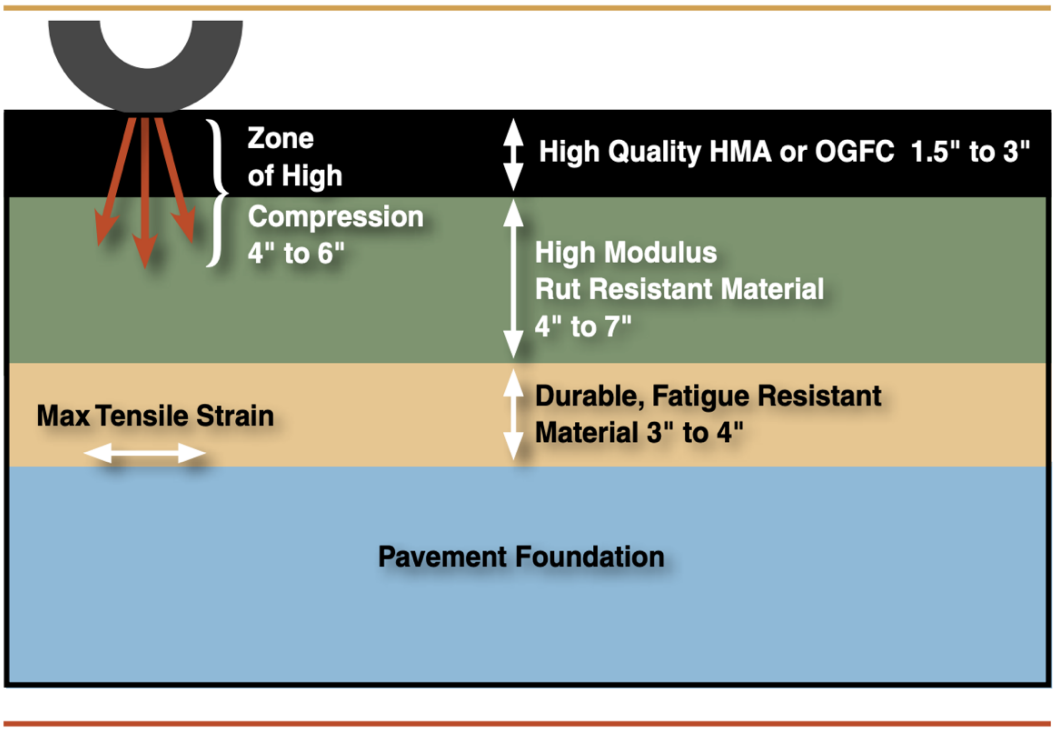

Figure 4 Perpetual pavements design concept (*14*)

The main difference in long-life pavement design (compared to standard designs) is that the responses below the "fatigue endurance limit" are not being considered in the damage accumulation. Since the structure should be designed in such a way that the majority of the critical responses, such as horizontal strain at the bottom of the asphalt layer for bottom-up cracking, are lower than the endurance limit, the damage in the damage accumulation model should be minimal.

Different design software can be used for long-life pavement design. They either use a single value for the endurance limit (AASHTOWare Pavement ME) or a criterion for strain distribution that can be controlled in specific percentiles (PerRoad). Recent studies showed that FEL in asphalt concrete is not a single value and it highly depends on several factors such as binder rheology, temperature, loading time and air void content (*20–22*). Both of these

approaches will be used in this study to analyze the performance of the MDOT pilot long-life projects.

AASHTOWare Pavement ME design software is probably the most common software that now is being used by State DOTs for designing or controlling the designs in the US. Recent pilot flexible long-life projects US-131 and I-475 have been designed using this software. In the earlier versions of MEPDG, an optional FEL ranging between 75 and 125 με was incorporated to the software, based on information from NCHRP project 9-38. Although, in the latest version (2.6.0) that is being currently used by MSU research team, the range has been decreased to 50 to 100 με.

PerRoad is a flexible perpetual pavement design software that was developed at National Center for Asphalt Technology (NCAT) at Auburn university in conjunction with Asphalt Pavement Alliance (APA), the National Asphalt Pavement Association (NAPA) and the State Asphalt Pavement Associations (SAPA). The software is based on layered elastic analysis and a statistical analysis procedure (Monte Carlo simulation) to predict the responses within the pavement. The criteria for pass/fail the design can be selected based on the pavement response or using transfer functions to convert the responses to different distresses in the pavement. The advantage of this software is that it can compare the distribution of the tensile strain at bottom of the HMA layer resulting from different loads, climatic condition and material stiffnesses with a predefined criterion for this distribution. The default values for the strain distribution criteria are developed through NCAT 2003 and 2006 test track experiments.

3.2 Material Selection Methods for Long-life Pavements

In order to design a perpetual or long-life pavement properly with current mechanistic empirical design procedures, it is essential to characterize the potential materials and use the

proper inputs for the design. The foundation of the pavement and each of the asphalt layers have a certain role in the structure of the pavement. The top course is a sacrificial layer in long-life pavements. This layer is usually designed to be rut resistant and cracking resistant. Proper surface drainage is another desirable property of the surface layer. The intermediate or levelling layer should provide durability and rut resistance. Since this layer usually experiences relatively lower strain levels compared to the top and base course, use of high percentages of reclaimed asphalt pavement (RAP) or recycled asphalt shingles (RAS) is probably more beneficial in the intermediate layer. The base course should be designed to have high durability and fatigue resistance. It is critical to understand the properties of these layers and the fluctuation in their behavior with the climatic and environmental conditions. Each of the components the asphalt mixture design including aggregates, binder type, percentage of RAP or RAS, design air voids and potential additives should be selected carefully for each of the layers to meet the desired properties in the pavement structure.

Public Act 175 requires MDOT to evaluate "…road materials and construction methods that, when implemented, could allow the department to build high-quality roads in this state that last longer than those typically constructed by the department, with a goal of roads lasting at least 50 years, with higher quality roads and reduced maintenance costs". As a result of this Public Act, MDOT has developed a New Material Evaluation Procedure to assess new materials, technologies and construction methods that could potentially improve the pavement performance. Public Act 259 of 2001 or Pavement Demonstration Program is another opportunity for MDOT to evaluate new materials, construction methods or design. This program allows MDOT to construct up to four demonstration projects to evaluate new materials and technologies.

This section focuses on the required properties and role of different layers in a typical flexible long-life asphalt pavement.

3.2.1 Foundation

The pavement foundation plays an important role during the construction and performance of a perpetual pavement. The foundation serves as working platform during the construction and has a significant role in providing assistance to the asphalt compactor to reach the desired density in the upper layers. Also, it should be properly designed to minimize volume changes in wet-dry and freeze-thaw cycles in soft clays and frost susceptible soils. Proper drainage design in unbound layers is a key element to the design of long-life pavements. In some of the States which frost design is considered for the pavement structure, the minimum total pavement structure thickness is required to be equal or higher than 50% of the expected design frost depth. Seasonal variations should also be evaluated to have a better estimation of moduli changes in different seasons. This evaluation plays an important role in the design process to use a rational value for using in mechanistic simulations. In-situ testing for pavement foundation material can be a good strategy to develop a better understanding of the performance. Different stabilization technics can be used to improve the performance and resilient modulus of the unbound layers.

3.2.2 Base course of HMA

The most important role of the base layer of HMA in long-life pavements is to resist fatigue cracking resulting from load repetitions due to traffic and distribution of loads to the underlying unbound layers effectively to prevent excessive stresses and strains. The most desirable material for the base course should be both flexible to endure high strain levels and stiff enough to resist rutting and distribute the load to the underlying layers. Increasing the thickness

of the structure results in lower strain levels at the bottom of the base course. Using polymer modified binder is suggested to improve the fatigue life in the asphalt base layer (*23*). Newcomb et. al (2002) suggests to use higher binder content and finer aggregates to improve the fatigue resistance of the mix (*1*). Additionally, higher binder content makes the mix more durable and facilitates the compaction of the HMA layer so that higher densities (lower air voids) can be achieved (*24–26*). He also suggests to use the Superpave mix design for lower pavement layers for this layer. According to Superpave mix design, mixes for lower pavement layers usually have higher NMAS (nominal maximum aggregate size) and coarser aggregates. In the wet-freeze areas, because of the prolonged contact with water, the moisture susceptibility of the base layer should be considered. Kassem et al. (2008) suggested that coarse Superpave mixes could be very permeable and moisture susceptible (*27*). Increasing the binder content and material density improves the moisture resistance of the mixture. The low PG of the binder is suggested to be similar to upper layers. The most important and informative performance tests for this layer are fatigue, stiffness and moisture susceptibility test.

3.2.3 Levelling course of HMA

The intermediate layer for long-life pavements should be designed to have adequate stability and durability (*1*). The contribution of aggregate skeleton in this regard is significant. Using crushed aggregates with large nominal maximum aggregate size and coarser aggregates can improve the aggregate interlock. Aggregate to aggregate contact leads to higher stability in this layer. To test the aggregate interlock of the alternative mixes for this layer, Bailey method can be used (*28*). The skeletal structure's relationship to volumetric, segregation and compaction can be characterized using this test (*1*).

For proper selection of the binder grade for this layer, the high PG grade of the binder is suggested to be same as the top layer to resist rutting (*29*). Although, according to the suggestion the low PG grade can be relaxed one grade since the temperature gradient is asphalt pavements is quite steep and this layer is estimated not to experience low temperatures similar to the surface layer. Performing a rutting test like flow number and moisture susceptibility test and dynamic modulus test should be considered for a proper design for this layer.

3.2.4 Top course of HMA

The top course requirements highly depend on local needs and experiences like traffic conditions and environment (29). Generally, rutting resistance, surface cracking resistance, wear resistance, impermeability, reducing the tire noise and surface drainage can be mentioned as desired requirements for this layer. This layer is usually designed to have an acceptable performance for 15 to 20 years and contain the surface distresses as a sacrificial layer that can be renewed periodically.

Stone matrix asphalt (SMA) is one of the recommended alternatives for this layer (14). This mix is usually designed by using polymer modified binders, relatively stiff binders with fibers or a mix of binder with specific mineral fillers. Some of the States like Maryland, Georgia and Wisconsin have successfully used this mix in high traffic roads. Harm et al. (2001) suggests to select the thickness of SMA based on the traffic level. The suggested thicknesses are 2 inches for low traffic level, 4 inches for medium traffic level and 6 inches for high traffic levels (>25 million ESAL) (12). Texas requires a 2 to 3 inches of SMA under an optional porous friction course (21).

Another alternative for using as a renewable sacrificial top course for long-life pavements is open graded friction course or OGFC (8). OGFC is a porous mix designed with polymer

modified binder or asphalt rubber binder to provide a wearing course that reduces tire splash, spray, noise, hydroplaning and aging (8). This mix has a relatively high void structure that enables it to move the water rapidly from the surface. This mix is similar to Gap Graded Superpave (GGSP) that Michigan is currently using as the surface layer for pilot long-life projects. GGSP is a binder rich, gap graded mix designed with polymer modified binder.

Based on the climatic conditions, high PG grade of the binder of the top course should be properly chosen to avoid rutting. The selection of the low PG grade of the binder is vital in mitigating thermal cracking. Since this layer is designed to be wear resistant, high-quality aggregates with low potential for abrasion should be selected. Using high percentages of RAP and RAS is not recommended in the wearing course.

3.3 Construction Practices and QC/QA specifications for Long-life Pavements

Proper construction of the pavement is so important in achieving the longevity in the life of the pavement. The variability in different construction factors can negatively impact the performance of long-life pavements. The construction of a long-life pavement begins with the subgrade and extends to the bottom of the asphalt layers. Each of the unbound layers serves as a part of the structure and a platform for the construction of the subsequent layer. Improving the properties of unbound layers with stabilization is one of the common technics used in the construction of the long-life pavements. Lime, Portland cement, asphalt and chemical admixtures are among the options that can be used to improve the properties of the unbound layers. Proper installation of the drainage system in the unbound layers is another key point in the construction of the unbound layers. A relatively more rigorous quality control and quality assurance plan for controlling the compaction and uniformity of compaction along the project can significantly help in achieving the desired longer life. Additionally, conducting field test such as dynamic cone

penetrometer (DCP), falling weight deflectometer (FWD) and light weight deflectometer can reveal the weak areas along the project during the construction.

Regarding the asphalt base course, mixtures with nominal maximum aggregate size (NMAS) of 19 to 25 mm designed with lower air voids, are relatively easier to compact in the field (*29*). Reducing the air voids results in higher modulus in HMA layers and makes them less permeable that leads to less susceptibility in moisture damages as well. Lower air voids result in higher durability in the mixture. It has been suggested that 3% more compaction can result in 15% less thickness required due to improved fatigue behavior (*2*, *30*).

For increasing the durability of the mixtures following suggestions are presented (12):

- Minimum lift thickness of 3 to 6 times greater than nominal maximum aggregate size to increase the density of the mix
- Dust control in the plant for better mixture production
- Tacking each lift before paving for increased bonding between the layers
- Reducing the variability in the bottom HMA layer by using virgin aggregates
- Using material transfer device to prevent segregation
- Revised in-place density testing to provide more uniform density in the layers
- Increased required density for the middle layer of HMA

One of the most common and significant construction issues is segregation. Segregation is defined as lack of homogeneity in the asphalt mix and may occur due to improper handling of the mix. It can occur due to either fine and coarse aggregate separation during production, transportation or placement of the HMA, or temperature differentials during paving or transportation. This issue can be reduced by using material transfer device to properly mix and place the mix during the construction. Material transfer device remixes the mixture before paving

and compaction that makes the mix and temperature more uniform. Segregation makes the pavement more susceptible to top-down cracking and consequent moisture damage (31, 32).

Another important construction issue is debonding. If debonding occurs, the structure of the pavement cannot transfer the load to the desired location and leads to higher stresses and strains in the upper layers and early pavement failures (*33*).

Longitudinal joints are another potential construction-related issue. Typically, longitudinal joints in construction have less density compared to other parts and these joints might be more permeable that makes the pavement more susceptible to moisture and other damages. The best practice in this regard is to use echelon paving or full width paving to eliminate the longitudinal joints. When echelon paving is not possible due to different limitations, other technics can be used to improve the joint quality like wedge joints, joint heaters and joint sealants (*34*).

The drainage system has a significant role in the performance of the pavements and in perpetual pavements it is extremely important. Proper construction of the underdrains designed for unbound materials in the pavement foundation has a great effect on the longevity of the pavement.

4 RESEARCH PLAN

4.1 CHAPTER 1: GATHERING POST-CONSTRUCTION DATA

As part of this task, the Roads Innovation Task Force (RITF) report, project plans, and available materials information was reviewed. The RITF report includes a comprehensive synthesis of the literature, inputs from other DOTs, county road associations (and county road departments), academia, industry, relevant associations, and pavement demonstration reports. A review of the RITF report revealed important information about potential enhancements to traditional pavement design and construction practices to achieve a longer structural life. A summary of the recommended enhancements listed in the RITF report to achieve long-life pavements is illustrated in Figure 5. As shown in Figure 5, structural design, materials characteristics, construction practices, and QC/QA specifications are all thoroughly considered, and recommendations have been made.

Table 3 and Table 4 summarize the recommended enhancements to HMA and PCC long-life projects and the information on whether these were or were not met (red shading) in the four pilot projects. It should be noted that the recommended enhancements shown in Figure 5 should be treated as wish list, not like a specification to be followed. Each project is different and some deviations from these recommendations is inevitable. The fact that there are some red shadings in these tables does not necessarily mean that there should be a concern for potential poor performance in those pavement sections.

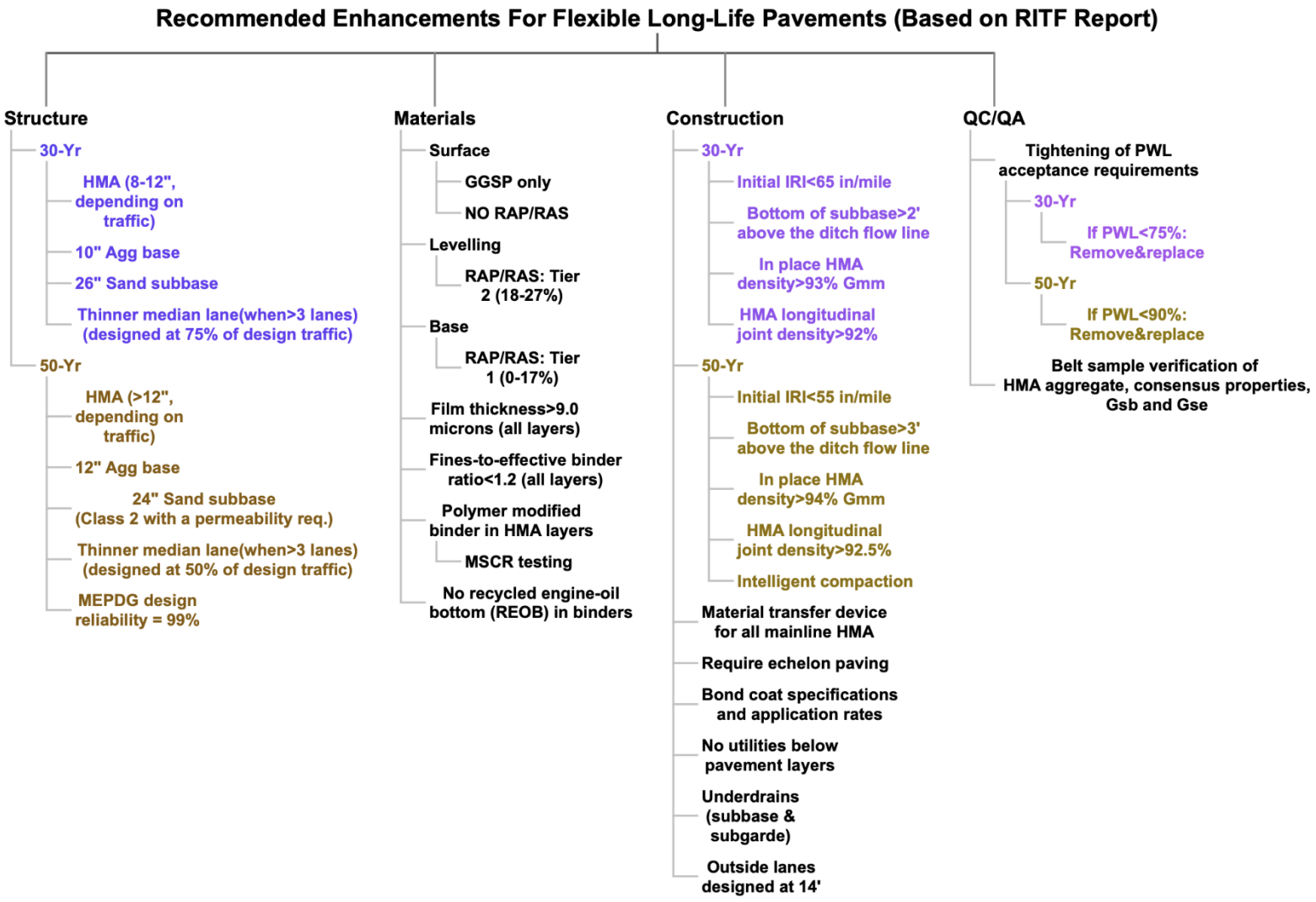

Figure 5 Recommended enhancements for flexible long-life pavements

Table 3 RITF recommended enhancements and comparison with implementations in US-131 HMA project

Pavement type and design life			Standard - 20 years	Long-life - 30 years		
Test section number			Test section 4 NB	Test section 1 NB	Test section 2 NB	Test section 3 NB
Structure		8-12" HMA	1.75"5E10	1.5" GGSP	1.5" GGSP	1.5" GGSP
			3" 3E10	2.5" 4E30	2.5" 4E30	2.5" 4E30
			4.5" 2E10	7.25" 3E30	7.25" 3E30	7.25" 3E30
		10" Agg base	6" Aggregate Base	12" Aggregate Base	12" Aggregate Base	12" Aggregate Base
		26" Sand subbase	18" Sand Subbase	24" Sand Subbase	24" Sand Subbase	24" Sand Subbase
		Thinner median lane (when > 3 lanes)	NA	Not applicable as it was a two-lane pavement.		
Materials	Surface	GGSP only	5E10	GGSP- No RAP/RAS	GGSP- No RAP/RAS	GGSP- No RAP/RAS
		No RAP/RAS	19%-Tier 2	GGSP- No RAP/RAS	GGSP- No RAP/RAS	GGSP- No RAP/RAS
	Leveling	RAP/RAS Tier 2:18-27%	16 %- Tier 1	9%- Tier 1	9%- Tier 1	9%- Tier 1
	Base	RAP/RAS Tier1: 0-17%	24 %- Tier 2	13 %- Tier 1	13 %- Tier 1	13 %- Tier 1
	Surface	Film thickness > 9.0 microns (all layers)	8.8	10	10	10
	Leveling		9.2	9.5	9.5	9.5
	Base		8.1	9.8	9.8	9.8
	Surface	Fines/effective binder ratio < 1.2 (all layers)	0.94	1.27	1.27	1.27
	Leveling		0.97	0.83	0.83	0.83
	Base		1.11	0.83	0.83	0.83
	Surface	Polymer modified binders in HMA Layers	64-28 (Virgin: PG 64-28)	70-28P (Virgin: PG 70-28P)	70-28P (Virgin: PG 70-28P)	70-28P (Virgin: PG 70-28P)
	Leveling		64-28 (Virgin: PG 64-28)	70-28P (Virgin: PG 70-28P)	70-28P (Virgin: PG 70-28P)	70-28P (Virgin: PG 70-28P)
	Base		58-22 (Virgin: PG58-28)	64-28 (Virgin: PG 64-28)	64-28 (Virgin: PG 64-28)	64-28 (Virgin: PG 64-28)
	All layers	MSCR testing	NA	No MSCR testing was required		
		No REOB in binders	NA	REOB not used		
		Limitations or prohibitions of recycled materials	NA	Recycled materials were used for unbound layers. (Recycled concrete aggregate base)		
Construction		Initial IRI < 65 in/mile	28.1 (in/mile)	29.2 (in/mile)		
		Bottom of subbase >2' above the ditch flow line	NA	Unknown		
		In place HMA density >93% Gmm	5E10 avg= 94.06%	GGSP avg= 91.60%		
			3E10 avg= 93.84%	4E30 avg= 95.30%		
			2E10 avg= 94.60%	3E30 avg=94.89%		
		HMA longitudinal joint density >92%	5E10 avg=92.27% 3E10 avg=92.44%	Echelon paving for the top layer. 4E30 avg= 93.36%		
		Material transfer device for all mainline HMA	NA	Unknown		
		Require echelon paving	NA	Only the top layer was paved using echelon paving.		
		Bond coat specifications and application rates	NA	Unknown		
		No utilities below pavement layers	NA	Gas pipe below the pavement crossing horizontally.		
		Underdrains (subbase and subgrade)	NA	Unknown		
		Outside lanes designed at 14'	NA	Outside lanes designed at 12'		
QC/QA		Tightening of PWL acceptance requirements	NA	No change in PWL acceptance requirements.		
		If PWL<75% Remove & replace	NA	No change in PWL acceptance requirements		
		Belt sample verification of HMA aggregate consensus properties, Gsb and Gse	NA	Unknown		

Table 4 RITF recommended enhancements and comparison with implementations in I-475 HMA project

Pavement type and design life			Standard - 20 years			Long-life - 50 years		
Test section number			TS-1 SB	TS-2 SB	TS-3 SB	TS-1 NB	TS-2 NB	TS-3 NB
Structure		Thickness >12" HMA	1.75" 5E10	1.75" 5E10	1.75" 5E10	2" GGSP	2" GGSP	2" GGSP
			2.5" 5E10	2.5" 5E10	2.5" 5E10	2.5" 4E30	2.5" 4E30	2.5" 4E30
			3.5" 3E10	3.5" 3E10	3.5" 3E10	6.5" 3E30	6.5" 3E30	6.5" 3E30
		12" Aggregate base	6" Agg. Base (RCA used)	6" Agg. Base	6" Agg. Base (RCA used)	12" Agg. Base (RCA used)	12" Agg. Base	12" Agg. Base
		24" Sand subbase (class 2 with a permeability req)	18" Sand Subbase	18" Sand Subbase	18" Sand Subbase	24" Sand Subbase	24" Sand Subbase	24" Sand Subbase
		Thinner median lane (when > 3 lanes)	NA			Not applicable as it was a two-lane project		
		MEPDG Design reliability= 99%	NA	NA	NA	95%	95%	95%
Materials	Surface	GGSP only	5E10	5E10	5E10	GGSP- No RAP/RAS	GGSP- No RAP/RAS	GGSP- No RAP/RAS
		No RAP/RAS	31%- Tier 3	31%- Tier 3	31%- Tier 3	GGSP- No RAP/RAS	GGSP- No RAP/RAS	GGSP- No RAP/RAS
	Leveling	RAP/RAS Tier 2:18-27%	31%- Tier 3	31%- Tier 3	31%- Tier 3	17%-Tier 1	17%-Tier 1	17%-Tier 1
	Base	RAP/RAS Tier1:0-17%	25%- Tier 2	25%- Tier 2	25%- Tier 2	19%-Tier 2	19%-Tier 2	19%-Tier 2
	Surface	Film thickness > 9.0 microns (all layers)	7.3	7.3	7.3	10	10	10
	Leveling		8.5	8.5	8.5	9.3	9.3	9.3
	Base		8.3	8.3	8.3	9.6	9.6	9.6
	Surface	Fines/effective binder ratio < 1.2 (all layers)	1.11	1.11	1.11	1.37	1.37	1.37
	Leveling		1.11	1.11	1.11	0.95	0.95	0.95
	Base		1.15	1.15	1.15	0.91	0.91	0.91
	Surface	Polymer modified binders in HMA Layers	PG 64-28 (Virgin: PG 58-34)	PG 64-28 (Virgin: PG 58-34)	PG 64-28 (Virgin: PG 58-34)	PG 70-28P (Virgin: 70-28P)	PG 70-28P (Virgin: 70-28P)	PG 70-28P (Virgin: 70-28P)
	Leveling		PG 64-28 (Virgin: PG 58-34)	PG 64-28 (Virgin: PG 58-34)	PG 64-28 (Virgin: PG 58-34)	PG 70-28P (Virgin: 70-28P)	PG 70-28P (Virgin: 70-28P)	PG 70-28P (Virgin: 70-28P)
	Base		PG 58-28 (Virgin: PG 52-34)	PG 58-28 (Virgin: PG 52-34)	PG 58-28 (Virgin: PG 52-34)	PG 64-28 (Virgin: PG 58-34)	PG 64-28 (Virgin: PG 58-34)	PG 64-28 (Virgin: PG 58-34)
	All layers	MSCR testing	NA			No MSCR testing was required		
		No REOB in binders	NA			No information		
		Limitations or prohibitions of recycled materials	NA			Recycled materials were used for unbound layers. (Recycled concrete aggregate base)		

Table 4 (cont'd)

Construction	Initial IRI < 55 in/mile	49.3 (in/mile)	46.4 (in/mile)
	Bottom of subbase >3' above the ditch flow line	NA	
	In place HMA density >94% Gmm	5E10 avg=94.69% 3E10 avg=94.91%	GGSP avg=95.91% 4E30 avg=95.28% 3E30 avg=95.16%
	HMA longitudinal joint density >92.5%	5E10 avg=90.80%	GGSP avg=96.12%
	Material transfer device for all mainline HMA	NA	No information
	Require echelon paving	NA	Only the top layer was paved using echelon paving.
	Bond coat specifications and application rates	NA	No information
	No utilities below pavement layers	NA	Some utility lines crossing perpendicular to the road, but those are not significant for pavement performance.
	Underdrains (subbase and subgrade)	NA	No information
	Outside lanes designed at 14'	NA	Outside lanes designed at 12'
	Intelligent compaction (50-yr)	NA	Not used.
QC/QA	Tightening of PWL acceptance requirements	NA	No change in PWL acceptance requirements.
	If PWL<90% Remove & replace	NA	No change in PWL acceptance requirements
	Belt sample verification of HMA aggregate consensus properties, Gsb and Gse	NA	No information

4.1.1 Pavement Cross-Sections

The cross-sections of the standard and the long-life sections were obtained from the letting plans and verified with the MDOT engineers during the interviews. The structural properties are shown in Table 3 for US-131 project and Table 4 for I-475 project.

4.1.2 Mix Designs

Job mix formulae (JMF) and concrete mix designs are critical information that can explain the behavior of the asphalt mixture and the concrete slab in the field and laboratory tests, respectively. Several concrete mix design documents were available, and their intended use was not always apparent. To identify the exact concrete mix designs used for the construction of the mainline pavement, it was necessary to summarize the mix design data. This activity allowed comparing the composition of the different mixes and knowing the w/cm ratios. Besides, the desired strength, F-T requirements, and other important information were summarized readily.

4.1.2.1 I-475 HMA Pavement Project

Table 5 presents the critical JMF details for all the mixes used in the different layers of both the standard and long-life sections of the project.

Table 5 I-475 Mixtures design characteristics

ID	PG	Layer	Pb (%)	NMAS (mm)	Design ESAL (Million)	Ndes	VMA (%)	VFA (%)
GGSP	70-28P	Top	6.27	19	N/A	109	17.79	83.14
4E30	70-28P	Leveling	5.58	12.5	50	109	14.87	79.82
3E30	58-34	Base	5.40	19	50	109	14.20	78.88
5E10-Top	58-34	Top	6.07	9.5	10	96	15.42	80.54
5E10-Lev	58-34	Leveling	6.07	9.5	10	96	15.42	80.54
3E10	52-34	Base	4.79	19	10	96	13.71	78.12
Notes: GGSP = Gap Graded Superpave, Ndes = number of design gyrations, Pb = Binder content, VMA = Voids in Mineral Aggregate, VFA = Voids Filled with Asphalt, PG = Performance Grade.								

4.1.2.2 US-131 HMA Pavement Project

Table 6 presents the critical JMF details for all the mixes used in the different layers of both the standard and long-life sections of the project.

Table 6 US-131 Mixtures design characteristics

ID	PG	Layer	P_b (%)	NMAS (mm)	Design ESAL (Million)	N_{des}	VMA (%)	VFA (%)
GGSP	70-28P	Top	6.39	9.5	N/A	109	18.28	83.59
4E30	70-28P	Leveling	5.21	12.5	30	109	15.21	80.28
3E30	64-28	Base	4.90	12.5	30	109	14.29	79.01
5E10	64-28	Top	5.90	9.5	10	96	16.14	81.41
3E10	64-28	Leveling	5.07	12.5	10	96	14.18	78.84
2E10	58-28	Base	4.48	19	10	96	13.08	77.06
Notes: GGSP = Gap Graded Superpave, N_{des} = number of design gyrations, Pb = Binder content, VMA = Voids in Mineral Aggregate, VFA = Voids Filled with Asphalt, PG = Performance Grade.								

4.1.3 Field Tests

The MDOT conducted different field tests on different layers of all four projects to estimate their in-field moduli. The field tests included light weight deflectometer (LWD), dynamic cone penetrometer (DCP), and falling weight deflectometer (FWD). This section presents the analyses of all the available data for each of these field tests.

4.1.3.1 Light Weight Deflectometer (LWD) Data Analysis

Light weight deflectometer (LWD) tests were conducted on each pavement foundation layer (base, subbase, subgrade layers). Results of LWD tests were analyzed to estimate elastic moduli of each pavement foundation layer. The following equation was used to calculate the force applied during the test (per drop) (*35*).

$$F_{LWD} = \sqrt{2mghC} \qquad \text{Equation 1}$$

where F_{LWD} is the force applied by the LWD equipment (lbs.), m is the drop mass (22 lbs.), g is the acceleration due to gravity (32.17 ft/s^2), h is the drop height (19.7 inches), and C is the spring

constant (267290 lb/ft) [18]. The following Boussinesq's elastic half-space equation was used to determine the LWD elastic modulus (*35*).

$$E_{LWD} = \frac{(1 - v^2)\sigma_0 r}{d_0} f \qquad \text{Equation 2}$$

where E_{LWD} is the LWD elastic modulus; *v* is the Poisson's ratio [0.35 and 0.40 for tests performed on base and subgrade layers, respectively]; σ_0 is the applied stress (ksi); r is the radius of the plate (12 inches); d_0 is the average deflection (mm); and *f* is the shape factor [8/3 (rigid plate on granular material) and $\pi/2$ (rigid plate on material with intermediate characteristics) for tests performed on base and subgrade layers, respectively] (*35*).

4.1.3.1.1 I-475 Project

Table 7 presents the descriptive statistics for the elastic moduli of unbound layers that estimated using the LWD data for the I-475 project. Figure 6 compares the different layer moduli calculated for the inner (IL) and outer lanes (OL) of the various test sections for both the long-life and standard sections. It is observed that the subgrade moduli vary significantly along the NB direction while such differences were not observed with between the IL and OL for the same sections. However, it was noticed that the subgrade moduli for both the NB and SB TS-3s are higher and more variable than that of TS-1 and TS-2.

Figure 6 provides a graphical comparison of the elastic modulus of test sections from LWD tests. Except for the TS-1 of the SB pavement, the variability of the subbase is not significant. Base moduli values do not vary much within the NB sections and have higher elastic moduli than the standard design pavement sections. Higher variation is observed for base moduli of the SB standard pavement sections. TS-2 and TS-3 have the highest base moduli among all the standard and long-life sections.

Table 7 Descriptive statistics of layer moduli obtained using LWD data – I-475 HMA project

Layer	Test section	Number of drops	Mean	Standard deviation	Minimum	Maximum
Long-life/ Northbound						
Subgrade modulus (ksi)	TS1	20	2.272	0.883	0.680	4.139
	TS2	22	1.107	0.474	0.570	1.913
	TS3	20	4.301	2.091	0.924	8.742
Subbase modulus (ksi)	TS1	22	4.895	0.446	4.020	5.826
	TS2	20	3.898	0.634	2.666	5.534
	TS3	22	4.122	0.498	2.953	4.830
Base modulus (ksi)	TS1	22	12.533	1.826	8.470	16.580
	TS2	22	11.823	1.820	7.997	13.942
	TS3	22	13.271	1.352	10.871	16.390
Standard/ Southbound						
Subgrade modulus (ksi)	TS1	22	1.367	1.112	0.460	3.819
	TS2	22	1.450	0.904	0.431	3.294
	TS3	22	4.603	3.131	0.493	11.262
Subbase modulus (ksi)	TS1	22	6.342	0.850	4.559	8.588
	TS2	22	4.180	0.400	3.378	4.902
	TS3	22	3.966	0.339	3.129	4.868
Base modulus (ksi)	TS1	22	7.279	1.802	3.256	10.603
	TS2	22	14.652	2.386	10.323	20.546
	TS3	22	9.188	0.959	7.808	11.212

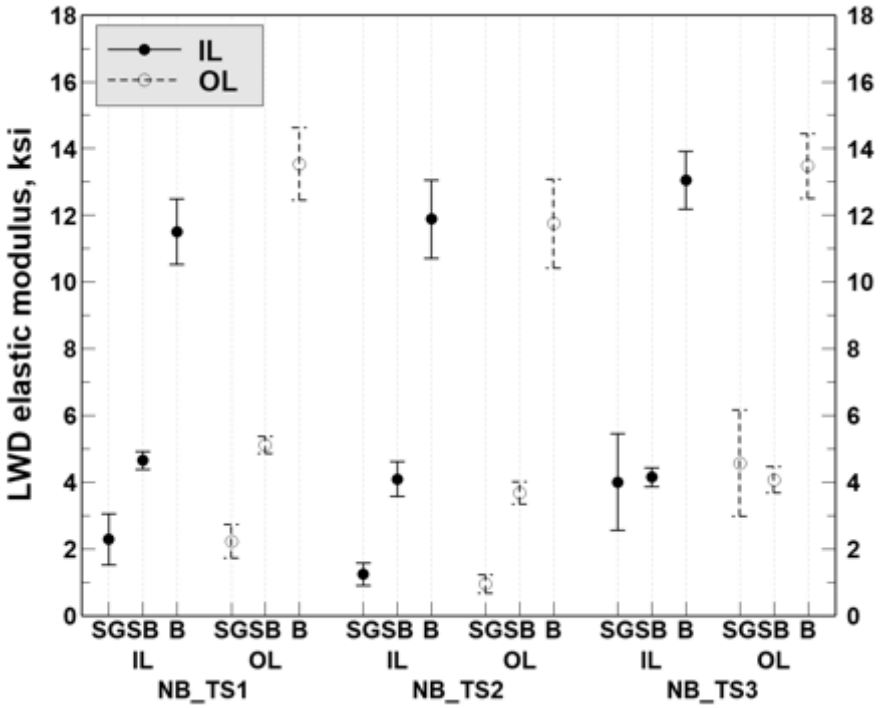

(a) Northbound long-life design

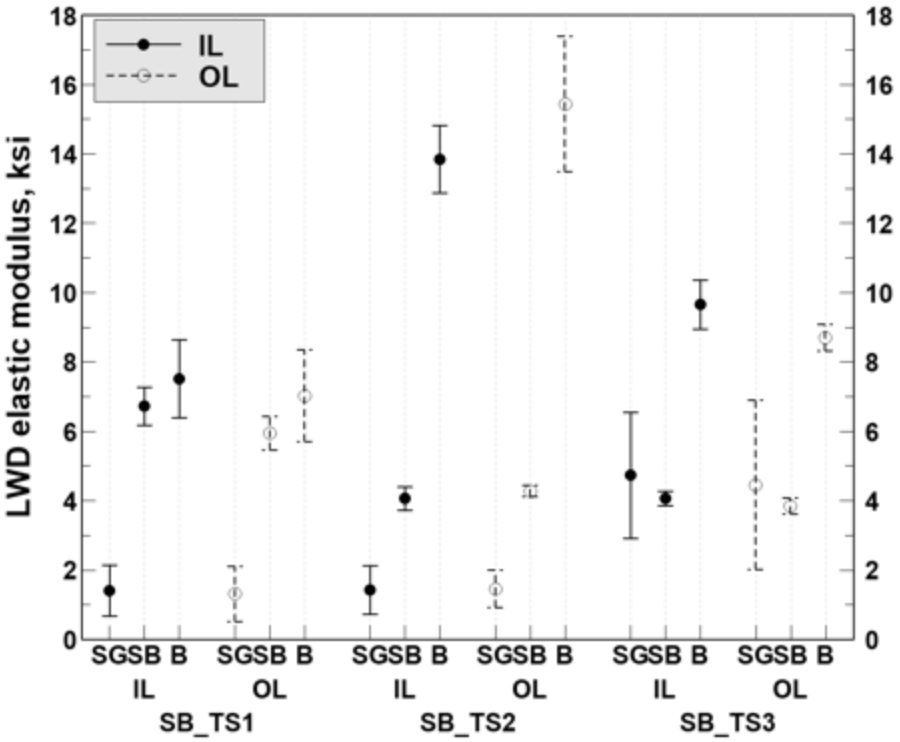

(b) Southbound standard design

Figure 6 Interval plots comparing subgrade (SG), subbase (SB), and base (B) moduli values between different lanes and test sections of the Northbound (NB) long-life and Southbound (SB) standard design pavements – I-475 HMA project

4.1.3.1.2 US-131 Project

Subgrade and base layer moduli of test sections in US-131 HMA project calculated using LWD data are reported in Table 8. No records were available for the subbase layer. Figure 7 shows the interval plots for each inner (IL) and outer lane (OL). Subgrade moduli of each test section on the long-life sections do not vary significantly. The base moduli values also exhibit less variation except for the TS-3 (long-life) and TS-4 (standard) where the base moduli are significantly different between the ILs and OLs.

Table 8 Descriptive statistics of layer moduli obtained using LWD data – US-131 HMA project

Layer	Test section	Design	Number of drops	Mean	Standard deviation	Minimum	Maximum
Subgrade modulus (ksi)	TS1	Long-life	7	6.069	1.020	3.957	7.164
	TS2		22	3.874	2.447	0.489	10.764
	TS3		6	3.710	2.096	1.364	7.418
	TS4	Standard	Nil	-	-	-	-
Base modulus (ksi)	TS1	Long-life	22	10.752	2.420	6.971	15.730
	TS2		22	11.695	2.267	7.086	15.846
	TS3		22	13.340	2.422	8.658	16.973
	TS4	Standard	22	12.664	3.068	8.891	19.608

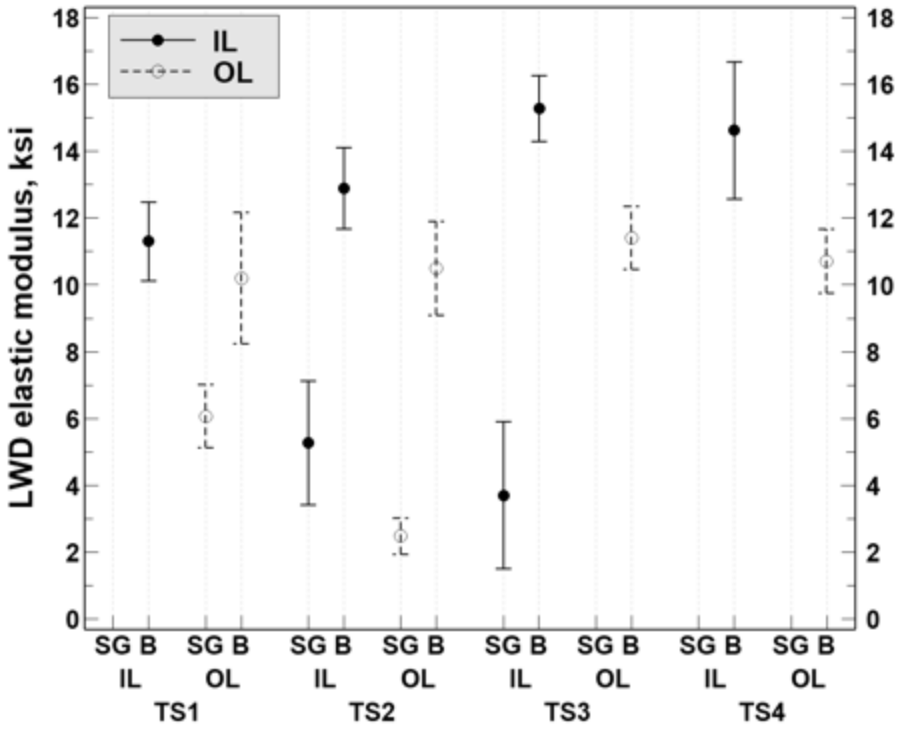

Figure 7 Interval plots comparing subgrade (SG) and base (B) moduli values between different lanes and test sections of the long-life (TS-1 through TS-3) and standard (TS-4) design pavements – US-131 HMA project

4.1.3.2 Falling Weight Deflectometer (FWD) Data Analysis

This section summarizes the back-calculated layer moduli for I-475 HMA and US-131 HMA sections and back-calculated layer moduli, LTE and k-values for I-69 JPCP, and US-131 JPCP projects using FWD deflections data. The team used FWD test results on flexible pavement sections (US131 and I475) to quantify the spatial variability of the moduli of asphalt, base and subgrade layers. The team could not to make conclusions about the relative performance of long-life and standard sections. This is because FWD tests on long life sections and standard sections were done at different dates (sometimes months apart) and subsurface temperature profiles were not measured. Subsurface temperature profiles can potentially be quite different even if the surface temperatures are the same and subsurface temperature profiles depend on the climatic conditions of previous days. When subsurface temperature profiles are

not known, it is not possible to reconcile the differences in the back calculated moduli of AC layers of long life and standard sections.

4.1.3.2.1 I-475 HMA Project

For the I-475 HMA project, FWD measurements were available for each of the AC layers (i.e., wearing course (WC), leveling course (LC), and base course (BC)) in both directions (i.e., northbound (NB) for long-life design, and southbound (SB) for standard design). The back-calculation results for the WC only are presented herein, while the results of the LC and BC AC layers can be found in Appendix A. The back-calculation was performed using MODULUS software on a 3-layer pavement structure, where the base and the subbase layers were combined. The descriptive statistics of the results obtained for the I-475 HMA project are summarized in Table 9, while Figure 8 displays the spatial variation within the layer moduli values for TS1 NB. A negligible variation in the AC layer moduli within each lane and between the lanes was observed. On the other hand, base and subgrade layers resulted having considerable differences between their back-calculated moduli at different stations within the section.

Figure 9 illustrates the back-calculated AC layer moduli for the I-475 HMA project between different lanes of each test section for both the long-life (NB) and standard (SB) pavement sections. It is observed that moduli of the AC layer in the standard sections are higher than those in the long-life sections. Moreover, high variability was observed in the NB TS-1 and SB TS-2 between the inner and outer lanes. The difference between the NB and SB sections can be attributed to the different pavement temperature conditions during FWD measurements (Figure 9(b)).

As mentioned earlier, a 3-layered structure with combined base and subbase layers was used for moduli back-calculation. Here following, the combined unbound layers will be referred

to as ‘Base’. Higher base moduli for the NB TS-1 compared to the other sections (Figure 10), and an overall low variability was observed for both ILs and OLs except for the TS-1 of the SB direction. Generally, the base moduli obtained from the back-calculation are between 25,000 to 40,000 psi. This range is acceptable considering that a base resilient modulus of 33,000 psi is used by MDOT at the design stage in the AASHTOWare Pavement-ME software.

Table 9 Descriptive statistics - I-475 HMA project back-calculated layer moduli

Design/ direction	FWD measured on	Lane	Layer	No. of FWD points	Mean (ksi)	Std. (ksi)	Minimum (ksi)	Maximum (ksi)
Test section 1 (650+00 – 660+00)								
Long-life/ NB	WC	IL	AC	11	577.98	32.41	537.93	644.37
		OL	AC	11	635.68	23.54	608.50	666.80
		IL	Base/SB	11	39.63	7.94	27.50	51.83
		OL	Base/SB	11	42.52	8.53	27.80	52.80
		IL	SG	11	26.51	4.68	17.60	32.20
		OL	SG	11	24.00	4.15	14.80	27.93
Standard/ SB	WC	IL	AC	11	994.7	97.4	890.7	1192.2
		OL	AC	11	932.6	65.7	890.0	1092.6
		IL	Base/SB	11	41.23	7.04	26.93	51.77
		OL	Base/SB	11	27.53	4.28	21.77	35.80
		IL	SG	11	14.49	2.173	12.70	19.53
		OL	SG	11	16.52	2.637	12.53	21.63
Test section 2 (745+00 – 755+00)								
Long-life/ NB	WC	IL	AC	11	579.8	37.5	514.4	633.2
		OL	AC	11	590.12	22.47	552.73	629.20
		IL	Base/SB	11	28.75	3.82	24.20	34.77
		OL	Base/SB	11	31.62	2.69	27.23	35.00
		IL	SG	11	23.82	7.88	13.83	36.07
		OL	SG	11	24.87	4.93	15.30	32.50
Standard/ SB	WC	IL	AC	11	844.7	44.9	754.8	896.0
		OL	AC	11	933.3	70.7	841.2	1037.2
		IL	Base/SB	11	32.23	6.52	19.93	41.27
		OL	Base/SB	11	27.97	6.07	20.10	36.53
		IL	SG	11	13.34	2.83	8.83	17.86
		OL	SG	11	13.34	3.02	8.50	17.36
Test section 3 (770+00 – 780+00)								
Long-life/ NB	WC	IL	AC	11	537.34	25.00	492.20	579.27
		OL	AC	11	549.32	17.44	522.23	574.67
		IL	Base/SB	11	25.28	3.01	20.76	29.96
		OL	Base/SB	11	25.62	2.79	20.06	29.83
		IL	SG	11	22.76	2.43	18.56	28.50
		OL	SG	11	23.72	3.91	20.63	34.67
Standard/ SB	WC	IL	AC	11	995.4	178.7	697.9	1172.7
		OL	AC	11	1094.0	48.4	1008.6	1168.7
		IL	Base/SB	11	37.93	7.32	23.70	48.40
		OL	Base/SB	11	32.56	6.55	20.03	42.23
		IL	SG	11	17.65	2.43	13.66	21.20
		OL	SG	11	17.93	2.57	14.20	22.16

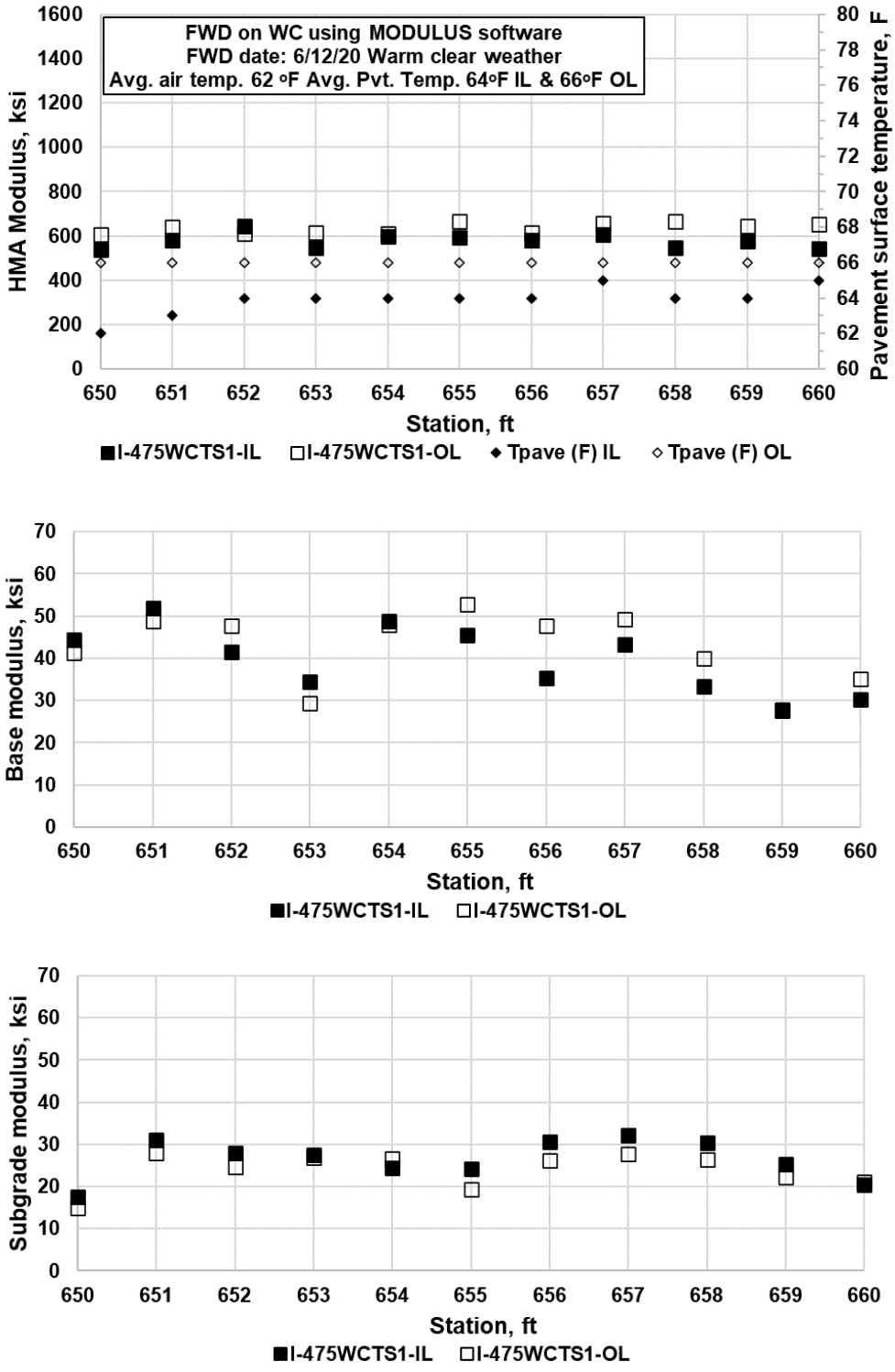

Figure 8 Spatial variation of back-calculated moduli within lanes for I-475 TS1 NB using MODULUS and deflections measured on wearing course

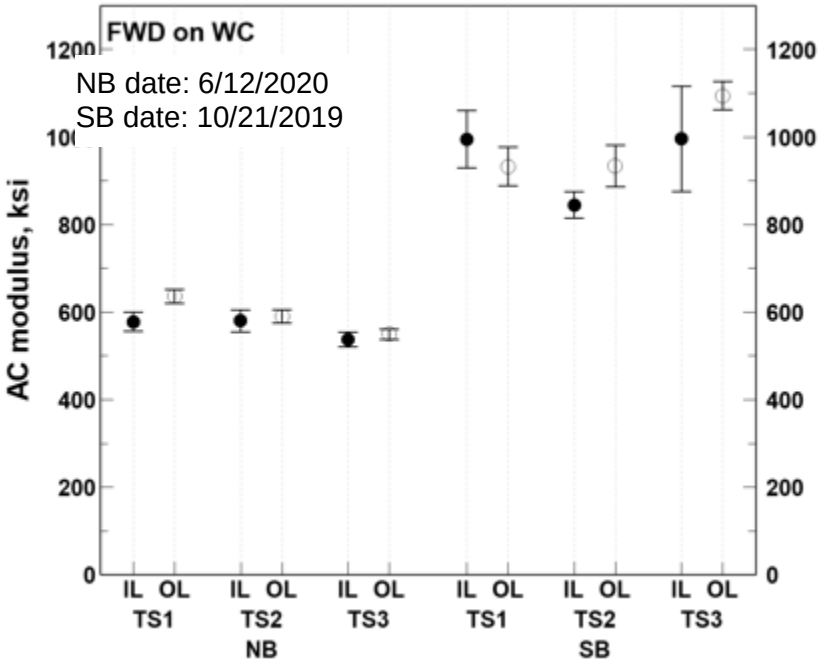

(a) Back-calculated AC moduli values

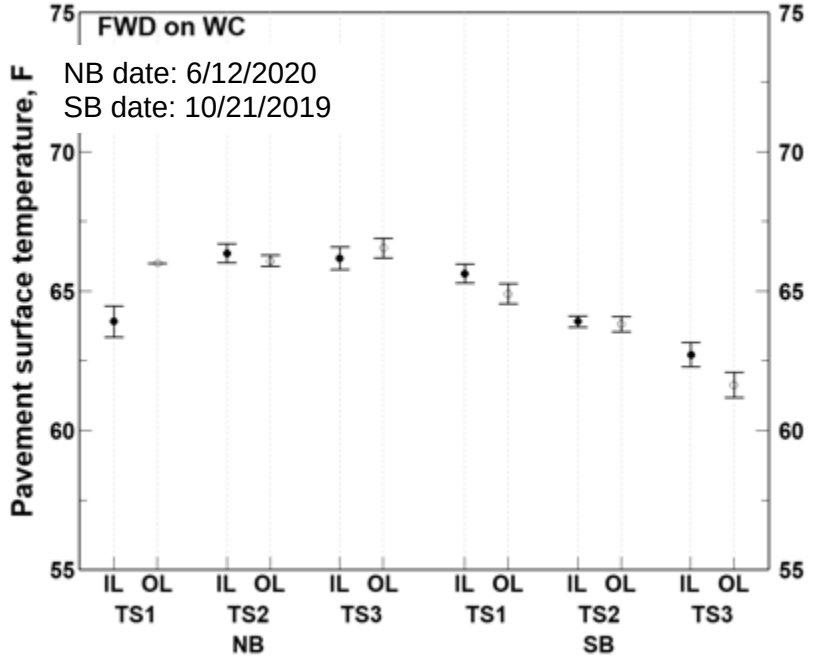

(b) Recorded pavement surface temperatures

Figure 9 Comparison between backcalculated AC moduli values – I-475 HMA standard and long-life pavement sections along with recorded surface temperatures

For subgrade (Figure 10), higher moduli were backcalculated for the long-life NB sections as compared to the standard (SB) sections. However, the NB direction showed also

higher variability. The subgrade moduli values for the long-life sections along the NB direction are about 25,000 psi while these are between 14,000 to 18,000 psi for the standard design sections along the SB direction. Although subgrade values variate spatially within a pavement lane, these are consistent between the inner and outer lanes on each test section.

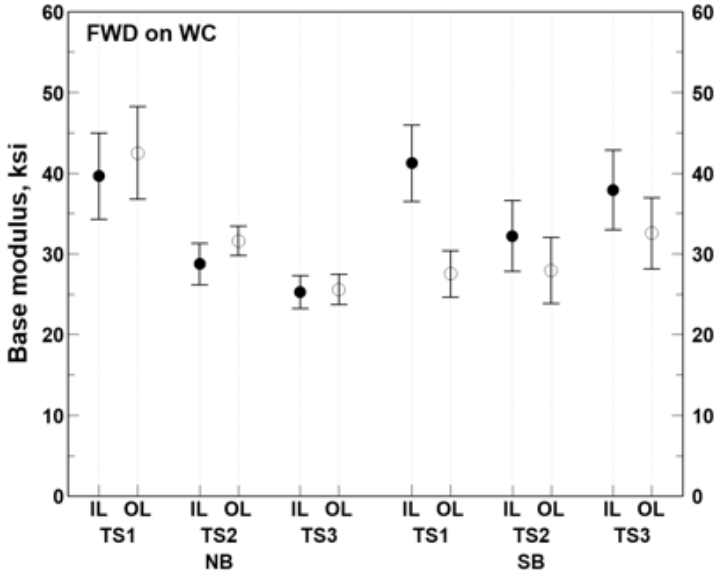

(a) Base moduli values

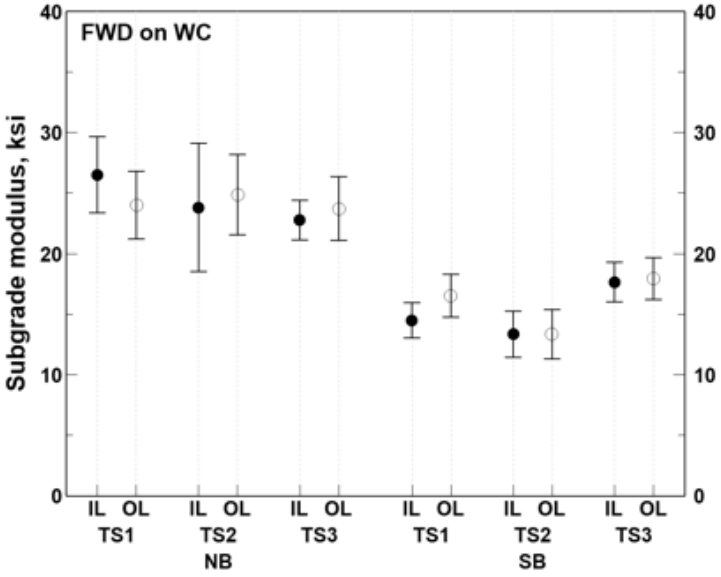

(b) Subgrade moduli values

Figure 10 Comparison between backcalculated base and subgrade moduli values – I-475 HMA standard and long-life pavement sections

4.1.3.2.2 US-131 HMA Project

For the US-131 30-year HMA project, FWD measurements were available for each of the AC layers (i.e., WC, LC, and BC) and all sections of the project. The results based on the FWD deflections measured over the WC are summarized herein, and other results are available in Appendix A. Table 10 and Figure 11 illustrate the descriptive statistics of the back-calculated layer. It can be noticed that the moduli for TS-1 and 3 (long-life pavement sections) significantly vary between the inner and the outer lanes. Additionally, outer lanes have higher AC layer moduli as compared to the inner lanes. This may be attributed to the lower surface temperatures recorded at the time of FWD testing at the outer lanes, as displayed in Figure 11b.

Table 10 Descriptive statistics – back-calculated layer moduli for US-131 HMA project

Design/ direction	Test section	Lane	Layer	No. of FWD points	Mean (ksi)	Std. (ksi)	Minimum (ksi)	Maximum (ksi)
Long-life/ NB	TS1	IL	AC	11	1069.6	101.5	938.6	1245.0
		OL	AC	11	1209.7	57.7	1149.1	1335.1
		IL	Base/SB	11	38.84	10.71	24.73	62.03
		OL	Base/SB	11	48.35	13.16	22.80	70.87
		IL	SG	11	22.18	4.71	17.20	31.53
		OL	SG	11	26.21	5.93	21.47	40.87
Long-life/ NB	TS2	IL	AC	11	1112.0	90.8	958.4	1281.4
		OL	AC	11	1160.6	66.4	1057.9	1265.2
		IL	Base/SB	11	38.99	6.10	30.37	51.87
		OL	Base/SB	11	42.11	4.89	36.03	49.30
		IL	SG	11	23.06	8.73	14.27	42.13
		OL	SG	11	23.49	6.76	15.37	37.00
Long-life/ NB	TS3	IL	AC	11	1074.2	73.8	1005.1	1222.4
		OL	AC	11	1173.8	48.9	1086.4	1234.3
		IL	Base/SB	11	32.20	7.34	19.97	40.47
		OL	Base/SB	11	56.25	11.09	33.87	79.10
		IL	SG	11	20.89	4.01	16.47	28.67
		OL	SG	11	22.28	3.91	18.60	32.77
Standard/ NB	TS4	IL	AC	11	1135.9	138.6	1012.5	1479.4
		OL	AC	11	1237.5	126.0	1003.8	1428.0
		IL	Base/SB	11	41.36	5.92	32.30	50.13
		OL	Base/SB	11	45.24	5.97	36.17	54.87
		IL	SG	11	16.47	4.50	10.23	25.70
		OL	SG	11	17.86	5.13	11.93	26.77

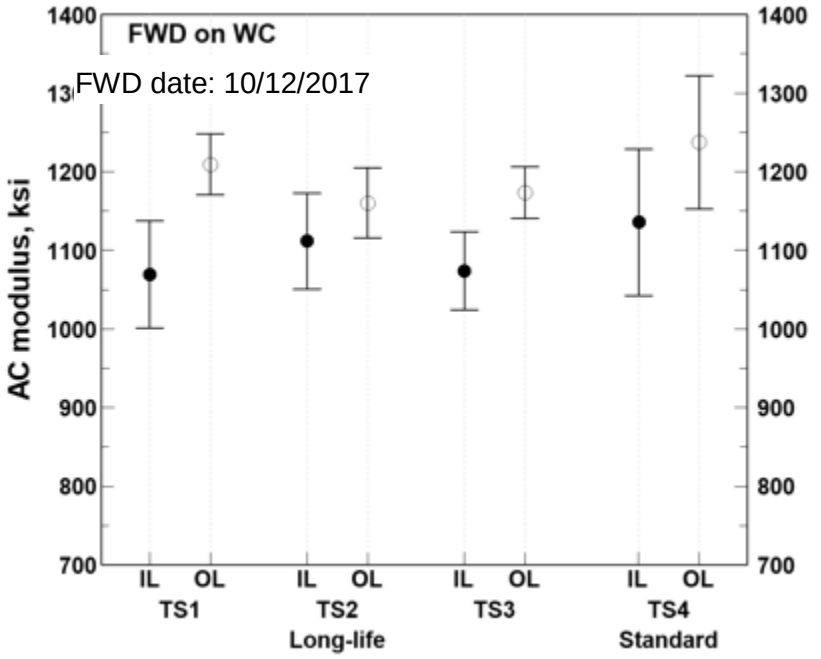

(a) Backcalculated AC moduli values

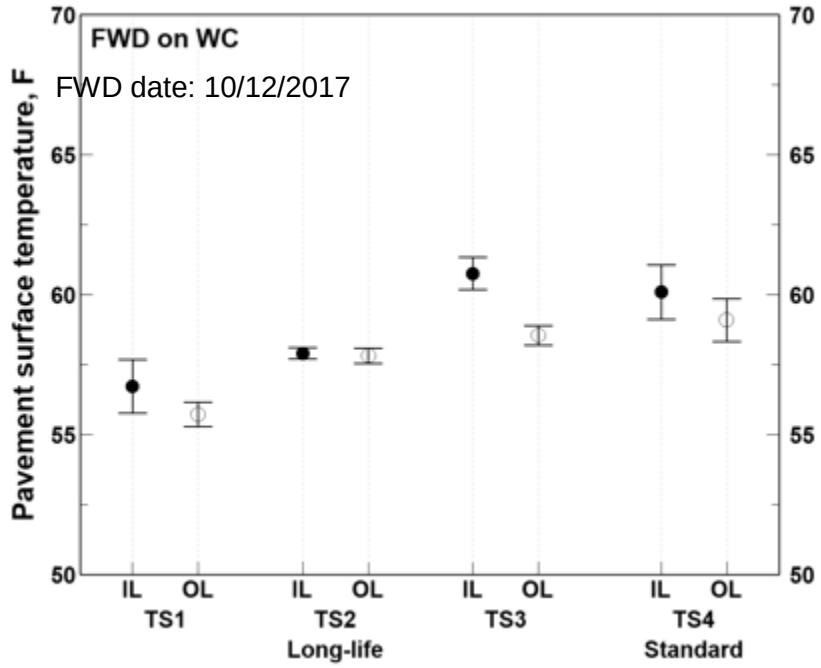

(b) Recorded pavement surface temperatures

Figure 11 Comparison between backcalculated AC moduli values – US-131 HMA standard and long-life pavement sections along with recorded pavement temperatures during FWD testing

Figure 12 illustrates the comparison of the back-calculated base and subgrade layer moduli values for the standard and the long-life pavement sections of the US-131 HMA project. The base moduli values show a significant difference between the inner and outer lanes of TS-3 of the long-life pavement section while they do not vary between the different lanes of the remaining test sections. The back-calculated base moduli values range between 35,000 to 50,000 psi, higher than the 33,000 psi commonly used by MDOT.

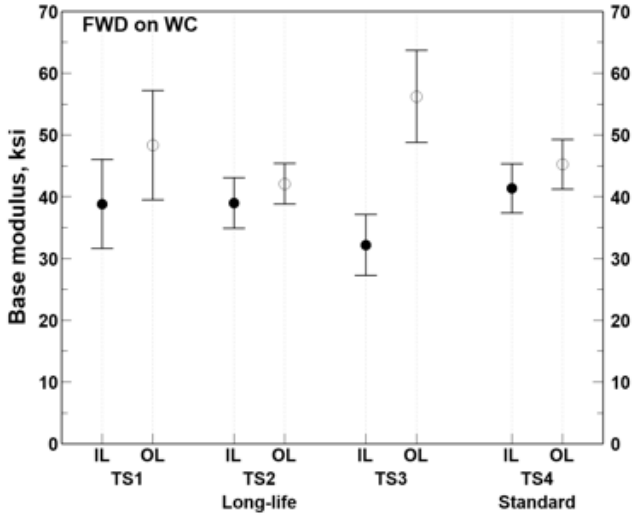

(a) Base moduli values

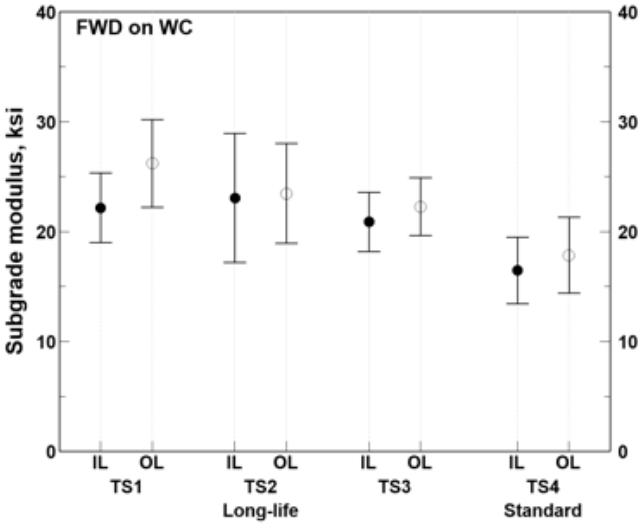

(b) Subgrade moduli values

Figure 12 Backcalculated base and subgrade moduli values - US-131 HMA long-life and standard pavement sections

The subgrade moduli display higher variability between the different lanes of TS-1 and 2 as compared to the other two sections as seen in Figure 12. However, the mean subgrade modulus value for either pavement lane of the long-life pavement sections ranges between 22,000 to 26,000 psi while it is around 18,000 psi for TS-4 (standard design section). In all cases, these values are 3 to 4 times higher than the typical subgrade modulus value of 5,000 psi used by the MDOT in the design process.

4.1.3.3 Dynamic Cone Penetrometer (DCP) Data Analysis

Dynamic cone penetrometer (DCP) test results for all projects were analyzed to calculate the resilient moduli of the subbase and subgrade layers. The following equations (Equations 3 to 7) were used to estimate the resilient modulus (Mr) of unbound materials from the DCP test results.

$$M_r\,(psi) = 2555 * CBR^{0.64} \quad \text{(NCHRP 1-37A)} \qquad \text{Equation 3}$$

$$M_r\,(psi) = \frac{151.8}{DCP(\frac{mm}{blow})^{1.096}} * 1000 \quad \text{(DCP direct model)} \qquad \text{Equation 4}$$

where Mr = resilient modulus, CBR = California bearing ratio, and DCP = dynamic cone penetrometer. CBR in Equation 3 is computed as follows depending on the classification of soils and subbase materials:

For all soils except for CL soils with CBR < 10 and CH soils:

$$\text{CBR} = 292/\text{DCP}^{1.12} \qquad \text{Equation 5}$$

For CL soils with CBR<10:

$$CBR = \frac{1}{(0.017019 * DCP)^2} \qquad \text{Equation 6}$$

For CH soils:

$$CBR = \frac{1}{0.002871 * DCP}$$ Equation 7

where DCP = DCP index in mm/blow.

4.1.3.3.1 I-475 HMA Project

Table 11 and Figure 13 present the descriptive statistics and the layer moduli of each subbase and subgrade layers that are calculated from the DCP data for the I-475 project. It is observed that the trend of DCP-based results is consistent with the LWD results presented above. The subgrade moduli are different in various sections along the NB direction but do not vary between lanes (IL vs OL) of the same section. Similar to the LWD elastic moduli results, the subgrade moduli of the TS-3 for both the NB and SB pavements (in general) are higher than that of other sections. As expected, subbase moduli of pavement foundation layers are consistently higher than that subgrade moduli regardless of project types (Figure 13).

Table 11 Descriptive statistics of layer moduli obtained using DCP data – I-475 HMA project

Layer	Test section	Number of drops	Mean	Standard deviation	Minimum	Maximum
Long-life/ Northbound						
Subgrade modulus (ksi)	TS1	20	10.89	4.05	5.01	20.07
	TS2	22	12.26	4.65	3.77	19.92
	TS3	22	17.14	5.35	6.98	27.35
Subbase modulus (ksi)	TS1	22	7.90	1.85	5.45	13.49
	TS2	22	6.81	0.95	4.61	8.30
	TS3	22	9.02	5.25	6.00	31.70
Standard/ Southbound						
Subgrade modulus (ksi)	TS1	22	14.30	5.93	4.55	26.91
	TS2	22	11.79	2.04	7.51	16.06
	TS3	22	21.90	11.12	6.73	49.71
Subbase modulus (ksi)	TS1	22	8.78	2.39	4.79	13.64
	TS2	22	7.57	1.26	5.45	9.78
	TS3	22	7.63	1.46	5.37	10.34

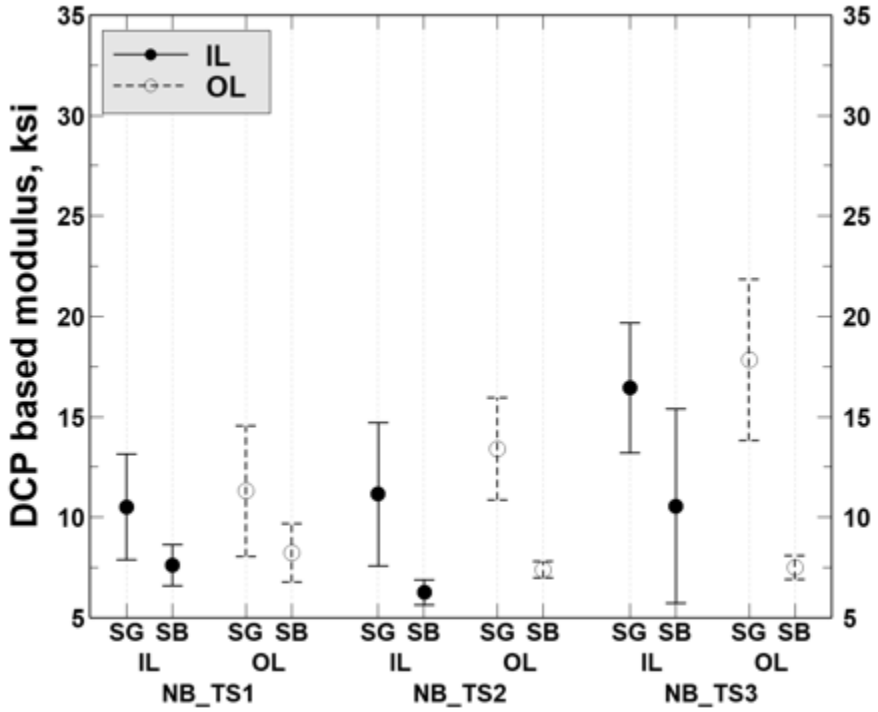

(a) Northbound long-life design

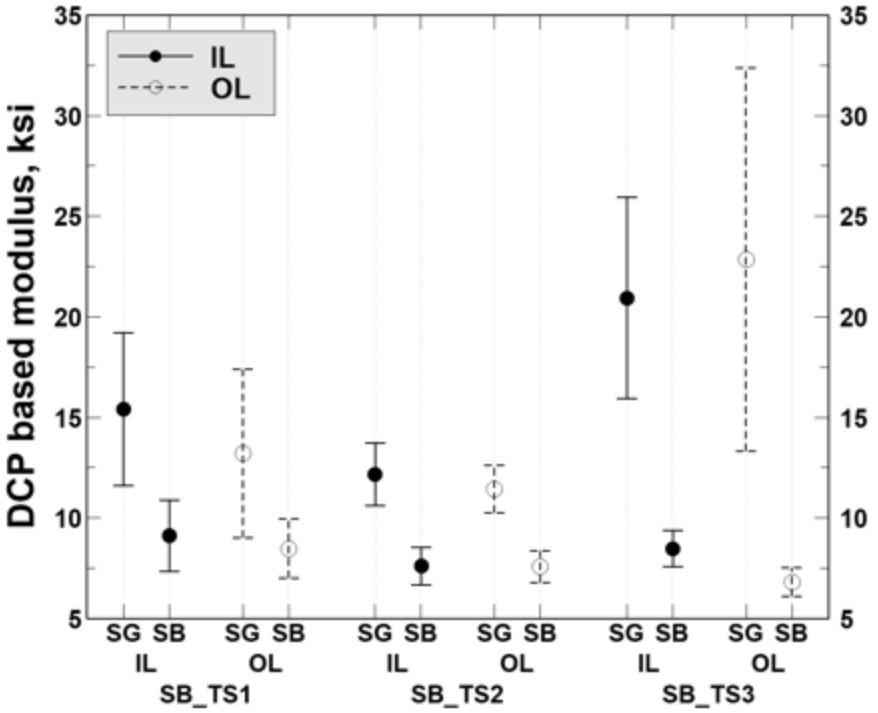

(b) Southbound standard design

Figure 13 Interval plots comparing DCP-based subgrade (SG) and subbase (SB) moduli values between different lanes and test sections of the Northbound (NB) long-life and Southbound (SB) standard design pavements – I-475 HMA project

4.1.3.3.2 US-131 HMA Project

The subgrade and subbase layer moduli of the test sections at US-131 HMA project (calculated from DCP data) are summarized in Table 12 and Figure 14. Subgrade moduli of the long-life sections (TS-1 through TS-3) are higher than that of the standard TS-4 even though they show higher variability. The same trend was also observed for the subbase layer moduli of test sections of both long-life and standard test sections.

Table 12 Descriptive statistics of layer moduli obtained using DCP data – US-131 HMA project

Layer	Test section	Design	Number of drops	Mean	Standard deviation	Minimum	Maximum
Subgrade modulus (ksi)	TS1	Long-life	6	59.16	9.26	50.10	73.26
	TS2		6	46.55	23.18	15.29	71.57
	TS3		6	56.65	15.36	39.26	82.03
	TS4	Standard	5	11.49	4.12	5.38	15.56
Subbase modulus (ksi)	TS1	Long-life	6	28.88	6.48	16.42	34.71
	TS2		6	36.22	13.30	22.42	52.88
	TS3		6	45.03	3.28	39.64	49.45
	TS4	Standard	6	17.13	8.39	10.55	32.81

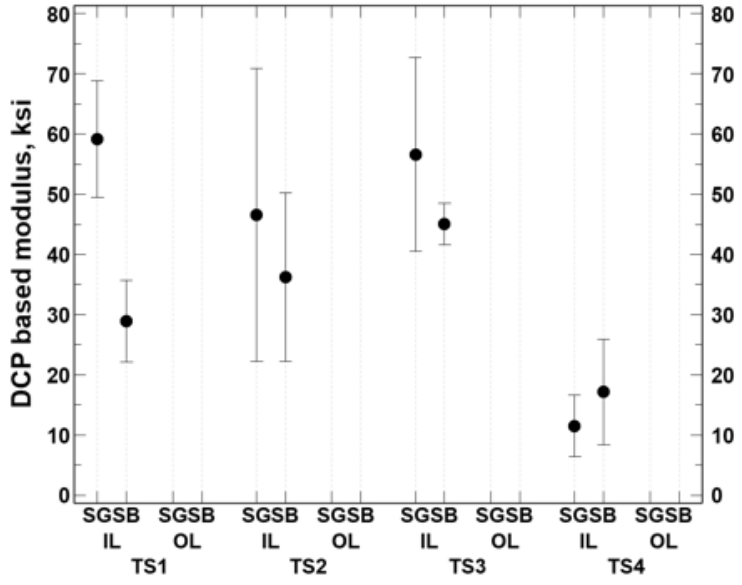

Figure 14 Interval plots comparing DCP-based subgrade (SG) and subbase (SB) moduli values between test sections of the long-life and standard design pavements – US-131 HMA project

4.2 CHAPTER 2: MATERIAL TESTING AND CHARACTERIZATION

4.2.1 Linear viscoelastic characterization of asphalt binders

The linear viscoelastic characterization of asphalt binders was conducted in general accordance with AASHTO T 315, Dynamic Shear Rheometer (DSR) test. The bitumen complex modulus (|G*|) and phase angle (δ) were obtained at the same loading frequencies and temperatures as the ones reported in MDOT RC-1593 report to generate the |G*| master curves. Table 13 shows the binders provided by MDOT for I-475. The binders used in the long-life and standard sections of the US-131 were tested as part of another project with MDOT.

Table 13 List of asphalt binders provided by MDOT, collected from I-475 project

Date	Direction	Binder Grade	Mix
8/24/2019	SB	52-34	3E10
8/25/2019	SB	52-34	3E10
10/11/2019	SB	58-34	5E10 LV (leveling)
10/13/2019	SB	58-34	5E10 LV (leveling)
10/17/2019	SB	58-34	5E10 TOP
10/18/2019	SB	58-34	5E10 TOP
11/05/2019	NB	58-34	3E30
6/20/2020	NB	70-28p	GGSP
6/04/2020	NB	70-28p	GGSP
5/27/2020	NB	70-28p	4E30
5/26/2020	NB	70-28p	4E30
5/31/2020	NB	70-28p	4E30
5/6/2020	NB	58-34	3E30
5/13/2020	NB	58-34	3E30
5/22/2020	NB	58-34	3E30
6/4/2020	NB	58-34	5E3
6/6/2020	NB	58-34	5E3

Asphalt binders were tested in their original and short-term aged conditions. Aged bitumen was obtained using the rolling thin-film oven (RTFO) in accordance with AASHTO 240-13. Data at different temperatures for the binders used in long-life and standard sections of I-475 and US-131 are shown in Figure 15 to Figure 18. As expected, asphalt binders with same PG from different HMA layers have similar complex modulus values. Test results also showed a

trend between PG and stiffness of the bitumen, as expected. The polymer modification used for the production of the PG 70-28P of the long-life sections in I-475 and the one used in the US-131 resulted in stiffer bitumen compared to both PG 58-34 and PG 64-28 used in the two projects. For both I-475 and US-131, the binder used in the base course of the standard sections (PG 52-34 for I-475 and PG 58-28 for US-131), is softer than the ones used in the top and leveling HMA layers. Using stiffer binders at high temperatures results in better performance in rutting. Therefore, mixtures with polymer modified binders (GGSP and 4E30) are expected to have better performance in rutting. Although the aggregate skeleton is another significant factor in rutting resistance. Softer binders in low temperatures might have more flexibility. Polymer modification is also shown to improve the fatigue performance.

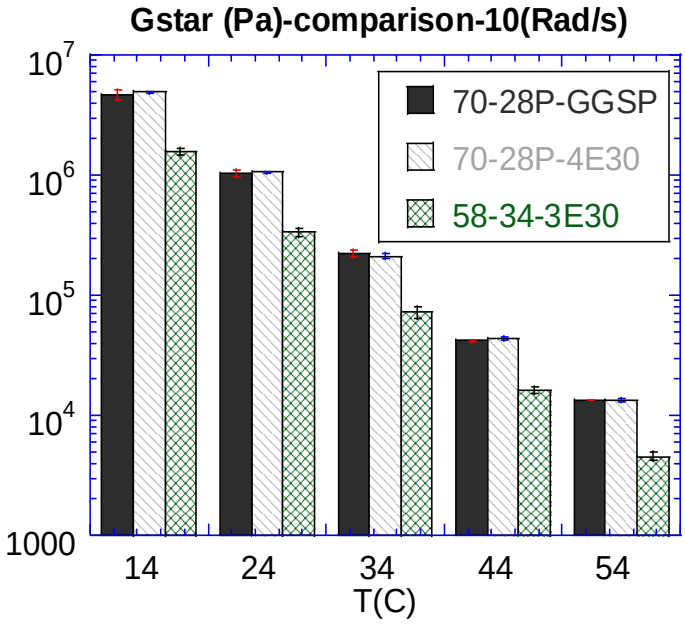

Figure 15 |G*| test raw data comparison – I-475 long-life mixtures binders – RTFO aged

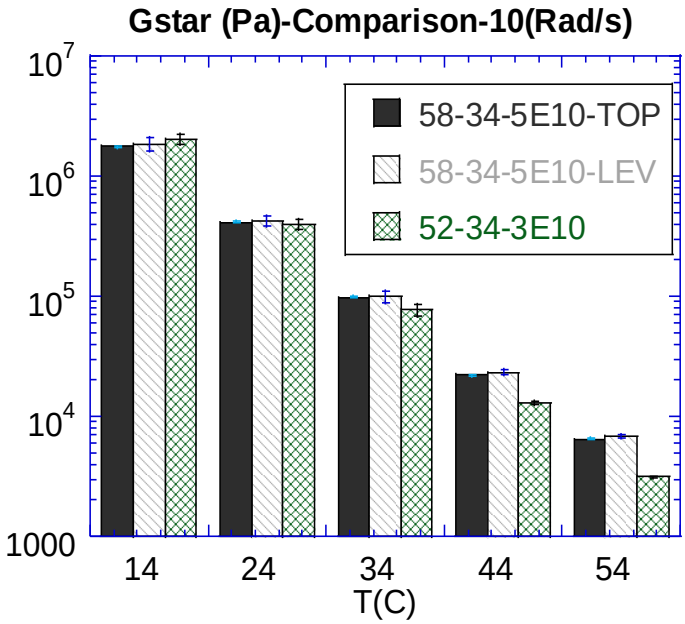

Figure 16 |G*| test raw data comparison – I-475 standard mixtures binders – RTFO aged

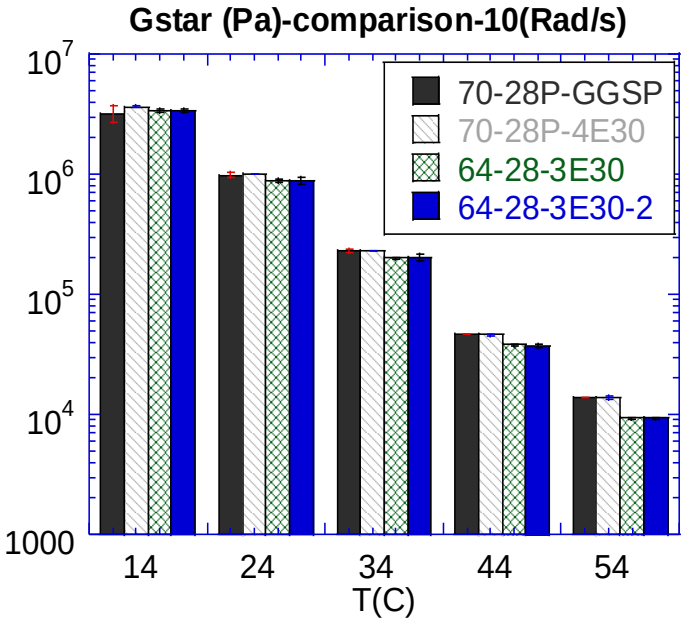

Figure 17 |G*| test raw data comparison – US-131 long-life mixtures binders – RTFO aged

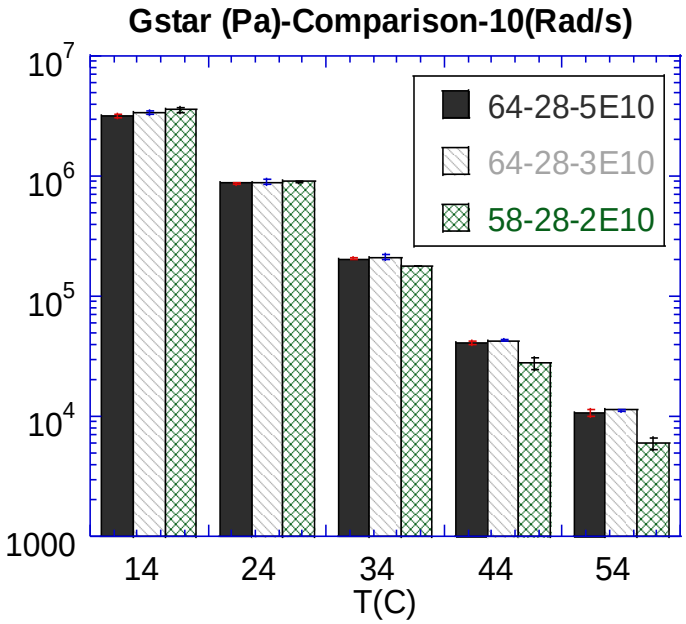

Figure 18 |G*| test raw data comparison – US-131 standard mixtures binders – RTFO aged

4.2.2 Asphalt Binder Multiple Stress Creep Recovery (MSCR) Test

The multiple stress creep recovery (MSCR) test was conducted by using the DSR system in accordance with AASHTO T 350. The test starts with the application of a low stress (0.1 KPa) for 10 creep/recovery cycles. Then the stress level increases to 3.2 KPa for 10 additional cycles. Nonrecoverable creep compliance (J_{nr}) is equal to the average non-recovered strain for the 10 creep and recovery cycles divided by the corresponding applied stress in those cycles. The average percent recovery is equal to the average ratio of recovered strain to maximum strain in every cycle under corresponding applied stress. All binder grades used in the long-life and standard sections of the I-475 and US-131 projects were tested. These binder grades include 70-28P, 58-34 and 52-34 for I-475 and 70-28P, 64-28 and 58-28 for US-131 project. All RTFO-aged binders were tested at 58°C, which corresponds to the high PG temperature required for Michigan's binders before traffic adjustments. The MSCR test uses two parameters, the percent recovery (%R) and the non-recoverable creep compliance (J_{nr}) at 3.2 kPa, to evaluate their potential to accumulate permanent deformations. The results of MSCR test on I-475 and US-131

projects are shown in Figure 19. The polymer-modified binders (PG 70-28P) used in both projects resulted in %R above the pass-fail threshold. However, differences were noticed in terms of non-recoverable creep compliance.

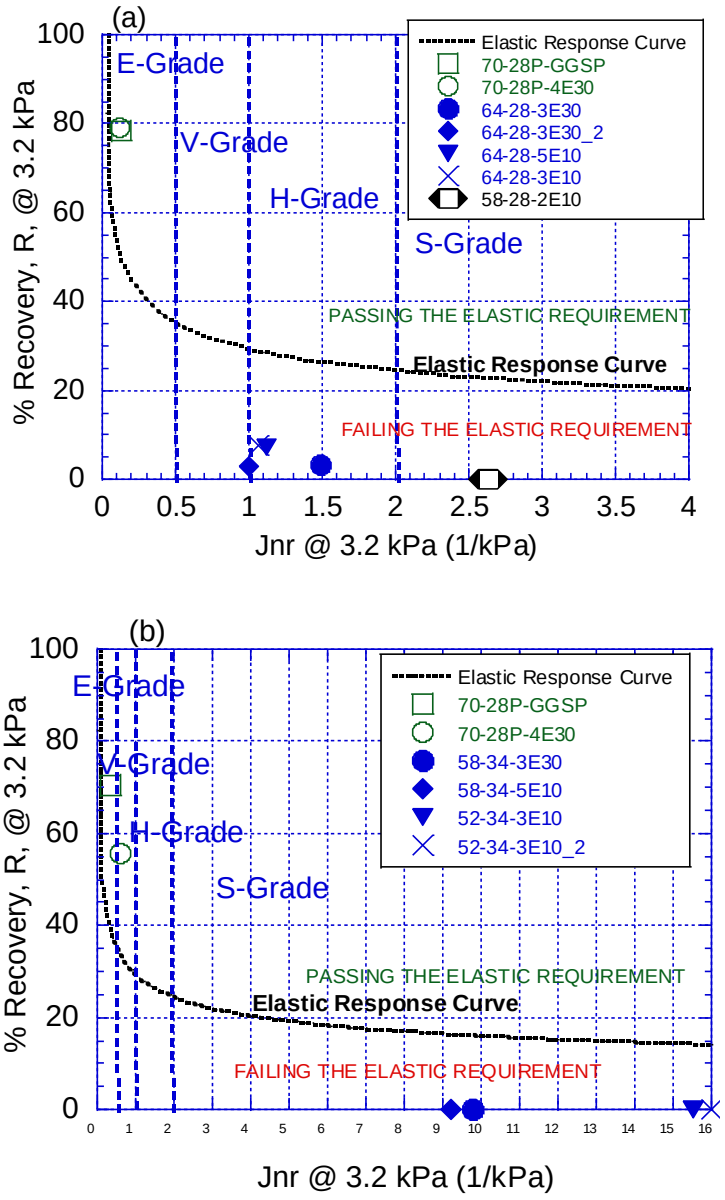

Figure 19 MSCR test results for (a) US-131 and (b) I-475 binders

In fact, while the two binders used on the US-131 can be both classified as "E" grade (i.e., suitable for extremely heavy traffic), the two PG70-22P used in the I-475 project belong to two different grades, "E" and "V" for the GGSP and 4E30, respectively. It shall be also noted

that the “E” grade of bitumen used in the GGSP mixture of the I-475 has a lower %R and higher Jnr3.2 compared to the “E” grades used in the US-131 project. All other non-polymer modified binders showed negligible rutting resistance.

4.2.3 Asphalt Mixture Dynamic Modulus (|E*|)

Dynamic Modulus (|E*|) tests were conducted on HMA mixtures of I-475 for all six test sections in accordance with AASHTO T342, and their master curves generated in accordance with the AASHTO R84. US-131 mixtures were also tested as part of another project with MDOT. For these tests, 4” diameter and 6” tall samples were prepared by cutting and coring gyratory compactor specimens. Target air voids for the samples was 7%±0.5%. Three replicates for each mixture were tested in uniaxial compression mode at different temperatures (-10°C, 4°C, 21°C, 37°C and 54°C) and loading frequencies (25, 10, 5, 1.0, 0.5, and 0.1 Hz). It is well known that the minimum temperature that the AMPT device is capable of controlling is approximately 0°C. To obtain |E*| data at -10°C, samples were conditioned overnight at -13°C using an external environmental conditioning system. Before each test, samples were quickly transferred into the AMPT chamber (which was kept at 0°C overnight) and tested. This procedure was validated by placing a thermocouple in a dummy sample and running a trial test, during which it was observed that the temperature of the sample was -10°C±0.5°C during the entire test. The duration of each |E*| test was approximately 3 minutes. The stress level is adjusted such that the strain level measured on the sample remains between 75 and 125 microstrains to ensure no damage accumulation during the test.

A summary of results of |E*| tests at the frequency of 10 Hz for I-475 and US-131 mixtures is shown in Figure 20 and Figure 21, respectively. As shown in the Figure 20(a) and (b), the top and levelling courses of the long-life sections (GGSP and 4E30) are generally stiffer than the corresponding layers in the standard sections (5E10-Top and 5E10-Lev). The difference

in the stiffness of these layers (GGSP vs 5E10-Top and 4E30 vs 5E10-Lev) is more significant at higher temperatures. These results can only be partially due to the polymer-modified binders. In addition, the gradation of the aggregate's skeleton plays a crucial role. The higher stiffness of the GGSP, for example, can be associated to the high number of stone-to-stone contacts in this Stone Matrix Asphalt – type of HMA, as opposed to the dense-graded mix of the 5E10. It is common understanding that stiffer surface layers are desirable if they are not brittle. A stiffer surface layer can, in fact, reduce the stress transmitted to lower layers and reduce their deformation under loading, hence reducing the potential for fatigue cracking damage. On the other side, the polymer modified binders used on the top layer of the long-life sections is expected to produce a ductile material and reduce the risk of top-down cracking typical of brittle surface HMAs.

It is worth also noting that no performance-related conclusion can be drawn solely based on dynamic modulus test results. These tests are performed in the linear-viscoelastic range of the HMA mechanical response, where damage does not accumulate. Hence, any comments based on |E*| test results would be purely indicative. Damage (e.g., tension-compression fatigue, three-point bending cylinder) as well as plastic strain-inducing (e.g., flow number) tests are needed to fully characterize the asphalt mixture performances.

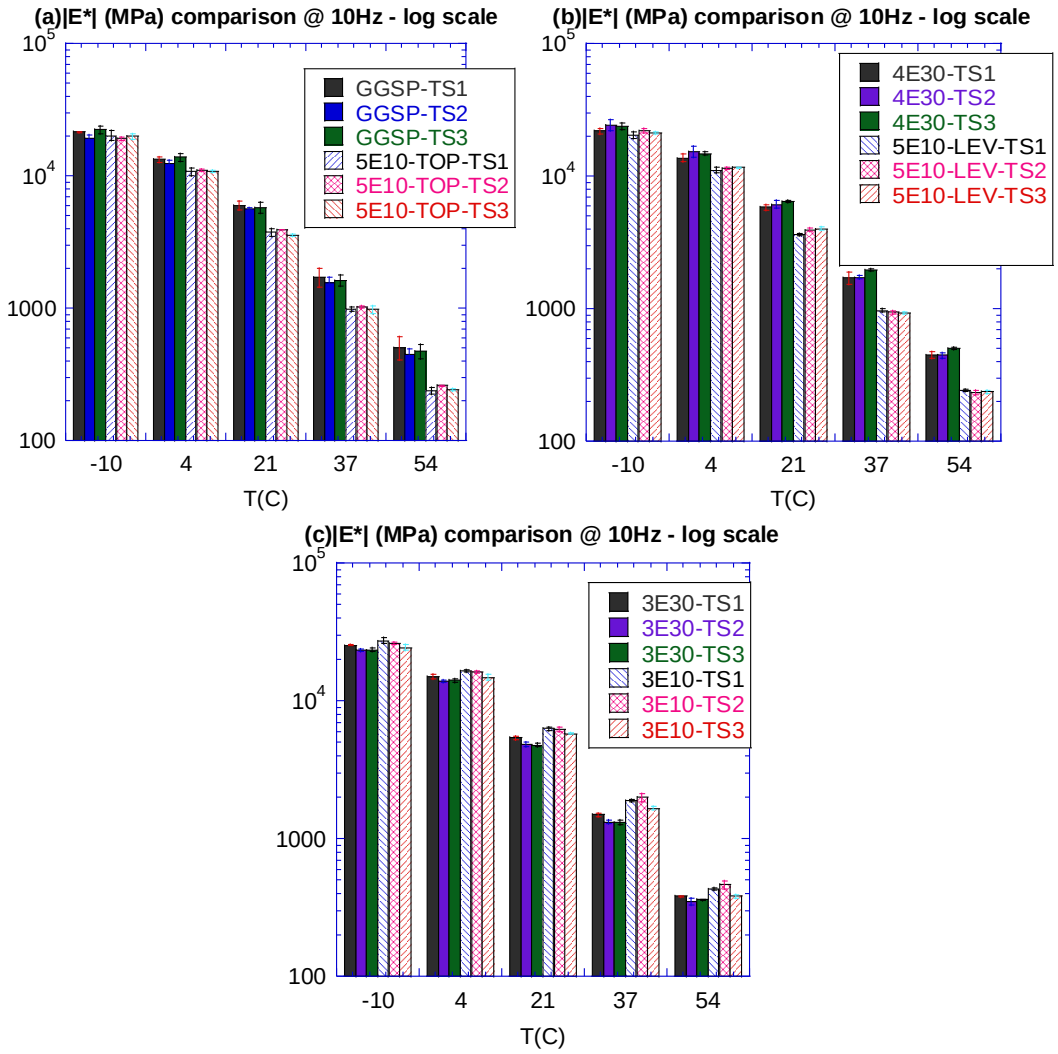

Figure 20 Summary of results of |E*| tests at 10 Hz for I-475 project: (a) GGSP (PG70-28P) vs 5E10-Top (PG58-34), (b) 4E30 (PG70-28P) vs 5E10-Lev (PG58-34) and (c) 3E30 (PG58-34) vs 3E10 (PG52-34)

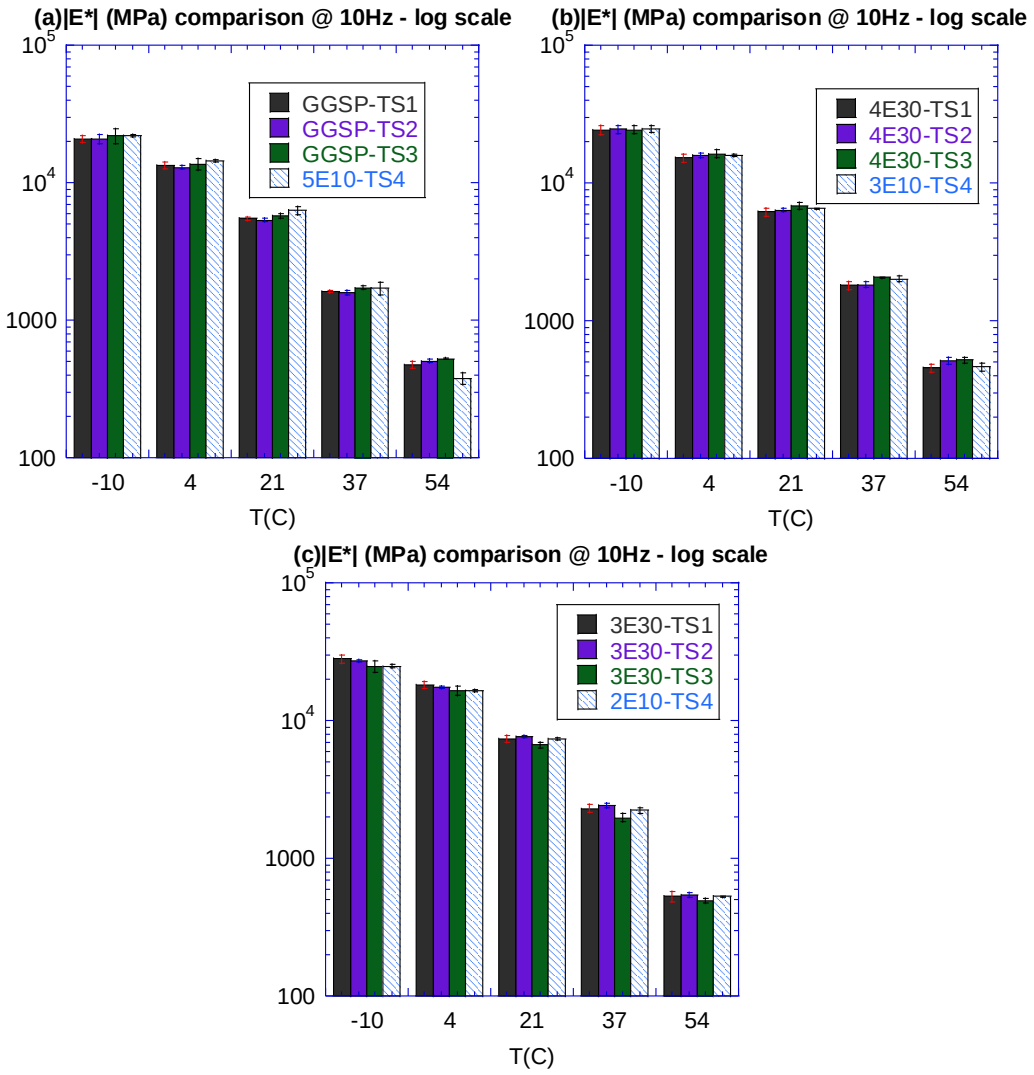

Figure 21 Summary of results of |E*| tests at 10 Hz for project US-131: (a) GGSP (PG70-28P) vs 5E10 (PG64-28), (b) 4E30 (PG70-28P) vs 3E10-LEV (PG64-28) and (c) 3E30 (PG64-28) vs 2E10 (PG58-28)

4.2.4 Asphalt Mixture Confined Dynamic Modulus (|E*|)

Confined dynamic modulus |E*| tests were conducted so that mixture-specific calibration coefficients of the MEPDG HMA rutting model can be computed. Tests were performed on the same samples used for unconfined dynamic modulus tests described above and following the same testing protocol, except for the application of a 10 psi (68.9 kPa) lateral confining pressure. The average of three replicates was used to generate |E*| master curves, in accordance with AASHTO R84. A comparison of confined and unconfined |E*| master curves is shown in Figure

22 and Figure 23 for I-475 and US-131 HMAs, respectively. The effect of lateral confinement can be clearly noticed at high temperatures (i.e., low frequencies).

The effect of confinement, in terms of ratio between confined and unconfined moduli, on different mixtures used in the long-life and standard sections of I-475 and US-131 projects were quantified and plotted in Figure 24 and Figure 25, respectively. The effect of confinement was less significant on GGSP and 4E30 mixtures of the I-475 compared to 5E10-Top and 5E10-Lev. This was possibly because of the polymer modified binders making the mixtures stiffer (Figure 24). On the other hand, the effect of confinement on the base courses (3E30 and 3E10) were similar. Similar trends have been noticed for the mixtures of the US-131 project (Figure 25). It should be noted that the input required by the AASHTOWare Pavement ME software is the unconfined |E*|. The software, in fact, performs the layered elastic analysis under the assumption of negligible confinement effect, while confinement is considered in the HMA rutting model through an empirical variable (k_z).

It is hypothesized that the mixtures that are less affected by confinement are better mixtures. This is because these mixtures do not need confinement to provide a given stiffness (i.e., dynamic modulus). It is well known that unbound materials (base and subbase) need significant confinement to provide sufficient stiffness to withstand traffic loading. If an asphalt mixture is like an unbound material where the confinement affects its stiffness, this means that the binder is not doing its job, or the gradation is not providing sufficient aggregate interlocking. As such, the mixtures whose dynamic moduli are not affected (or affected minimally) by the confinement are better and more stable mixtures. Based on the data provided herein, the GGSP and 4E30 mixtures are much more stable mixtures (not as significantly affected by confinement as other mixtures).

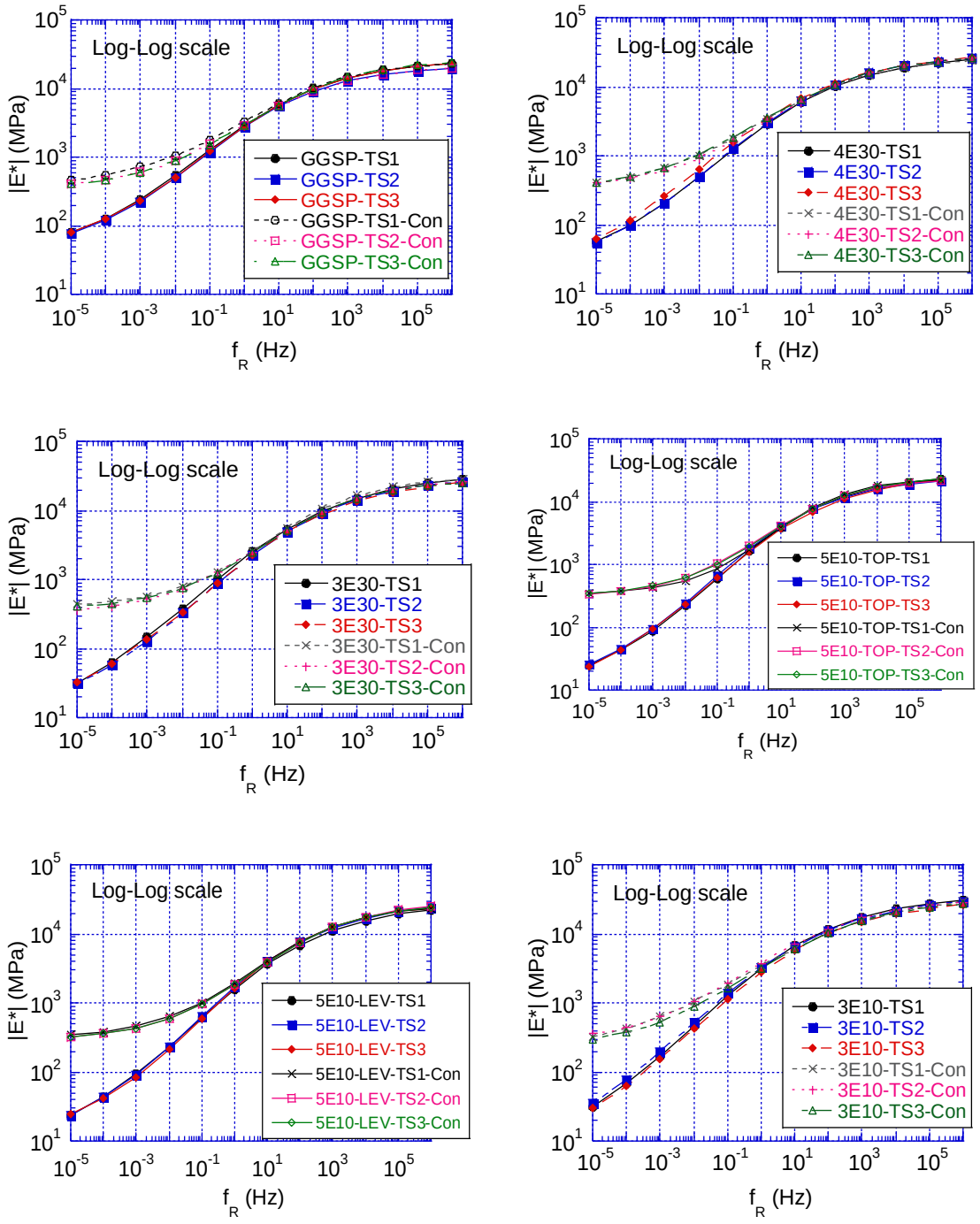

Figure 22 Comparison of confined and unconfined |E*| master curves of the mixtures for the long-life and the standard sections of I-475 project

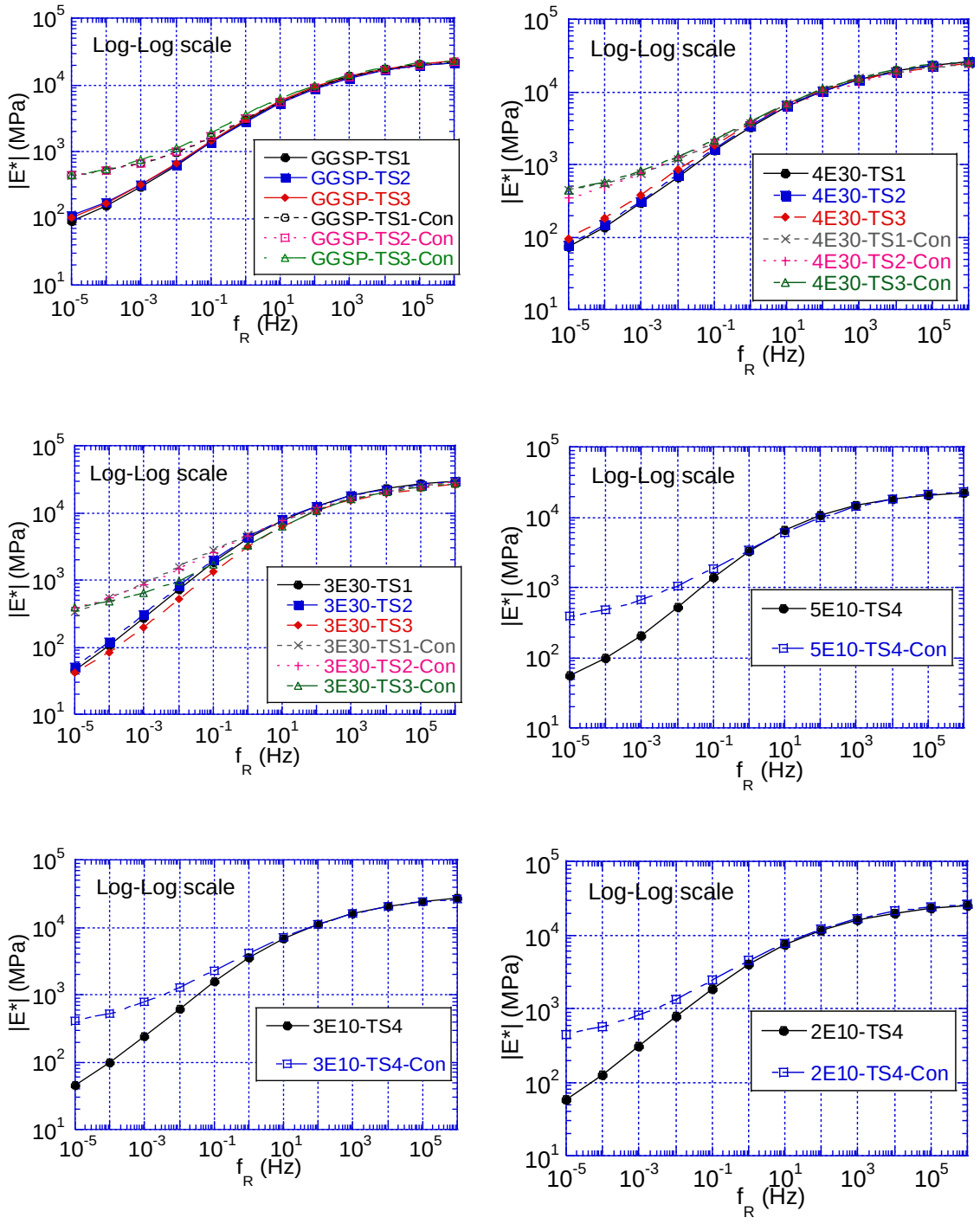

Figure 23 Comparison of confined and unconfined |E*| master curves of the mixtures for the long-life and the standard sections of US-131 project

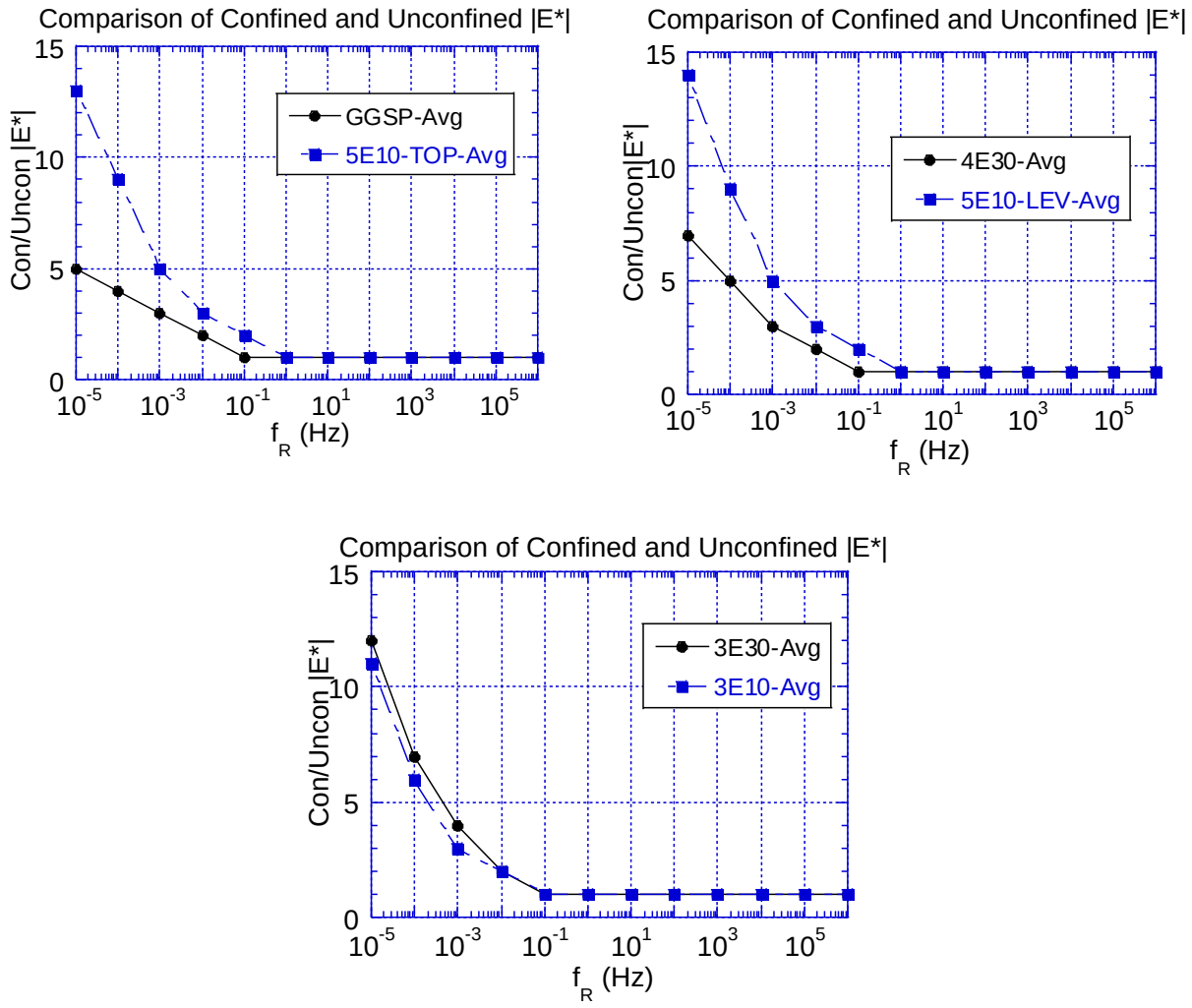

Figure 24 The effect of confinement on long-life and standard mixtures for I-475 project

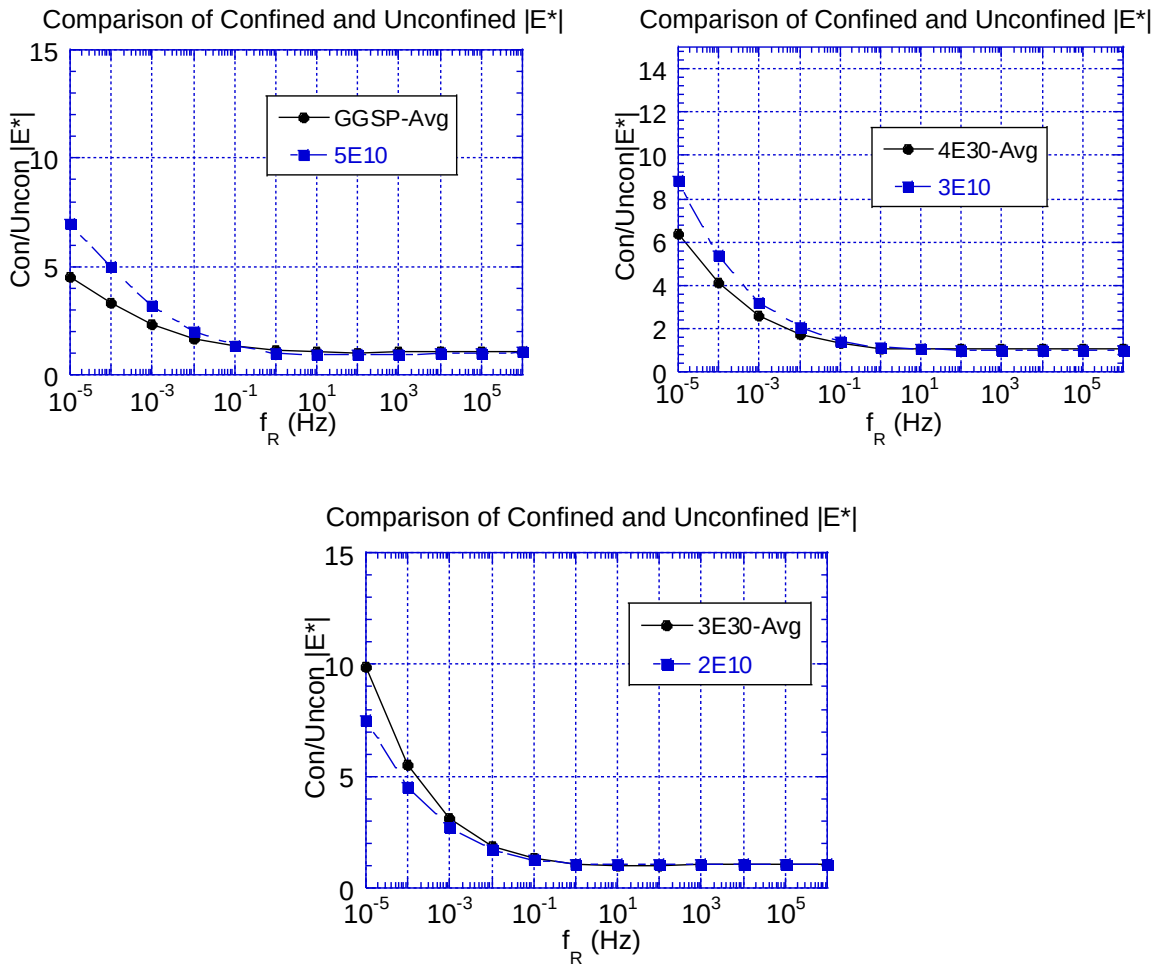

Figure 25 The effect of confinement on long-life and standard mixtures for US-131 project

4.2.5 Asphalt Mixture Repeated Load Permanent Deformation (RLPD) Test

The RLPD tests (also known as Flow Number tests) were conducted in accordance with AASHTO T 378-17 to evaluate the susceptibility of asphalt mixtures to rutting. Laboratory fabricated cylindrical specimens, produced for dynamic modulus test, were subjected to a haversine axial compressive load pulse of 0.1s followed by a 0.9s rest period. The test duration was set equal to 10,000 load repetitions, and samples were tested at repeated deviatoric stress of 482.6 kPa (70 psi), constant confined stress level of 68.9 kPa (10 psi), at a single temperature of 54°C.

None of the mixtures exhibited tertiary flow at the stress state they were tested. A summary of the results obtained on the US-131 HMAs is provided in Figure 26, where the plastic strain accumulated after 10000 cycles is reported. Despite the GGSP and 5E10 |E*| values were comparable (see Figure 20a), and GGSP had higher binder content than 5E10 (see Table 5), GGSP performed better than 5E10. This confirms that performance indications based solely on dynamic modulus results can be misleading. GGSP's aggregate skeleton, combined with polymer modified binder are the two potential reasons for its superior performance. The 4E30 (leveling course, long-life section) also performed better than the material of the corresponding layer in the standard section (3E10), although their stiffnesses were comparable (see Figure 20b). This can be attributed to the fact that the 4E30 mix has been designed using a higher number of gyrations, which probably provides better aggregates' interlocking between compared to the one achieved in the 3E10 mix. The accumulated plastic strain in the HMA Base (3E30 and 2E10) were similar on average, with high variability observed between the long-life test sections.

Similar results were obtained on the HMAs of the I-475 (Figure 27). The surface and intermediate layers of long-life sections (GGSP and 4E30) exhibited lower accumulated plastic strain as compared to those of the standard sections (5E10). The two HMAs used for base course, the 3E30 and 3E10, resulted in similar performance.

Based on these results, the overall rutting susceptibility of the structure used in the long-life sections is generally lower than the one of the standard sections in both projects.

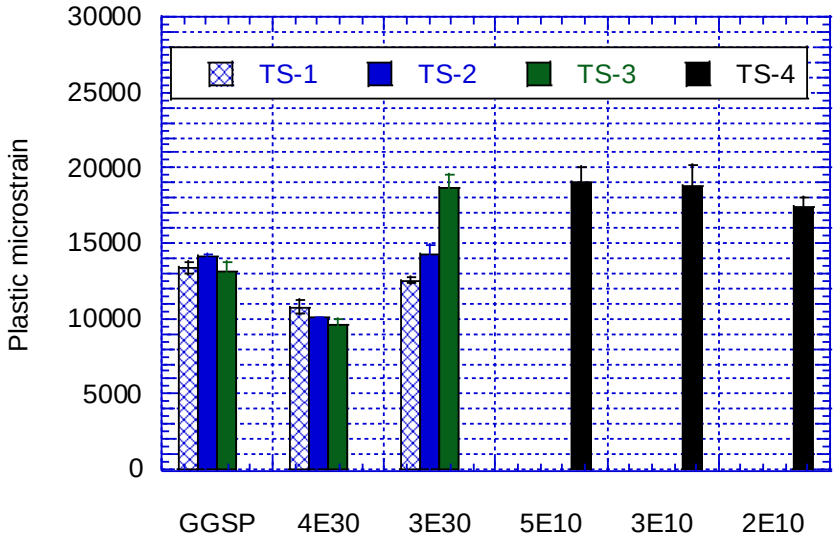

Figure 26 RLPD test results summary for US-131 HMAs

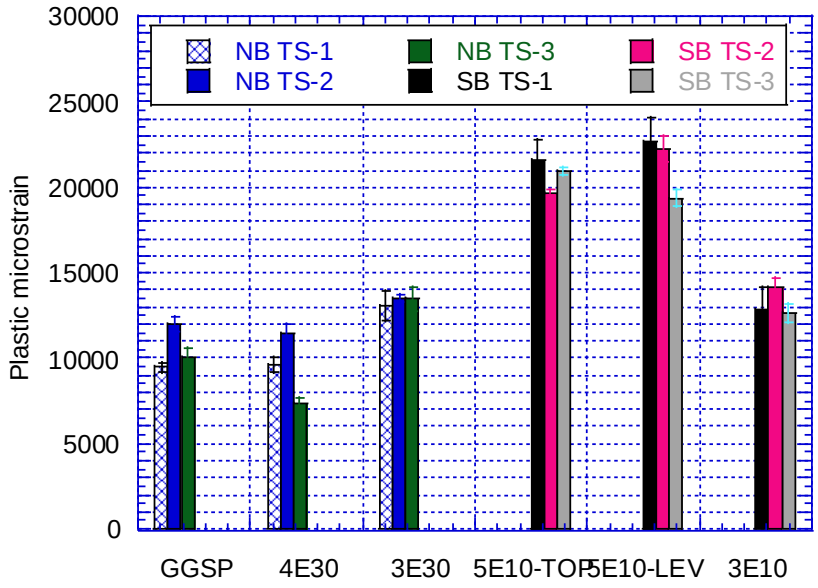

Figure 27 RLPD test results summary for I-475 HMAs

As mentioned above, results of the RPLD tests were coupled with the confined dynamic modulus test results to calibrate the MEPDG HMA rutting model. The details of the calibration procedure are described in Appendix L and results of the calibration are shown in Table 14 and Table 15.

Table 14 Rutting model calibration coefficients based on the flow number test results US-131

Test section	Mix type	Br1	k1	k2	k3
			-2.4545	3.01	0.22
			Log Br1	Br2	Br3
TS-1	GGSP	118759	5.07	-0.3035	0.7451
TS-1	4E30	17252	4.24	-0.2025	0.8927
TS-1	3E30	2431	3.39	-0.0648	1.0177
TS-2	GGSP	74746	4.87	-0.2730	0.7605
TS-2	4E30	25547	4.41	-0.2268	0.8380
TS-2	3E30	1686	3.23	-0.0405	1.0669
TS-3	GGSP	161450	5.21	-0.3208	0.7328
TS-3	4E30	33769	4.53	-0.2456	0.8145
TS-3	3E30	93	1.97	0.1422	1.1829
TS-4	5E10	655	2.82	0.0296	1.0561
TS-4	3E10	253	2.40	0.0903	1.1505
TS-4	2E10	2208	3.34	-0.0429	1.0598

Table 15 Rutting model calibration coefficients based on the flow number test results I-475

Direction	Test section	Mix type	Br1	k1	k2	k3
				-2.4545	3.01	0.22
				Log Br1	Br2	Br3
NB	TS-1	GGSP	123296	5.09	-0.3294	0.7371
NB	TS-1	4E30	216204	5.33	-0.3711	0.7613
NB	TS-1	3E30	36248	4.56	-0.2466	0.9038
NB	TS-2	GGSP	350143	5.54	-0.3820	0.7211
NB	TS-2	4E30	380887	5.58	-0.3929	0.7433
NB	TS-2	3E30	59863	4.78	-0.2812	0.8827
NB	TS-3	GGSP	652287	5.81	-0.4306	0.6802
NB	TS-3	4E30	198199	5.30	-0.3770	0.7645
NB	TS-3	3E30	34139	4.53	-0.2429	0.8913
SB	TS-1	5E10-TOP	1627	3.21	-0.0541	1.1606
SB	TS-1	5E10-LEV	742	2.87	0.0082	1.1167
SB	TS-1	3E10	14444	4.16	-0.1862	0.9441
SB	TS-2	5E10-TOP	3075	3.49	-0.0889	1.0579
SB	TS-2	5E10-LEV	1998	3.30	-0.0547	1.0658
SB	TS-2	3E10	219257	5.34	-0.3519	0.8493
SB	TS-3	5E10-TOP	2045	3.31	-0.0594	1.0589
SB	TS-3	5E10-LEV	3612	3.56	-0.0986	1.0299
SB	TS-3	3E10	86275	4.94	-0.3085	0.9103

4.2.6 Asphalt Mixture Low-Temperature Indirect Tensile Test (IDT)

The low-temperature indirect tensile tests (IDT) were conducted on mixtures obtained from the I-475 project in accordance with AASHTO T-322-07. The IDT strength tests were performed at -10°C by applying a monotonic displacement-controlled load along the diameter of a cylindrical sample at a rate of 12.5 mm per minute. Samples had a diameter of 150 mm and typical thickness of 38 mm. The maximum load before sample failure is used to calculate the IDT strength of the sample using the following formula:

$$\sigma_s = \frac{2P}{\pi D t_s} \qquad \text{Equation 8}$$

where σ_s is the IDT strength (psi), P the max load (lbs), D is the diameter of the sample (in) and t_s the thickness of the sample (in).

The average of three replicates was used to calculate the IDT strength for each mixture. Typically, for each test section, two samples were in the 7%±0.5% range of air voids, while the third one was slightly out of this range. Tests were performed on all asphalt layers for I-475 Northbound (GGSP, 4E30 and 3E30) and Southbound (5E10 Top, 5E10 Leveling and 3E10 Base) and all test sections (TS1, TS2 and TS3) as part of this project. The US-131 mixtures were instead tested as part of another project with MDOT.A summary of the IDT test results for I-475 is shown in Figure 28. GGSP and 4E30 show higher IDT strength values compared to 3E30. As expected, 5E10-Top and 5E10-Lev showed similar behavior. The differences of IDT strength values for all of the three mixtures in the standard sections (5E10-Top, 5E10-Lev, and 3E10) are negligible. The raw data of the IDT tests were also used for calculating the Work of Fracture (WOF). The WOF is defined as the area under the IDT load-displacement curve, and it indicates the potential for dissipating energy before failure (Table 16). Mixtures with high WOF typically perform better in the field. Although a direct comparison can be made for all mixtures and

among those of the same layer, it is worth focusing on differences between mixes used for wearing course, since thermal cracking initiates at the surface and then propagate into the pavement structure. The WOF is consistently higher for HMAs used in the long-life sections and, consequently, better thermal cracking performance are expected.

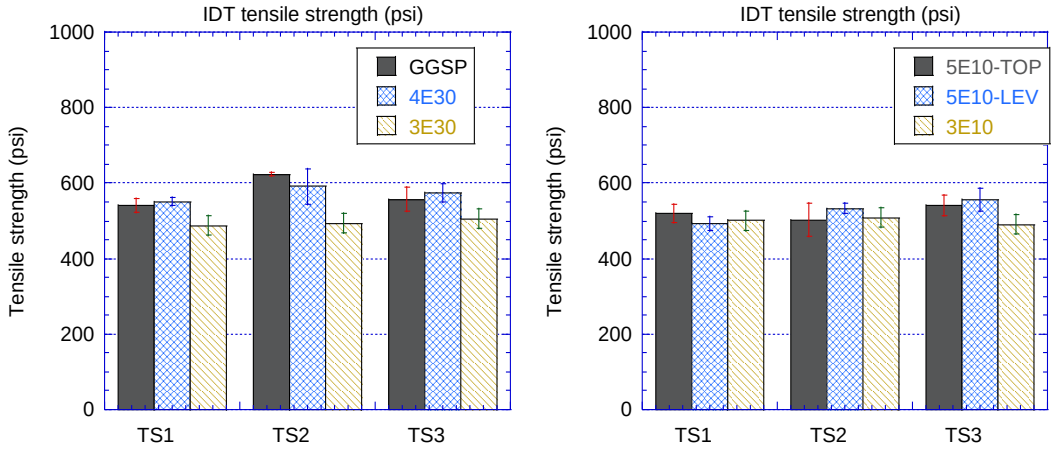

Figure 28 Summary of IDT test results I-475

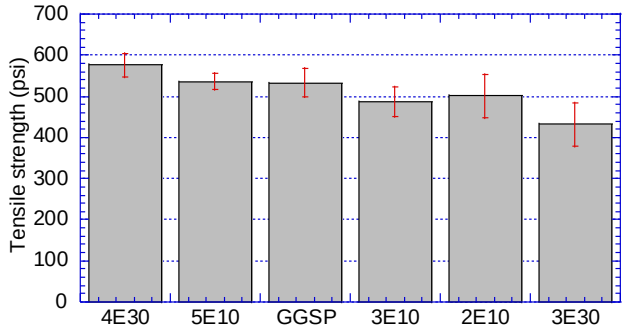

Figure 29 The Indirect Tensile Strength values of the asphalt mixture samples at -10C(Average of TS1, TS2 and TS3 are shown for GGSP, 4E30 and 3E30)

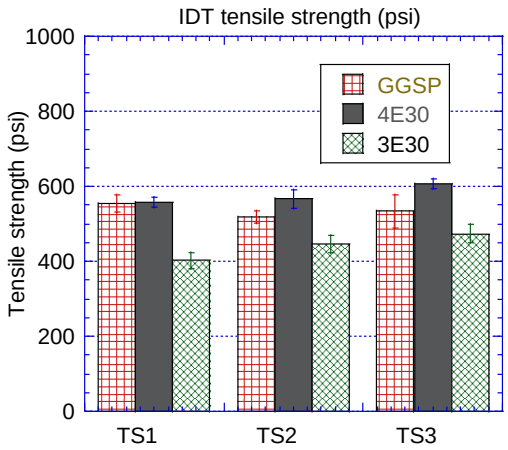

Figure 30 Comparison of US-131 Long-life sections IDT results

Table 16 IDT fracture work summary

Project	Mixtures	GGSP	4E30	3E30	5E10-Top	5E10-Lev	3E10
I-475	Average W_f (Joule)	56.5	39.9	55.2	48.9	45.5	43.5
	Standard deviation	20.3	5.9	10.1	4.0	7.2	10.4
	Mixtures	GGSP	4E30	3E30	5E10	3E10	2E10
US-131	Average W_f (Joule)	64.5	37.3	35.6	32.0	28.5	37.1
	Standard deviation	7.9	6.2	7.2	4.3	1.9	9.9

4.2.7 Asphalt Mixture Three-point Bending Cylinder (3PBC) Test

The 3PBC test was developed as part of NCHRP IDEA 20-30/IDEA 218 project (*36*). The 3PBC test is run to determine the fatigue life (i.e., number of cycles to failure, N_f) of asphalt mixtures using cylindrical samples subjected to cyclic three-point bending (*37*). A picture of the testing setup is shown in Figure 31. The tests have been conducted on the 68 mm diameter samples obtained by vertically coring a gyratory compactor sample obtained using the loose mixtures collected throughout the project. No further sample preparation (e.g., cutting) was required. The air voids content of each sample was 7±0.5%. The fatigue test was performed in a displacement-controlled mode, and it was conducted at a frequency of 5 Hz. Tests were repeated at two temperatures (10 and 20°C), two replicates at each temperature.

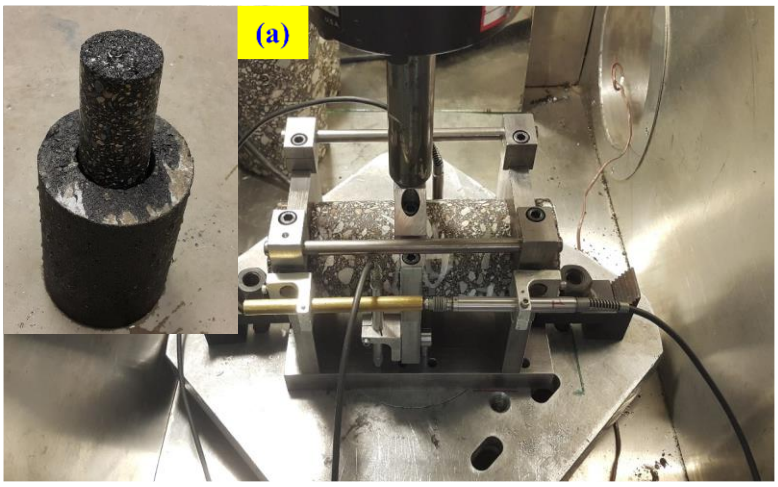

Figure 31 A picture of the 3PBC setup in the material testing system (MTS) with the 68 mm sample

The HMA bottom-up fatigue cracking model implemented in the AASHTOWare Pavement ME software correlates the fatigue life (N_f) to tensile strain (ε_t) and modulus (E) of the asphalt mixture. In this study, first, the raw data of the 3PBC test was analyzed using the Viscoelastic Continuum Damage (VECD) theory (*38–40*). The VECD model is based on the elastic–viscoelastic correspondence principle and Schapery's work potential theory to model the mechanical behavior of asphalt mixtures (*40*). The application of the VECD formulations allow the prediction of N_f values at different temperatures, strain levels, and frequencies, from a limited set of laboratory data. This eliminates the need to run time consuming fatigue tests at multiple temperatures and strain levels.

The number of cycles to failure (N_f) from the 3PBC tests for surface and base mixes of the I-475 project are displayed in Figure 32 for 300 micro strain level). As shown, the fatigue cracking performance of the GGSP mixture is, on average, better than any other mixture tested, including the 5E10 mixture used for the surface layer of the traditional section. The HMAs for base layers, 3E30 and 3E10, exhibited a mixed trend. The 3E30 performed better than 3E10 at 10°C but worse at 20°C. This may be an indication of these two mixtures being equivalent. It is

worth noting that the long-life sections are designed quite thick so that no bottom-up cracking develops throughout its service life. Therefore, even if 3E30 were to be less resistant that 3E10, the cracks would not develop because of the low strain levels at the bottom of the asphalt. On the other hand, top-down cracking is quite possible in thick asphalt pavements. The fact that the GGSP mix performed better in fatigue compared to 5E10 mix is a positive finding and may indicate that the long-life sections will perform better in terms of top-down cracking.

Figure 33 summarizes the results of fatigue tests for US-131 surface and base mixes. Also, in this case, the GGSP with polymer-modified binder is performing better compared to the 5E10 mixture at both 10 and 20°C. It is worth mentioning that the 5E10 mix has been produced with 19%-Tier 2 RAP, which might have played a role in the results obtained. The comparison of the 3E30 vs. 2E10 base mixes indicates that the two mixes have similar performance at 20°C while 2E10 has slightly better performance at 10°C.

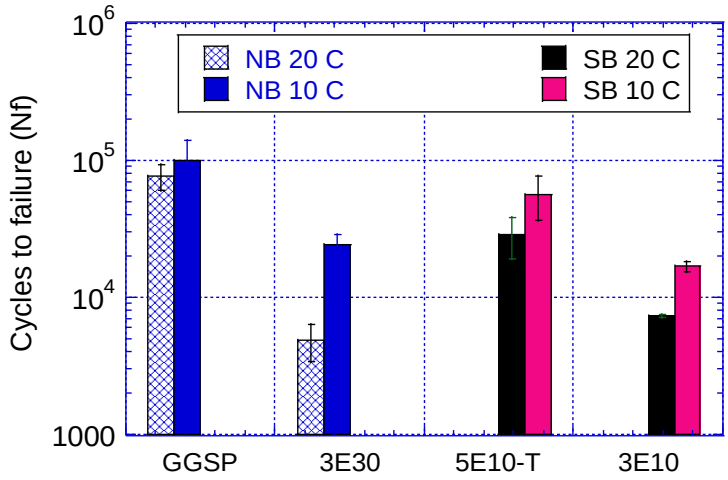

Figure 32 The summary of fatigue testing on surface and base mixtures of I-475 at 300με

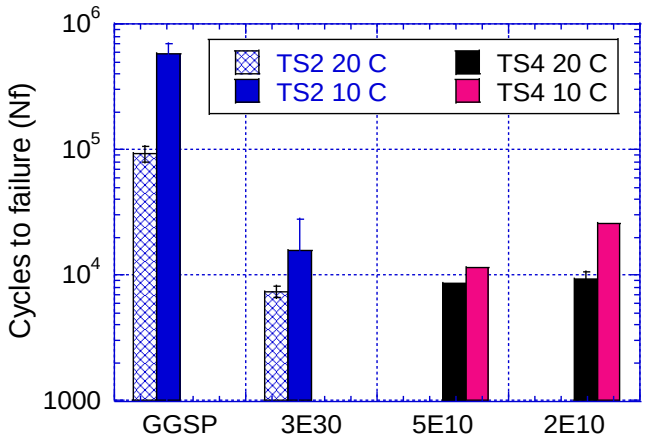

Figure 33 3PBC fatigue testing summary on the surface and base mixtures of US-131 HMA project at 300με

4.2.8 HMA Pavement Core Testing

For each test section of the I-475 project, three cores were provided from the HMA top course, levelling course, and base course. For the long-life test sections separate cores were taken from the 1st lift and 2nd lift of the base course (3E30). Core thicknesses are shown in Table 17 and Table 18 for long-life and standard sections, respectively. As shown, the core thickness variability was about 10% (based on the coefficient of variation - COV) for long-life sections and the average thicknesses were very close to the design thicknesses. Core thickness variability (COV) in standard sections varied from 4.4% to 21.2% and top course was slightly thicker than the design and leveling course was slightly thinner. Overall thickness of the standard sections was slightly lower than the design thickness.

Core air voids of long life and standard sections are shown in Table 19 and Table 20 respectively. As shown, the air voids ranged from 4-5% on average for the long-life sections whereas the air voids for standard sections were slightly above 5% on average. Overall, all these air voids are quite good and shows good compaction characteristics for both standard and long-life sections.

Core thicknesses of US131 project are shown in Table 21 and Table 22 for long-life and standard sections, respectively. Overall, the core thickness variability was low in both sections however, standard section thicknesses were a bit lower than the design thickness. Core air voids of US131 are shown in Table 23 and Table 24. All air voids were about 5-6%, except the GGSP layers where higher air voids were observed (~9% on average).

Table 17 Core thicknesses for I-475 project: Long-life sections

	Thickness (in)													
AC Layer	TS 1-1	TS 1-2	TS 1-3	TS 2-1	TS 2-2	TS 2-3	TS 3-1	TS 3-2	TS 3-3	Avg	COV (%)	Min	Max	Design
GGSP (NB Top)	2.01	2.56	2.20	2.01	1.93	2.05	1.81	2.28	1.77	2.07	11.9%	1.77	2.56	2.00
4E30 (NB Leveling)	2.48	2.40	2.68	2.48	2.60	2.76	1.85	2.68	2.68	2.51	10.9%	1.85	2.76	2.50
3E30 (NB Base, lift 2)	3.58	2.99	3.66	3.15	3.23	2.68	3.07	3.39	3.11	3.21	9.5%	2.68	3.66	3.25
3E30 (NB Base, lift 1)	3.19	3.54	2.48	3.35	2.83	3.46	3.15	3.50	3.23	3.19	10.8%	2.48	3.54	3.25
Total	11.26	11.50	11.02	10.98	10.59	10.94	9.88	11.85	10.79	10.98	5.1%	9.88	11.85	11.00

Table 18 Core thicknesses for I-475 project: Standard sections

	Thickness (in)													
AC Layer	TS 1-1	TS 1-2	TS 1-3	TS 2-1	TS 2-2	TS 2-3	TS 3-1	TS 3-2	TS 3-3	Avg	COV (%)	Min	Max	Design
5E10 (SB Top)	2.0	2.2	2.3	2.1	2.0	2.4	1.7	2.1	2.0	2.08	10.2%	1.65	2.40	1.75
5E10 (SB Leveling)	2.7	2.4	2.7	1.7	1.8	1.9	1.7	1.7	1.9	2.04	21.2%	1.65	2.72	2.50
3E10 (SB Base)	3.7	3.4	3.3	3.6	3.4	3.5	3.2	3.5	3.3	3.44	4.4%	3.19	3.70	3.50
Total	8.35	7.95	8.31	7.32	7.24	7.80	6.50	7.28	7.24	7.55	7.9%	6.50	8.35	7.75

Table 19 Core air voids for I-475 project: Long-life sections

	Core Air Voids (%)												
AC Layer	TS 1-1	TS 1-2	TS 1-3	TS 2-1	TS 2-2	TS 2-3	TS 3-1	TS 3-2	TS 3-3	Avg	COV (%)	Min	Max
GGSP (NB Top)	4.9	4.8	3.3	4.9	5.2	3.1	4.0	3.1	3.5	4.09	20.9%	3.13	5.19
4E30 (NB Leveling)	4.5	4.1	3.7	4.4	5.7	4.6	6.3	4.1	5.1	4.72	17.3%	3.73	6.27
3E30 (NB Base, lift 2)	4.9	5.2	4.9	5.6	5.7	5.3	4.3	4.7	5.5	5.14	9.0%	4.33	5.72
3E30 (NB Base, lift 1)	3.5	4.2	4.4	4.2	5.6	4.7	5.7	4.7	3.8	4.54	16.7%	3.48	5.71

Table 20 Core air voids for I-475 project: Standard sections

	Core Air Voids (%)												
AC Layer	TS 1-1	TS 1-2	TS 1-3	TS 2-1	TS 2-2	TS 2-3	TS 3-1	TS 3-2	TS 3-3	Avg	COV (%)	Min	Max
5E10 (SB Top)	7.0	5.0	5.7	4.7	4.9	5.6	5.5	5.2	4.0	5.28	15.6%	3.97	6.96
5E10 (SB Leveling)	6.1	4.0	5.2	5.1	4.8	4.6	5.1	4.7	4.5	4.89	12.2%	3.97	6.12
3E10 (SB Base)	6.8	6.7	5.3	5.3	5.4	5.7	4.4	3.3	5.1	5.35	20.1%	3.30	6.80

Table 21 Core thicknesses for US-131 project: Long-life sections

	Thickness (in)													
AC Layer	TS 1-1	TS 1-2	TS 1-3	TS 2-1	TS 2-2	TS 2-3	TS 3-1	TS 3-2	TS 3-3	Avg	COV (%)	Min	Max	Design
5-Top	1.50	1.63	1.63	1.63	1.63	1.63	1.50	1.38	1.50	1.56	5.9%	1.38	1.63	1.50
4-Leveling	2.38	2.38	2.38	2.75	3.00	3.00	1.75	2.13	2.50	2.47	16.3%	1.75	3.00	2.50
3-Base	3.25	3.75	4.00	3.63	4.38	4.38	3.75	3.75	3.00	3.77	12.2%	3.00	4.38	3.63
3-Base	3.88	3.00	2.75	3.13	3.25	3.38	3.00	3.00	4.38	3.31	15.5%	2.75	4.38	3.63
Total	11.01	10.76	10.76	11.14	12.26	12.39	10.00	10.26	11.38	11.11	7.3%	10.00	12.39	11.25

Table 22 Core thicknesses for US-131 project: Standard sections

	Thickness (in)							
AC Layer	TS 4-1	TS 4-2	TS 4-3	Avg	COV (%)	Min	Max	Design
5-Top	1.88	2.00	2.00	1.96	3.5%	1.88	2.00	1.75
3-Leveling	2.75	2.75	2.25	2.58	11.2%	2.25	2.75	3.00
2-Base	4.25	3.88	3.63	3.92	8.0%	3.63	4.25	4.50
Total	8.88	8.63	7.88	8.46	6.1%	7.88	8.88	9.25

Table 23 Core air voids for US-131 project: Long-life sections

	Core Air Voids (%)												
AC Layer	TS 1-1	TS 1-2	TS 1-3	TS 2-1	TS 2-2	TS 2-3	TS 3-1	TS 3-2	TS 3-3	Avg	COV (%)	Min	Max
5-Top	8.70	8.70	8.60	9.20	9.20	7.30	9.60	9.30	10.00	8.96	9%	7.30	10.00
4-Leveling	5.60	6.80	5.30	4.80	5.30	3.90	5.90	6.60	4.30	5.39	18%	3.90	6.80
3-Base	5.90	5.10	6.40	5.90	5.80	5.70	4.50	6.20	5.00	5.61	11%	4.50	6.40
3-Base	5.20	5.40	4.30	5.50	6.80	6.50	3.80	5.30	5.90	5.41	18%	3.80	6.80

Table 24 Core air voids for US-131 project: Standard sections

	Core Air Voids (%)						
AC Layer	TS 4-1	TS 4-2	TS 4-3	Avg	COV (%)	Min	Max
5-Top	4.80	6.30	4.80	5.30	16%	4.80	6.30
3-Leveling	4.10	6.70	8.20	6.33	33%	4.10	8.20
2-Base	5.20	5.10	5.60	5.30	5%	5.10	5.60

4.2.9 Unbound Material Testing

Unbound material testing included thirty (30) samples that were collected from I-475, and US 131 projects. A summary of the material information is provided in Table 25.

Table 25 Unbound material samples information

Location	Pavement Type	TS	Direction	Start Location	End Location	Type of Layer Tested
I-475	HMA	1	NB	0650+00	0660+00	Base, Subbase, Subgrade
		2	NB	0745+00	0755+00	Base, Subbase, Subgrade
		3	NB	0770+00	0780+00	Base, Subbase, Subgrade
		1	SB	0650+00	0660+00	Base, Subbase, Subgrade
		2	SB	0745+00	0755+00	Base, Subbase, Subgrade
		3	SB	0770+00	0780+00	Base, Subbase, Subgrade
US 131	HMA	1	NB	1090+00	1100+00	Base, Subbase, Subgrade
		2	NB	1127+52	1137+81	Base, Subbase, Subgrade
		3	NB	1170+00	1180+00	Base, Subbase, Subgrade
		4	SB	1210+10	1220+00	Base, Subbase, Subgrade

4.2.9.1 Index Properties and Compaction Characteristics

This section presents the index properties of all unbound materials including gradation, soil classification, Atterberg limits and compaction characteristics of the pavement foundation materials.

The particle size distribution of the granular materials was determined in accordance with ASTM C136, D6913, and D7928 and the Atterberg limits were determined in accordance with ASTM D4318. The material classification was performed according to the Unified Soil Classification System (USCS) (ASTM D2487) and the American Association of State Highway and Transportation Officials (AASHTO) soil classification system (AASHTO M 145).Table 26, Table 27, and Table 28 summarize the index properties of the base, subbase, and subgrade materials, respectively. For some of the test sections, due to the similarity of the material, the materials were combined across the test sections.

Table 26 Index properties of base materials

Base Material	Gravel (%)	Sand (%)	Fines (%)	C_u	C_c	LL	PI	AASHTO	USCS
I-475(HMA)_TS1(SB)_Base	51.3	40.0	8.7	80.0	0.6	NA	NP	A-1-a	GP-GM
I-475(HMA)_TS2(NB)_Base	59.6	36.2	4.2	47.8	1.5	NA	NP	A-1-a	GW
US 131(HMA)_TS1(NB) &TS2(NB)&TS3(NB) &TS4(SB)_Base	66.1	30.7	3.2	29.2	2.4	NA	NP	A-1-a	GW

Fines = silt and clay; C_u = uniformity coefficient; C_c = coefficient of curvature; LL = liquid limit; PI = plasticity index; AASHTO = American Association of State Highway and Transportation Officials; USCS = Unified Soil Classification System; NP = non-plastic; NA = not available.

Table 27 Index properties of subbase materials

Subbase Material	Gravel (%)	Sand (%)	Fines (%)	C_u	C_c	LL	PI	AASHTO	USCS
I-475(HMA)_TS1(SB)_Subbase	1.5	93.2	5.3	2.5	1.3	NA	NP	A-3	SP-SM
I-475(HMA)_TS2(NB)_Subbase	5.1	90.3	4.6	2.9	1.0	NA	NP	A-3	SP
US 131(HMA)_TS2(NB) &TS3(NB)_Subbase	11.9	83.7	4.4	2.9	1.0	NA	NP	A-1-b	SP
US 131(HMA)_TS4(SB)_Subbase	29.6	65.4	5.0	6.5	0.6	NA	NP	A-1-b	SP

Fines = silt and clay; C_u = uniformity coefficient; C_c = coefficient of curvature; LL = liquid limit; PI = plasticity index; AASHTO = American Association of State Highway and Transportation Officials; USCS = Unified Soil Classification System; NP = non-plastic; NA = not available.

Table 28 Index properties of subgrade materials

Subgrade Material	Gravel (%)	Sand (%)	Fines (%)	C_u	C_c	LL	PI	AASHTO	USCS
I-475(HMA)_TS1(SB)_Subgrade	2.9	41.3	55.8	NA	NA	21.4	10.1	A-4	CL
I-475(HMA)_TS1(NB)_Subgrade	6.6	26.5	66.9	NA	NA	24.7	12	A-6	CL
I-475(HMA)_TS2(NB)_Subgrade	2.7	31.3	66.0	NA	NA	24.7	11.6	A-6	CL
I-475(HMA)_TS3(SB)_Subgrade	3.3	28.2	68.5	NA	NA	22.9	10.1	A-4	CL
US 131(HMA)_TS1(NB) &TS2(NB)_Subgrade	2.2	94.8	3.0	2.6	1.1	NA	NP	A-1-b	SP
US 131(HMA)_TS3(NB)_Subgrade	23.9	72.5	3.6	3.8	1.0	NA	NP	A-1-b	SP
US 131(HMA)_TS4(SB)_Subgrade	3.5	43.3	53.2	NA	NA	22.0	6.6	A-4	CL-ML

Fines = silt and clay; C_u = uniformity coefficient; C_c = coefficient of curvature; LL = liquid limit; PI = plasticity index; AASHTO = American Association of State Highway and Transportation Officials; USCS = Unified Soil Classification System; NP = non-plastic; NA = not available.
[a]There are unstabilized and cement-stabilized (with 5% cement) subgrade materials. However, for the determination of the index properties, only the unstabilized subgrade materials were used.

The maximum dry unit weight (MDU) and optimum moisture content (OMC) values of the materials are reported in Table 29, Table 30 and Table 31 for base, subbase, and subgrade, respectively. The MDU values of the unbound base materials ranged from 133.9 pcf to 136.6 pcf. For the same materials, the OMCs were between 8.3% and 9.5%. For subbase samples, the

MDU values varied between 117.1 pcf and 122.8 pcf, while the OMCs were between 9.5% to 12.1%. In both cases, the range of variation of the subbase properties were higher than that of the base materials. Finally, for the subgrade materials, the MDU values ranged between 115.7 pcf and 132.6 pcf, and the OMCs were between 6.9% and 13.0%.

Table 29 Compaction test results for base materials

Base Material	MDU (pcf)	OMC (%)
I-475(HMA)_TS1(SB)_Base	135.3	9.5
I-475(HMA)_TS2(NB)_Base	133.9	8.3
US 131(HMA)_TS1(NB)&TS2(NB)&TS3(NB)&TS4(SB)_Base	136.6	8.7

MDU = maximum dry unit weight; OMC = optimum moisture content; NA = not available.

Table 30 Compaction test results for subbase materials

Subbase Material	MDU (pcf)	OMC (%)
I-475(HMA)_TS1(SB)_Subbase	117.1	12.1
I-475(HMA)_TS2(NB)_Subbase	122.8	9.8
US 131(HMA)_TS2(NB)&TS3(NB)_Subbase	120.4	9.5
US 131(HMA)_TS4(SB)_Subbase	129.8	8.3

MDU = maximum dry unit weight; OMC = optimum moisture content.

Table 31 Compaction test results for subgrade materials

Subgrade Material	MDU (pcf)	OMC (%)
I-475(HMA)_TS1(SB)_Subgrade	130.1	9.8
I-475(HMA)_TS1(NB)_Subgrade	132.6	11.2
I-475(HMA)_TS2(NB)_Subgrade	131.7	11.6
I-475(HMA)_TS3(SB)_Subgrade	130.2	13.0
US 131(HMA)_TS1(NB)&TS2(NB)_Subgrade	115.7	6.9
US 131(HMA)_TS3(NB)_Subgrade	119.8	9.0
US 131(HMA)_TS4(SB)_Subgrade	127.1	9.8

MDU = maximum dry unit weight; OMC = optimum moisture content.

4.2.9.2 Resilient Modulus Testing

Resilient modulus (M_R) tests were performed on all samples at room temperature following the methodology described in the AASHTO T 307 to measure the stiffness of the materials. The conventional Mechanistic-Empirical Pavement Design Guide (MEPDG) model shown in Equation 9 was used to determine the M_R characteristics of the materials using the elastic deformations recorded during the last five cycles of each testing sequence (*41*).

$$M_R = k_1 P_a \left(\frac{\theta}{P_a}\right)^{k_2} \left(\frac{\tau_{oct}}{P_a} + 1\right)^{k_3} \quad \text{Equation 9}$$

where k_1, k_2, and k_3 are the fitting parameters, P_a is the atmospheric pressure (ksi), θ is the bulk stress ($\theta = \sigma_1 + \sigma_2 + \sigma_3 = \sigma_1 + 2\sigma_3$) (ksi), σ_1, σ_2, and σ_3 are the principal stresses (ksi), and τ_{oct} is the octahedral shear stress [$\tau_{oct} = 1/3\sqrt{(\sigma_1 - \sigma_2)^2 + (\sigma_1 - \sigma_3)^2 + (\sigma_2 - \sigma_3)^2}$] (ksi).

Summaries of the M_R test results of the base, subbase, and subgrade materials are provided in Table 32, Table 33, and Table 34, respectively. Overall, the base materials showed an average SM_R value of 34.66 ksi, about two and three times higher than those observed for subbase and unstabilized subgrade samples which have average values of 17.83 ksi and 11.78 ksi, respectively. For the base materials, the highest SM_R value was observed on the US 131 project. Among the subbase samples, I-475_TS2(NB)_Subbase showed the highest SM_R value (30.06 ksi) while I-475_TS1(NB)_Subbase yielded the lowest SM_R value (12.38 ksi). Finally, within the subgrade materials, the highest SM_R values were observed in I-475_TS2 and US 131(HMA)_TS1 & TS2 (NB) the lowest was observed in US 131(HMA)_TS4 (NB).

Table 32 Resilient modulus (MR) test results for base materials

Base Material	Fitting Parameters			R^2	SM_R (ksi)	SD (ksi)
	k_1	k_2	k_3			
I-475(HMA)_TS1(SB)_Base	1422.31	0.93	-0.78	0.95	30.07	0.51
I-475(HMA)_TS2(NB)_Base	1326.10	0.76	-0.11	0.91	32.21	0.62
US 131(HMA)_TS1(NB) &TS2(NB)&TS3(NB)&TS4(SB)_Base	1900.74	0.63	-0.13	0.93	41.70	2.38

k_1, k_2, and k_3 = fitting parameters in Equation (9); SM_R = summary M_R; SD = standard deviation.
Note: SM_R values were determined at the bulk stress (θ) and the octahedral shear stress (τ_{oct}) corresponding to the 6th sequence of the base/subbase testing sequences (AASHTO T 307) (θ = 30 psi and τ_{oct} = 7 psi).

Table 33 Resilient modulus (MR) test results for subbase materials

Subbase Material	Fitting Parameters			R^2	SM_R (ksi)	SD (ksi)
	k_1	k_2	k_3			
I-475(HMA)_TS1(SB)_Subbase	1152.86	0.51	-1.2	0.86	12.38[a]	2.94
I-475(HMA)_TS2(NB)_Subbase	1376.23	0.62	-0.12	0.88	30.06[b]	0.84
US 131(HMA)_TS2(NB)&TS3(NB)_Subbase	1556.20	0.80	-1.10	0.96	16.07[a]	0.55
US 131(HMA)_TS4(SB)_Subbase	1480.30	0.90	-2.00	0.91	12.80[a]	0.53

k_1, k_2, and k_3 = fitting parameters in Equation (9); SM_R = summary M_R; SD = standard deviation.
[a]SM_R values were determined at the bulk stress (θ) and the octahedral shear stress (τ_{oct}) corresponding to the 13th sequence of the subgrade testing sequences (AASHTO T 307) (θ = 12 psi and τ_{oct} = 3 psi).
[b]SM_R values were determined at θ and τ_{oct} corresponding to the 6th sequence of the base/subbase testing sequences (AASHTO T 307) (θ = 30 psi and τ_{oct} = 7 psi).

Table 34 Resilient modulus (MR) test results for subgrade materials

Subgrade Material	Fitting Parameters			R^2	SM_R (ksi)	SD (ksi)
	k_1	k_2	k_3			
I-475(HMA)_TS1(SB)_Subgrade	1480.30	0.49	-4.00	0.93	9.77	0.30
I-475(HMA)_TS1(NB)_Subgrade	2115.57	0.35	-3.83	0.94	14.78	2.04
I-475(HMA)_TS2(NB)_Subgrade	2540.64	0.41	-4.11	0.94	16.71	4.74
I-475(HMA)_TS3(SB)_Subgrade	1276.40	0.44	-3.86	0.92	8.73	2.34
US 131(HMA)_TS1(NB)&TS2(NB)_Subgrade	1512.23	0.69	-1.17	0.81	15.78	2.92
US 131(HMA)_TS3(NB)_Subgrade	1719.86	1.00	-3.30	0.89	11.61	0.16
US 131(HMA)_TS4(NB)_Subgrade	549.40	0.34	-2.23	0.87	5.09	0.00

k_1, k_2, and k_3 = fitting parameters in Equation (9); SM_R = summary M_R; SD = standard deviation.
Note: SM_R values were determined at the bulk stress (θ) and the octahedral shear stress (τ_{oct}) corresponding to the 13th sequence of the subgrade testing sequences (AASHTO T 307) (θ = 12 psi and τ_{oct} = 3 psi).

Table 35 and Figure 34 report the SM_R values for the pavement foundation layers for the two projects. Tests performed on the base layer of the US 131 resulted in the highest average SM_R value (41.70 ksi). Within the samples collected from the subbase layers, the ones from the I-475 project provided the highest M_R values. The subgrade values for the US-131 and I-475 projects are comparable.

Table 35 Summary resilient modulus (SM_R) values for pavement foundation layers

Foundation Layer	I-475 (HMA)		US 131 (HMA)	
	SM_R (ksi)	SD (ksi)	SM_R (ksi)	SD (ksi)
Base	31.14	1.51	41.70	NA
Subbase	21.22	12.50	14.43	2.31
Subgrade	12.50	3.85	10.83	5.39

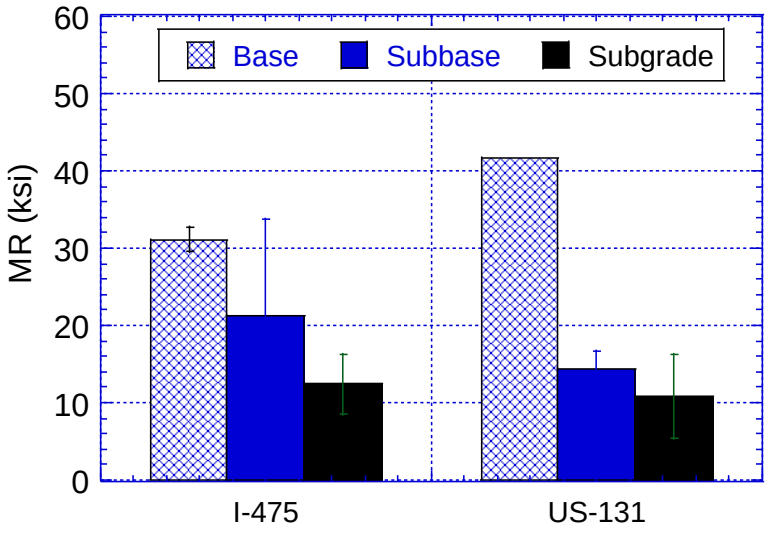

Figure 34 Summary resilient modulus (SM_R) values for pavement foundation layers

4.2.9.3 Discussion on Various Modulus Values Obtained from Different Tests

As part of this project, several methods (laboratory, FWD, LWD and DCP) were used to estimate the modulus of sublayers of standard and long-life pavement sections. This section includes a brief discussion on comparisons of moduli obtained from different methods and the values selected for mechanistic-empirical (ME) analysis.

A comparison of unbound layer moduli for I-475 project is shown in Figure 35. The following observations can be made from these figures:

- Subgrade moduli obtained from lab M_r tests and DCP tests were relatively close to each other, except the standard section. On the other hand, the LWD tests revealed unreasonably low moduli values for typical subgrade soils. FWD backcalculated moduli for both standard and long-life sections were higher than laboratory measurements, which is consistent with the literature. It is typical for lab M_r results to be 2-5 times lower than the FWD results, and it is a common practice to reduce FWD backcalculated values by a factor and use them in design and analysis. Therefore, it was decided to use the lab M_r tests results for subgrade in ME analyses.

- Subbase moduli obtained from DCP and LWD tests were simply too low, and they did not make sense. FWD backcalculation could only provide an 'average' base/subbase modulus, but they were not too far from the lab M_r values. Therefore, lab M_r was thought to be the most representative subbase moduli to be used in ME analysis.
- Base moduli from lab and FWD were very close, which makes sense because although FWD-based modulus is for base/subbase combination, it is affected more by the base modulus because it is closer to the surface load. LWD data was too low and did not make sense. Therefore, lab M_r was used in the ME analyses.

Figure 36 shows a comparison of unbound layer moduli for the US-131 project. The following observations can be made from these figures:

- Again, the LWD tests revealed unreasonably low moduli, and DCP results for long life sections resulted in unreasonably high moduli for subgrade soils. Lab Mr results were lower than FWD backcalculated values (as expected). It was decided to use the lab M_r tests results for subgrade in ME analyses.
- Subbase moduli obtained from lab and DCP tests agreed reasonably well for the standard section. However, the DCP modulus from long life section was unreasonably high for a subbase. Therefore, lab Mr of subbase was used in ME analyses.

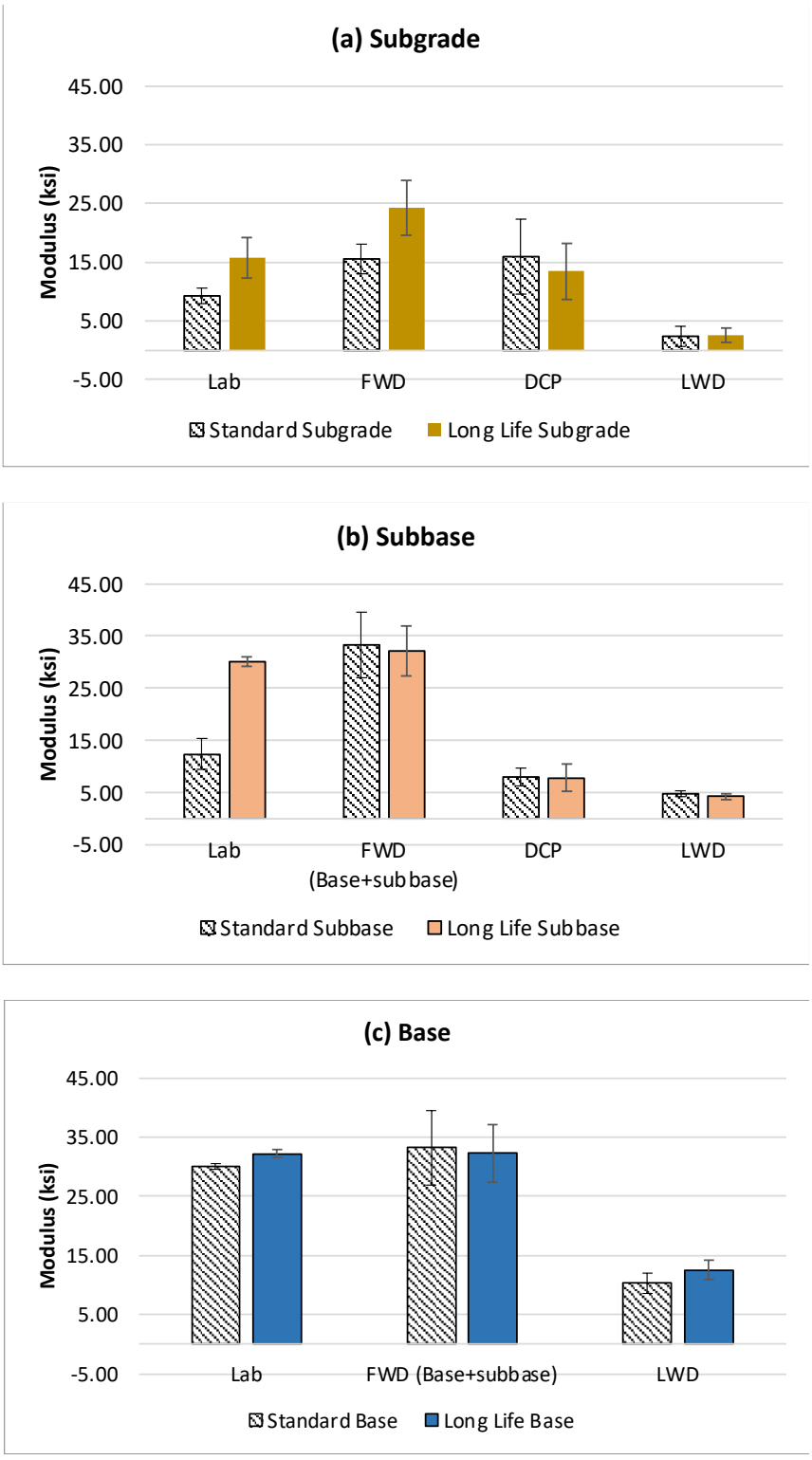

Figure 35 Comparison of unbound layer moduli for I-475 project. Note: DCP data was not available for the base layer

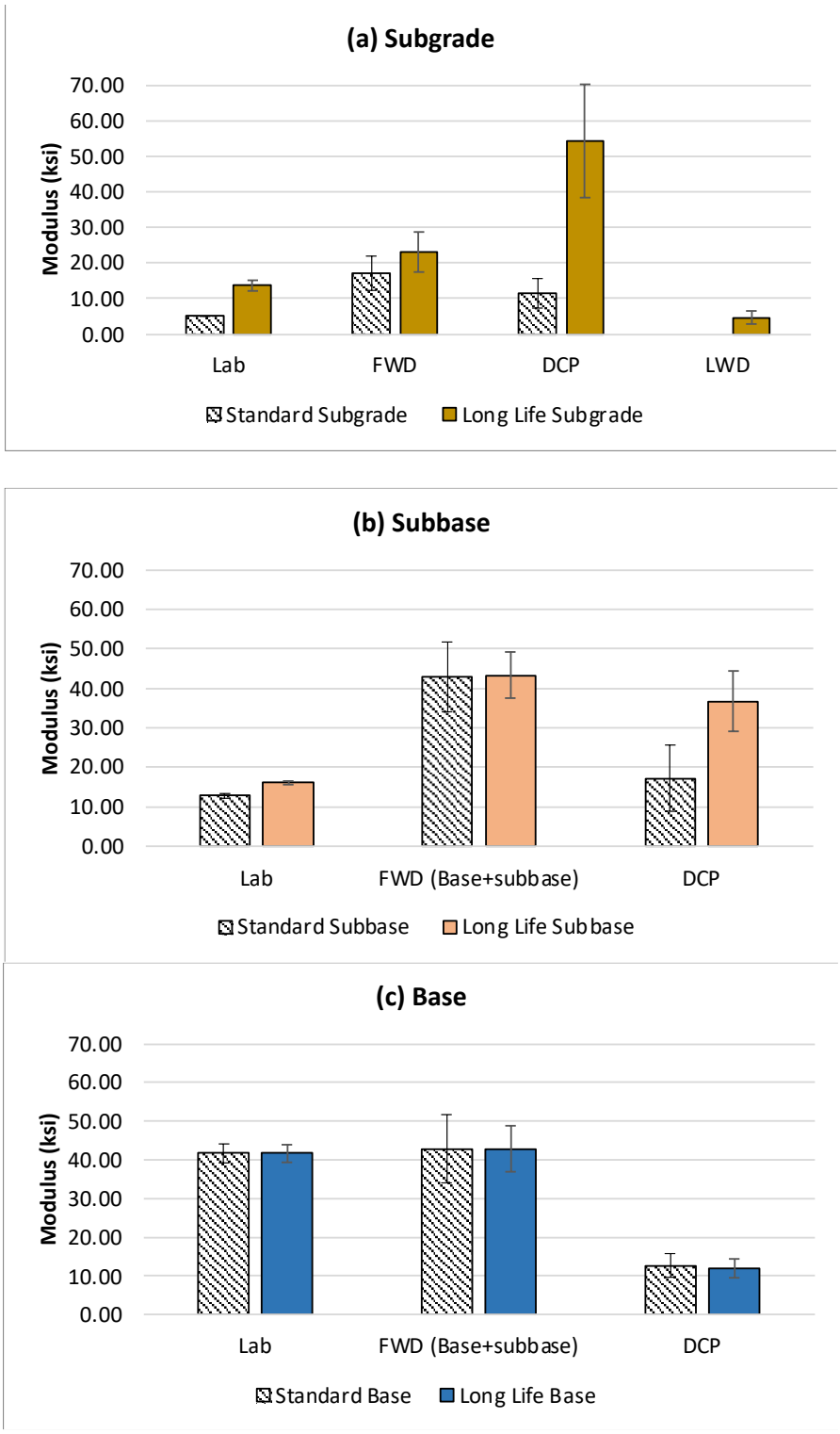

Figure 36 Comparison of unbound layer moduli for US-131 project. Note: There was no LWD data available for subgrade of standard section, subbase and base of both sections

- Base moduli from lab and FWD were very close, and DCP data was too low and did not make sense. Therefore, lab Mr was used in the ME analysis.

4.3 CHAPTER 3: PAVEMENT PERFORMANCE PREDICTIONS AND ANALYSIS

Since as-built material properties and their variability during construction and other structural design elements have significant impacts on achieving the long-life purpose of the four pilot projects, it is essential to evaluate the long-term performance of the pavement structures using tools like the AASHTOWare Pavement ME using the as-built input data collected throughout the project. Therefore, for evaluation of the two flexible pavement pilot projects, I-475 and US-131, the AASHTOWare Pavement ME V.2.3 and V.2.6, MEAPA and PerRoad were used for performance prediction. Pavement ME V.2.3 is currently adopted by MDOT and Michigan calibration coefficients are available for this version. Pavement ME V.2.6 is the latest version of the software, which mainly differ from the previous one for the new top-down cracking mode. PerRoad is a flexible perpetual pavement design software that has been developed at Auburn University in collaboration with the Asphalt Pavement Alliance (APA), the National Asphalt Pavement Association (NAPA), and the State Asphalt Pavement Associations (SAPA). The software is based on layered elastic analysis and a statistical analysis procedure (Monte Carlo simulation) to predict the responses within the pavement structure. Pass/fail criteria can be selected based on the pavement response or using transfer functions to convert the responses to different distresses within the pavement. The main advantage of this software is that it can compare the distribution of the tensile strain at the bottom of the HMA layers resulting from different load, climatic condition, and material stiffnesses with a predefined criterion for this distribution. The default values for the strain distribution criteria were developed based on the NCAT (National Center for Asphalt Technology) test track experiment results.

Table 36 and Table 37 show the inputs used in AASHTOWare Pavement ME simulations for I-475 and US-131, respectively. Pavement structures were evaluated in AASHTOWare Pavement ME for a service life of 50 and 30 years for the I-475 and US-131, respectively. A new flexible pavement project type with an initial International Roughness Index (IRI) of 67 in/mi and 95% reliability level were used for the analysis. Average annual daily truck traffic (AADTT), vehicle class distribution, growth factors, monthly adjustment factors were provided by MDOT.

Table 36 Pavement ME inputs for I-475 project

Section	ID	PG	Layer	|E*|	|G*|	IDT strength	Air voids (%)	Layer thickness (in)	Creep compliance	Unbound layers properties
Long-life sections	GGSP	70-28P	Top	LM	LM	LM	LM	LM	Calculated from |E*|	LM
	4E30	70-28P	Lev	LM	LM	LM	LM	LM	Calculated from |E*|	LM
	3E30	58-34	Base	LM	LM	LM	LM	LM	Calculated from |E*|	LM
Standard sections	5E10-top	58-34	Top	LM	LM	LM	LM	LM	Calculated from |E*|	LM
	5E10-leveling	58-34	Lev	LM	LM	LM	LM	LM	Calculated from |E*|	LM
	3E10	52-34	Base	LM	LM	LM	LM	LM	Calculated from |E*|	LM

Notes: GGSP = Gap Graded Superpave, LM= Lab measured, DV=Design values, Lv3= Level 3

Table 37 Pavement ME inputs for US131 project

	ID	PG	Layer	|E*|	|G*|	IDT strength	Air voids (%)	Layer thickness (in)	Creep compliance	Unbound layers properties
Long-life sections	GGSP	70-28P	Top	LM	LM	LM	LM	LM	Calculated from |E*|	LM
	4E30	70-28P	Lev	LM	LM	LM	LM	LM	Calculated from |E*|	LM
	3E30	64-28	Base	LM	LM	LM	LM	LM	Calculated from |E*|	LM
Standard section	5E10	64-28	Top	LM	LM	LM	LM	LM	Calculated from |E*|	LM
	3E10	64-28	Lev	LM	LM	LM	LM	LM	Calculated from |E*|	LM
	2E10	58-28	Base	LM	LM	LM	LM	LM	Calculated from |E*|	LM

Notes: GGSP = Gap Graded Superpave, LM= Lab measured, DV=Design values, Lv3= Level 3

The results of the simulations using the AASHTOWare Pavement ME 2.6 are shown in Figure 37 and Figure 38, and observations can be summarized as follows:

- The predicted bottom-up cracking for both projects is minimal, as observed in Figure 37 and Figure 38. Although the predicted top-down cracking of the long-life sections starts earlier than standard sections, the final distress magnitude for all sections of both the I-475 and US-131 is below the pass-fail threshold at the end of 50 years.
- Two of the I-475 long-life sections and all the US-131 test sections fail for thermal cracking.
- The rutting performance of all the test sections is acceptable, with the long-life sections slightly outperforming the standard sections.
- Regarding IRI, all of the test sections of I-475 and US-131 fail relatively early in the design life. This might be partially due to the early thermal and top-down cracking developed. It also may be because of the significant vertical shift due to the 95% reliability calculations. Initial IRI values at 95% reliability are close to 100 in/mile, which

is quite high. The team do not think Pavement ME's vertical shift is reasonable for these pavements. Therefore, failure of these pavements due to roughness is not probable.

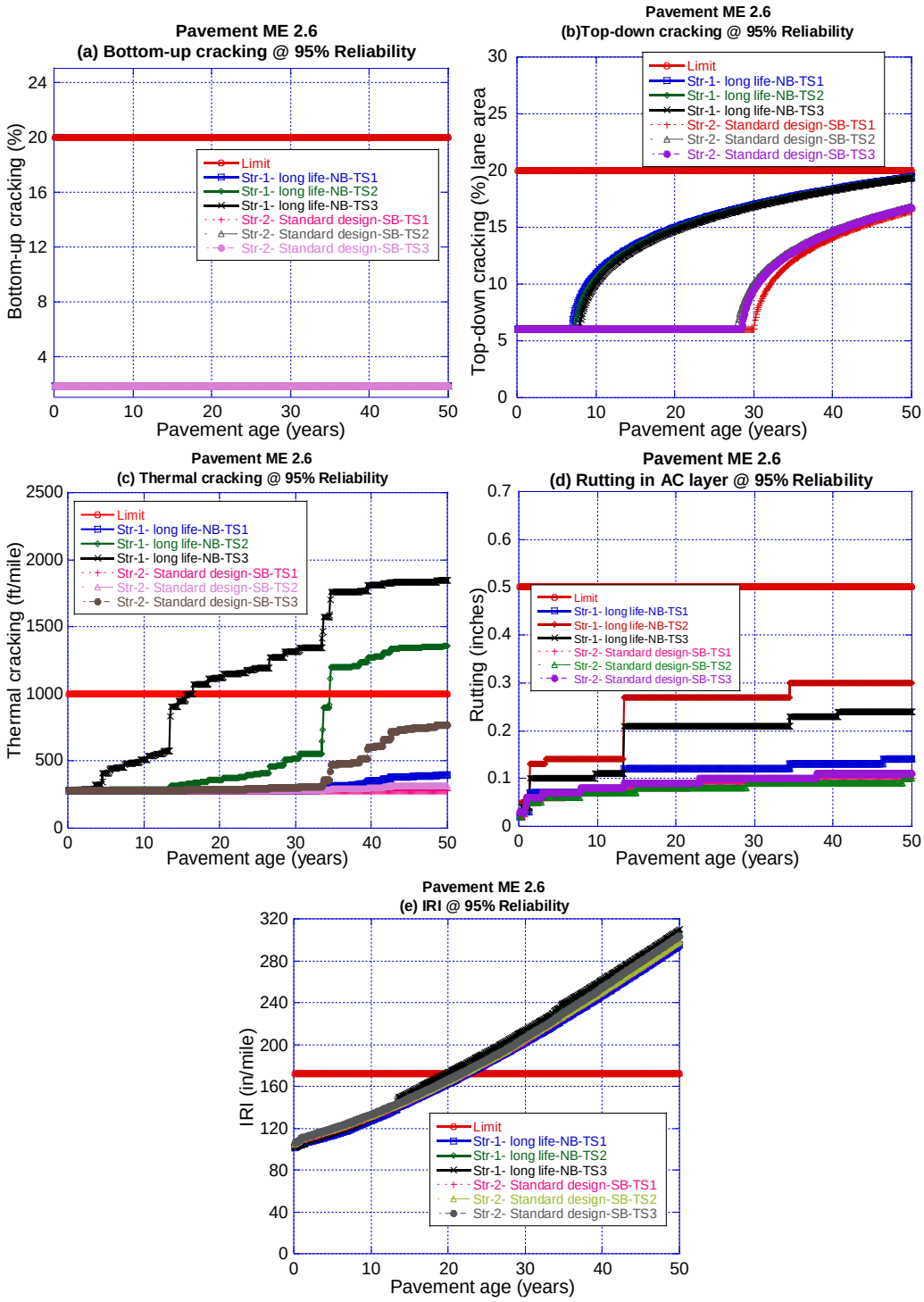

Figure 37 I-475 Pavement ME 2.6 predicted distresses (a)bottom-up cracking, (b) top-down cracking, (c)thermal cracking, (d) rutting in AC, (E) IRI

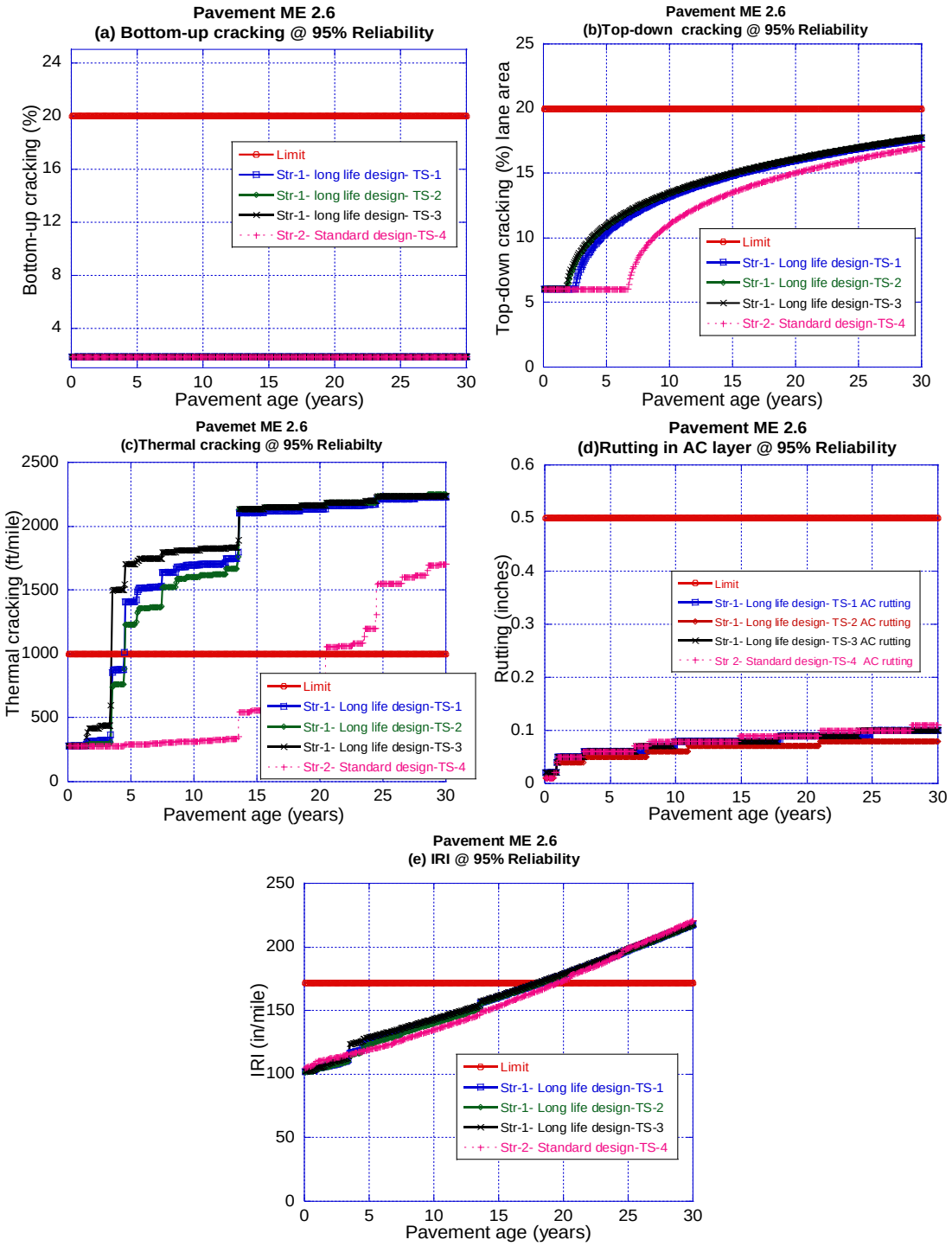

Figure 38 US-131 Pavement ME 2.6 predicted distresses (a) bottom-up cracking, (b) top-down cracking, (c)thermal cracking, (d) rutting in AC, (e) IRI

The results of the simulations using the AASHTOWare Pavement ME 2.3 are shown in Figure 39 and Figure 40, and observations can be summarized as follows:

- The predicted bottom-up cracking for both projects is acceptable with the long-life sections outperforming the standard sections. The standard sections of the I-475 project fail for top-down cracking, while no failure was predicted for the long-life pavement structures.
- The predicted thermal cracking is negligible regardless of the project and sections analyzed.
- The standard sections of the I-475 project fail for HMA rutting, while all other pavement sections analyzed do not.
- The predicted IRI of all I-475 section exceed the pass-fail threshold between 30-40 years of service life. On the contrary, all the US-131 test sections are below the limits until end of the design life.

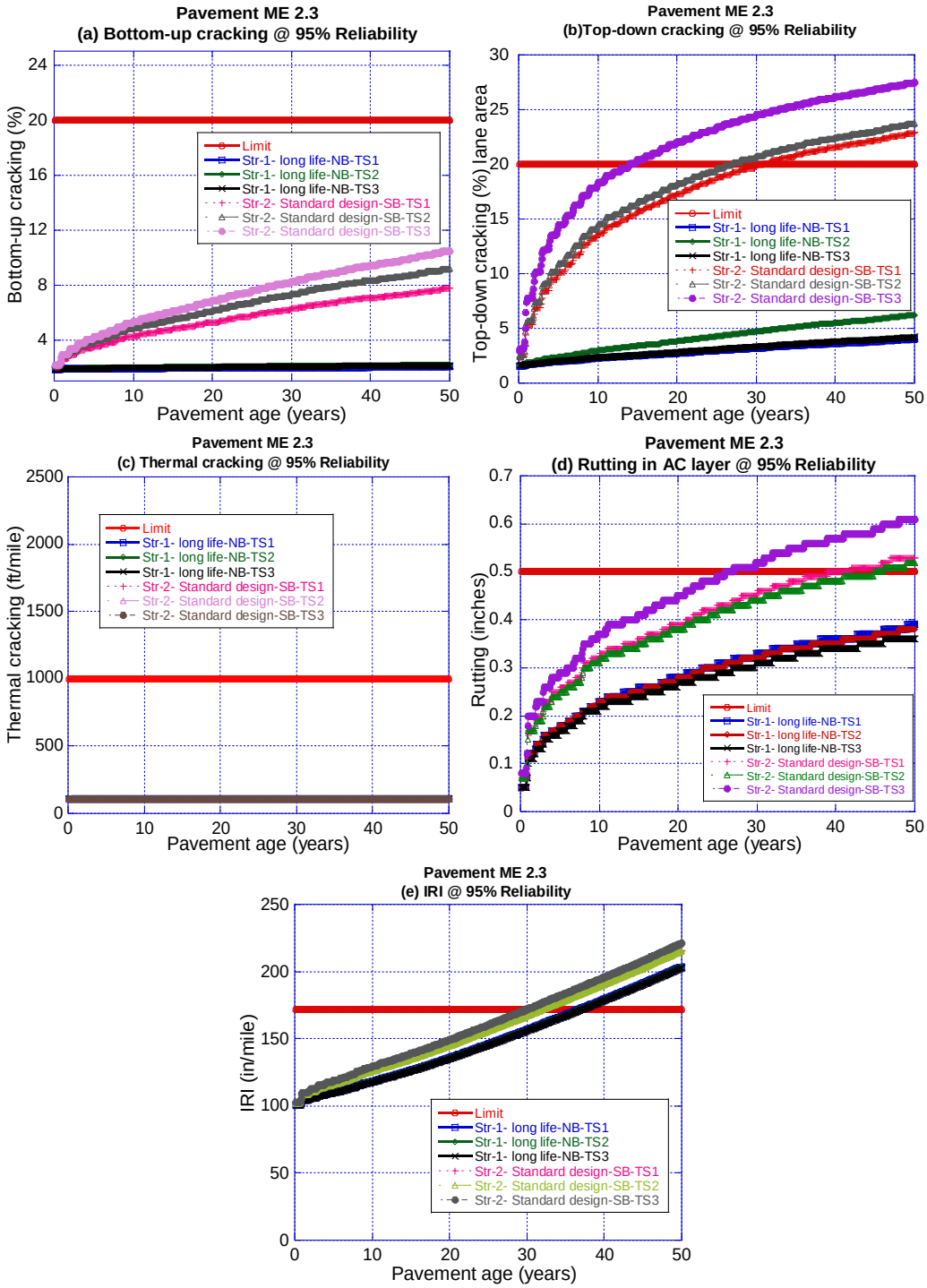

Figure 39 I-475 Pavement ME 2.3 predicted distresses (a)bottom-up cracking, (b) top-down cracking, (c)thermal cracking, (d) rutting in AC, (e) IRI

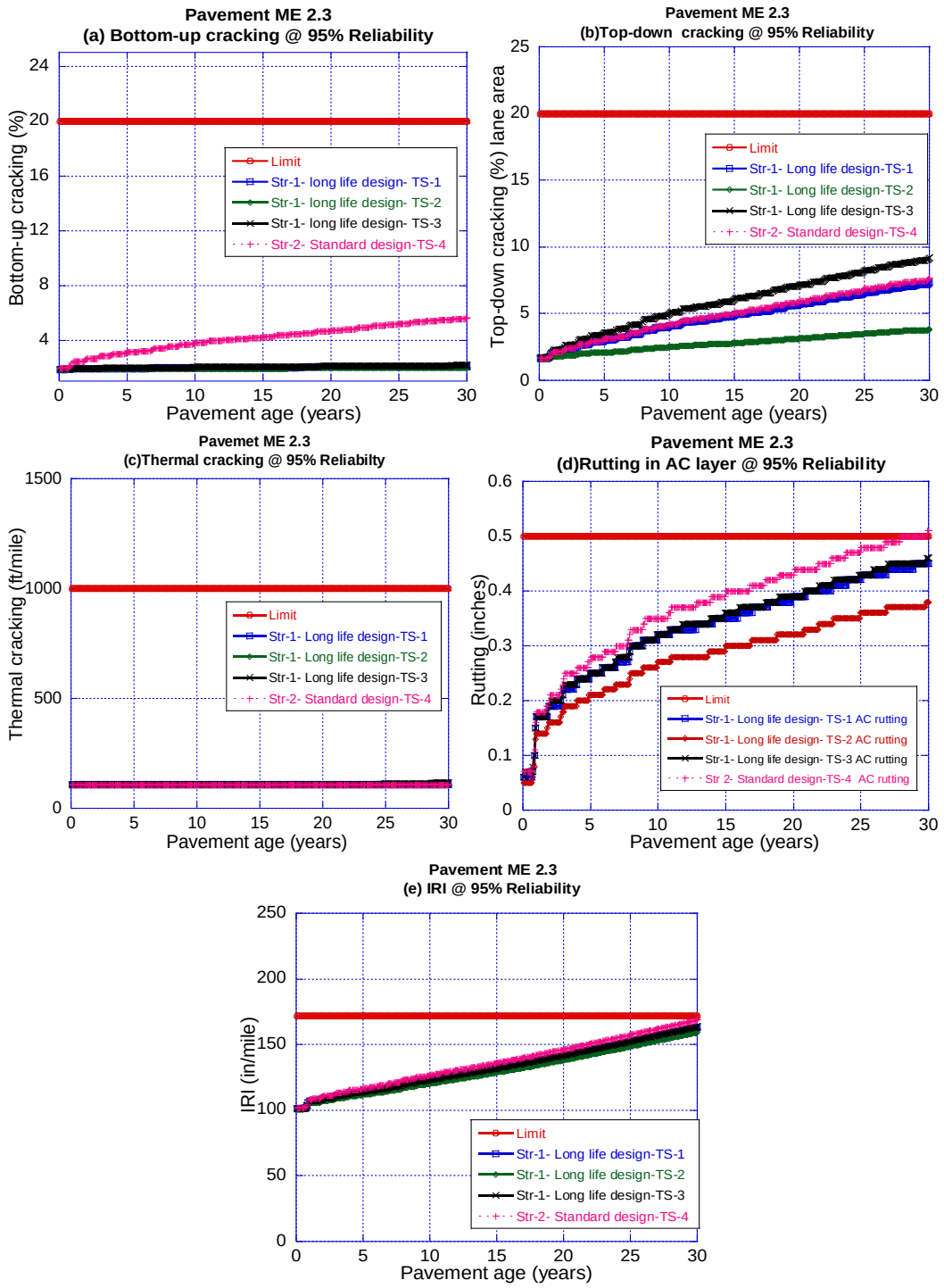

Figure 40 US-131 Pavement ME 2.3 predicted distresses (a)bottom-up cracking, (b) top-down cracking, (c)thermal cracking, (d) rutting in AC, (e) IRI

The results of the simulations using the MEAPA are shown in Figure 41 and Figure 42, and observations can be summarized as follows:

- As it can be seen in Figure 41 and Figure 42, the predicted bottom-up cracking for the standard sections for both projects is higher than the limit. The long-life sections have an acceptable performance in bottom-up cracking. The standard sections of the I-475 and three test sections of US-131 fail in top-down cracking.
- The predicted thermal cracking using MEAPA 2.0 for both projects is minimal.
- The standard sections of the I-475 project fail in rutting. Test sections 3 and 4 (one long-life and one standard test section) for the US-131 project fail in rutting at the end of the design life.
- Regarding IRI, the performance of US-131 test sections are acceptable but the I-475 test sections fail in this distress.

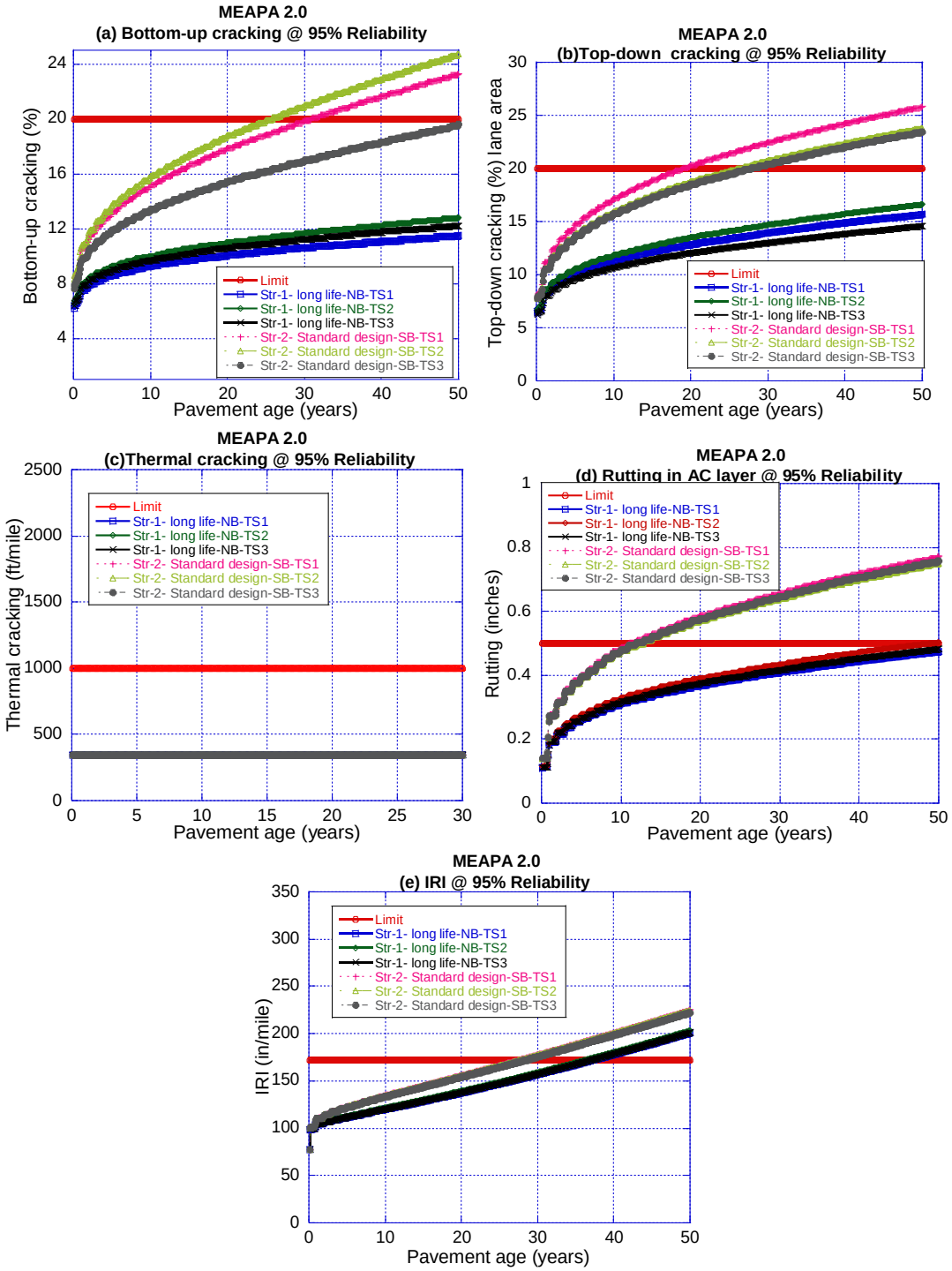

Figure 41 I-475 MEAPA 2.0 predicted distresses (a)bottom-up cracking, (b) top-down cracking, (c)thermal cracking, (d) rutting in AC, (E) IRI

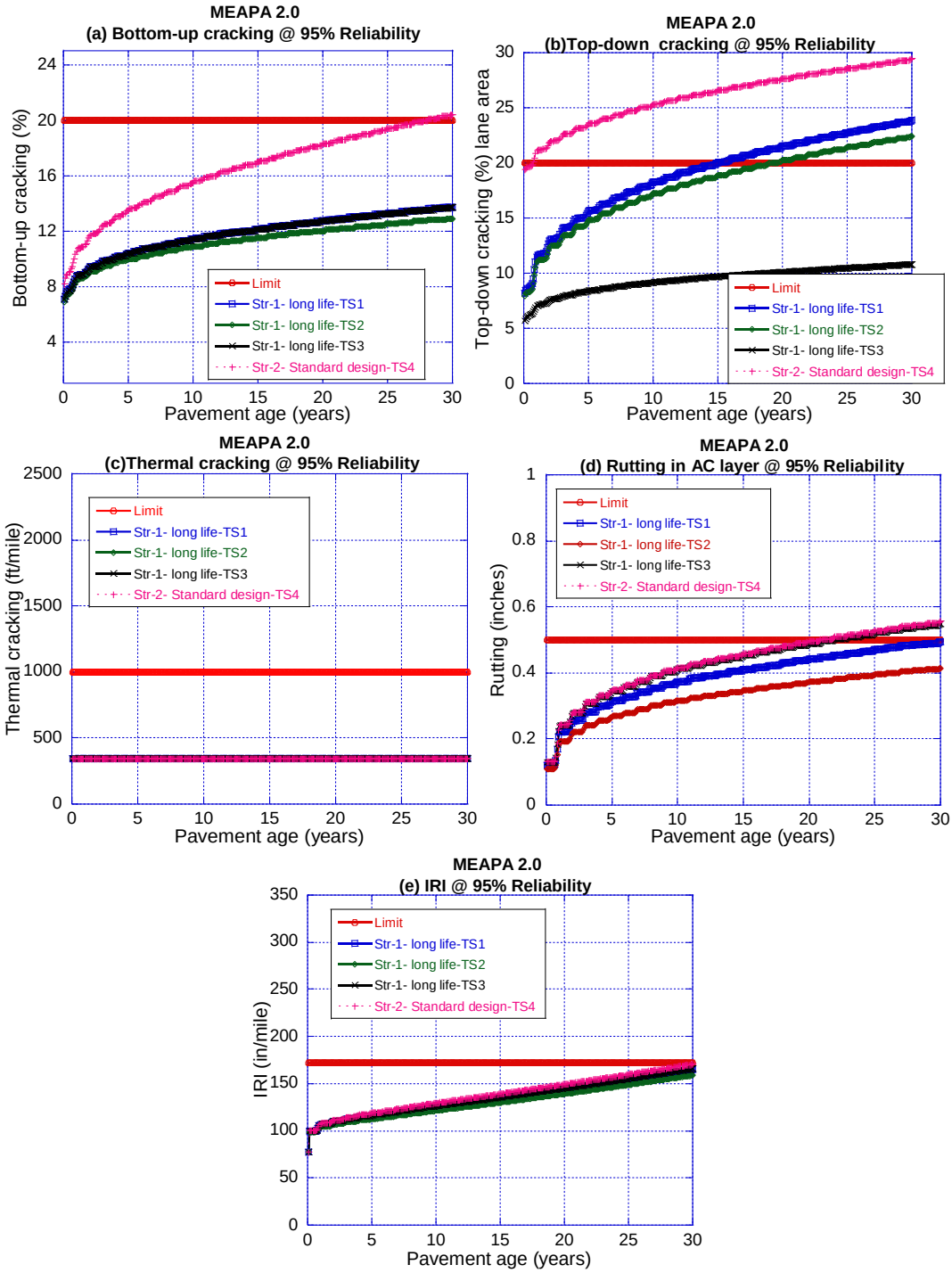

Figure 42 US-131 MEAPA 2.0 predicted distresses (a)bottom-up cracking, (b) top-down cracking, (c)thermal cracking, (d) rutting in AC, (E) IRI

In order to calculate seasonal pavement moduli for the PerRoad simulations, 52 weeks of the year were divided into four 13-weeks period representing the four seasons. Average monthly air temperatures were extracted from the corresponding AASHTOWare Pavement ME climatic files. Seasonal pavement moduli for HMA layers were calculated based on dynamic modulus master curves for the seasonal temperatures and frequency of 10 Hz. The COV (coefficient of variation) used in these simulations is the highest COV observed for each mixture in the dynamic modulus test. Due to the limited number of layers that can be implemented in the software, base and subbase layers were combined into one layer using Odemark's equivalent thickness method. The lab measured resilient modulus values for unbound layers were used for these calculations. The resilient modulus values for unbound layers were considered constant in different seasons. The thicknesses and variation in the thicknesses for HMA layers is based on the analysis of cores described in the previous chapter. An example of seasonal and structural inputs for I-475 NB test section 1 is shown in Figure 43.

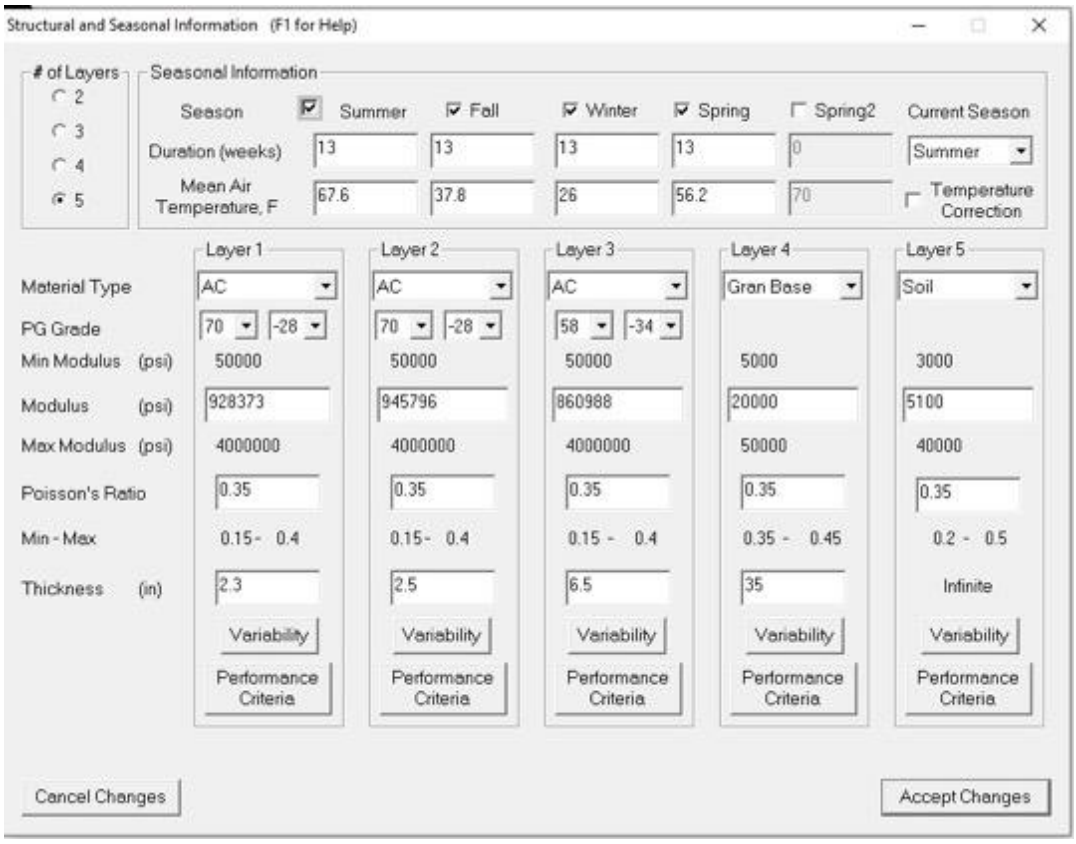

Figure 43 PerRoad structural and seasonal inputs- I-475 NB test section 1

The performance criteria for evaluation of the performance of the long-life and standard test sections of US-131 and I-475, were defined at 4 locations in the pavement structure:

- Principal strain at the top of the top HMA course (indication of top-down cracking)
- Horizontal strain distribution at the bottom of the base HMA course (indication of bottom-up cracking)
- Vertical strain at the middle of the combined base and subbase layer (indication of rutting)
- Vertical strain at the top of the subgrade layer (indication of rutting)

Pavement performance criteria and values used in this study are summarized in Table 38.

Table 38 Pavement performance criteria for PerRoad simulations

Location		Performance criteria	Threshold limit	
Layer	Position			
Top HMA layer	Top	Principal strain	-100 με	
Base HMA layer	Bottom	Horizontal strain distribution	Percentile	με
			95th	-257
			85th	-194
			75th	-158
			65th	-131
			55th	-110
Combined base and subbase	Middle	Vertical strain	150 με	
Subgrade	Top	Vertical strain	200 με	

Based on the above performance criteria, all the long-life and standard test sections resulted in acceptable performance and passed the PerRoad criteria. The results for I-475 NB test section-1 are listed in Table 39. As shown, the strain distribution at the bottom of the HMA layer is significantly lower than the failing criteria. Additionally, vertical strains at the middle of the combined base and subbase layer and top of the subgrade layer are also significantly lower than the target values. The cumulative distribution of the defined performance criteria for I-475 and US-131 are shown in Figure 44 and Figure 45, respectively. As shown in these figures, all the predicted principal strains at the top of the HMA surface layer are below the defined target value. This prediction could be an indication of good performance in top-down cracking. The cumulative distribution of the horizontal strains at the bottom of the AC layer shows that all the long-life and standard section pass the PerRoad horizontal strain distribution criteria, since all of them are on the left side of the PerRoad limits. Additionally, the predicted values for the long-life sections are less than standard sections for a given percentile. There is a similar trend in the vertical strain response at the middle of the base layer. This can be an indication of acceptable performance in terms of rutting in the unbound layers. Similar results were obtained for all long-life and standard test sections of the US-131 and I-475 projects.

Table 39 PerRoad analysis results- I-475 NB test section 1

Perpetual Pavement Design Results: Percentile Responses							
Layer	Location	Criteria	Target	Units	Target percentile	Actual percentile	Pass/Fail?
1	Top	Principal Strain	-100	microstrain	50	100	Pass
1	Bottom	Tensile Strain	-257	microstrain	95	100	Pass
			-194	microstrain	85	100	Pass
			-158	microstrain	75	100	Pass
			-131	microstrain	65	100	Pass
			-110	microstrain	55	100	Pass
4	Middle	Vertical Strain	150	microstrain	50	100	Pass
5	Top	Vertical Strain	200	microstrain	50	100	Pass

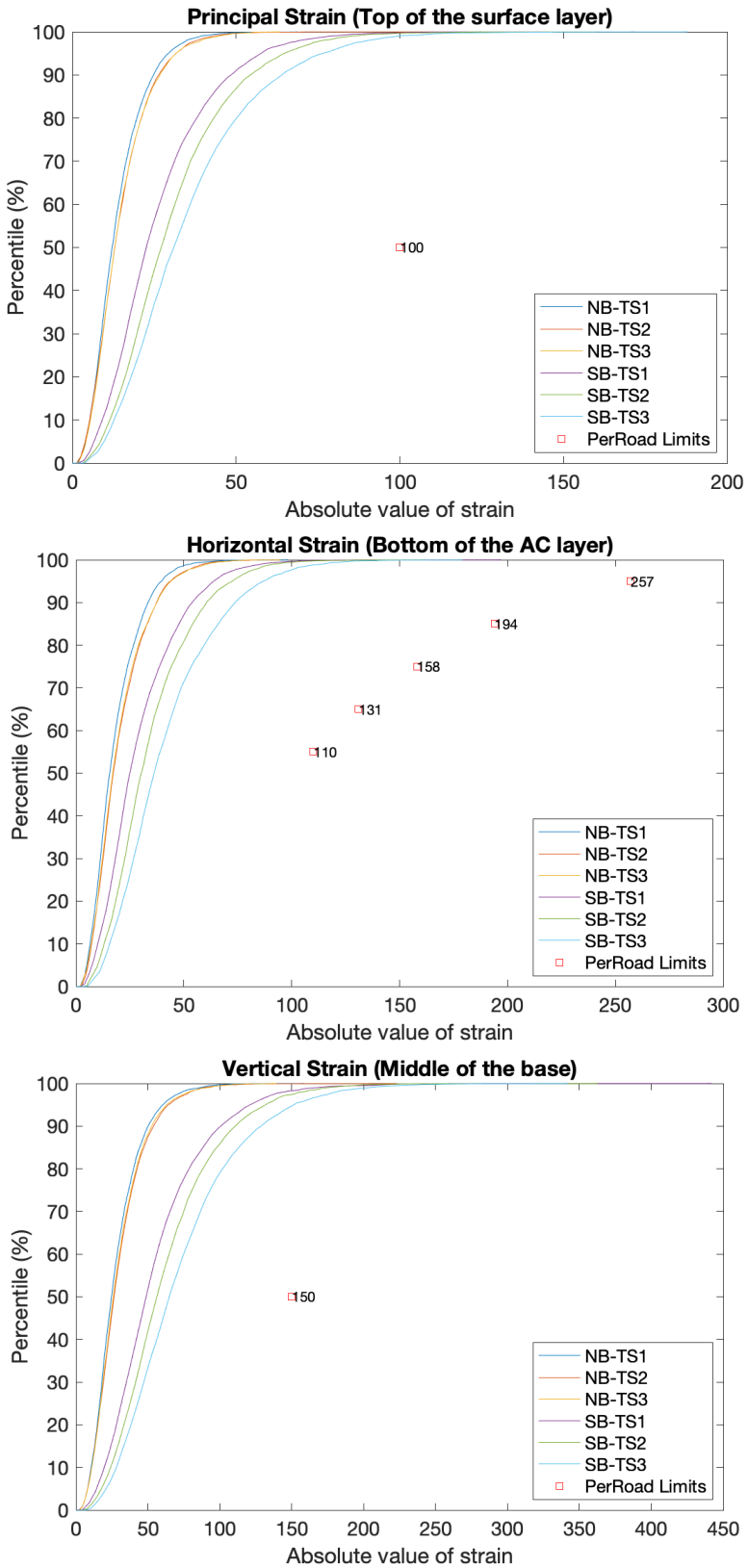

Figure 44 Cumulative distribution of defined performance criteria in PerRoad – I-475

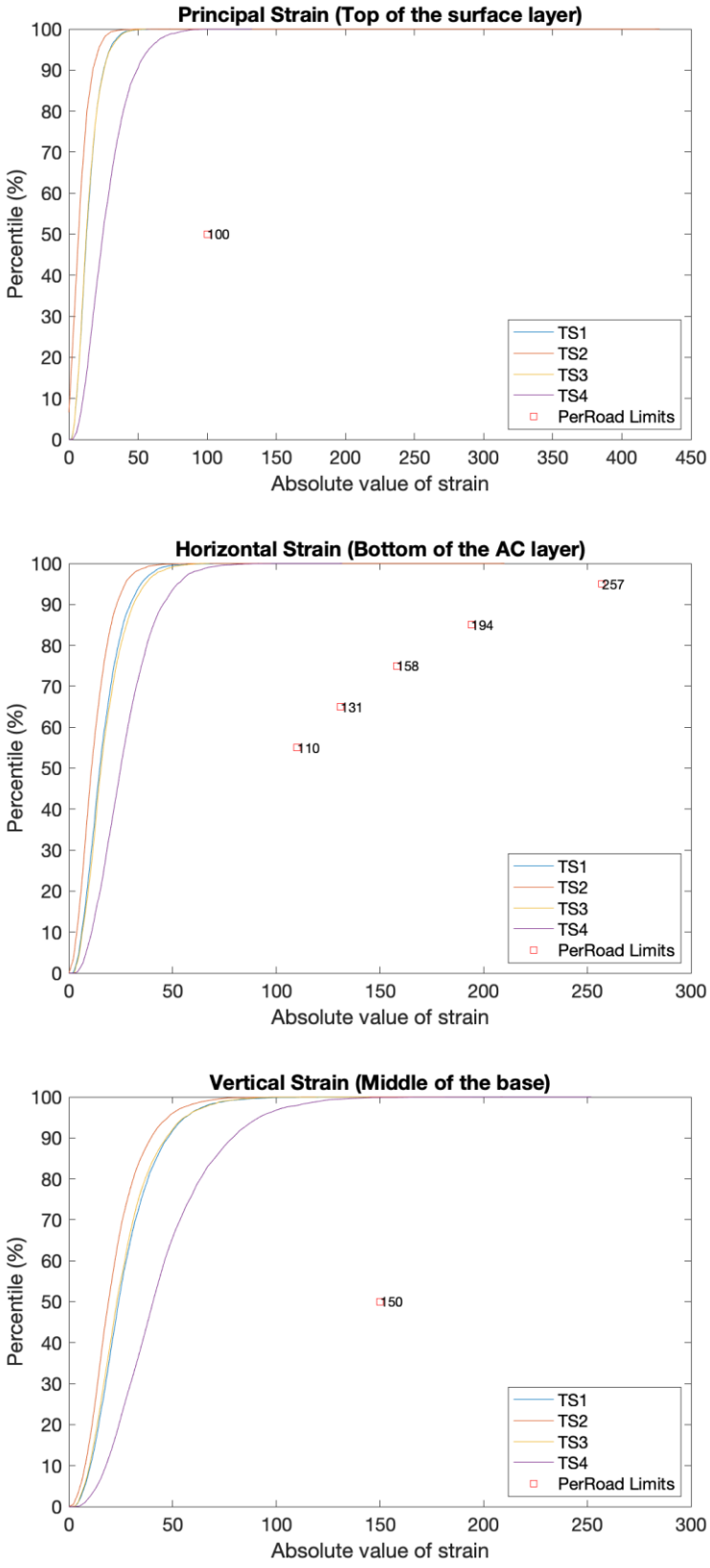

Figure 45 Cumulative distribution of defined performance criteria in PerRoad – US-131

4.4 CHAPTER 4: ENHANCED MECHANISTIC-EMPIRICAL ANALYSIS OF THE LONG-LIFE PROJECTS WITH VARIABLE FATIGUE ENDURANCE LIMIT

In this part of the study, a fatigue endurance limit (FEL) prediction model, developed as a result of a project by the National Cooperative Highway Research Program (NCHRP 9-44A)(*42*) is implemented in the Mechanistic Empirical Asphalt Pavement Analysis (MEAPA) software to have a better prediction of the performance of the US-131 and I-475 projects. As part of this task, FEL mastercurves will be developed for the mixtures used in the long-life and standard sections in these two projects based on NCHRP 9-44A FEL prediction model. Development of FEL mastercurves helps MDOT in future long-life designs with application of the fatigue endurance limit.

4.4.1 Fatigue Endurance Limit

Long-life or perpetual pavements are usually designed to last longer than 50 years without a major structural rehabilitation, other than periodic surface renewal due to surficial distresses. A key point in designing such pavements is to limit the tensile strains at the bottom of the asphalt layer to prevent accumulation of fatigue damage. This limiting strain is defined as fatigue endurance limit (FEL). This is the strain level below which no fatigue damage occurs in the pavement structure.

During the past 50 years, FELs ranging from 70 to 300 με have been reported by different researchers. In one of the first studies related to FEL, Monismith (*43*) proposed a FEL of 70. More recent studies have proposed higher FELs ranging from 70 to 100 (*16*, *44*), 90 to 300 (*45*), 115 to 250 (*46*), 75 to 200 (*20*), 200 (*47*) and 96 to 158 (*48*). These FEL values were estimated either by applying different analytical methods to fatigue test data (*16*, *19*, *20*, *44*, *46*, *49*, *50*) or

analyzing long-life pavements sections (*17*, *47*, *51*). Based on the fatigue performance of certain well performing test tracks at National Center for Asphalt Technology (NCAT), Willis and Timm (*21*) showed that pavements can experience strain levels higher than laboratory determined FELs without showing fatigue damage. They proposed a strain distribution criterion for long-life pavements based on the performance of test tracks with minimal fatigue damage. Recent studies showed that FEL in asphalt concrete is not a single value and it highly depends on several factors such as binder rheology, temperature, loading time and air void content (*20–22*). Understanding the effect of applying FEL in pavement analysis and design is essential for not only the long-life pavements, but also the traditional pavements. Zeiada et al. (*52*) estimated FEL values from six different analytical models (ranging from 37 to 162 με) and applied them in AASHTOWare Pavement ME for six different pavement structures. They reported the required asphalt layer thickness ranged from 11 cm to 23 cm based on different FEL values to obtain a perpetual pavement (*52*). The drawback of this analysis method is that the current implementation of the FEL concept in AASHTOWare Pavement ME allows the user to enter a single FEL value, which remains fixed during the entire analysis period. However, as noted in NCHRP 9-44A project, the FEL varies for different stiffnesses (i.e., temperatures / frequencies / materials). Therefore, FEL in the Pavement ME analysis should vary for each quintile, each month and for each vehicle speed in the analysis.

Kenneth and Timm (*53*) compared the FEL values estimated using the NCHRP 9-38 and NCHRP 9-44A procedures in designing perpetual pavements and studied their impact on asphalt layer thickness for 20 asphalt mixtures of the NCAT test track. They found that the NCHRP 9-44A method led to lower FELs, thus thicker layers in design as compared to the NCHRP 9-38 method.

4.4.2 NCHRP 9-44A FEL Prediction Model

Witczak et al. demonstrated in NCHRP 9-44a report (*22*) that the FEL value is significantly impacted by the healing that takes place during rest periods. Healing is defined as the capability of a material to partially self-recover its mechanical properties upon closure of micro-cracks during rest periods (i.e., when they are unloaded). They also proposed that FEL depends on many factors such as binder type and content, mixture air voids, temperature, strain level, number of load cycles, and rest period between load cycles (healing). They conducted numerous bending beam fatigue (BBF) tests on 19-mm Superpave designed mixtures with three asphalt binder grades (PG 58-25, PG 64-22 and PG 76-16), two binder contents (4.2% and 5.2%), two mixture air voids (4.2% and 9.5%), three strain levels (low, medium, high), three test temperatures (4°C, 21°C, 38°C) and four rest periods (0 s, 1 s, 5 s, and 10 s). The results from a total of 468 BBF tests were used to develop a FEL prediction model based on a regression analysis. In this model, the initial stiffness of the mixture (E_0) was used as a surrogate for the binder content, binder grade, mixture air voids, and temperature. The NCHRP 9-44A FEL prediction model is provided in Equation *10* :

$$SR = 2.0844 - 0.1386 * \text{Log}(E_0) - 0.4846 * \text{Log}(\varepsilon_t) - 0.2012 * \text{Log}(N) + 1.4103 * \tanh(0.8471 * RP) + 0.0320 * \text{Log}(E_0) * \text{Log}(\varepsilon_t) - 0.0954 * \text{Log}(E_0) * \tanh(0.7154 * RP) - 0.4746 * \text{Log}(\varepsilon_t) * \tanh(0.6574 * RP) + 0.0041 * \text{Log}(N) * \text{Log}(E_0) + 0.0557 * \text{Log}(N) * \text{Log}(\varepsilon_t) + 0.0689 * \text{Log}(N) * \tanh(0.2594 * RP)$$

Equation 10

where,

SR = stiffness ratio

E_0 = initial flexural stiffness (Ksi)

ε_t = applied tensile microstrain (the tensile portion of the tension-compression loading cycle, or half peak to peak) (10^{-6} in./in.)

RP = rest period (s)

N = number of loading cycles

In this equation, the stiffness ratio (SR) parameter is defined as the stiffness of mixture at any cycle divided by the stiffness of mixture at 50th cycle, which is assumed to be the undamaged state after the 'conditioning' of the sample during the first 50 cycles of a BBF test. A constant SR = 1.0 during the test is an indicator of balanced condition between the fatigue damage and healing of micro-cracks. Therefore, they suggested that by substituting SR = 1.0 in Equation 1, the calculated strain value becomes the FEL for different E_0, N, and rest period (*22*). It has been reported that, after certain cycles, number of load cycles had minimal effect on the calculated FEL value, especially for rest periods higher than 1 s. Thus, the use of 200,000 loading cycle was recommended. The results of BBF tests in NCHRP 9-44A also showed that the rest period threshold value ranged from 5 s to 10 s for a loading duration of 0.1 s. In other words, further healing in the BBF tests were not observed for the rest periods higher than this range.

4.4.3 Mechanistic-Empirical Asphalt Pavements Analysis (MEAPA)

The Mechanistic-Empirical Asphalt Pavement Analysis (MEAPA) is a web-based application developed at Michigan State University to predict flexible pavement performance. Figure 46 illustrates the project detail page of MEAPA web site. The MEAPA analysis engine includes implementation of the original formulations of the Mechanistic-Empirical Pavement Design Guide (MEPDG), with few improvements and simplifications on climatic model and improvements on the top-down cracking model. The rest of the formulations implemented in MEAPA are identical to those of the original MEPDG (*54*, *55*). The main analysis engines of MEAPA were coded in MATLAB, including the layered elastic analysis algorithm, called MatLEA (*56*). The MatLEA is publicly available and formulations and computational steps are identical to those of the MnLayer software (*57*). The web-based application interface of MEAPA is composed of many sub-algorithms written in several languages including JAVA, Python,

JavaScript, HTML and CSS. In addition, the project data is saved in and retrieved from a MySQL database, which is integrated into the JAVA codes.

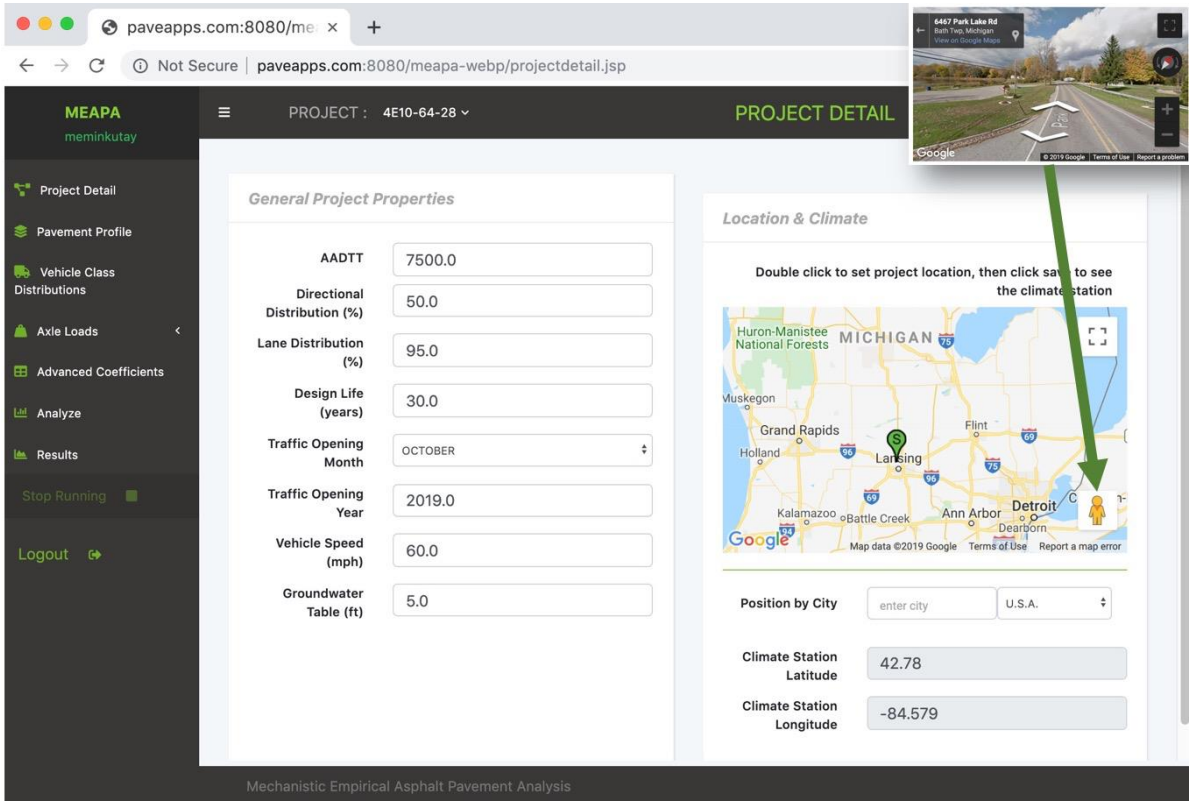

Figure 46 Project detail page in MEAPA web application

The MEAPA web application predicts pavement temperature profile with depth based on an improved climatic-materials-structural (CMS) model, which originally developed at the University of Illinois (*58*). Main improvement is on the computation of downwelling shortwave radiation (D-SWR) from the sun, downwelling longwave radiation (D-LWR) from the atmosphere, and upwelling longwave radiation (U-LWR) (*59*). Another improvement is on the calculation of sun-rise and sunset times, which are important in calculation of net radiation flux at the pavement surface (*58*).

The fatigue cracking model in MEAPA is based on the traditional fatigue life formulation implemented in the MEPDG (NCHRP 2004) as shown in Equation 10:

$$N_f = C_H C \beta_{f1} k_{f1} \left(\frac{1}{\varepsilon_t}\right)^{\beta_{f2} k_{f2}} \left(\frac{1}{E}\right)^{\beta_{f3} k_{f3}}$$ Equation 11

$$C = 10^{4.84\left(\frac{V_{be}}{V_a + V_{be}} - 0.69\right)}$$ Equation 12

$$C_{H-bu} = \left(b_{bu1} + \frac{b_{bu2}}{1 + exp(b_{bu3} - b_{bu4}.h_{ac})}\right)^{-1}$$ Equation 13

where:

N_f = number of cycles to failure;

ε_t = critical tensile strain (in/in);

E = equivalent modulus (at the given temperature/frequency) (psi);

V_{be} = effective asphalt content by volume (%);

V_a = air voids in the HMA mixture (%);

k_{f1}, k_{f2}, k_{f3} = global field calibration coefficients (k_{f1} = 0.007566, k_{f2} = 3.9492, and k_{f3} = 1.281, based on the NCHRP 1-40D research);

β_{f1}, β_{f2}, β_{f3} = local or mixture specific calibration coefficients;

h_{ac} = height of the AC layer (in),

b_{bu1} = 0.000398;

b_{bu2} = 0.003602;

b_{bu3} = 11.02;

b_{bu4} = 3.49.

For top-down fatigue cracking, major principal tensile strain near the tire within top 0.5" (1.27 cm) of the asphalt pavement layer was used in the calculation of fatigue life in Equation 9.

4.4.4 Implementation of NCHRP 9-44A Model in MEAPA

The objective of this chapter was to investigate the effect of variable FEL values computed for different mixtures, pavement structures, and rest periods on the predicted bottom-up fatigue cracking. To meet this objective, the NCHRP 9-44A FEL prediction model was implemented in MEAPA to evaluate the fatigue cracking performance, with and without implementation of variable FEL in the analysis. Example analyses were performed to illustrate the importance of FEL implementation for different structures and materials.

4.4.5 Methodology

In the first phase of this study, three typical pavement structures designed for; (i) LTV (Low Traffic Volume) roads (1 million ESALs), (ii) MTV (Medium Traffic Volume) roads (3 million ESALs), and (iii) HTV (High Traffic Volume) roads (10 million ESALs) were analyzed using constant rest periods. The analysis period was 20 years for all cases. According to the MEPDG manual of practice, the FEL concept is only applicable to the bottom-up fatigue cracking (*61*) . Thus, the focus of this study was on bottom-up fatigue cracking. In the MEAPA analysis engine, the critical tensile strains and equivalent elastic modulus at the bottom of the asphalt layer were calculated for five temperature quantiles in each month during the pavement design life. These values were used in calculation of fatigue life (N_f) in Equation 2, which was subsequently used in Miner's law of damage growth using the corresponding applied traffic data, as shown in Equation 13:

$$Damage_m = \sum_{i=1}^{m} \sum_{j=1}^{5} \sum_{k=1}^{4} \sum_{l=1}^{N_k} \frac{1}{5} \cdot \frac{n_{i,k,l}}{N_{f_{i,j,k,l}}} \qquad \text{Equation 14}$$

where:

m = total number of months;

i = indicator of month number during pavement life;

j = indicator of each temperature quantile in each month;

k = indicator of each axle types (single, tandem, tridem, and quad);

l = indicator of each load level in each axle type;

N_k = number of load levels at k^{th} axle type.

$Damage_m$ = damage level at the m^{th} month;

$n_{i,k,l}$ = number of axle repetitions at i^{th} month, k^{th} axle type, and l^{th} load level;

$N_{f\,i,j,k,l}$ = fatigue life at i^{th} month, j^{th} temperature quantile, k^{th} axle type, and l^{th} load level;

In order to implement the NCHRP 9-44A model in MEAPA fatigue cracking analysis, FEL values were calculated for different rest periods at each temperature quantile of each month during the pavement life. For a given rest period, the use of N = 200,000 and SR = 1.0 is recommended by the model developers (*22*). Therefore, the only variable of FEL prediction model at a certain temperature quantile would be the stiffness (E_0), which was assumed to be equal to dynamic modulus of the bottom sub-layer of asphaltic layer at that temperature quantile. If the critical bottom-up fatigue strain at each temperature quantile/month was less than the calculated FEL value, the damage accumulation of that specific temperature quantile/month was excluded from the analysis. This procedure can be expressed in Equation 14:

$$Damage_m = \sum_{i=1}^{m}\sum_{j=1}^{5}\sum_{k=1}^{4}\sum_{l=1}^{N_k}\frac{1}{5}.\frac{n_{i,k,l}}{N_{f_{i,j,k,l}}} \quad \forall \ \varepsilon_{i,j,k,l} > FEL_{i,j} \qquad \text{Equation 15}$$

where:

$FEL_{i,j}$ = calculated FEL value at i^{th} month and j^{th} temperature quantile.

In order to evaluate the effect of rest period, five different rest periods of 1.0 s, 2.0 s, 5.0 s, 10.0 s, and 20.0 s were used in the MEAPA analysis, consistent with the values used in the literature (*52*) . General information and properties of the asphalt layers employed in this study are provided in Table 40. The structural properties of the typical LTV, MTV, and HTV roads are shown in Table 41. The analysis inputs used for the MEAPA analysis are also presented in Table 42.

In the second phase of this study, the long-life and standard sections of the flexible pilot long-life projects, I-475 and US-131, were analyzed using estimated field rest periods calculated from the weigh in motion (WIM) data provided by MDOT. For estimation of the rest periods from WIM data, initially two WIM stations close to the I-475 and US-131 were selected. Each vehicle pass (class 5 and higher) was considered as one load application and the time intervals between load application were calculated for each station. The histograms and cumulative distribution of the rest periods were generated for each station. Then the rest periods were divided to 5 quantiles per each month based on the distribution. The FEL values were calculated for each temperature quantile for 5 rest period quantiles per each month. The FEL in Equation 16 in this approach will be in the following form:

$FEL_{i,j,k}$= calculated FEL value at i^{th} month and j^{th} temperature quantile and k^{th} rest period quantile

Table 36 and Table 37 show the inputs used in MEAPA simulations for I-475 and US-131, respectively. Pavement structures were evaluated in MEAPA for a service life of 50 and 30 years for the I-475 and US-131, respectively. A new flexible pavement project type with an initial International Roughness Index (IRI) of 67 in/mi and 95% reliability level were used for

the analysis. Average annual daily truck traffic (AADTT), vehicle class distribution, growth factors, monthly adjustment factors were provided by MDOT.

4.4.6 Results and Discussion

Figure 47 shows the calculated FEL values predicted by NCHRP 9-44A model for different rest periods at each month. These FEL values were applied to the bottom-up fatigue cracking model in the MEAPA over the pavement life. The statistical summary of these results is also shown in Table 43. These results show that FEL values increases considerably as the rest period increases.

Table 40 Details and properties of HMAs

Pavement section	MDOT Mix Type	HMA ID [(1)]	Binder PG	V_a [(2)] [%]	V_{be} [(3)] [%]	VMA [(4)] [%]	VFA [(5)] [%]
HTV	5E10	S01	70-22P	6.5	12.0	18.5	64.9
	4E10	L01	70-22P	6.5	10.6	17.1	62.0
	3E10	B01	58-22	6.4	9.6	16.0	60.0
MTV	5E3	S02	70-28P	7.1	11.2	18.3	61.2
	4E3	L02	70-28P	6.7	10.9	17.6	61.9
LTV	4E1	S03	58-28	7.0	12.0	19.0	63.2
	4E1	L03	58-28	7.0	11.2	18.2	61.5

Note: [(1)] S, L, and B stand for surface, leveling, and base courses, respectively, [(2)] V_a= air voids, [(3)] V_{be}= Effective binder content, [(4)] VMA = Voids in Mineral Aggregate, [(5)] VFA = Voids Filled with Asphalt

Table 41 Structural properties of LTV, MTV and HTV roads

Layer	Property	HTV	MTV	LTV
HMA	Thickness (in)	2.0	2.0	1.3
	HMA ID	S01	S02	S03
	Thickness	2.0	2.0	1.2
	HMA ID	L01	L02	L03
	Thickness	4.0	-	-
	HMA ID	B01		
Base (Crushed gravel)	Thickness (in)	6.0	6.0	4.0
	Modulus (psi)	33,000	33,000	33,000
Subgrade (A-6)	Modulus (psi)	15,000	15,000	15,000

Table 42 MEAPA design inputs

Pavement section	LTV	MTV	HTV
Initial annual average daily truck traffic (AADTT)	300	1200	3500
Equivalent single axle load (ESAL) repetition	1.1 million	3.9 million	11.3 million
Lane distribution factor	90%	90%	90%
Direction distribution factor	51%	51%	51%
Vehicle speed	30 mph	60 mph	60 mph
Design life	20 years	20 years	20 years
Climate station	Lansing, MI	Lansing, MI	Lansing, MI
Latitude	42.78°	42.78°	42.78°
Longitude	-84.58°	-84.58°	-84.58°
Ground water table	10 ft	10 ft	10 ft

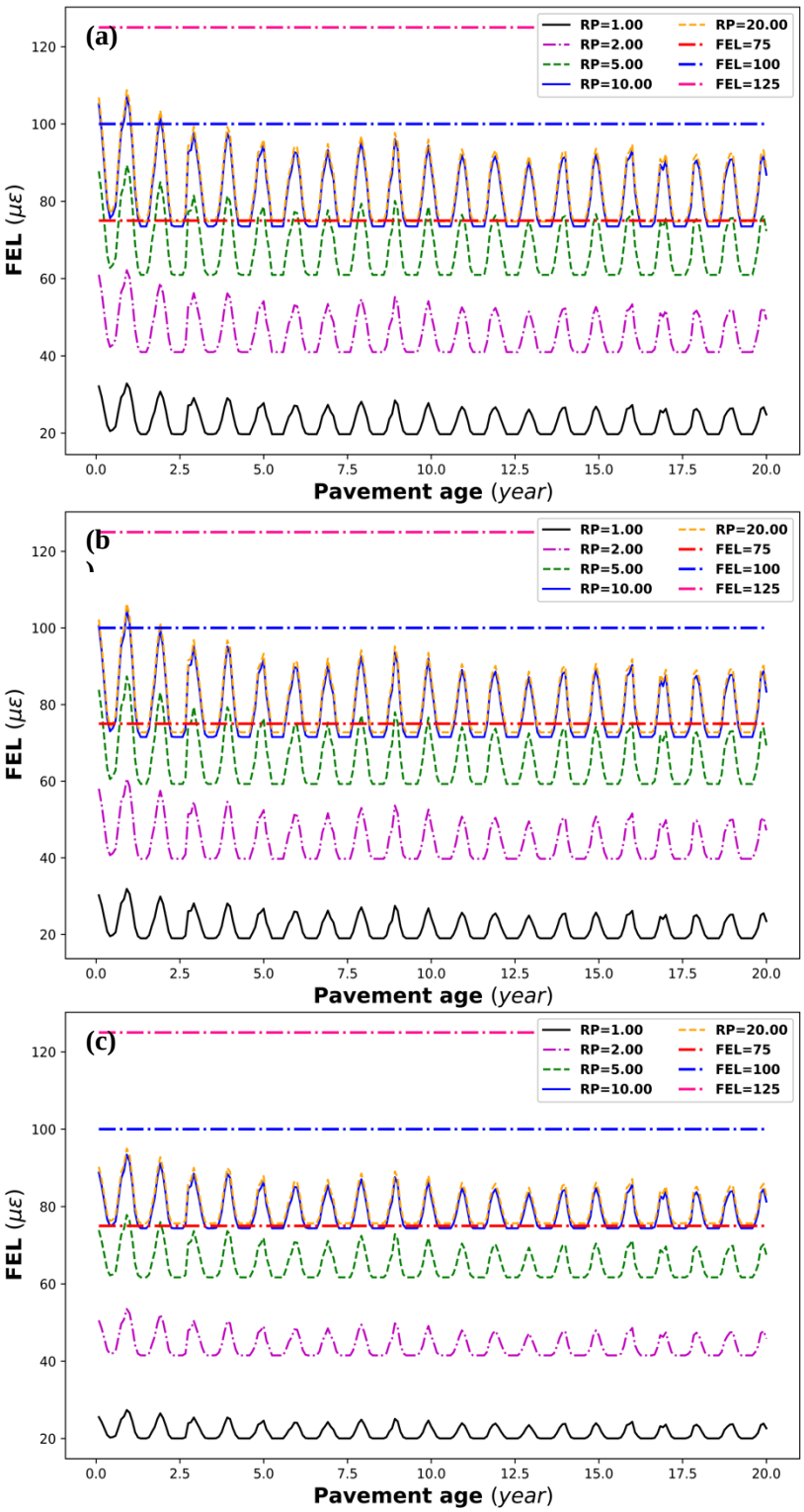

Figure 47 Calculated FEL values for different rest periods during the pavement life for (a) LTV, (b) MTV, and (c) HTV roads

Table 43 Statistical summary of the calculated FEL values

FEL Calculation type	Pavement section type	LTV	MTV	HTV
NCHRP, RP=1.0 s	Minimum FEL	19.71	18.97	20.03
	Mean FEL	22.62	21.61	21.51
	Maximum FEL	32.84	31.88	27.37
NCHRP, RP=2.0 s	Minimum FEL	40.97	39.73	41.51
	Mean FEL	45.74	44.08	43.95
	Maximum FEL	62.16	60.65	53.50
NCHRP, RP=5.0 s	Minimum FEL	60.95	59.28	61.69
	Mean FEL	67.39	65.14	64.98
	Maximum FEL	89.33	87.34	77.82
NCHRP, RP=10.0 s	Minimum FEL	73.49	71.51	74.37
	Mean FEL	81.10	78.44	78.26
	Maximum FEL	106.97	104.63	93.42
NCHRP, RP=20.0 s	Minimum FEL	74.75	72.74	75.64
	Mean FEL	82.48	79.78	79.60
	Maximum FEL	108.75	106.37	94.99
Pavement ME suggested range	Minimum FEL	75	75	75
	Mean FEL	100	100	100
	Maximum FEL	125	125	125

As shown in Figure 47, the FEL values ranged from 18.97 με at 1.0 s rest period in MTV road to 108.75 με at 20 s rest period in LTV road. This observation strengthens the importance of choosing the proper rest period for the analysis. The NCHRP 9-44A report contemplated that the rest period should correlate with the AADTT data from the field, but a correlation was not developed as part of that study (*22*).

Figure 47 also shows that the FEL graphs for rest periods of 10.0 s and 20.0 s were almost identical, which means that the threshold of influence of rest period is 10 s no further healing is expected in the mixture for rest periods longer than 10 s. This observation agrees with results of Zeiada et al. (*52*) and NCHRP 9-44A report. In this regard, Zeiada et al. (*52*) performed a simple traffic volume analysis and reported the average overhead time of 58-86 s between vehicles. As the change in FEL values with the rest periods greater than 10.0 s was minimal, they used 10.0 s rest period for calculation of the FEL. Figure 47 also shows that for a

given rest period, the FEL values exhibited a cyclic pattern, which is because of the changes in the stiffness (E_o), which varies due to the fluctuations of pavement temperature profile at each month at each quintile. Figure 47 also shows that the recommended range of the FEL values in AASHTOWare Pavement ME V2.5 (75 to 125 με) is typically higher than those calculated using NCHRP 9-44A model. Especially, the FEL values of 100 and 125 με were considerably higher than calculated FEL values. Table 43 also shows that for a given rest period, the magnitudes of FEL values of different structures (LTV, MTV and HTV roads) are relatively close to each other. This is because the NCHRP 9-44A model is a mixture-dependent model. As mentioned above, FEL values at each rest period were calculated using N = 200,000 cycles, and SR = 1.0. Therefore, the only variable influencing the FEL value for a given rest period is the modulus at the bottom of asphalt layer at a given month/quintile combination, for a given vehicle speed. Since the range of dynamic modulus of the mixtures used in this study were relatively close to each other, the range of the predicted FELs were also close to each other for all three structures.

A comparison of actual critical strains used in bottom-up fatigue cracking is plotted along with the FEL values in Figure 48. It is noted that this graph is provided to serve as an example for 18-kip single axle load. The MEAPA computes the critical strains for many different load levels of all four axle types (single, tandem, tridem and quad).

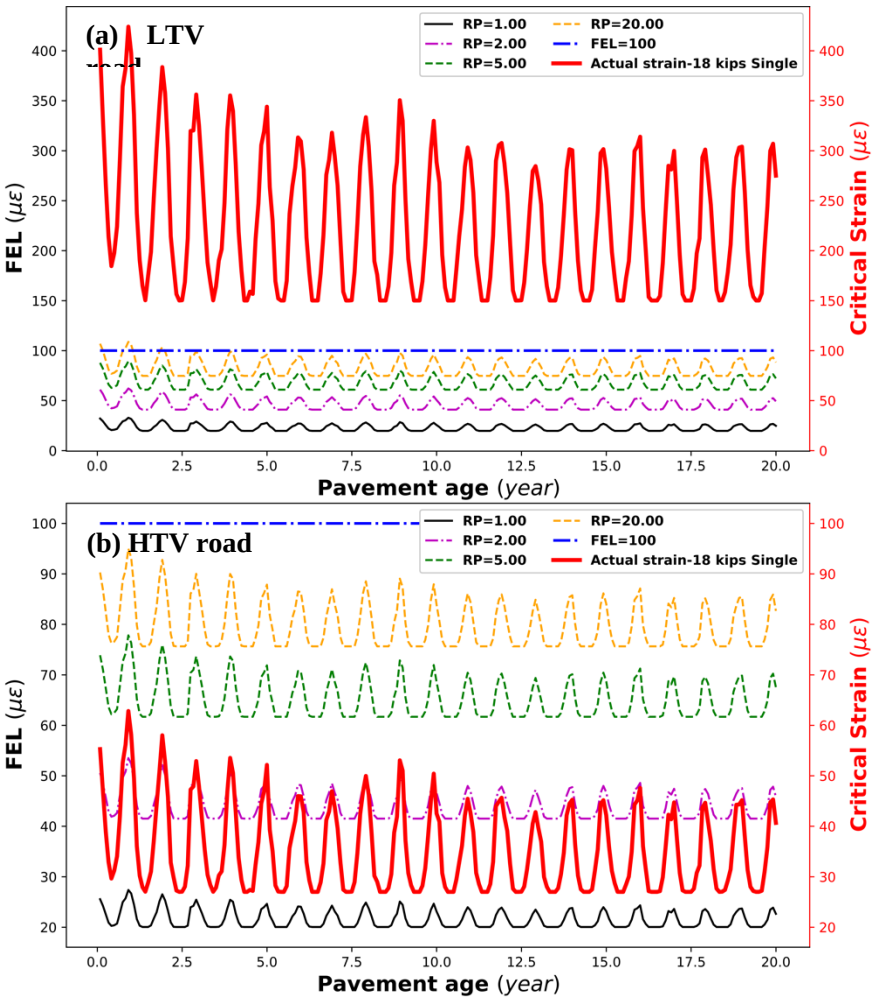

Figure 48 Comparison of the actual critical bottom-up fatigue strains (for 18 kips single axle load) with the calculated FEL values at different rest periods for (a) LTV, (b) HTV roads

Figure 48 (a) also shows that the critical strains for the LTV road were higher than the FEL values, regardless of the rest periods. As a result, the damage computations at this load level were unaffected by the FELs. This does not mean that FELs do not affect the damage in LTV roads. The critical strain levels at lower load levels might have intersected with the FEL values, which could have affected the damage computations. Figure 48 (b) shows that thick pavement structure of the HTV road, which resulted in considerably lower critical strain of the same axle load level. Thus, no damage accumulation is expected for rest periods of greater than 5.0 s. However, at higher load levels, critical strain may be higher than the FEL values. The true effect

of FELs can be observed by accumulating the damage at all load levels and axles and computing the fatigue cracking during the service life of the pavement, which is presented later in this section.

The pavement sections considered in this study were analyzed for 20 years. As a result, for each axle type (single, tandem, tridem, and quad) and load level in each axle type, 1200 critical bottom-up fatigue strains (20 years x 12 months x 5 quintiles) were computed within MEAPA analysis engine. These critical strains for each pavement structure (LTV, MTV, and HTV roads), axle types and three selective load levels (including standard axle load, one load level higher and lower than standard) were plotted using the boxplots, as shown in Figure 49. For each box in Figure 49, the central mark is the median, and the edges of the box are the 25th and 75th percentiles. The whiskers extend to the most extreme critical strain. As this figure shows, most of the critical strains of different axle configurations and load levels in LTV road were considerably higher than those of MTV and HTV roads. This is mainly because of the differences in the thicknesses of the pavements.

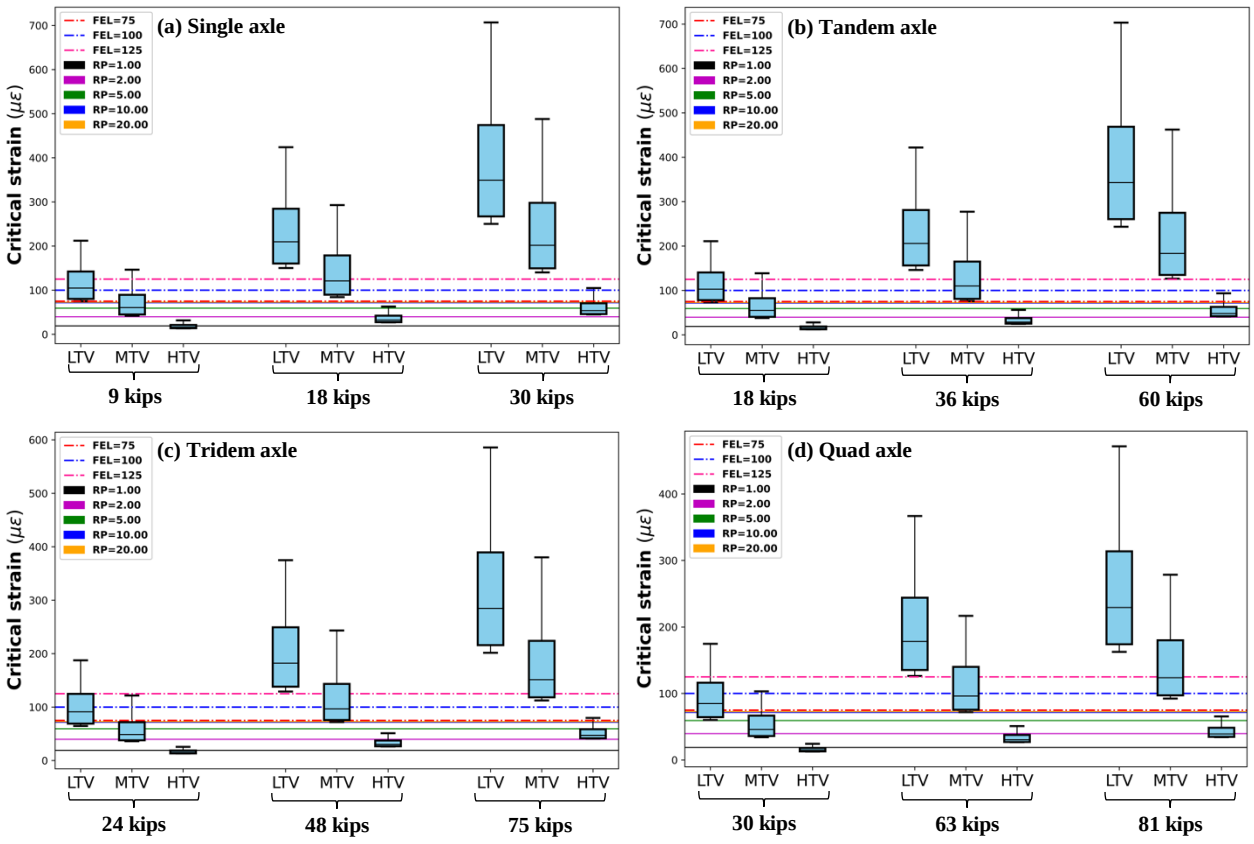

Figure 49 Statistical box plot of critical bottom-up fatigue strains for different pavement structures and axle configurations: (a) single, (b) tandem, (c) tridem, and (d) quad axles

Figure 49 also shows that most of the critical strains in the LTV road were higher than the FEL values predicted by NCHRP 9-44A model. Therefore, implementation of the FEL concept in the analysis of LTV was expected to have minimal effect on the predicted bottom-up fatigue cracking, regardless of the duration of the rest period. On the other hand, most of the critical strains of HTV road were less than the predicted FEL values. Therefore, implementation of FEL concept in the analysis of HTV is expected to significantly reduce the predicted bottom-up cracking. As the critical strains in the HTV were close to the FEL values, the amount of reduction in the predicted bottom-up fatigue cracking is also expected to be sensitive to the duration of rest periods.

Figure 50 shows the predicted bottom-up fatigue cracking for LTV, MTV, and HTV roads with and without implementation of FEL concept during the design life with different rest periods (1.0 s, 2.0 s, 5.0 s, 10.0 s, and 20.0 s) and constant FEL values of 75 με, 100 με, and 125 με. It can be observed that implementation of FEL concept had minimal effect on the bottom-up fatigue performance of LTV road. This is because most of the critical strains were higher than FEL values for almost all the rest periods (see Figure 49). The only considerable effect of FEL implementation in bottom-up cracking of LTV road has been observed when the relatively high FEL value of 125 με was used. As discussed before, FEL value of 125 με was noticeably higher than those computed with the NCHRP 9-44A model. On the other hand, the bottom-up fatigue predictions for MTV road for different rest periods were considerably different; especially for rest periods greater than 5.0 s. This implies the importance of selecting proper rest period when using the NCHRP 9-44A FEL prediction model.

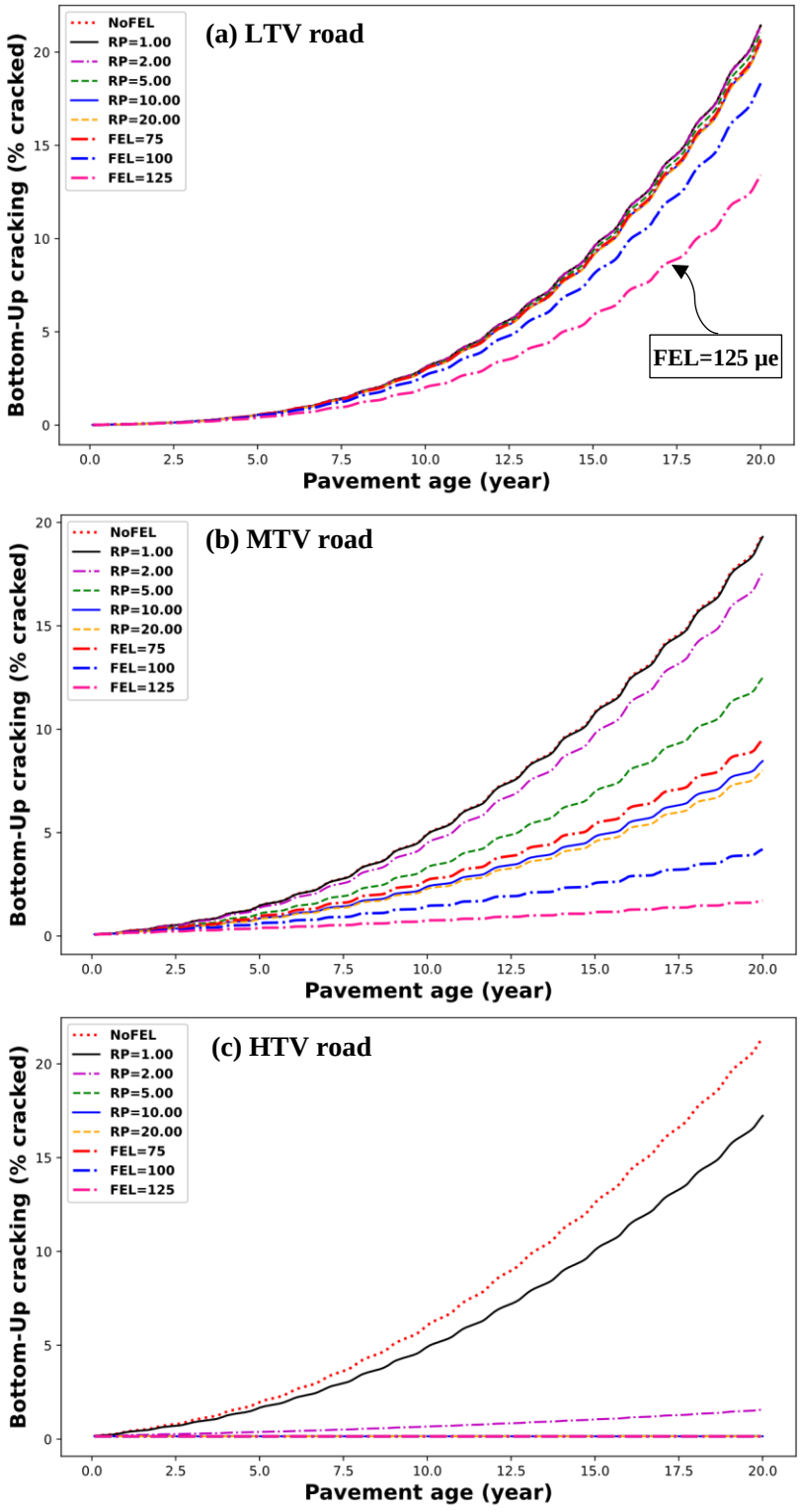

Figure 50 Effect of FEL on the bottom-up fatigue cracking prediction in (a) LTV, (b) MTV, and (c) HTV roads

The most significant effect of implementing FEL concept in bottom-up fatigue cracking prediction was observed in the HTV road. As it can be seen in Figure 50 (c), the maximum predicted fatigue cracking for HTV was about 22%, which reduced to almost 0% after implementing FEL concepts with rest periods of 2.0 s and above. This is because majority of the critical strains in HTV road were lower than the calculated FEL values. It worth noting that even the use of low rest periods can considerably reduce the predicted bottom-up fatigue cracking of HTV road. In summary, Figure 50 shows that the effect of implementing FEL concept on the predicted bottom-up fatigue cracking was highly dependent on the asphalt layer thickness (pavement structure).

Figure 50 also shows that the bottom-up fatigue cracking of the three typical structures (LTV, MTV, and HTV roads) was originally predicted about 20%. Implementation of the FEL concept leads to lower predictions of the bottom-up fatigue cracking. Thus, the AC layer thickness can be reduced by implementation of the FEL concept so that the same bottom-up cracking (20%) prediction is achieved. In this regard, Table 44 shows the percent reduction in AC layer thickness due to the implementation of FEL concept at different rest periods. As this table shows, in terms of the bottom-up fatigue cracking, implementation of the FEL concept resulted in up to 32.7% reduction in the AC layer thicknesses.

Table 44 Percent reduction in AC layer thicknesses due to the implementation of FEL concept

FEL at different rest periods	LTV	MTV	HTV
NCHRP 9-44A, RP=1.0 s	0.0 %	0.0 %	1.9 %
NCHRP 9-44A, RP=2.0 s	0.0 %	3.1 %	14.6 %
NCHRP 9-44A, RP=5.0 s	4.8 %	7.3 %	26.4 %
NCHRP 9-44A, RP=10.0 s	5.2 %	11.6 %	32.2 %
NCHRP 9-44A, RP=20.0 s	5.3 %	12.2 %	32.7 %

As mentioned before, in the second phase of this study, the long-life and standard sections of the pilot long-life projects were analyzed using varying FEL method using estimated

field rest periods calculated from the weigh in motion (WIM) data provided by MDOT. For estimation of the rest periods from WIM data, initially two WIM stations close to the I-475 and US-131 were selected. Each vehicle pass (class 5 and higher) was considered as one load application and the time intervals between load application were calculated for each station. The histograms and cumulative distribution of the rest periods were generated for each station. Then the rest periods were divided to 5 quantiles per each month based on the cumulative distribution. Table 45 shows the monthly rest period quantiles for station 40-3069 on US-131 based on 2019 WIM data. This data was used for analyzing US-131 project as estimated rest period. Similar approach was used for station 25-6119 on I-75 for analysis of the I-475 project. An example of the histogram of the rest periods for station number 40-3069 for June 2019 is shown in Figure 51.

Table 45 Monthly rest period quantiles for station 40-3069 based on 2019 WIM data

	Q1 (s)	Q2 (s)	Q3 (s)	Q4 (s)	Q5 (s)
Jan	21.2	56.1	102.4	174.3	316.8
Feb	22.4	58.2	107.1	182.9	325.0
Mar	23.3	59.8	105.1	174.7	311.1
Apr	18.6	47.7	86.3	147.6	265.3
May	14.4	37.4	68.4	116.9	213.7
Jun	14.9	37.4	70.0	118.1	216.3
Jul	13.9	35.5	66.4	112.5	204.1
Aug	13.1	33.0	61.8	105.0	194.6
Sep	13.4	34.4	63.9	107.2	202.8
Oct	12.4	31.6	59.7	103.5	191.6
Nov	13.7	36.2	66.9	116.3	218.3
Dec	16.7	43.6	81.6	139.3	257.2

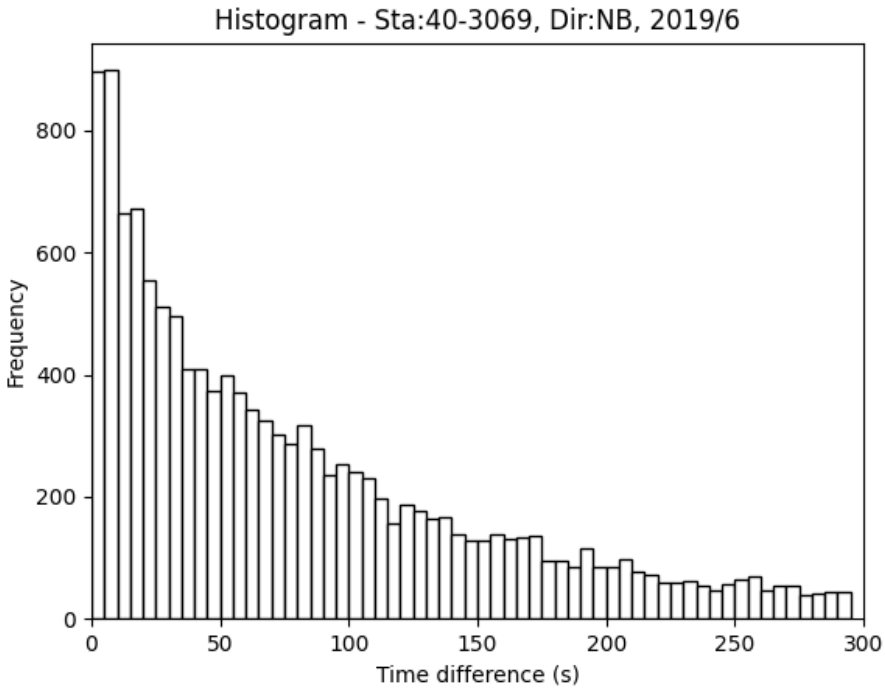

Figure 51 Histogram of the time intervals between load applications for station 40-3069 - June 2019

Figure 52 and Figure 53 show the predicted bottom-up fatigue cracking for I-475 and US-131 long-life and standard test sections with and without implementation of FEL concept during the design life with different rest periods (1.0 s, 2.0 s, 5.0 s, 10.0 s, 20.0 s and estimated rest periods from WIM data) and constant FEL values of 75 με, 100 με, and 125 με. It can be observed that implementation of FEL concept had less effect on the long-life sections as compared to the standard section. This can be attributed to the fact that long-life sections are thicker pavements and the critical strains are lower than the standard test sections. Since the critical strains are quite low in the long-life sections, the effect of applying FEL in the analysis is not as significant as the standard sections. On the other hand, the application of FEL on the standard sections has a significant effect on the predicted bottom-up cracking. In the standard

sections, the effect of application of FEL with different rest periods is also significantly important.

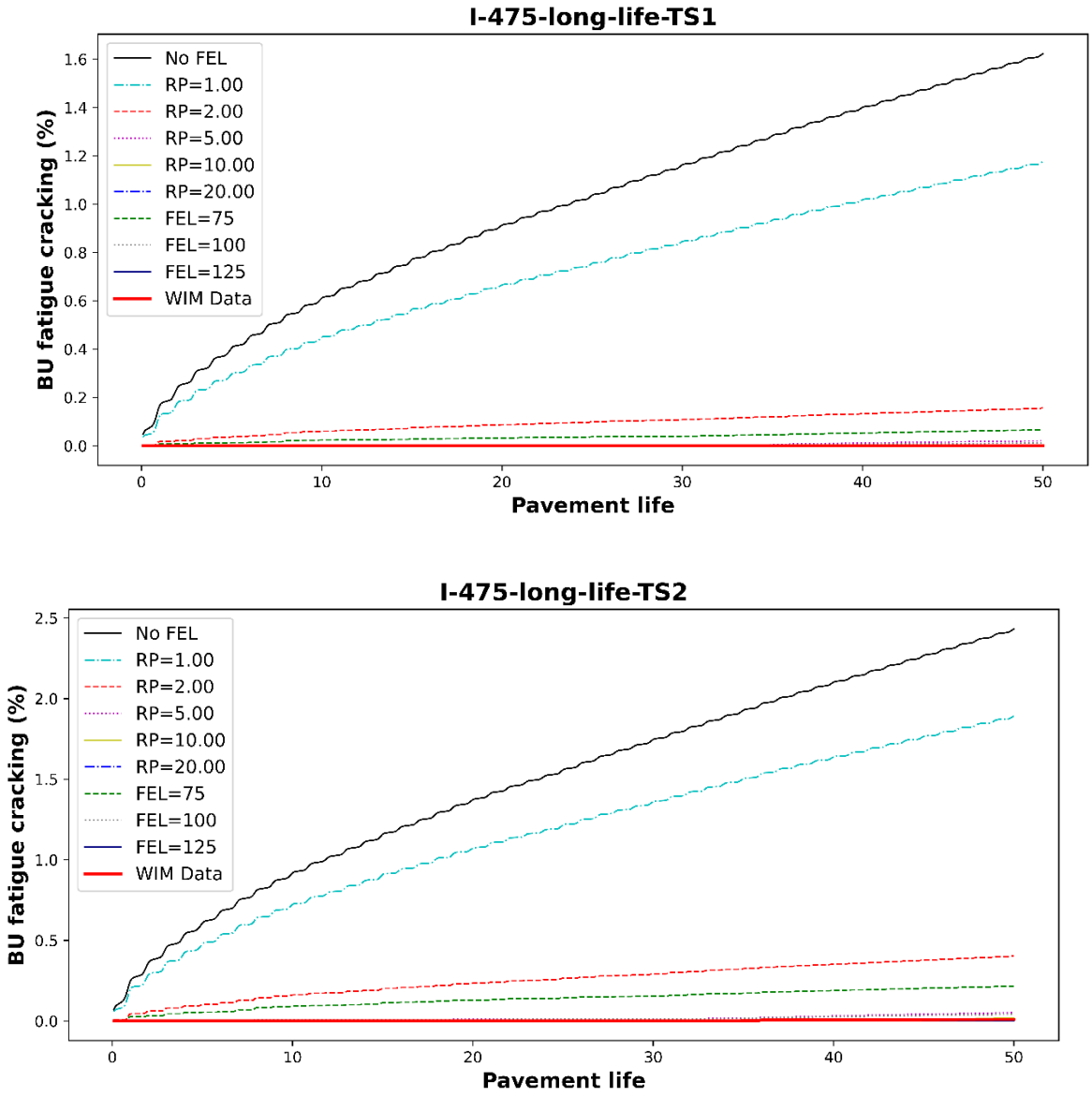

Figure 52 Effect of FEL on the bottom-up fatigue cracking prediction in the long-life and standard sections of I-475 project

Figure 52 (cont'd)

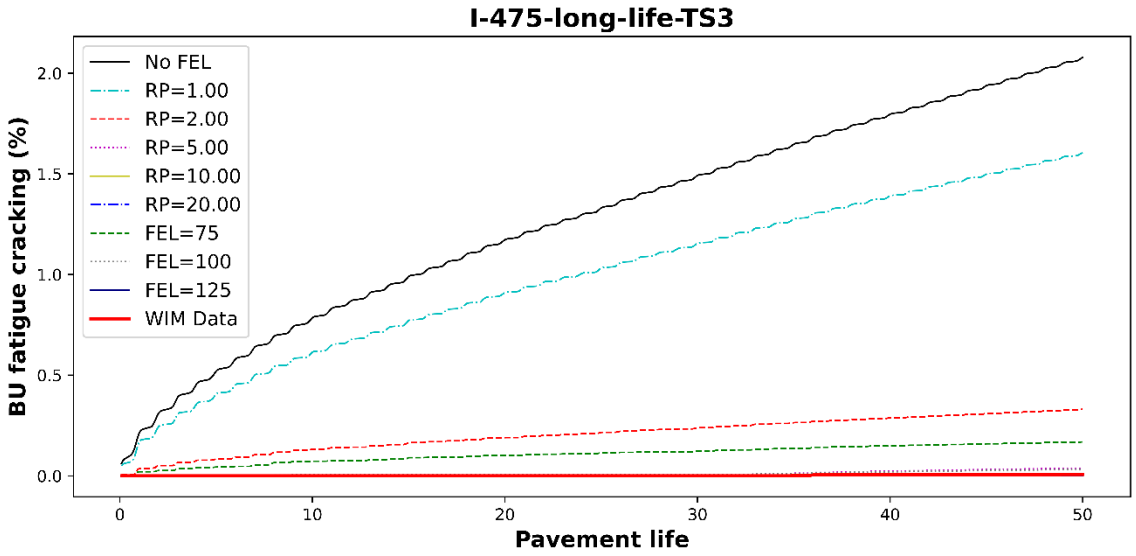

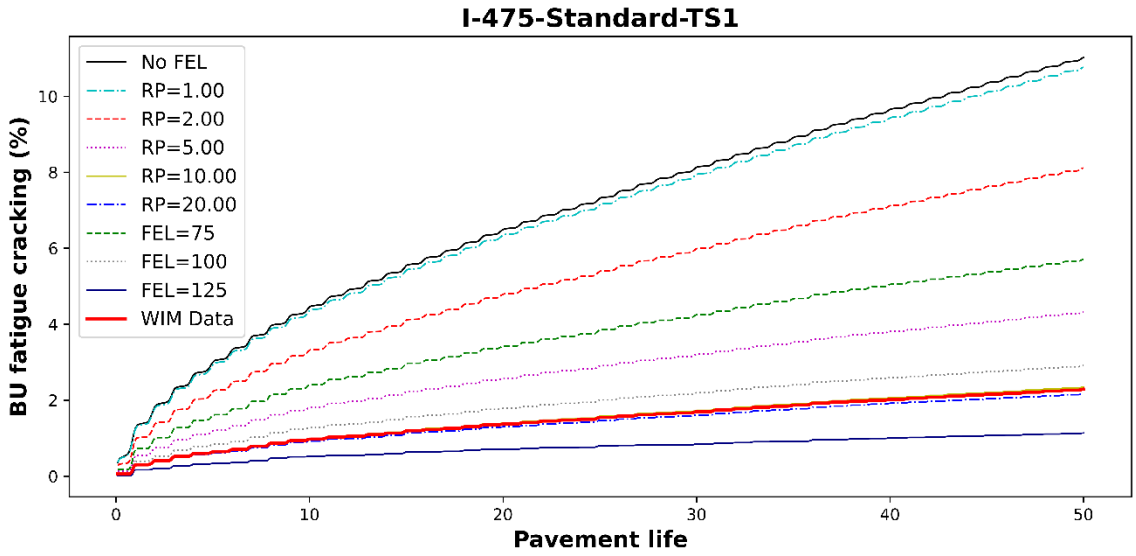

Figure 52 (cont'd)

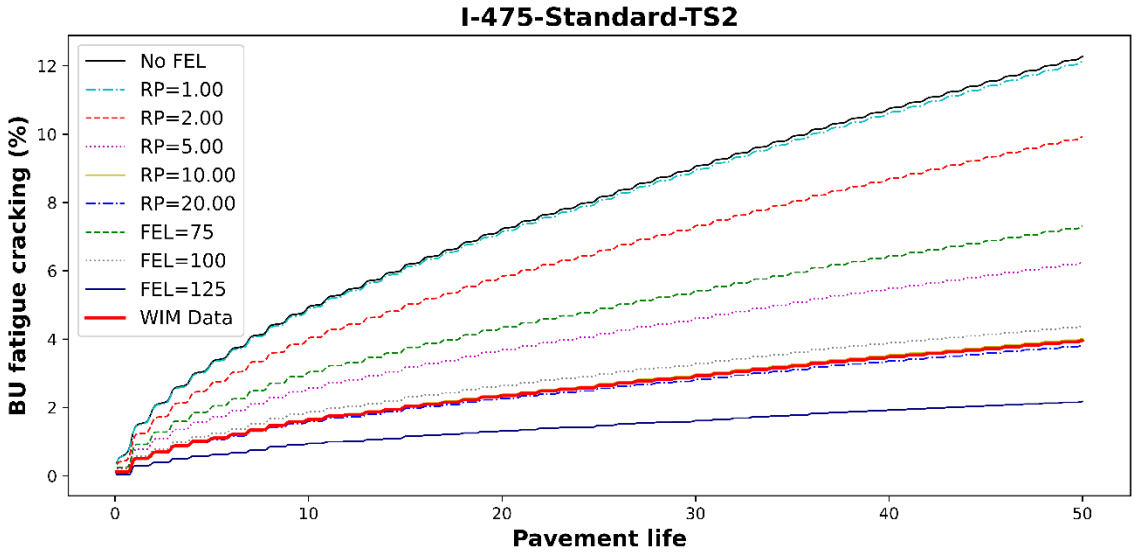

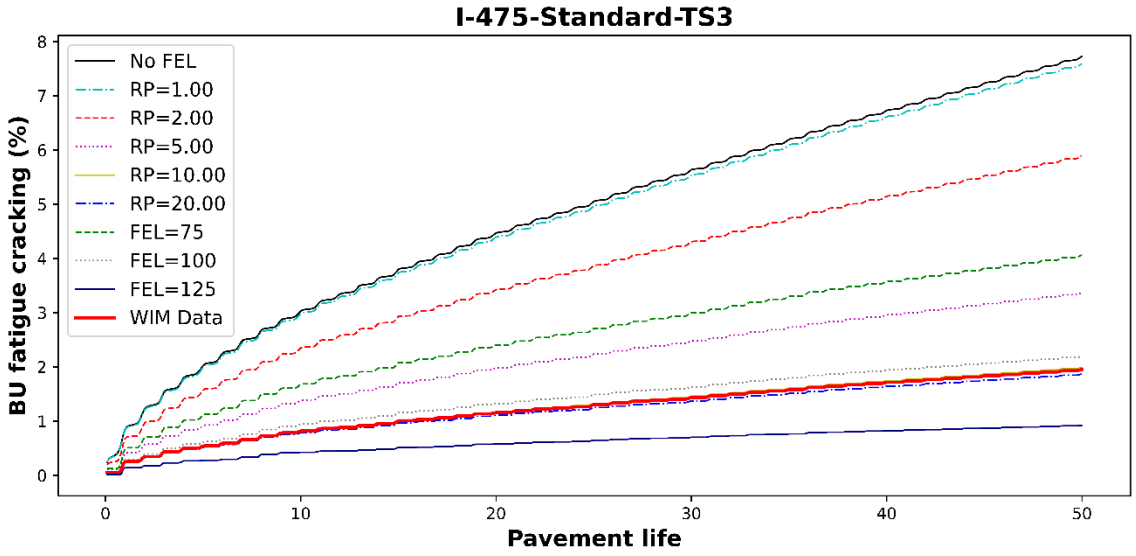

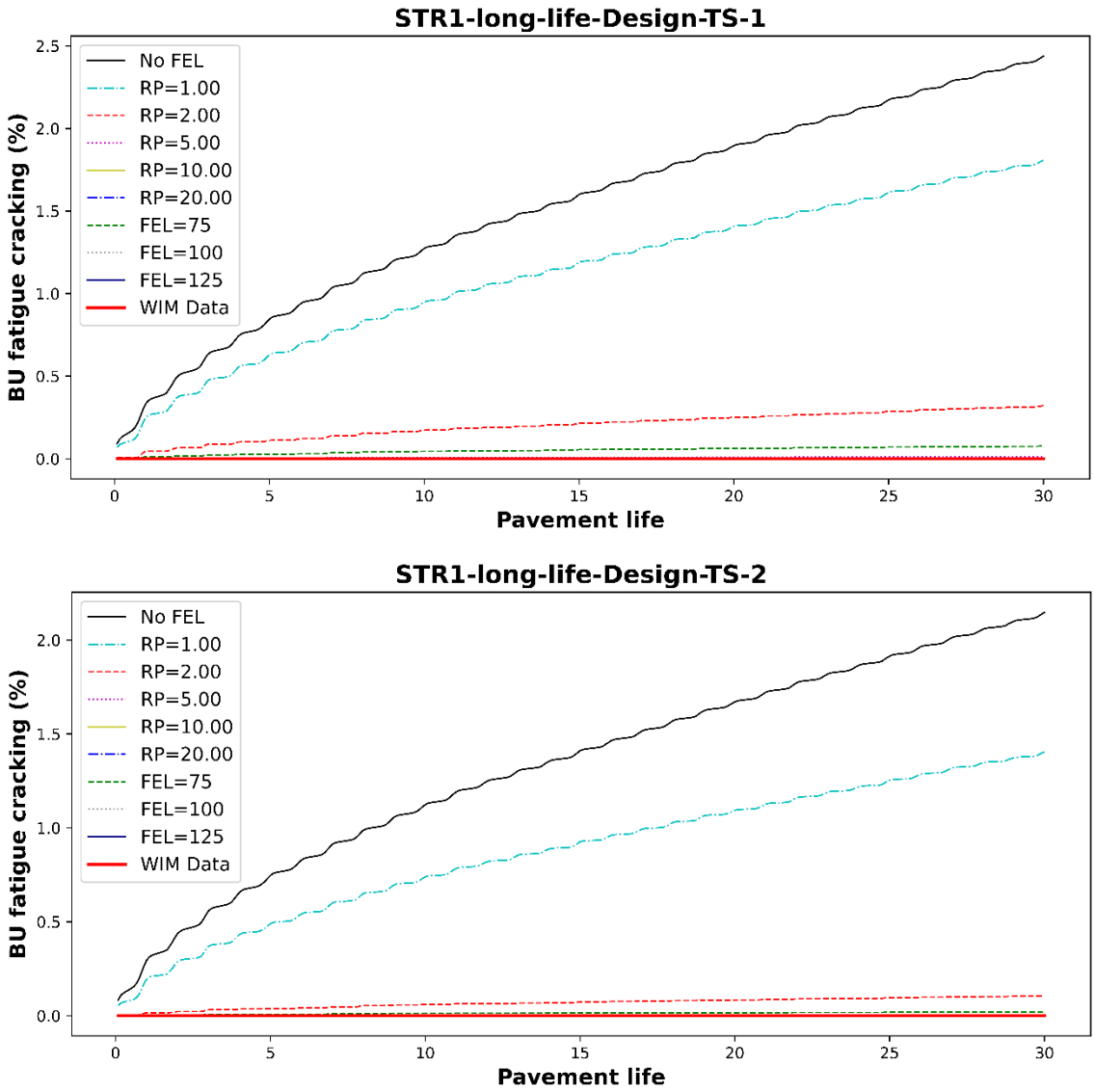

Figure 53 Effect of FEL on the bottom-up fatigue cracking prediction in the long-life and standard sections of US-131 project

Figure 53 (cont'd)

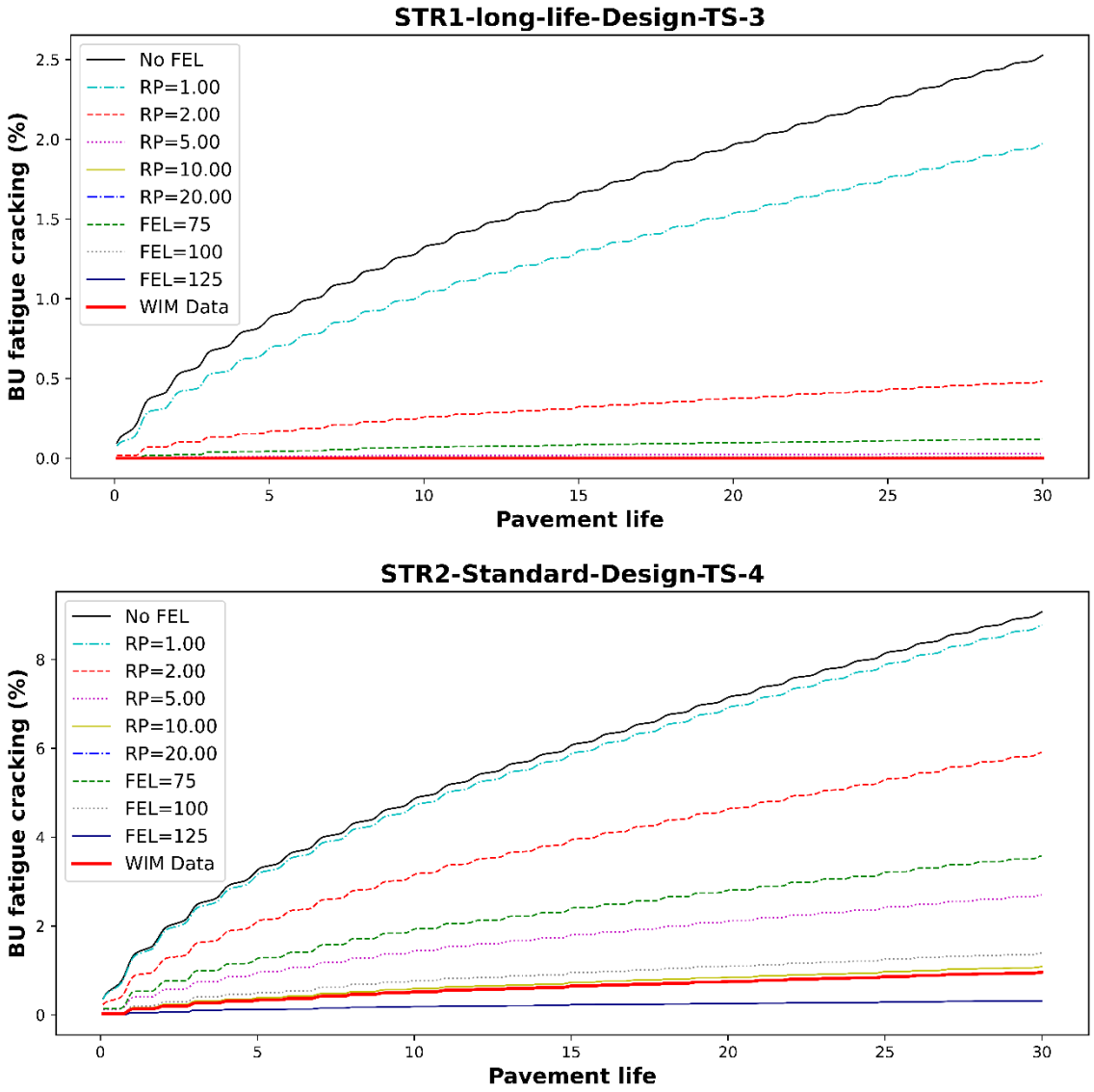

The critical strains for the standard and long-life sections of I-475 and US-131, for four axle types and three selective load levels (including standard axle load, one load level higher and lower than standard) were plotted using the boxplots, as shown in Figure 54 and Figure 55 for I-475 and US-131, respectively. For each box in these figures, the column in light blue shows the critical strains the central mark is the median, and the edges of the box are the 25th and 75th percentiles. The whiskers extend to the most extreme critical strain. The other color codes show the range of the FELs predicted for a specific rest period and a certain load level. As this figure

shows, the critical strains for the long-life sections are considerably lower than the standard sections in higher load levels. It is also shown that he ranges of the critical strains for the long-life sections are close or smaller than the range of the FELs predicted for 1.0 second rest period. This shows that the effect of choosing different rest periods for analyzing the long-life sections will not be significant.

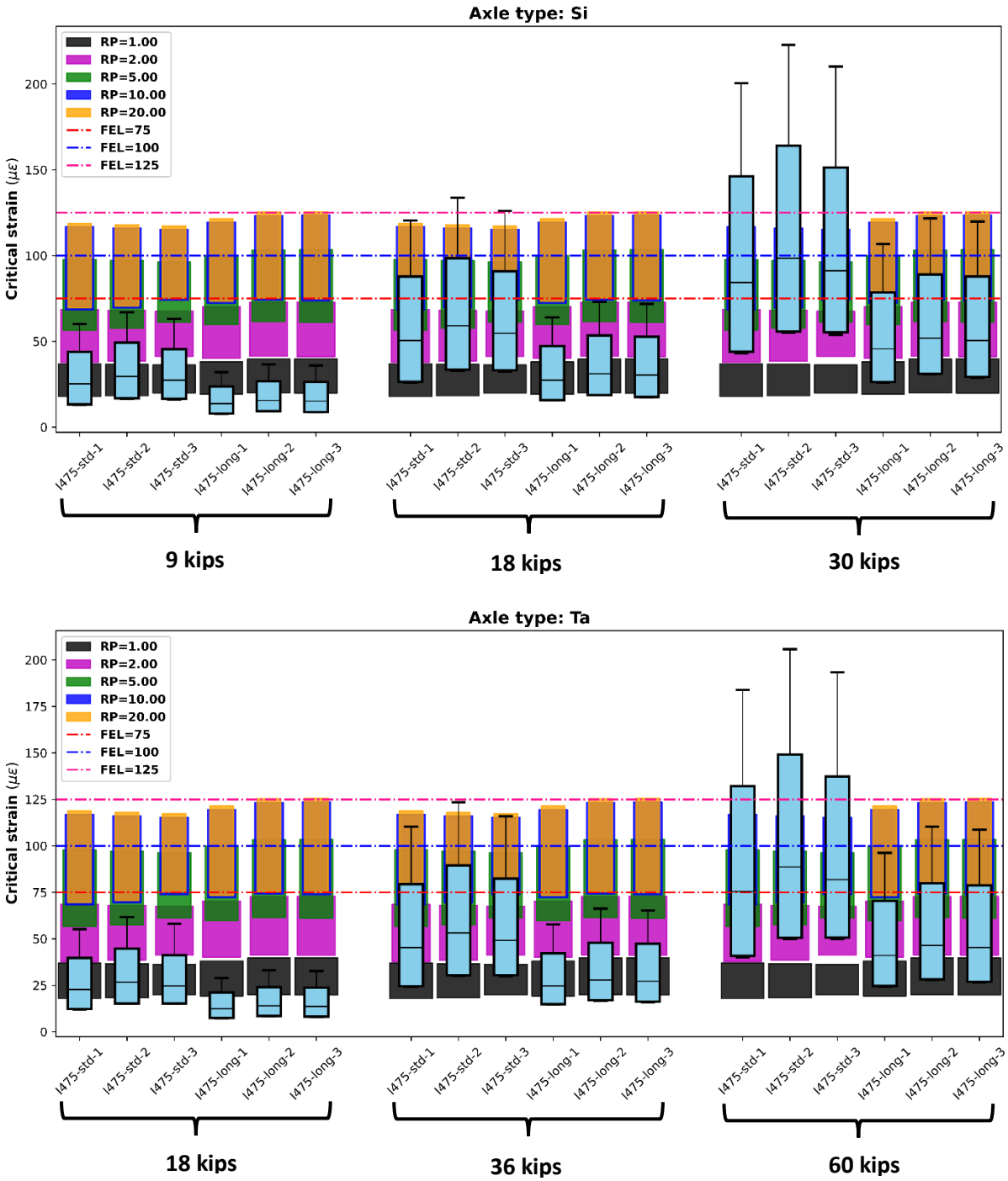

Figure 54 Statistical box plot of critical bottom-up fatigue strains for different pavement structures and axle configurations – I-475: (a) single, (b) tandem, (c) tridem, and (d) quad axles

Figure 54 (cont'd)

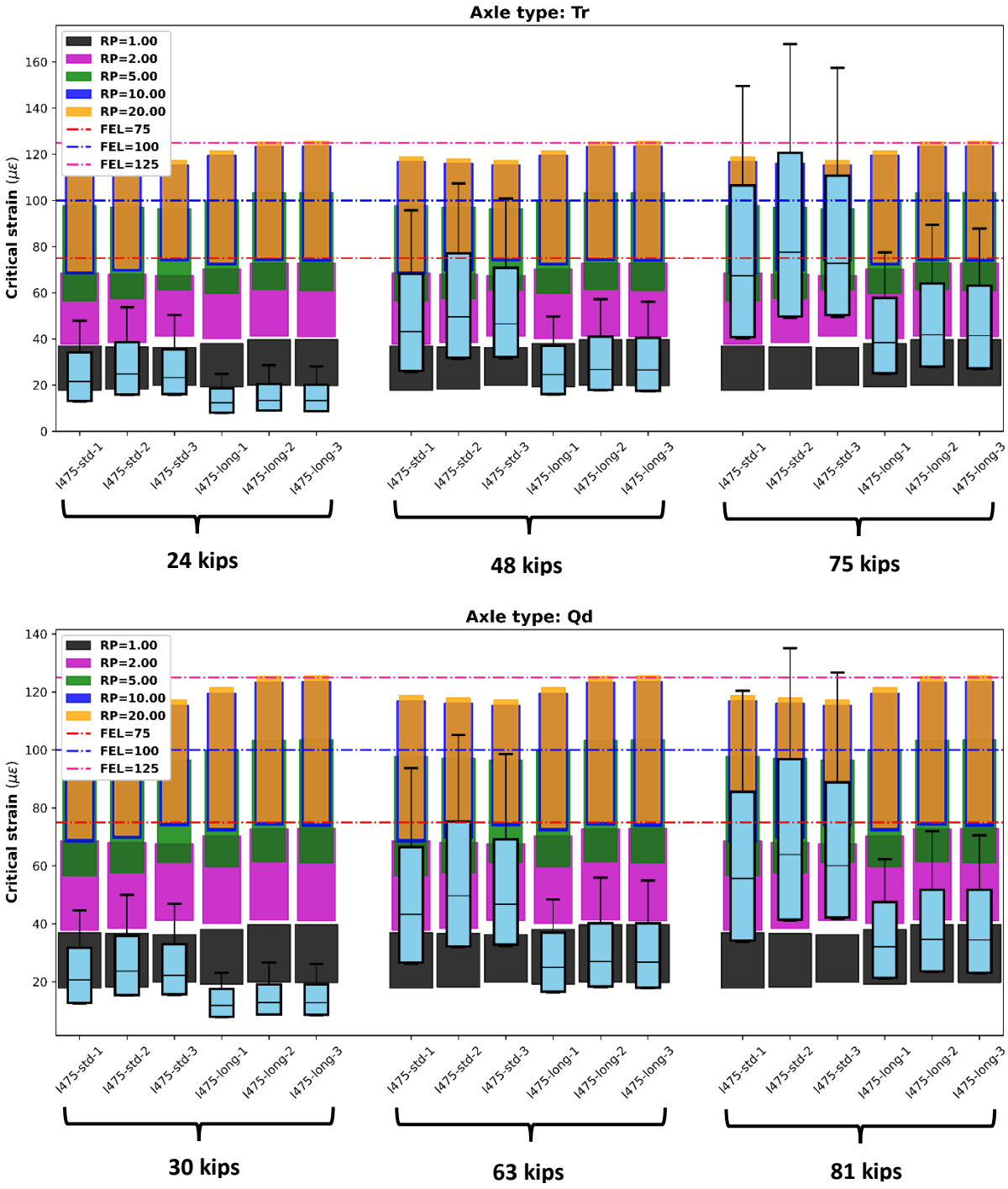

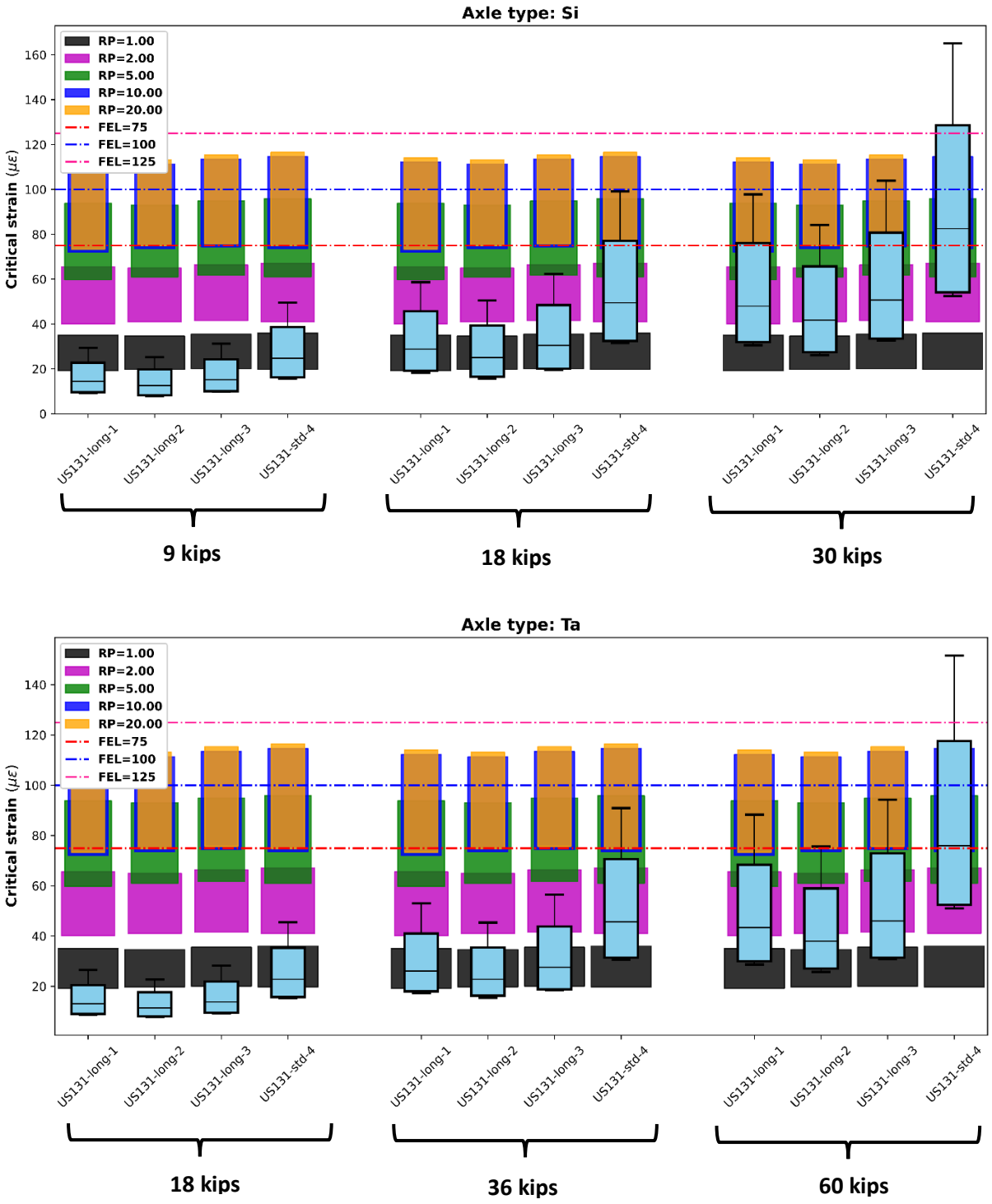

Figure 55 Statistical box plot of critical bottom-up fatigue strains for different pavement structures and axle configurations – US-131: (a) single, (b) tandem, (c) tridem, and (d) quad axles

Figure 55 (cont'd)

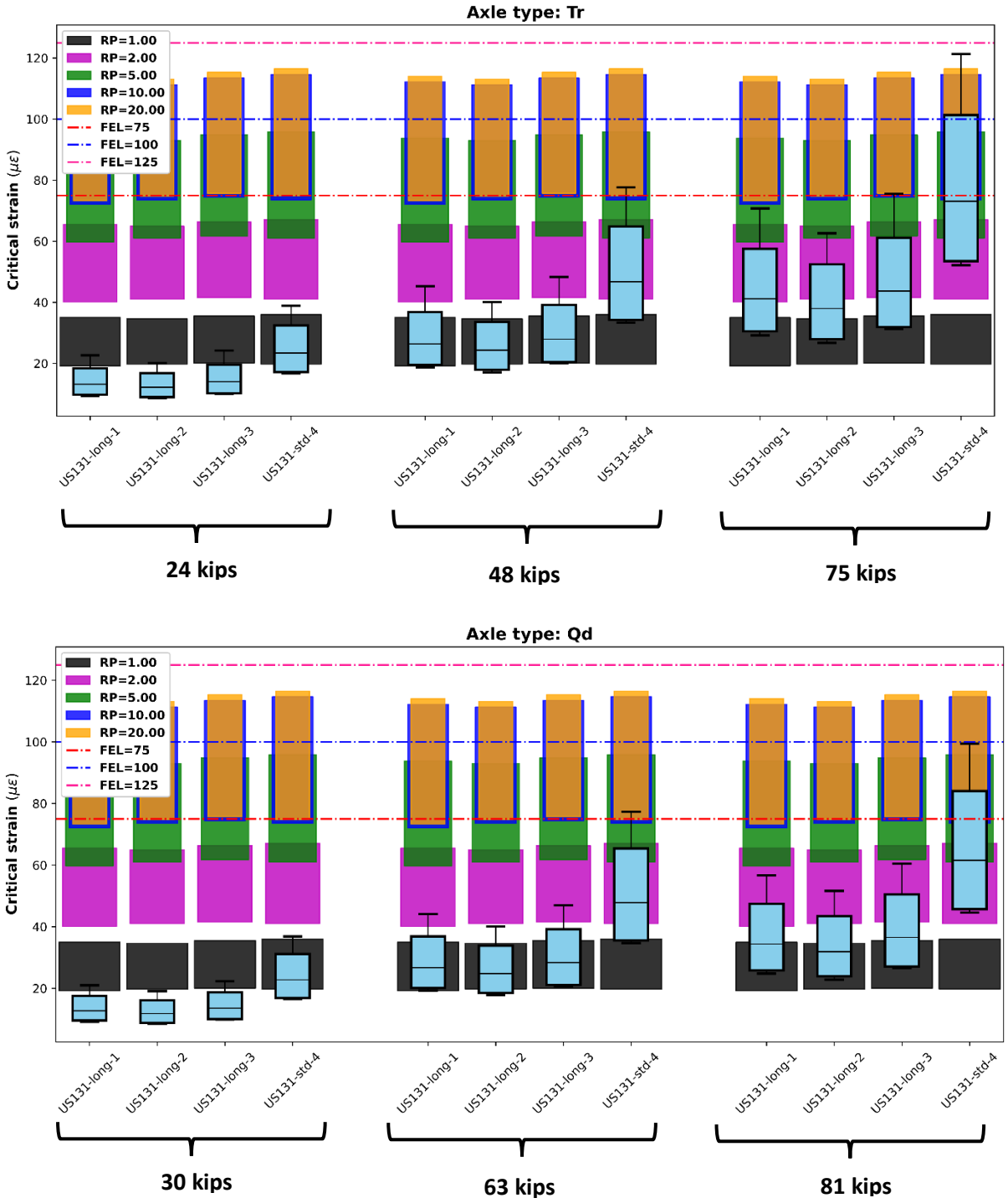

4.4.7 Conclusions

In this chapter, NCHRP 9-44A FEL prediction model was implemented in a mechanistic-empirical asphalt pavements analysis procedure (in this case MEAPA web application) and the impact of implementing FEL concept on the bottom-up fatigue cracking prediction was investigated. For this purpose, in the first phase, three typical road sections in Michigan (representing low-, medium-, and high-traffic volume roads) were analyzed. Five different rest periods of 1.0 s, 2.0 s, 5.0 s, 10.0 s, and 20.0 s as well as three constant FEL values in the range of AASHTOWare Pavement ME software (75 με, 100 με, and 125 με) were used in the analysis. In the second phase of this study the two flexible pilot long-life projects, I-475 and US-131, were analyzed using estimated rest period from the WIM data provided by MDOT. The major findings of this study can be summarized as follows:

- The FEL values calculated with the NCHRP 9-44A model increased with increasing rest periods until a rest period of 10.0 s, after which no further change was observed. In other words, rest periods longer than 10.0 s did not significantly improve healing.
- The recommended range for selecting a single FEL value in AASHTOWare Pavement ME software (75 με to 125 με) were higher than those calculated using the NCHRP 9-44A model, regardless of the rest period.
- The FEL values computed for a given structure in MEAPA exhibited a sinusoidal pattern. This was primarily because of the fluctuations of the pavement layer temperatures in different months and quintiles.
- Implementation of FEL concept had a minimal effect on the predicted bottom-up fatigue cracking of LTV road. However, the fatigue cracking predictions for MTV and HTV roads were significantly affected by the FEL values. It may be concluded that relatively

thick pavements are more significantly affected by the consideration of FEL in the analyses as compared to the thin pavements.

- In terms of the bottom-up fatigue cracking, implementation of the FEL concept resulted in up to 5.3%, 12.2%, and 32.7% reduction in AC layer thicknesses, for LTV, MTV, and HTV roads, respectively.

As mentioned above, the FEL is not a single value and fluctuates during a pavement's life (even for a given structure/material). The use of NCHRP 9-44A FEL prediction model is a reasonable method to estimate the FEL throughout an analysis period. One drawback of this method is the assumption of the duration of a rest period, which is somewhat difficult to estimate. Further studies are needed to find such estimates, perhaps by developing correlations between the field traffic patterns and the rest period.

4.5 CHAPTER 4: DEVELOP AN IMPROVED DESIGN FRAMEWORK FOR FUTURE LONG-LIFE PROJECTS

4.5.1 BACKGROUND

Perpetual or long-life pavements are designed such that there are no deep structural distresses such as bottom-up fatigue cracking and structural rutting throughout the design life. The role of the top layer is to serve as a sacrificial layer to maintain the surficial distresses such as top-down cracking, thermal cracking and asphalt rutting within the top layer of the structure. This sacrificial layer requires periodic surface treatment or replacement during the design life of the pavement. The MDOT flexible pilot long-life projects are relatively thick pavements with Gap Graded Superpave (GGSP) as the top layer. The HMA thickness for I-475 and US-131 long-life sections are 11 and 11.25 inches, respectively. The cross-sections for both standard and long-life sections for I-475 and US-131 are shown in Figure 56 and Figure 57, respectively.

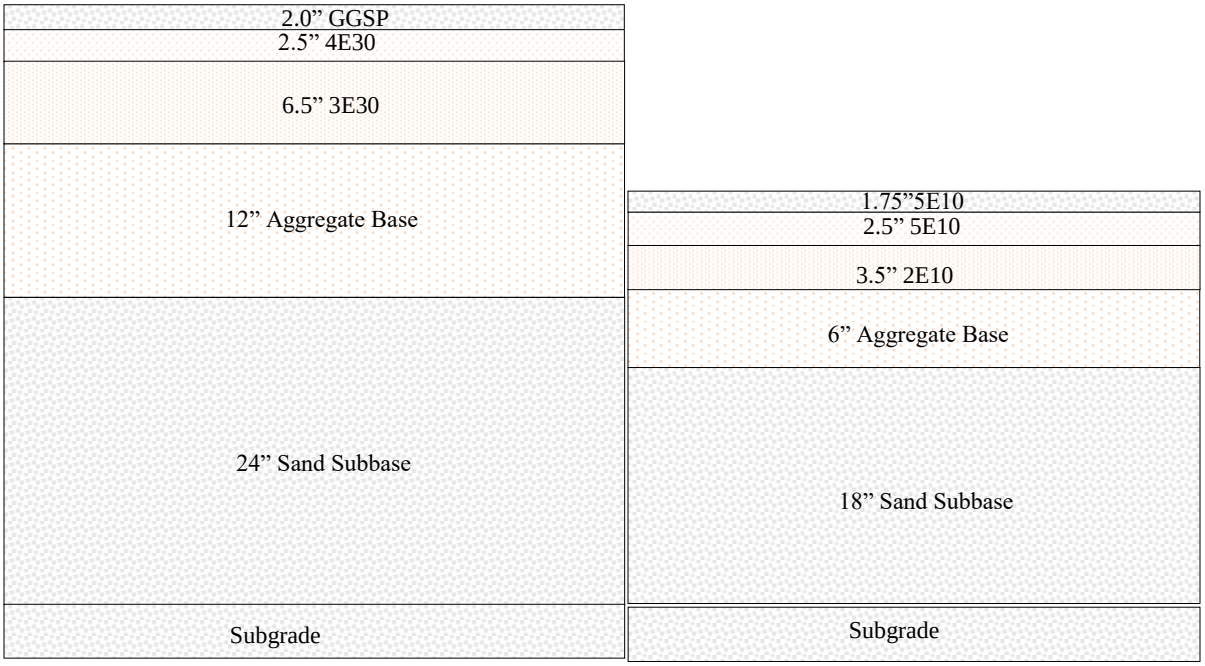

(a) Long-life section

(b) Standard section

Figure 56 Cross-sections – I-475 HMA Project

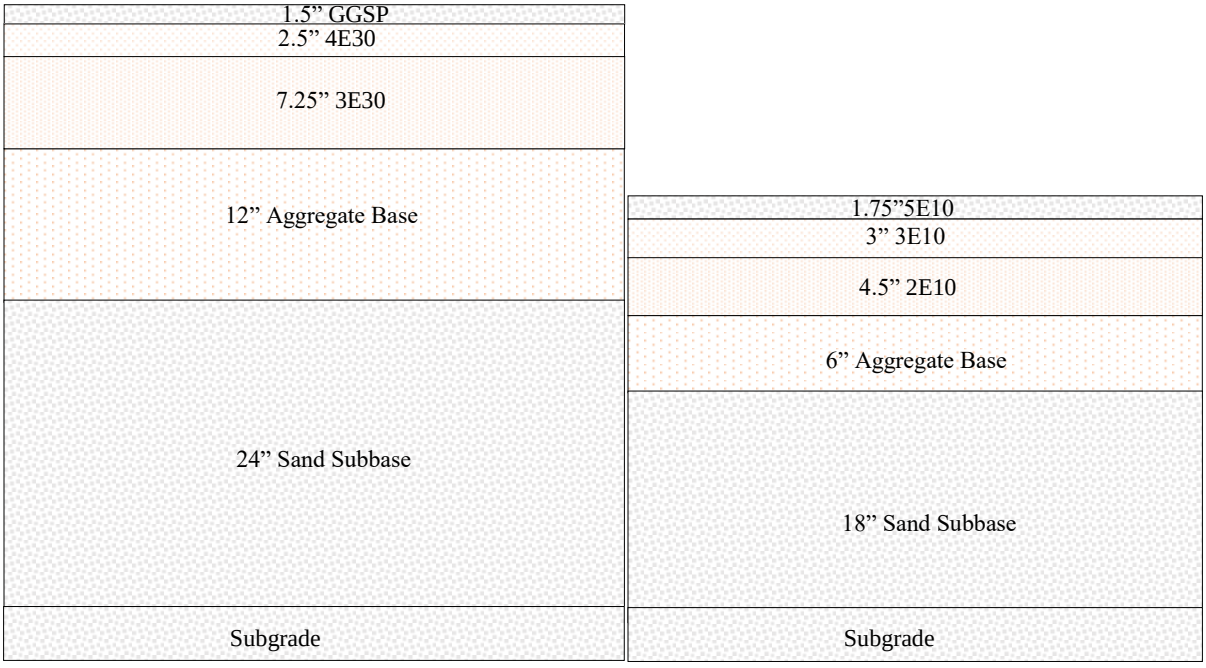

(a) Long-life section

(b) Standard section

Figure 57 Cross-sections US-131 Project

The predicted performance of these two projects with MEAPA 2.0 is presented in Figure 41 and Figure 42. The Level-1 material inputs for the AC layers (i.e., |E*|, |G*|, IDT strength, etc.) and the local calibration coefficients of Michigan have been used for these simulations. The pavement structures were evaluated in MEAPA 2.0 for a design life of 50 years for I-475 and 30 years for US-131 as new flexible pavement. The initial international roughness index (IRI) value of 67 in/mi was used in the analysis. A reliability level of 95% was used in the analysis. Average annual daily truck traffic (AADTT), vehicle class distribution, growth factors, monthly adjustment factors were provided by MDOT.

Based on these results, bottom-up fatigue cracking for long-life sections is relatively low as expected (about to 12 to 14 percent at the end of the design life). In this alternative design method, the pavement will be designed to have minimal bottom-up cracking during the design life with pre-designed periodical rehabilitation (mill & overlay) for the surface layer to mitigate the surface layer distresses. The preliminary results for the pilot flexible long-life projects show that this can be done with reducing the total thickness of the asphalt layer. This reduction in thickness result in lower initial cost for these projects. MDOT's LCCA approach includes periodic maintenance activities based on historical maintenance done on its pavements. For example, on average, first maintenance activity is done at 8 years after the initial construction and Distress Index (DI) reduces by 6 points after the maintenance. There are several other maintenance activities before pavement is allowed to fail, i.e., when DI is equal to 50 (DI = 0 means freshly constructed pavement). A similar approach will be used herein to develop a new design procedure using LCCA approach.

To achieve this goal, the overlay design in MEAPA will be enhanced. Characterization of the existing structure has been a challenge in the overlay design in all mechanistic empirical

pavement analysis software. To simulate the damage in the existing layer in the overlay design in MEAPA, a reduction factor is applied to the modulus of the existing HMA layer based on the condition of the pavement. This reduction results in an accelerated rutting early in the overlay design life and the densification of the existing layer is not considered. As part of this chapter, an anisotropic layered elastic analysis will be implemented in MEAPA to differentiate between the horizontal modulus that contributes to the fatigue cracking (horizontal strain) and the vertical modulus that contributes to rutting (vertical strain). This will lead to improved predictions of the rutting and bottom-up cracking in the overlay design.

4.5.2 Alternative design method

Preliminary results for US-131-TS-3 (see **Figure** 58) show that by decreasing the HMA layers thicknesses to 1.5 “GGSP, 2.0” 4E30 and 5.75” 3E30 (about 18% reduction in the HMA thickness), the bottom-up cracking at the end of the design life is still below the limit. The comparison between the original structure and the structure with the reduced thickness is shown in Figure 58. These results show that the sacrificial layer needs to be milled and overlaid in almost ten years. In this case, top-down cracking is the governing distress for the rehabilitation. This reduction in thickness results in significant savings in terms of materials and initial cost of the pavement.

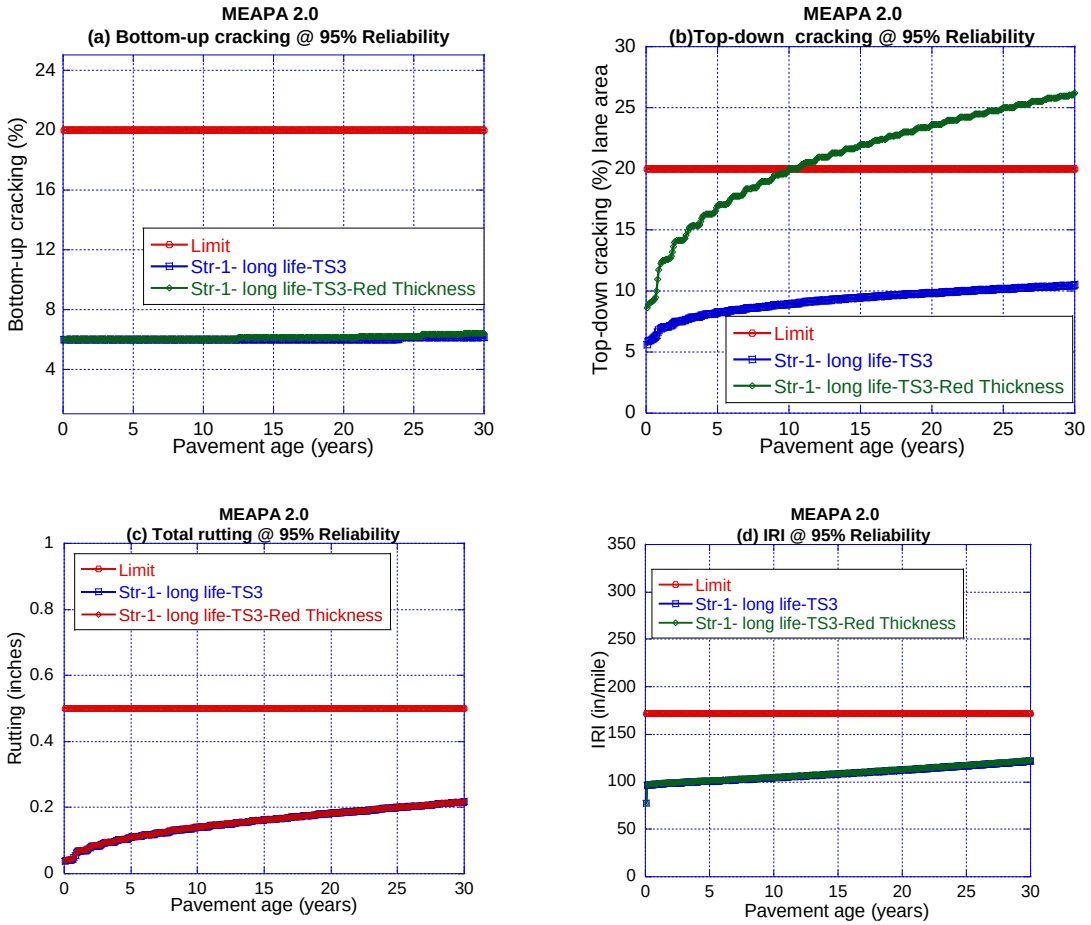

Figure 58 Preliminary results US-131-TS3 – Original structure (11.25") and reduced thickness (9.25")

For achieving more realistic results, the overlay design in MEAPA was enhanced. To simulate the damage in the existing layer in the overlay design in MEAPA, a reduction factor is applied to the modulus of the existing HMA layer based on the condition of the pavement. This reduction results in an accelerated rutting early in the overlay design life and the densification of the existing layer is not considered. As part of this chapter, an anisotropic layered elastic analysis was implemented in MEAPA to differentiate between the horizontal modulus that contributes to the fatigue cracking (horizontal strain) and the vertical modulus that contributes to rutting (vertical strain). For this purpose, two multipliers were used in the overlay design. The E_x-multiplier was defined as a reduction factor to simulate the damage in the existing layer in the

horizontal direction and the E_z-multiplier was defined as an adjustment factor to simulate the densification of the existing layer in the horizontal direction. For the first overlay deign, E_x-multiplier was selected to be 0.9 and the E_z-multiplier was selected to be 1.5. These coefficients were changed to 0.85 and 1.6 for the second overlay design. The results of the predicted distresses for the proposed alternative design method and the original design in 30 years design life are shown in Figure 59.

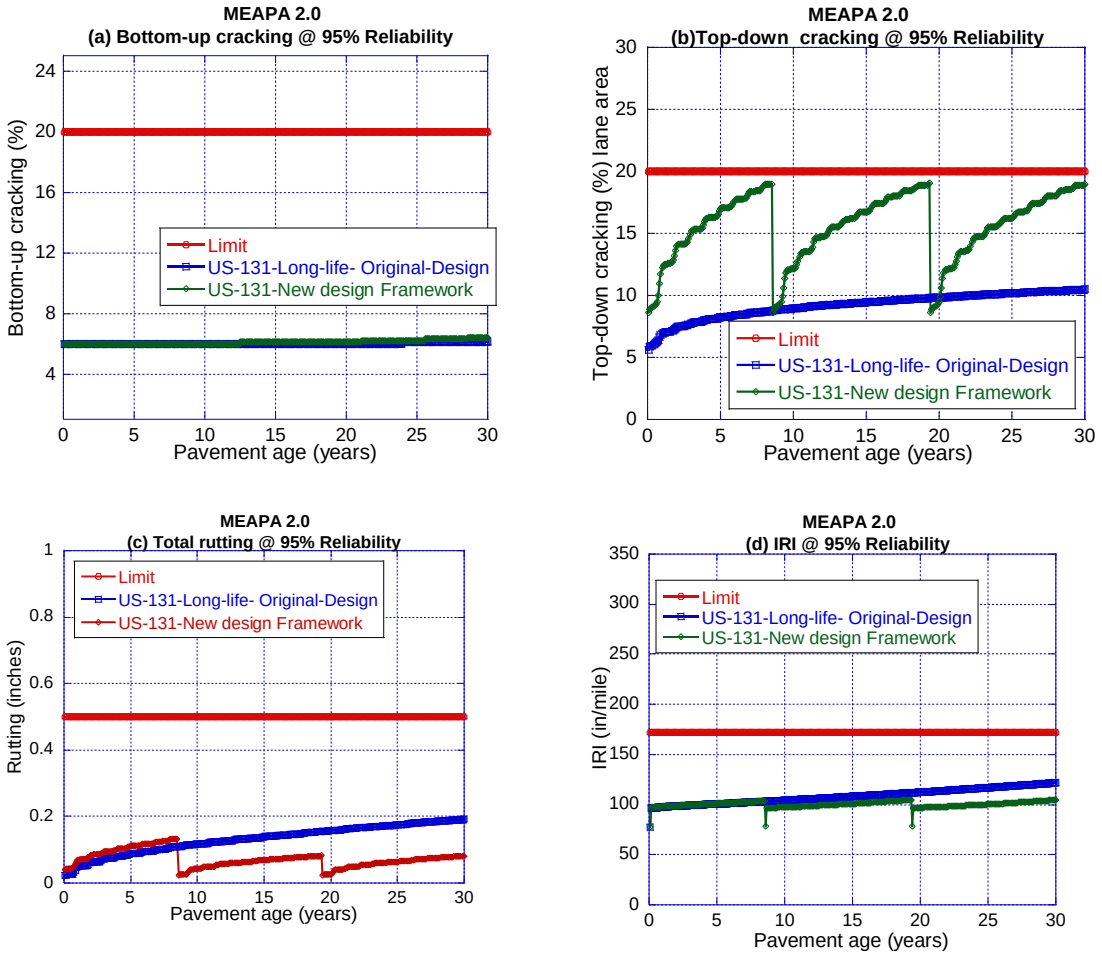

Figure 59 Predicted distresses for the original design and the proposed alternative design method

4.5.3 Simplified LCCA comparison

The cross-section cost (cost for the pavement section per lane mile) and overall cost of these two projects for the long-life and standard sections are listed in Table 46. The proposed design framework has the potential to reduce the difference between the long-life and standard sections and lower the life cycle cost of future long-life projects.

Table 46 Overall Cost and Cross-section Cost for the Pilot Long-life Projects

Project	Design	Cross-Section Cost [1] (per lane mile)	% Difference	Total Project Cost [2]	% Difference
US-131	20 yr. design	$436,550	42.50%	$1,338,765	13.90%
	30 yr. design	$622,195		$1,524,410	
I-475	20 yr. design	$510,354	59.30%	$1,892,846	16.00%
	50 yr. design	$812,875		$2,195,367	

Notes: All costs are per lane-mile of mainline pavement and are from the as-bid results using the bid amounts for the winning bidder.

It should be noted that these cost increases are project specific and should not be used for network analysis. For example, specification enhancements that resulted in increased costs may vary from contractor to contractor depending on their material sources, quality control measures, etc. In particular, the total project costs can vary significantly from project to project depending on the full scope of work involved for each project. Furthermore, the actual performance life of these long-life pavements will not be known until sometime in the future and thus we can only assume that the percentage increase in cost will result in longer life pavement.

1 - Cost for the pavement and shoulder cross-section pay items. I-475 is the only one that includes ramps - all other projects built all the ramps as 20-year designs.

2 - Total project costs include everything but pay items for structures work and lane rental bids. Calculated as: Total bid amount - structures bid amount (if part of the contract) - lane rental bid amount (if part of the contract) - total cross-section costs (all designs). This was then divided by total pavement lane miles. This is the "other costs" amount that is then added to each cross-section cost.

The reduction in thickness, based on the proposed design approach, results in lower initial cost for these projects. According to the alternative design proposed for the US-131 project and the bid amounts for this project, 2” reduction in the HMA structure results in around $55,731 (or about 11%) reduction in the cross-section cost of the US-131 30-year design section. MDOT's LCCA approach includes periodic maintenance activities based on historical maintenance done on its pavements. For example, on average, first maintenance activity is done at 8 years after the initial construction and Distress Index (DI) reduces by 7 points after the maintenance. There are several other maintenance activities before pavement is allowed to fail, i.e., when DI is equal to 50 (DI = 0 means freshly constructed pavement). Table 47 shows this

strategy for a new/reconstructed flexible pavement. The table shows that the service life of a new or reconstructed HMA pavement is 37 years with four preventive maintenance (PM) treatments.

Table 47 New/reconstructed HMA pavement preservation strategy (*62*)

Activity	Approx. age	DI (before)	DI (after)	RSL (yrs) (before fix)	Life (yrs) (extension)	RSL (yrs) (after fix)	Cost/ lane-mile	Time to fix one lane-mile (days)
Initial const.	0	-	0	-	-	18	Computed	-
PM*	8	9	2	10	5	15	$28,071**	0.48
PM	13	9	2	10	5	15	$41,342**	0.63
PM	17	7	1	11	5	16	$44,005**	0.65
PM	22	7	2	11	4	15	$32,411**	0.55
Rehabilitation/ reconstruction	37	-	-	-	-	-	-	-

For a simplified LCCA comparison of the current MDOT's strategy and the proposed design framework, the historical pavement preservation and maintenance data was evaluated to estimate the cost (per lane-mile) of cold milling and overlay for the US-131 project. Based on the average cost of five cold milling and overlay projects on different stretches of US-131, the average cost per mile for the mill and overlay on the US-131 was estimated to be $65,176. Based on this estimation the proposed pavement rehabilitation/preservation plan is presented in Table 48.

Table 48 Rehabilitation/preservation strategy for the proposed design framework

Activity	Approx. age	DI (before)	DI (after)	Life (yrs) (extension)	RSL (yrs) (after fix)	Cost/ lane-mile
Initial const.	0	-	0	-	18	Computed
Cold milling & Overlay	9	9	2	10	15	$65,176
Cold milling & Overlay	20	9	2	10	15	$65,176
Cold milling & Overlay	30	7	1	10	15	$65,176
Rehabilitation/ reconstruction	40	-	-	-	-	-

Comparison of the two scenarios leads to total cost of $768,024 per lane-mile for the original design for a service life of 37 years (initial cost and maintenance costs) and a total cost of $761,992 per lane-mile for the propose design approach for a service of 40 years. It also should be noted that the number of maintenance/rehab events in the proposed design approach is less than the current MDOT's practice. This might have significant effect on the user-delay costs.

5 CONCLUSIONS

The scope of this study included a thorough analysis of pilot long life pavement projects constructed by MDOT near Grand Rapids and Flint, MI. Field data collected after the construction of the projects (e.g., Light Weight Deflectometer, Falling Weight Deflectometer, Dynamic Cone Penetrometer) were analyzed and evaluated. Material samples were collected from different layers of the pavements (HMA, base, subbase and subgrade) were tested in the laboratory. HMA testing program included unconfined and confined dynamic modulus, flow number, three-point bending fatigue and indirect tensile strength (IDT) at low temperatures. Base, subbase and subgrade materials were tested for their index properties and resilient modulus. All the data gathered in the laboratory was used as Level 1 input to the mechanistic-empirical (ME) models. Three different ME models were used to forecast the performance of the long-life projects: AASHTOWARE Pavement ME, MEAPA and PerRoad. Furthermore, new methods of designing long life pavements were proposed and they will be investigated during the remaining part of this study. A list of general conclusions based on the data and observations gathered during this project are summarized in the subsections below.

5.1 Structural design improvements

Long life pavements were designed as thick pavements with no potential for bottom-up cracking. This goal was indeed achieved because the Pavement ME software predicted no bottom-up cracking. In addition, the strain distribution predicted by PerRoad software was significantly lower than the thresholds. Therefore, it is highly unlikely that any bottom-up cracking will develop in these pavements during their service lives.

5.2 Material improvements

Laboratory dynamic modulus, fatigue, rutting and indirect tensile strength experiments all showed better performance of the GGSP and 4E30 mixtures, over their standard counterparts (5E10 and 3E10). The main reasons for this superior performance are probably the use of the polymer modified binder, limiting the amount of recycled materials and high film thickness (>9microns) in GGSP and 4E30. Another reason could be the use of higher quality aggregates that are specified in E30 and GGSP mixtures. In future long-life projects, in surface layer, it is strongly recommended to use polymer modified binder, limit the RAP/RAS to Tier 1, specify high film thickness (>9microns) and use E30 (or higher mixtures, i.e., follow the aggregate specs that come along with E30 and higher mixtures).

In RITF report, it was recommended to have fines/effective binder ratio < 1.2. However, the GGSP performed exceptionally well in lab tests (fatigue, rutting, and low-temperature cracking) even though its fines/effective binder ratio was greater than 1.2. Therefore, this RITF report recommendation probably does not apply to GGSP (or similar Stone Matrix Asphalt) mixtures.

5.3 Construction-related improvements

In-place HMA density was recommended in the RITF report to be greater than 93% Gmm. This was achieved in all layers of I-475 but only leveling and base layers of US-131. The top GGSP layer had an in-place density of 91.6% (i.e., air voids of 8.4%) on average. It is recommended to monitor the performance of the top GGSP layer in US-131 and potentially consider one of the pavement preservation treatments (e.g., spray-on rejuvenator, micro-surfacing, etc.) to minimize the potential effect of high air voids.

It appeared that sufficient joint density was achieved in both I-475 and US-131 projects, probably because of the echelon paving of the surface (GGSP) layer. Echelon paving of the surface layer is strongly recommended to be implemented in future long-life projects.

Designing outside lane at 14 ft instead of 12 ft would potentially have increased wheel wander standard deviation and reduce the rate of damage accumulation. However, the impact of wheel wander standard deviation in Pavement ME simulation results is not very significant (see Figure 60 and Figure 61). Therefore, the wider outside lane is probably not needed. So, keeping the I-475 and US-131 pavement lanes 12' wide was a good decision.

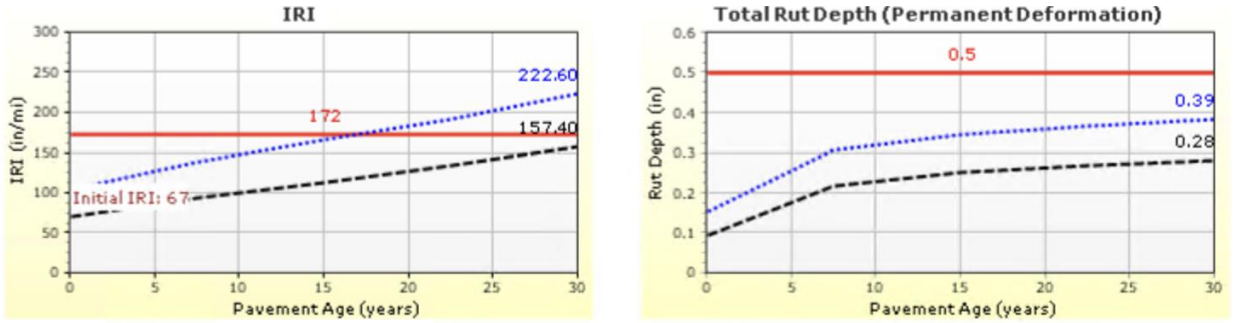

Figure 60 US-131-long-life-TS1: wheel wander standard deviation = 10"

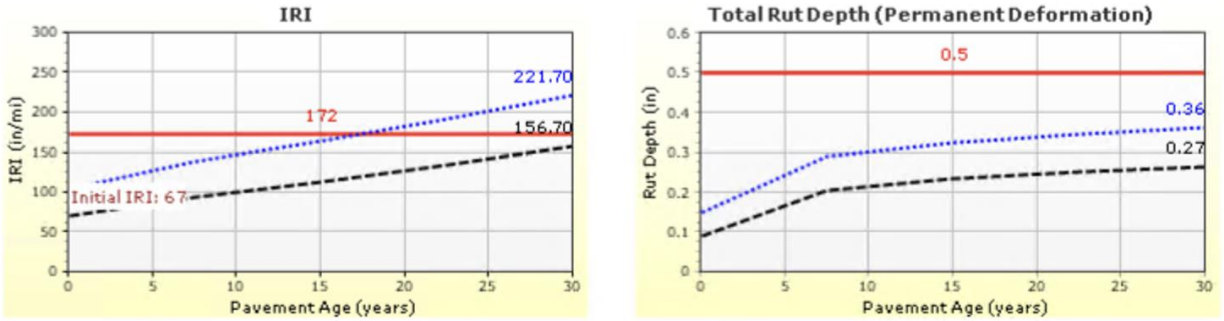

Figure 61 US-131-long-life-TS1: wheel wander standard deviation = 20"

Intelligent compaction was not used in any of the projects. Intelligent compaction would have probably reduced the variability of in-place air voids. In I-475 and US-131 projects, coefficient of variation (COV = standard deviation/mean) of core air voids ranged from 9% to

21%. While these COV values are not very large, potentially lower COV of air voids (i.e., more uniformity) could have been achieved with intelligent compaction.

5.4 QC/QA improvements for both flexible and rigid long-life pavements

The RITF report recommended tightening Percent Within Limits (PWL) requirements for QC/QA testing. For long life pavements, it was recommended to specify remove/replace when PWL<75 and when PWL<90 for 30- and 50-year design, respectively. Although this was not done in these projects and MDOT's standard PWL specs were used, the reviewed QC/QA data did not lead to a specific concern regarding the quality control/quality assurance.

5.5 Initial Costs

The initial costs per mile of the long-life pavements and their standard counterparts are shown in Table 49. As shown, based on cross-section cost only, long-life pavements were more expensive by 42.5% to 59.4%. However, focusing on cross-section costs may be misleading. Based on the total project cost (per lane mile), the difference ranged from 13.9% to 16.0%. Total project cost can be considered cross-section costs plus the "other costs" needed to construct that cross section. Since a pavement cannot be constructed without the "other costs", "other costs" will be paid regardless of whether long-life or standard cross sections are selected. Since the "other costs" are quite significant, selecting a long-life cross-section over a standard cross-section does not change the overall cost significantly.

Table 49 also shows the expected lives without maintenance (fix life) based on Pavement ME simulations. As shown, the difference in expected life is significantly higher than the difference in the total project costs. Therefore, long-life pavements are expected to be more cost-effective than the standard counterparts. An accurate life cycle cost analysis cannot be performed

because of a lack of actual performance data, when the maintenance treatments would be applied to these pavements, and how those treatments would extend their lives.

Table 49 Long-life pilot projects initial costs per lane mile

Project	Design (yr.)	Cross-Section Cost[1]	% Difference (Cross-Section Cost1)	Total Project Cost[2]	% Difference (Total Project Cost)	Expected Life Pavement ME* (yr.)	% Difference (Expected Life)
US-131 30 Year HMA	20	$436,550	42.5%	$1,338,765	13.9%	27	22.2%
	30	$622,195		$1,524,410		33	
	30	$820,829		$2,279,626		50	
I-475 50 Year HMA	20	$510,354	59.3%	$1,892,846	16.0%	26	42.3%
	50	$812,875		$2,195,367		37	

Notes: All costs are per lane-mile of mainline pavement and are from the as-bid results using the bid amounts for the winning bidder.

It should be noted that these cost increases are project specific and should not be used for network analysis. For example, specification enhancements that resulted in increased costs may vary from contractor to contractor depending on their material sources, quality control measures, etc. In particular, the total project costs can vary significantly from project to project depending on the full scope of work involved for each project. Furthermore, the actual performance life of these long-life pavements will not be known until sometime in the future and thus we can only assume that the percentage increase in cost will result in longer life pavement.

1 - Cost for the pavement and shoulder cross-section pay items. I-475 is the only one that includes ramps - all other projects built all the ramps as 20-year designs.

2 - Total project costs include everything but pay items for structures work and lane rental bids. Calculated as: Total bid amount - structures bid amount (if part of the contract) - lane rental bid amount (if part of the contract) - total cross-section costs (all designs). This was then divided by total pavement lane miles. This is the "other costs" amount that is then added to each cross-section cost.

3 - The expected lives shown in this table are predicted values and it is too early to determine if these are accurate estimates.

5.6 Comments on Future Testing

The LWD data did not provide useful information regarding modulus of the layers, therefore, running this test is not recommended. The DCP data provided reasonable results only in certain sections, and in other sections, the DCP results were not useful to derive the modulus of the layers. While these tests may be useful to assess the relative variability at different locations along a project length, they are not very useful to estimate moduli of unbound layers,

especially for the purpose of using ME analyses. Pavement ME versions 2.3 and 2.6, Mechanistic Empirical Asphalt Pavement Analysis, and PerRoad software have been used to analyzed the long-life and standard test sections of the pilot projects. The analysis has been done for 50 years for the long-life sections and 30 years for the standard sections

FWD backcalculations did provide reasonable moduli, but, because of limitations of existing backcalculation algorithms, sublayer (HMA top, HMA intermediate, HMA base, unbound base, subbase and subgrade, etc.) moduli could not be obtained. Therefore, FWD is also not very useful to obtain moduli of individual sublayers, for the purpose of performing ME analyses. But FWD may be very useful tool to identify the variations on the structural capacity of different spatial locations along a pavement project.

Instead of intense testing of LWD, DCP and FWD, MDOT should consider collecting material samples from different layers and perform laboratory testing. These tests include HMA |E*|, unbound layer M_R, concrete compressive strength, modulus of rupture and CTE. Sampling frequency can be determined based on the expected variations on the 'batches' of materials transported to the site, as well as the project length. The ongoing 'testing protocol and ME recalibration' project will provide more recommendations on the testing intervals.

BIBLIOGRAPHY

1. Newcomb, D. Perpetual Pavements-A Synthesis. 2002.

2. Harvey, J., C. Monismith, R. Horonjeff, M. Bejarano, B. W. Tsai, and V. Kannekanti. Long-Life AC Pavements: A Discussion of Design and Construction Criteria Based on California Experience. 2004.

3. European Asphalt Pavement Association. Long-Life Asphalt Pavements - Technical Version. 2007.

4. Hall, K., D. Dawood, S. Vanikar, R. Tally Jr, T. Cackler, A. Correa, P. Deem, J. Duit, G. Geary, A. Gisi, A. Hanna, S. Kosmatka, R. Rasmussen, S. Tayabji, and G. Voigt. Long-Life Concrete Pavements in Europe and Canada. 2007.

5. Mahoney, J. P. Study of Long-Lasting Pavements in Washington State. Transportation Research Circular, Vol. 503, 2001, pp. 88–95.

6. Tarefder, R. A., and D. Bateman. Design of Optimal Perpetual Pavement Structure. Journal of Transportation Engineering, Vol. 138, No. 2, 2011, pp. 157–175. https://doi.org/10.1061/(ASCE)TE.1943-5436.0000259.

7. Romanoschi, S. A., A. J. Gisi, M. Portillo, and C. Dumitru. First Findings from the Kansas Perpetual Pavements Experiment. Transportation Research Record, No. 2068, 2008, pp. 41–48. https://doi.org/10.3141/2068-05.

8. St Martin, J., J. T. Harvey, F. Long, E. B. Lee, C. L. Monismith, and K. Herritt. Long-Life Rehabilitation Design and Construction: I-710 Freeway, Long Beach, California. Transportation Research Circular, No. 503, 2001.

9. Thompson, M., and S. Carpenter. Considering Hot-Mix-Asphalt Fatigue Endurance Limit in Full-Depth Mechanistic-Empirical Pavement Design. Urbana, Vol. 51, 2006, pp. 61801–2350.

10. Timm, D., and D. Newcomb. Perpetual Pavement Design for Flexible Pavements in the US. International Journal of Pavement Engineering - INT J PAVEMENT ENG, Vol. 7, 2006, pp. 111–119. https://doi.org/10.1080/10298430600619182.

11. Walubita, L. F., T. Scullion, and Texas Transportation Institute. Texas Perpetual Pavements: New Design Guidelines. Publication 0-4822-P6. 2010.

12. Harm, E. Illinois Extended-Life Hot-Mix Asphalt Pavements. Transportation Research Circular, Vol. 503, 2001, pp. 108–112.

13. Tayabji, and Lim. Long-Life Concrete Pavements: Best Practices and Directions from the States. Publication FHWA-IF-07-030. 2007.

14. Newcomb, D. E., M. Buncher, and I. J. Huddleston. Concepts of Perpetual Pavements.

15. Curtis Bleech. Roads Innovation Task Force Report. Michigan Department of Transportation, 2016.

16. Carpenter, S. H., K. A. Ghuzlan, and S. Shen. Fatigue Endurance Limit for Highway and Airport Pavements. Transportation research record, Vol. 1832, No. 1, 2003, pp. 131–138.

17. Von Quintus, H. Application of the Endurance Limit Premise in Mechanistic-Empirical Based Pavement Design Procedures. Presented at the International Conference on Perpetual Pavements, Columbus, Ohio, 2006.

18. Monismith, C. L., and F. Long. Overlay Design for Cracked and Seated Portland Cement Concrete (PCC) Pavement--Interstate Route 710. 1999.

19. Peterson, R. L., P. Turner, M. Anderson, and M. Buncher. Determination of Threshold Strain Level for Fatigue Endurance Limit in Asphalt Mixtures. Presented at the International Symposium on Design and Construction of Long-Lasting Asphalt Pavements, 2004, Auburn, Alabama, USA, 2004.

20. Swamy, A. K. Validating the Fatigue Endurance Limit for Hot Mix Asphalt. 2010.

21. Willis, J. R. Field-Based Strain Thresholds for Flexible Perpetual Pavement Design. 2009.

22. Witczak, M., M. Mamlouk, M. Souliman, and W. Zeiada. Laboratory Validation of an Endurance Limit for Asphalt Pavements. NCHRP Report, No. 762, 2013.

23. Molenaar, A and van de VerPoot, MR and Liu, X and Scarpas, A and Scholten, EJ and Klutz, R. Modified Base Courses for Reduced Pavement Thickness and Increased Longevity. 2009.

24. Crovetti, J. Analysis of Load-Induced Strains in a Hot Mix Asphalt Perpetual Pavement. Transportation Reports with the Wisconsin Department of Transportation, 2009.

25. Materials Characterization and Analysis of the Marquette Interchange HMA Perpetual Pavement. Midwest Regional University Transportation Center, 2008.

26. Monismith, CL and Long, F. Mix Design and Analysis and Structural Section Design for Full Depth Pavement for Interstate Route 710. 1999.

27. Kassem, E., L. Walubita, T. Scullion, E. Masad, and A. Wimsatt. Evaluation of Full-Depth Asphalt Pavement Construction Using X-Ray Computed Tomography and Ground Penetrating Radar. Journal of Performance of Constructed Facilities, Vol. 22, No. 6, 2008, pp. 408–416. https://doi.org/10.1061/(ASCE)0887-3828(2008)22:6(408).

28. Vavrik, W. R., W. J. Pine, and S. H. Carpenter. Aggregate Blending for Asphalt Mix Design: Bailey Method. Transportation Research Record, Vol. 1789, No. 1, 2002, pp. 146–153. https://doi.org/10.3141/1789-16.

29. Newcomb, D. E., D. H. Timm, and J. R. Willis. Perpetual Pavements: A Manual of Practice. 2020.

30. Harvey, J., F. Long, and J. A. Prozzi. Applications of CAL/APT Results to Long Life Flexible. 1999.

31. Harmelink, D., S. Shuler, and T. Aschenbrener. Top-down Cracking in Asphalt Pavements: Causes, Effects, and Cures. Journal of Transportation Engineering, Vol. 134, No. 1, 2008, pp. 1–6.

32. Lu, L., D. Wang, and X. Than. Predicted Model of Asphalt Pavement Non-Segregated Zone. 2007.

33. Willis, J. R., and D. H. Timm. Forensic Investigation of Debonding in Rich Bottom Pavement. Transportation research record, Vol. 2040, No. 1, 2007, pp. 107–114.

34. Brown, E. R. Basics of Longitudinal Joint Compaction. Transportation Research Circular, EC105, Factors Affecting Compaction of Asphalt Pavements, 2006, pp. 86–95.

35. Vennapusa, P., and D. White. Comparison of Light Weight Deflectometer Measurements for Pavement Foundation Materials. Geotechnical Testing Journal, Vol. 32, No. 3, 2009, pp. 1–13. https://doi.org/10.1520/GTJ101704.

36. Seitllari, A., M. Hasnat, and M. E. Kutay. Development of Three Point Bending Cylinder (3PBC) Asphalt Mixture Fatigue Test System. NCHRP-IDEA Program Project Final Report, No. 218, 2022.

37. Seitllari, A., and M. Kutay. Development of 3-Point Bending Beam Fatigue Test System and Implementation of Viscoelastic Continuum Damage (VECD) Theory. J Assoc Asphalt Paving Technol, Vol. 88, 2019, pp. 783–810.

38. Kim, Y. R., H.-J. Lee, and D. N. Little. FATIGUE CHARACTERIZATION OF ASPHALT CONCRETE USING VISCOELASTICITY AND CONTINUUM DAMAGE THEORY (WITH DISCUSSION). In Asphalt Paving Technology 1997Association of Asphalt Paving Technologists (AAPT), No. 66, 1997.

39. Kutay, M. E., N. H. Gibson, and J. Youtcheff. Conventional and Viscoelastic Continuum Damage (VECD)-Based Fatigue Analysis of Polymer Modified Asphalt Pavements (With Discussion). In Asphalt Paving Technology 2008, No. 77, 2008.

40. Kutay, M. E., and M. Lanotte. Viscoelastic Continuum Damage (VECD) Models for Cracking Problems in Asphalt Mixtures. International Journal of Pavement Engineering, Vol. 19, No. 3, 2018, pp. 231–242. https://doi.org/10.1080/10298436.2017.1279492.

41. Laboratory Determination of Resilient Modulus for Flexible Pavement Design. Transportation Research Board, Washington, D.C., 2004.

42. Witczak, M., M. Mamlouk, M. Souliman, and W. Zeiada. Laboratory Validation of an Endurance Limit for Asphalt Pavements. NCHRP Report, No. 762, 2013.

43. Monismith, C. C., and D. B. McLean. Structural Design Considerations. Road, Journal of the Road Engineering Association, Vol. 1, No. 1, 1976.

44. Thompson, M. R., and S. H. Carpenter. Considering Hot-Mix-Asphalt Fatigue Endurance Limit in Full-Depth Mechanistic-Empirical Pavement Design. 2006.

45. Carpenter, S. H., and S. Shen. Effect of Mixture Variables on the Fatigue Endurance Limit for Perpetual Pavement Design. Columbus, Ohio, 2009.

46. Bhattacharjee, S., A. K. Swamy, and J. S. Daniel. Application of Elastic–Viscoelastic Correspondence Principle to Determine Fatigue Endurance Limit of Hot-Mix Asphalt. Transportation Research Record, Vol. 2126, No. 1, 2009, pp. 12–18. https://doi.org/10.3141/2126-02.

47. Nishizawa, T., S. Shimeno, and M. Sekiguchi. Fatigue Analysis of Asphalt Pavements with Thick Asphalt Mixture Layer. 1997.

48. Wu, Z., Z. Q. Siddique, M. Hossain, and A. J. Gisi. Kansas Turnpike: An Example of Long-Lasting Asphalt Pavement. 2004.

49. Shen, S., and S. H. Carpenter. Application of the Dissipated Energy Concept in Fatigue Endurance Limit Testing. Transportation Research Record, Vol. 1929, No. 1, 2005, pp. 165–173. https://doi.org/10.1177/0361198105192900120.

50. Zeiada, W. A., M. I. Souliman, K. E. Kaloush, and M. Mamlouk. Endurance Limit for HMA Based on Healing Concept Using Uniaxial Tension-Compression Fatigue Test. Journal of Materials in Civil Engineering, Vol. 26, No. 8, 2014, p. 04014036. https://doi.org/10.1061/(ASCE)MT.1943-5533.0000917.

51. Wu, Z., Z. Q. Siddique, M. Hossain, and A. J. Gisi. Kansas Turnpike: An Example of Long-Lasting Asphalt Pavement. Presented at the International Symposium on Design and Construction of Long-Lasting Asphalt Pavements, 2004, Auburn, Alabama, USA, 2004.

52. Zeiada, W. A., B. S. Underwood, and K. E. Kaloush. Impact of Asphalt Concrete Fatigue Endurance Limit Definition on Pavement Performance Prediction. International Journal of Pavement Engineering, Vol. 8436, 2017, pp. 1–12. https://doi.org/10.1080/10298436.2015.1127372.

53. Tutu, K. A., and D. H. Timm. Asphalt Fatigue Endurance Limit Estimation and Impact on Perpetual Pavement Design. International Journal of Pavement Engineering, 2020, pp. 1–9. https://doi.org/10.1080/10298436.2020.1797735.

54. Ghazavi, M., A. Seitllari, and M. E. Kutay. Performance Evaluation of Long-Life Pavements Using the Mechanistic-Empirical Asphalt Pavement Analysis (MEAPA) Web Application. 2020.

55. Kutay, M., and M. Lanotte. Formulations of the Pavement Performance Prediction Models in the Mechanistic-Empirical Asphalt Pavement Analysis (MEAPA) Web Application.

56. Kutay, M. E., M. Hasnat, and E. Levenberg. Layered Nonlinear Cross Anisotropic Model for Pavements with Geogrids. 2020.

57. Khazanovich, L., and Q. (Chuck) Wang. MnLayer: High-Performance Layered Elastic Analysis Program. Transportation Research Record, Vol. 2037, No. 1, 2007, pp. 63–75. https://doi.org/10.3141/2037-06.

58. Dempsey, B. J. A HEAT-TRANSFER MODEL FOR EVALUATING FROST ACTION AND TEMPERATURE RELATEDEFFECTS IN MULTILAYERED PAVEMENT SYSTEMS. University of Illinois at Urbana-Champaign, 1969.

59. Alam-Khan, S., B. Cetin, B. A. Forman, M. E. Kutay, S. Durham, and C. W. Schwartz. Evaluation of Shortwave and Longwave Radiation Models for Mechanistic-Empirical Pavement Analysis. International Journal of Pavement Engineering, Vol. 0, No. 0, 2021, pp. 1–11. https://doi.org/10.1080/10298436.2021.1895155.

60. Nchrp. Guide for Mechanistic-Empirical Design of New and Rehabilitated Pavement Structures, Appendix Ll-1: Calibration of Fatigue Cracking Models for Flexible Pavements. Transportation Research Board of the National Research Council, No. February, 2004, p. 311. http://pubsindex.trb.org/view.aspx?id=703699.

61. AASHTO. Mechanistic-Empirical Pavement Design Guide: A Manual of Practice. AASHTO, 2020.

62. Pavement Selection Manual, Michigan Department of Transporayion,2021.

APPENDIX A |G*| MASTERCURVES

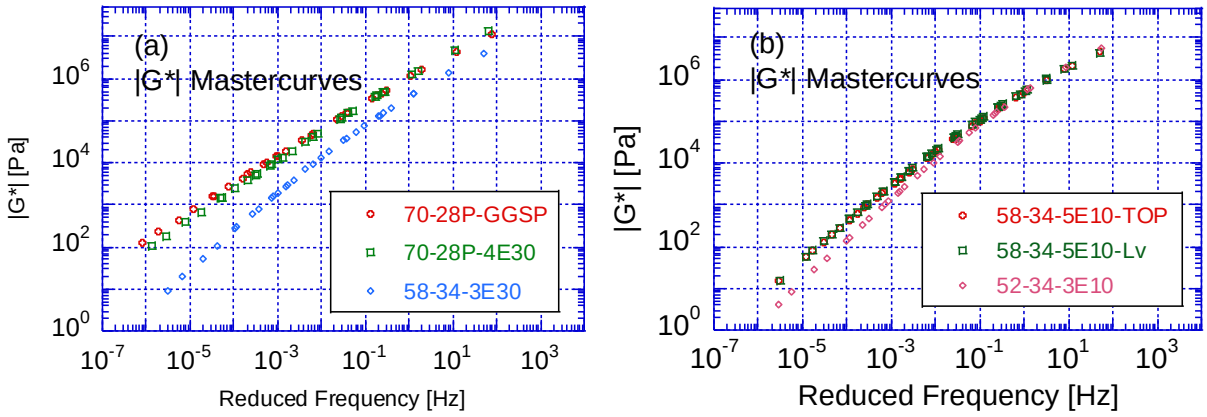

Figure B- 1 |G*| master curves for RTFO aged binders for I-475: a) 70-28P and 58-34 (Long-life section binders), b) PG 58-34 and 52-34 (Standard section binders)

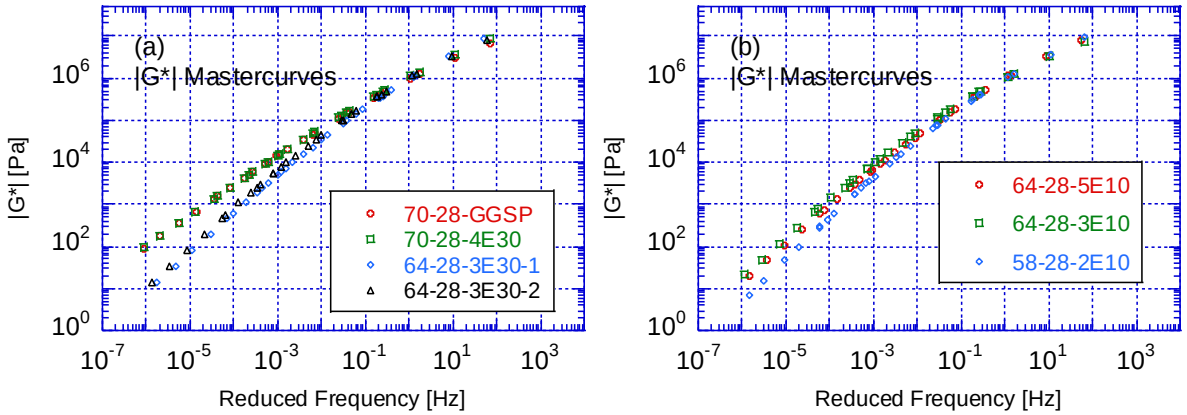

Figure B- 2 |G*| master curves for RTFO aged binders for US-131: a) 70-28P and 64-28 (Long-life section binders), b) PG 64-28 and 58-28 (Standard section binders)

APPENDIX B |E*| MASTERCURVES

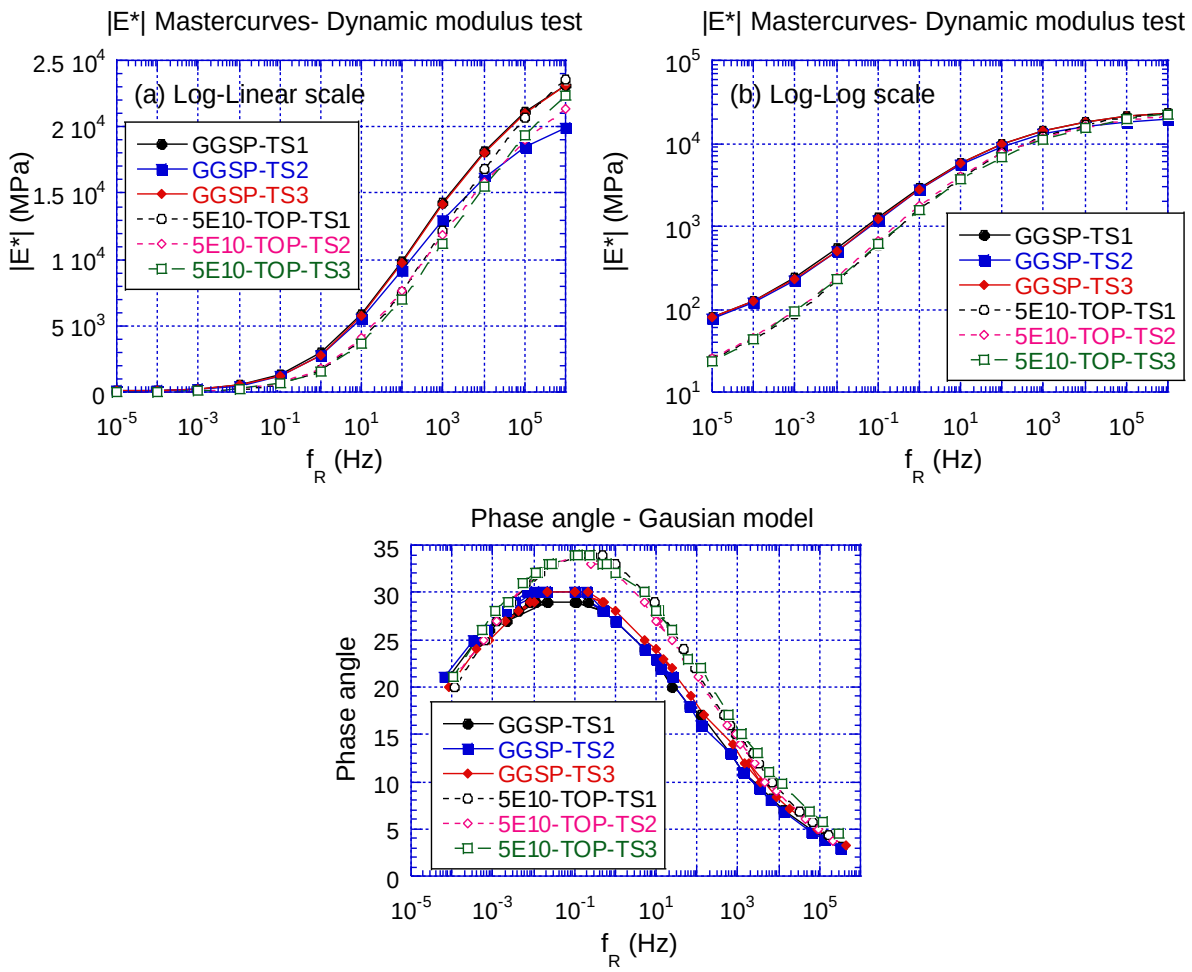

Figure C- 1 Comparison of |E*| master curves of the top courses for the I-475 long-life and the standard sections: (a) Log-Linear Scale, (b) Log-Log Scale, (c) Phase angle

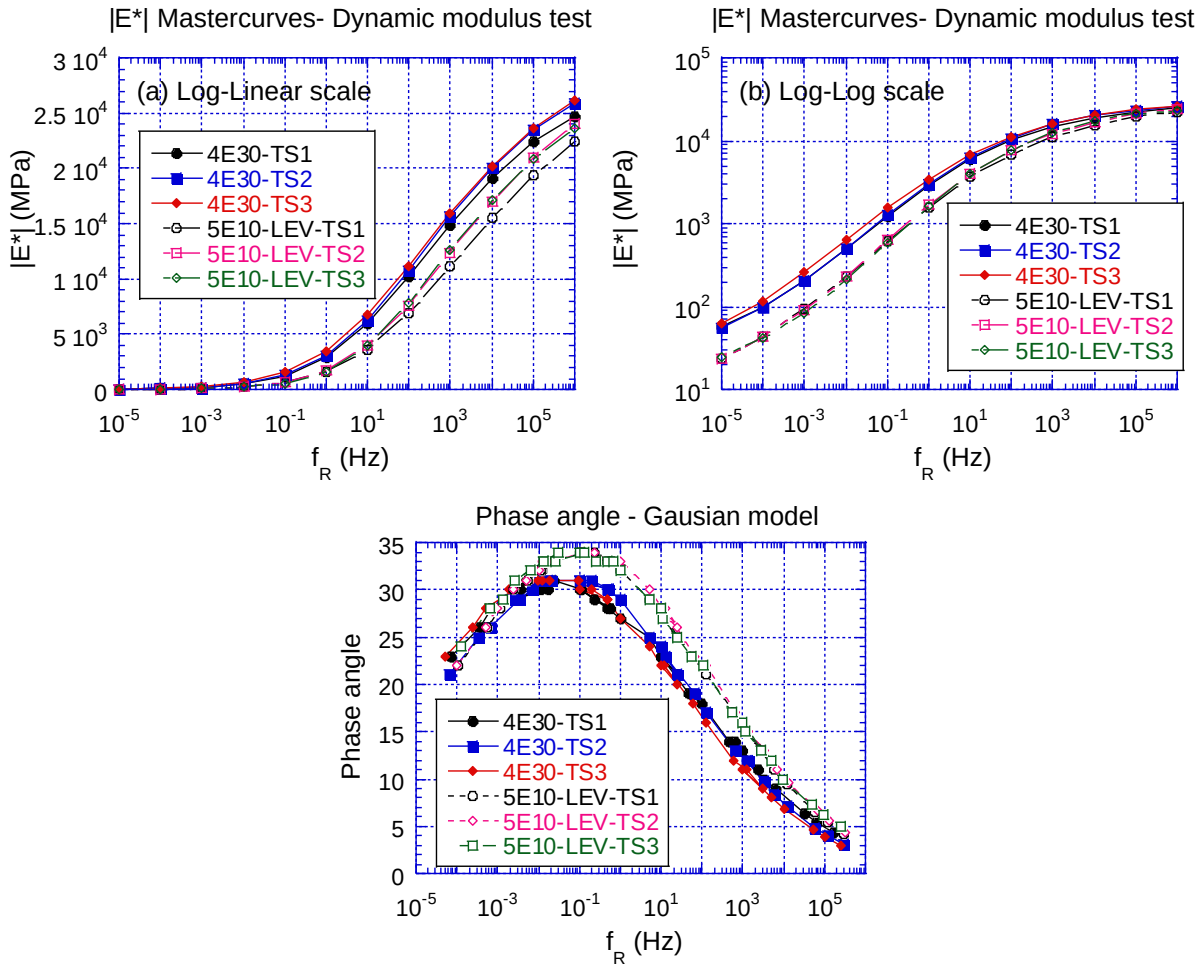

Figure C- 2 Comparison of |E*| master curves of the levelling courses for the I-475 long-life and the standard sections: (a) Log-Linear Scale, (b) Log-Log Scale, (c) Phase angle

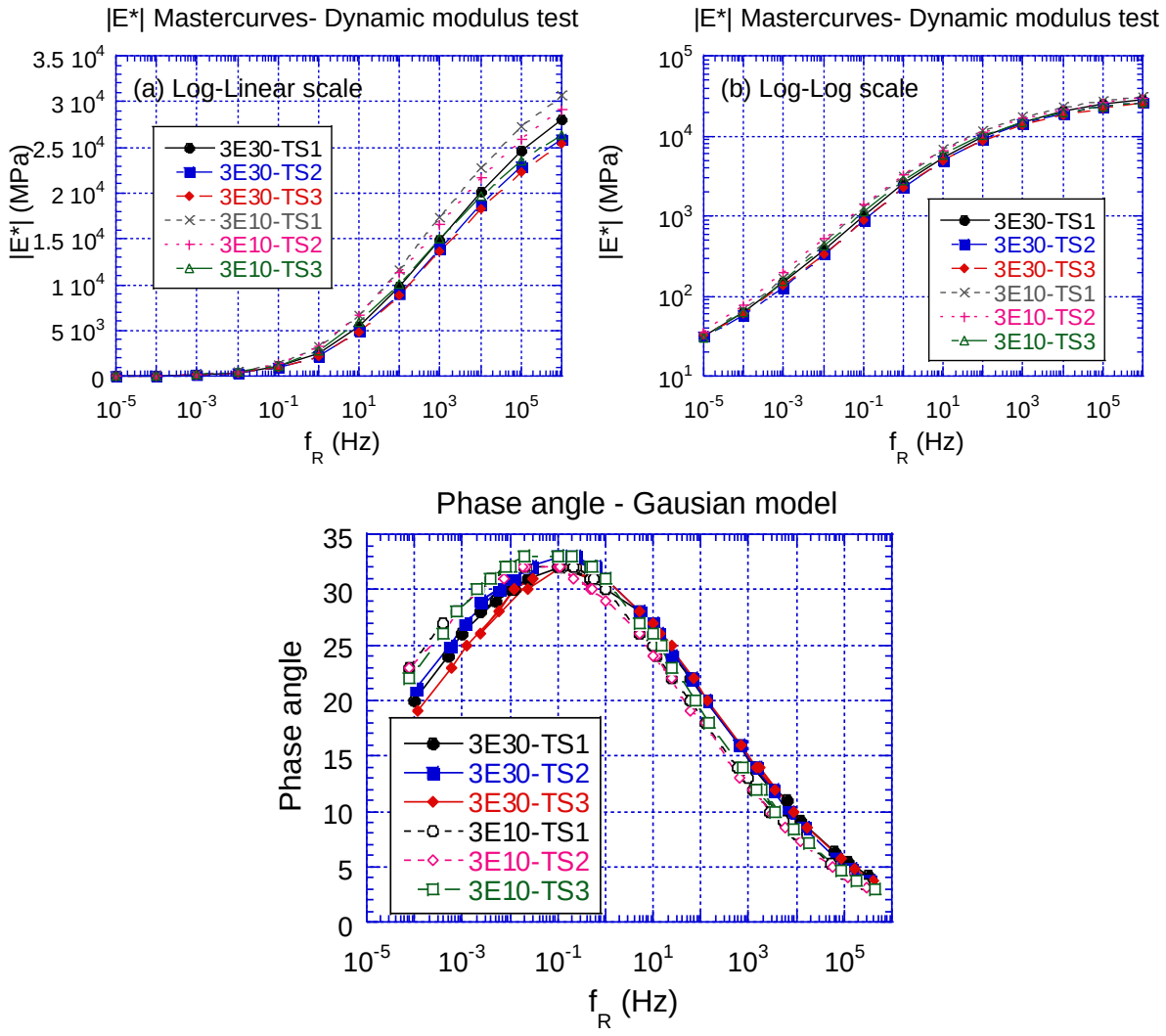

Figure C- 3 Comparison of |E*| master curves of the base courses for the I-475 long-life and the standard sections: (a) Log-Linear Scale, (b) Log-Log Scale, (c) Phase angle

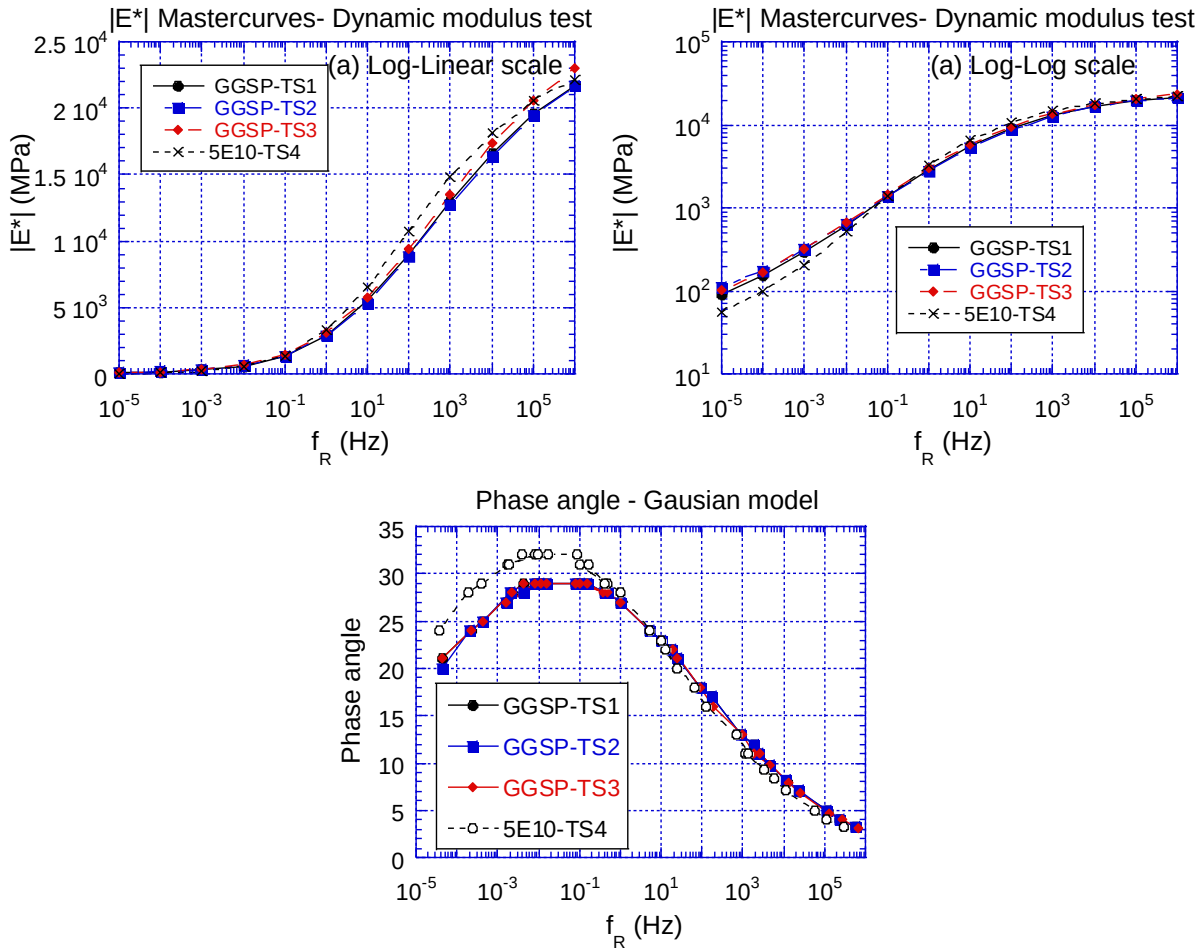

Figure C- 4 Comparison of |E*| master curves of the top courses for the US-131 long-life and the standard sections: (a) Log-Linear Scale, (b) Log-Log Scale, (c) Phase angle

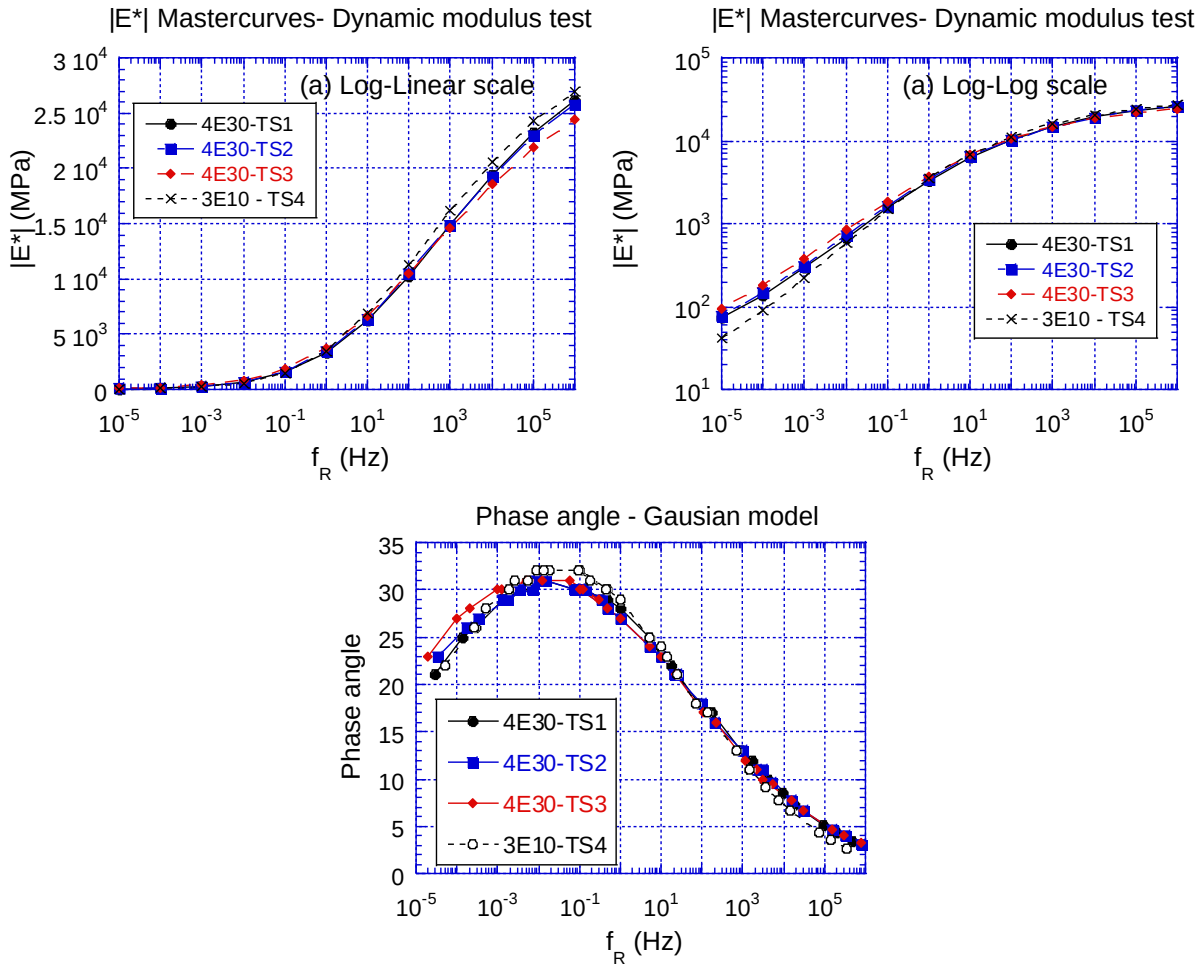

Figure C- 5 Comparison of |E*| master curves of the levelling courses for the US-131 long-life and the standard sections: (a) Log-Linear Scale, (b) Log-Log Scale, (c) Phase angle

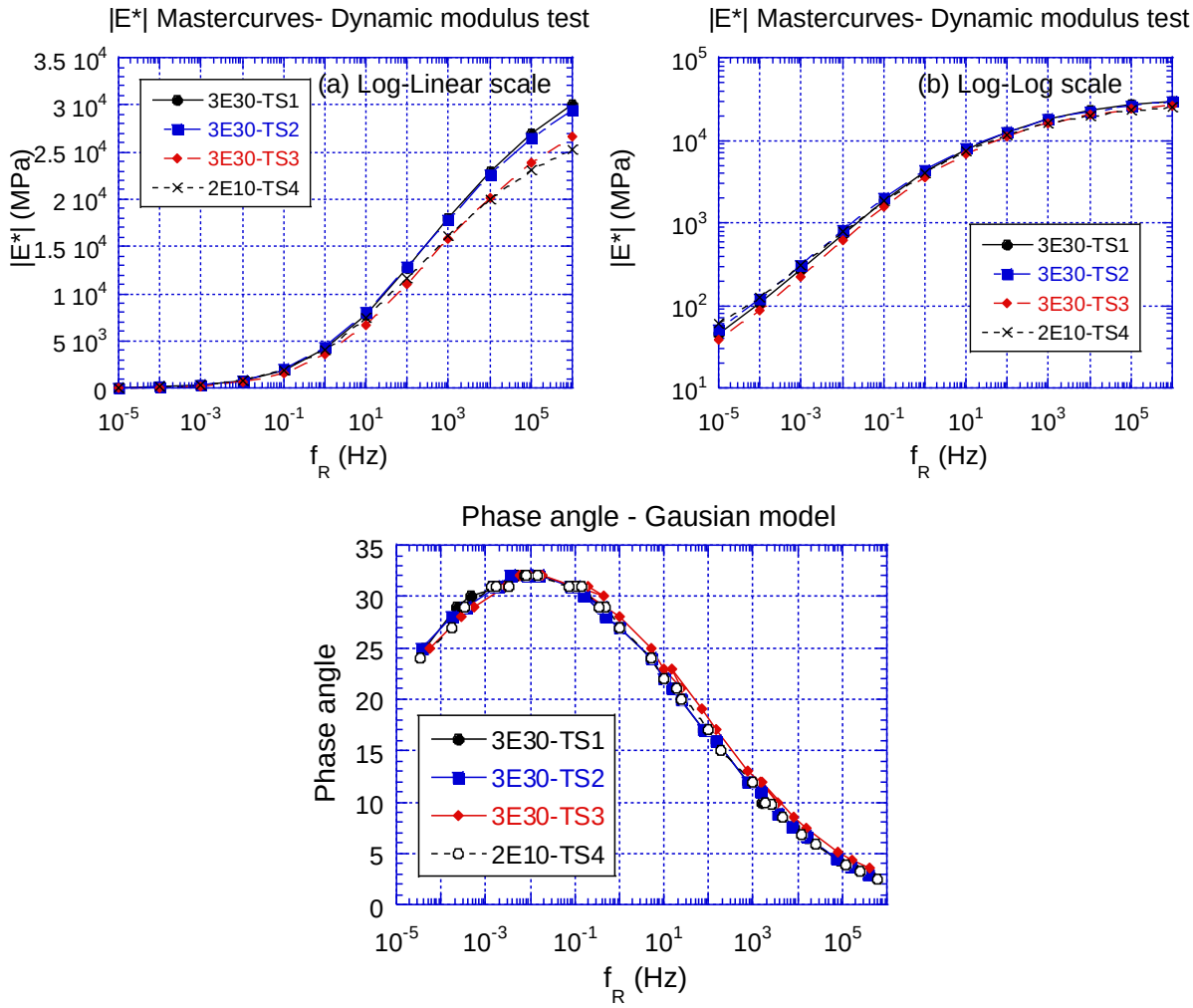

Figure C- 6 Comparison of |E*| master curves of the base courses for the US-131 long-life and the standard sections: (a) Log-Linear Scale, (b) Log-Log Scale, (c) Phase angle

APPENDIX C FLOW NUMBER TEST RESULTS

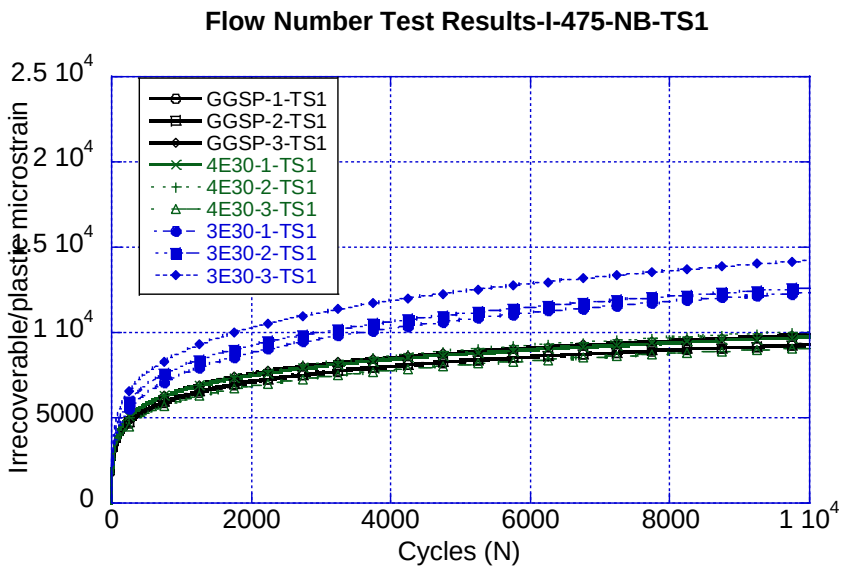

Figure D- 1 Flow number test results for I-475 Northbound TS1

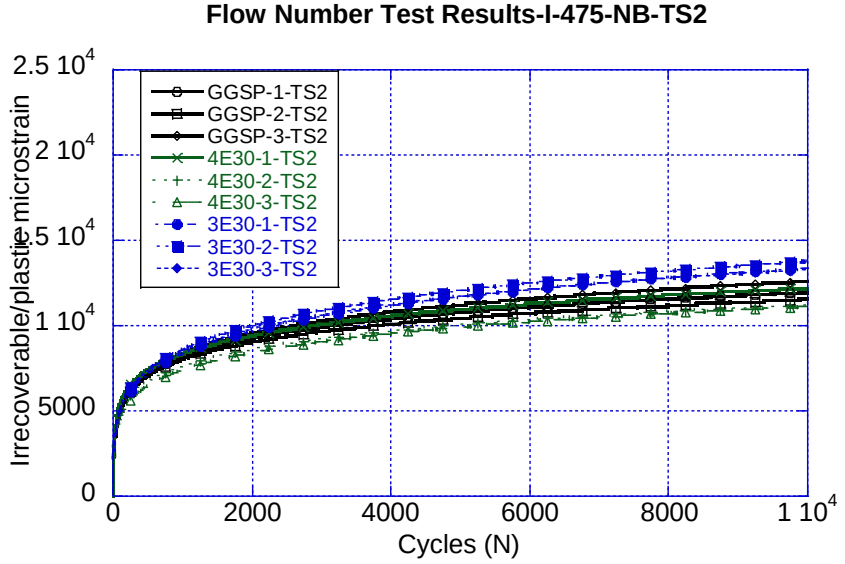

Figure D- 2 Flow number test results for I-475 Northbound TS2

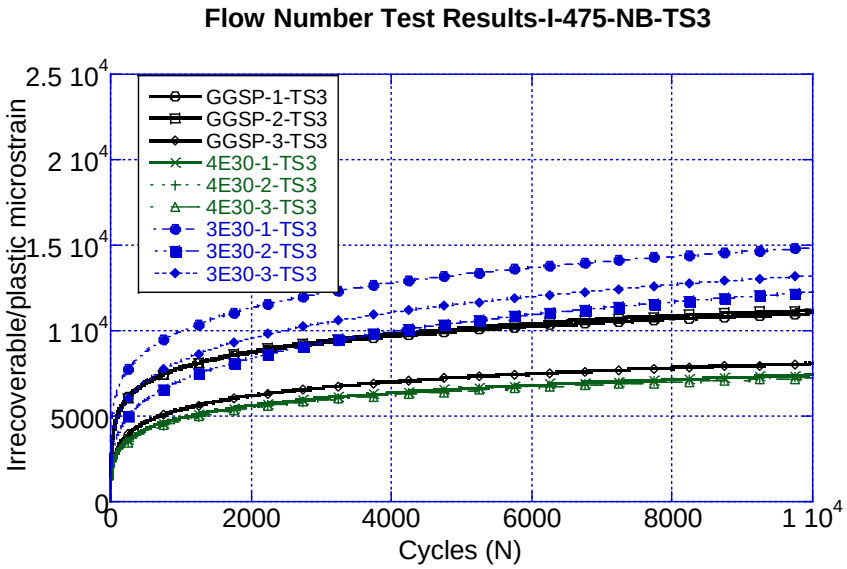

Figure D- 3 Flow number test results for I-475 Northbound TS3

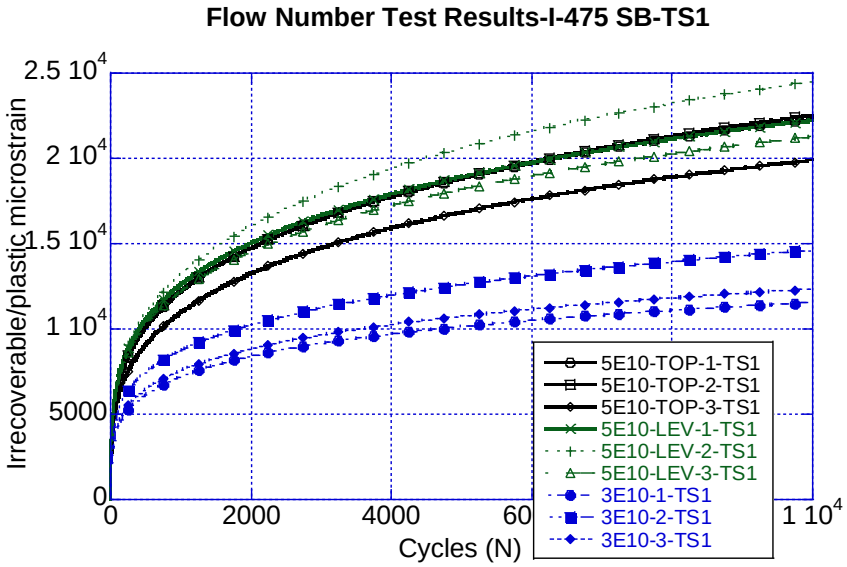

Figure D- 4 Flow number test results for I-475 Southbound TS1

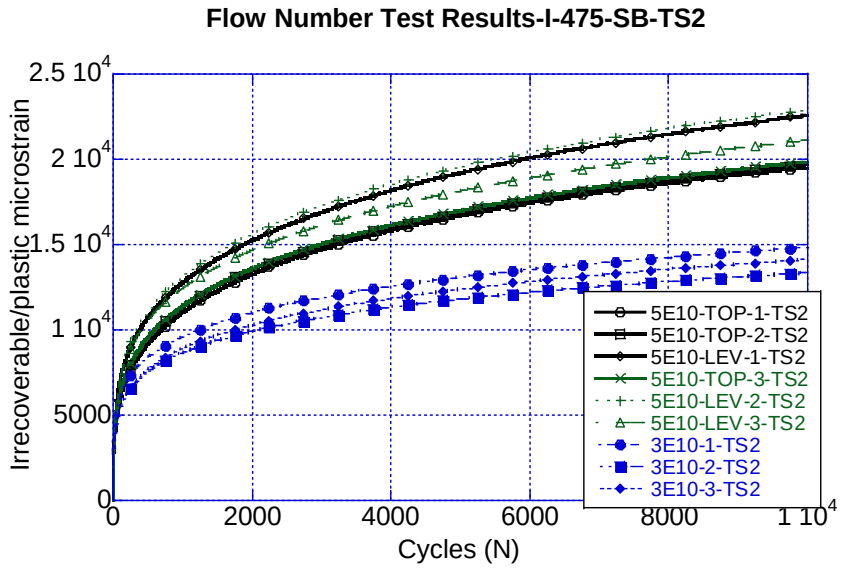

Figure D- 5 Flow number test results for I-475 Southbound TS2

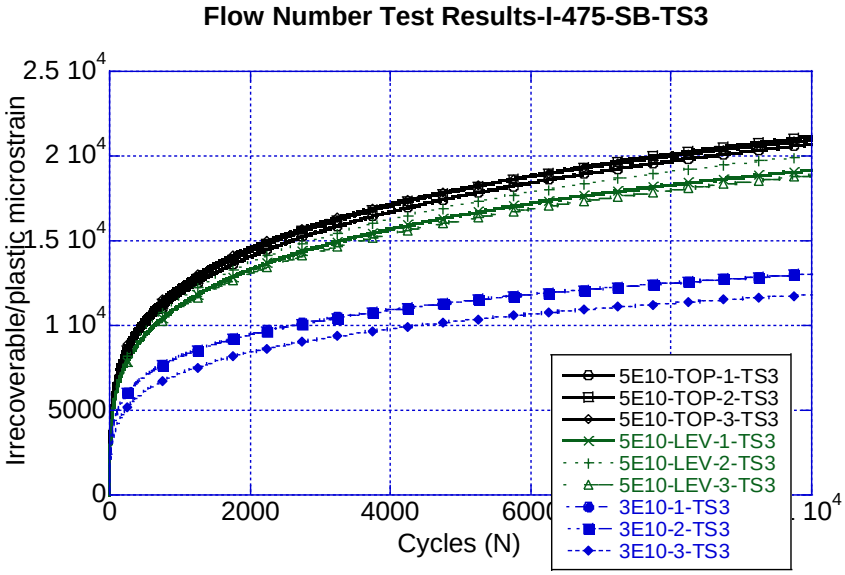

Figure D- 6 Flow number test results for I-475 Southbound TS3

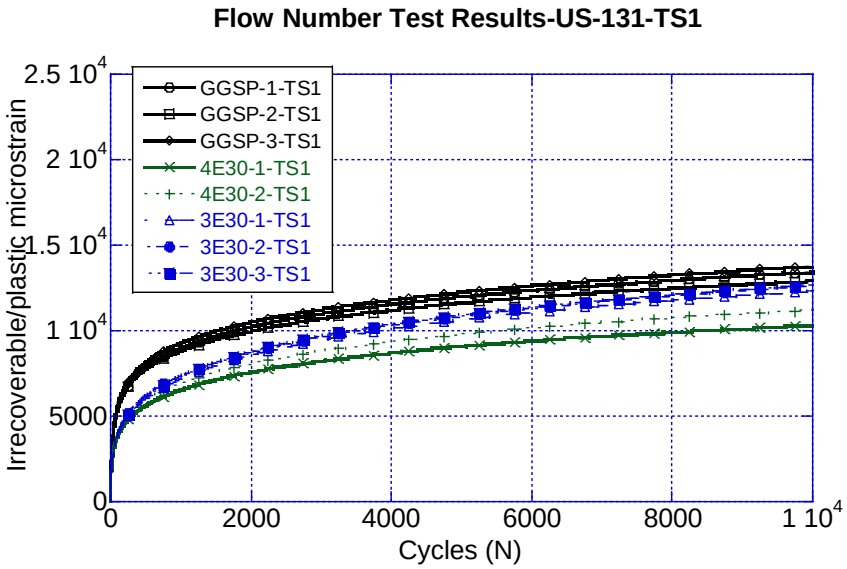

Figure D- 7 Flow number test results for US-131 TS1

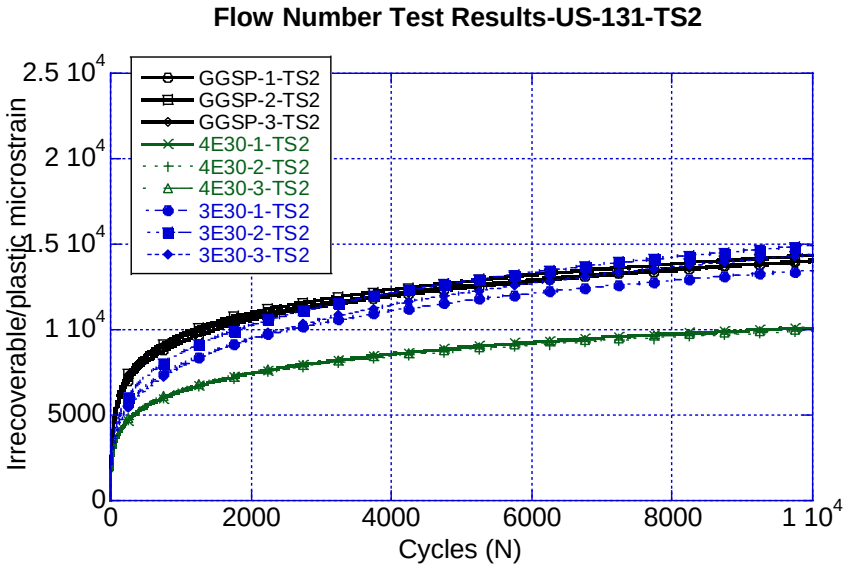

Figure D- 8 Flow number test results for US-131 TS2

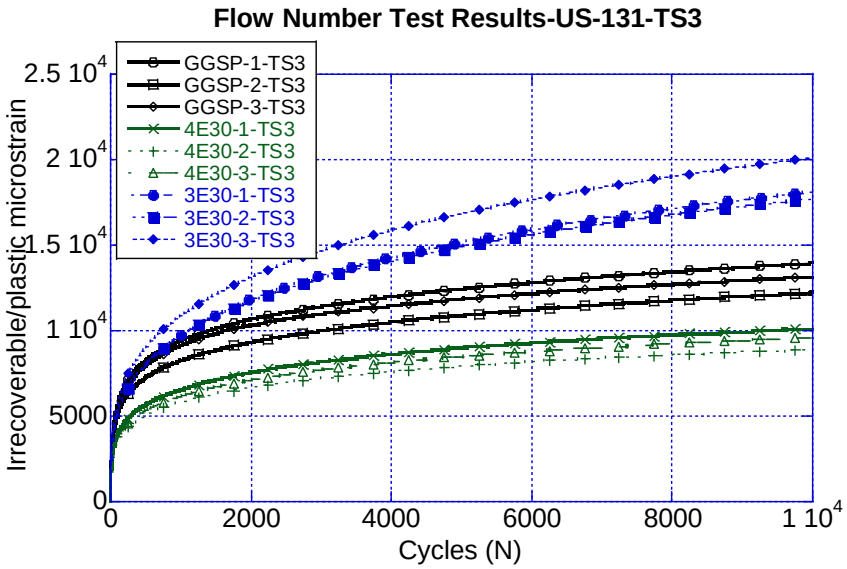

Figure D- 9 Flow number test results for US-131 TS3

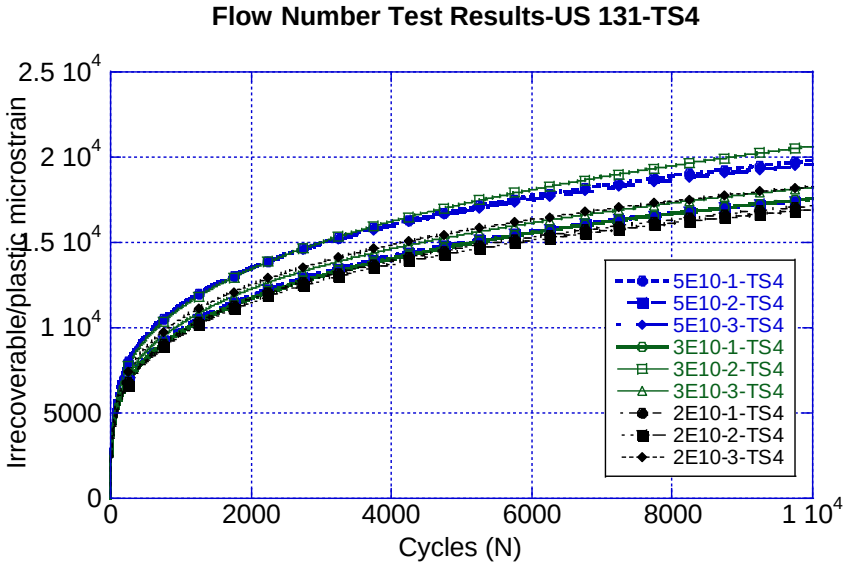

Figure D- 10 Flow number test results for US-131 TS4

APPENDIX D IDT TEST RESULTS

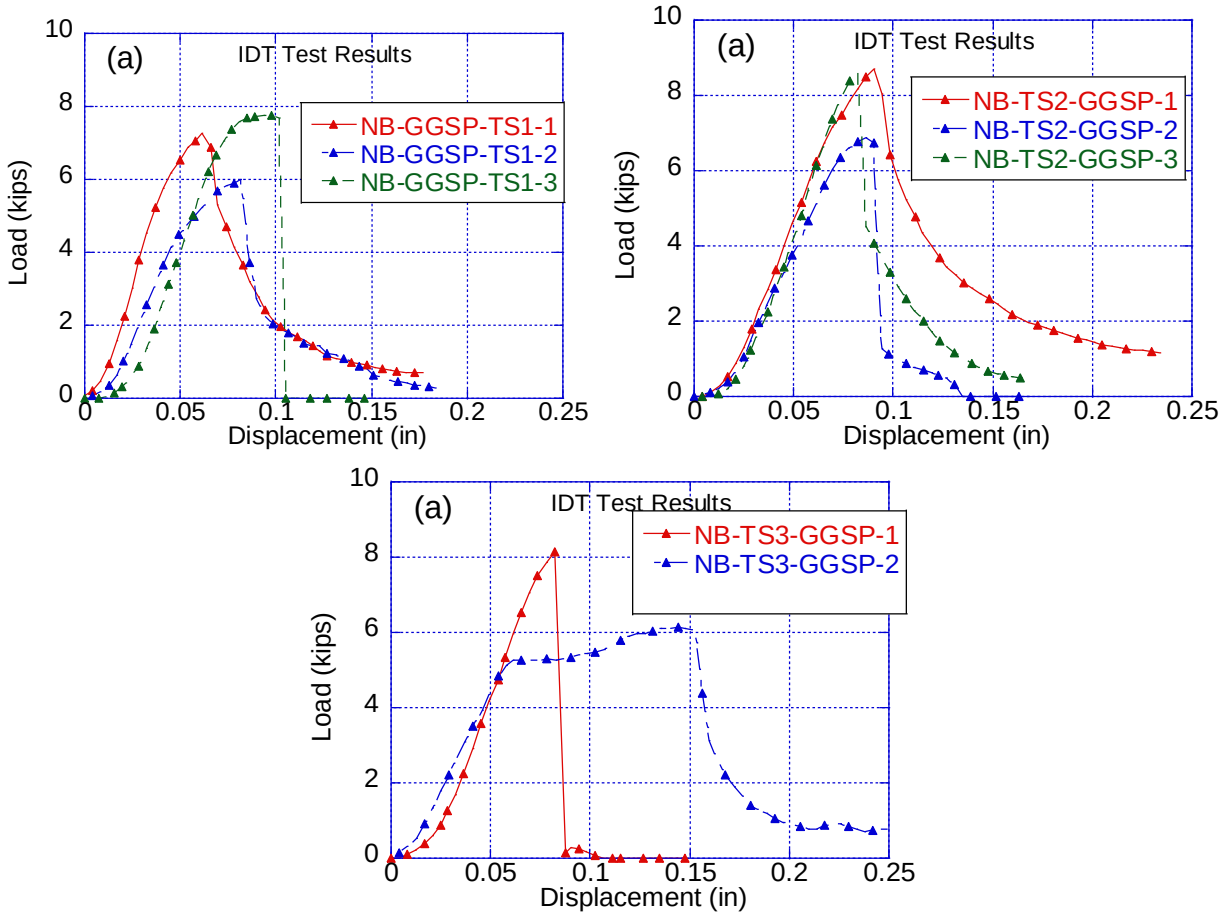

Figure E- 1 IDT test results GGSP I-475-NB: (a) test section 1, (b) test section 2 and (c) test section 3

Table E- 1 GGSP air voids (%)- IDT samples I-475

GGSP Air voids (%)	1	2	3
TS-1	6.6	8.7	7.0
TS-2	7.2	8.8	7.1
TS-3	6.7	8.5	7.0

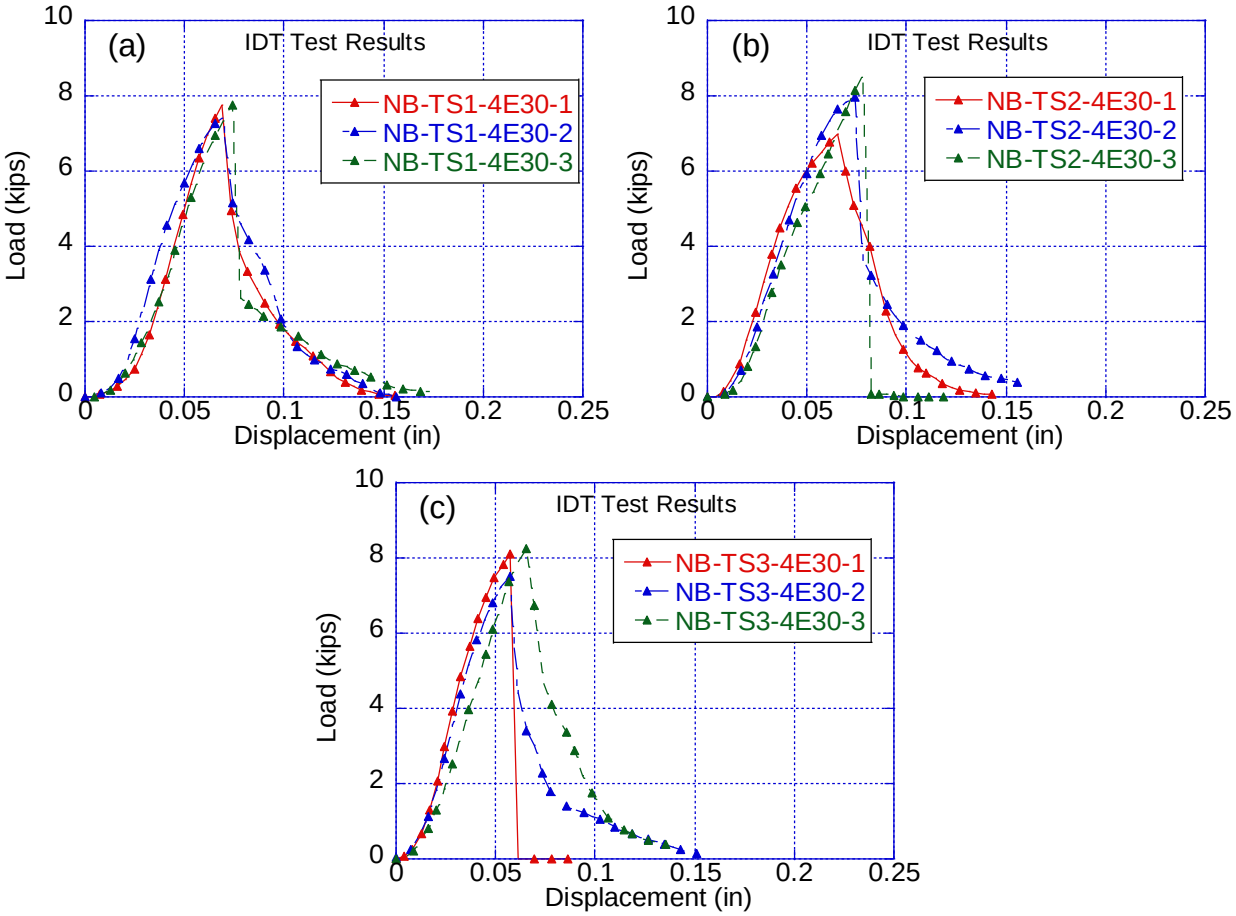

Figure E- 2 IDT test results 4E30 I-475-NB: (a) test section 1, (b) test section 2 and (c) test section 3

Table E- 2 4E30 air voids (%)- IDT samples I-475

4E30 Air voids (%)	1	2	3
TS-1	7.3	8.5	7.4
TS-2	7.3	8.7	7.4
TS-3	7.5	9.0	7.4

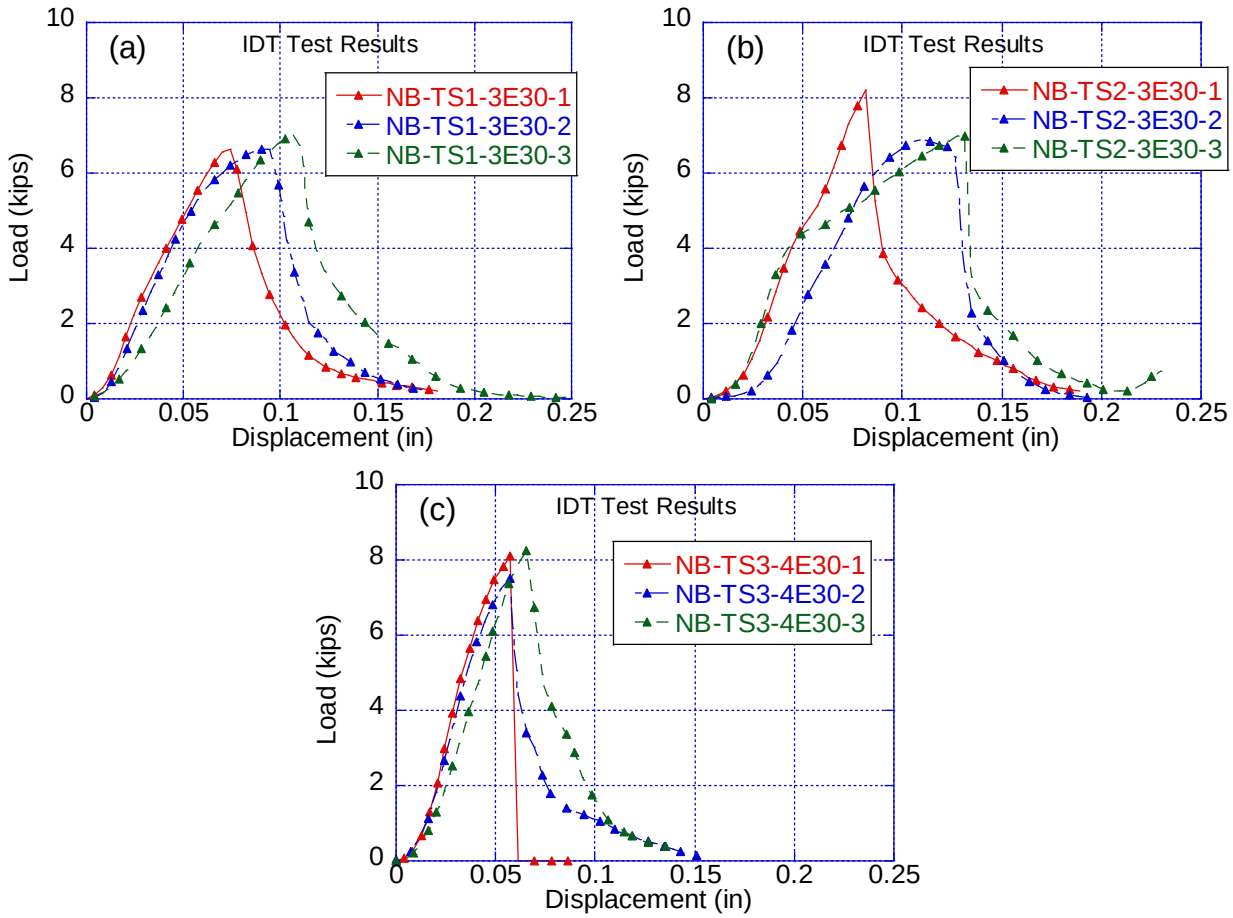

Figure E- 3 IDT test results 3E30 I-475-NB: (a) test section 1, (b) test section 2 and (c) test section 3

Table E- 3 3E30 air voids (%)- IDT samples I-475

3E30 Air voids (%)	1	2	3
TS-1	6.1	7.4	7.0
TS-2	6.5	8.1	7.0
TS-3	8.0	6.9	7.2

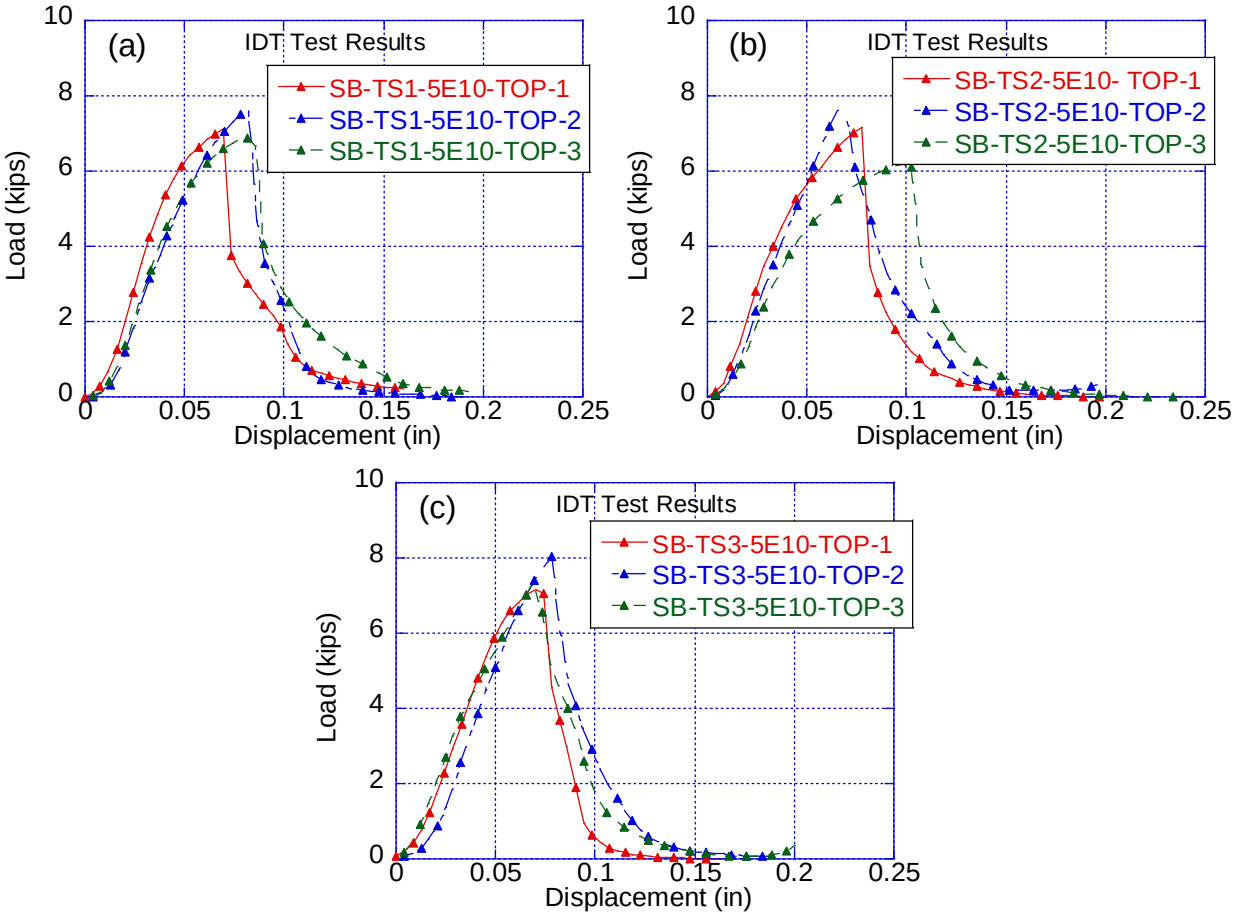

Figure E- 4 IDT test results 5E10-TOP I-475-SB: (a) test section 1, (b) test section 2 and (c) test section 3

Table E- 4 5E10-TOP air voids (%)- IDT samples I-475

5E10-TOP Air voids (%)	1	2	3
TS-1	6.5	7.2	6.2
TS-2	6.5	7.3	6.2
TS-3	6.6	6.4	7.1

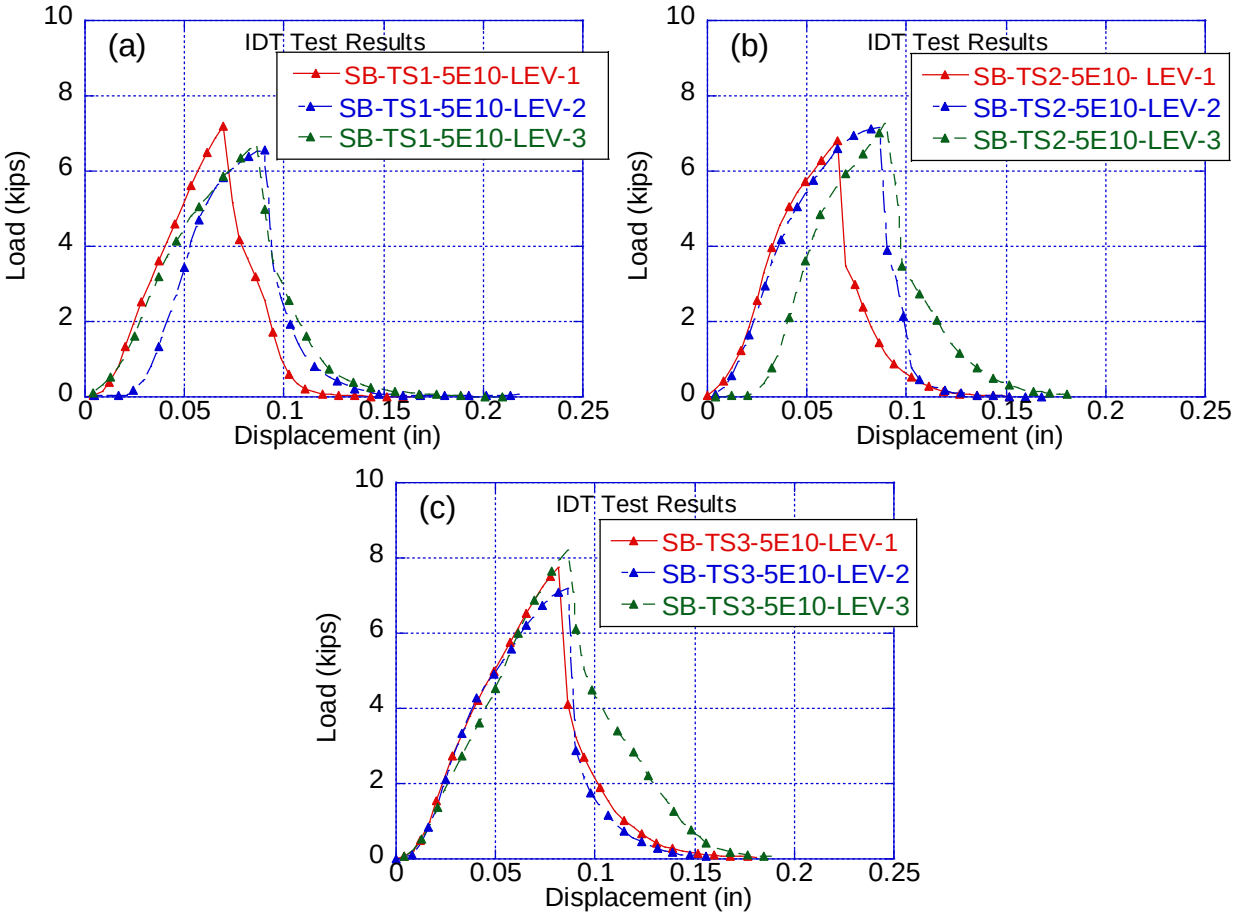

Figure E- 5 IDT test results 5E10-LEV I-475-SB: (a) test section 1, (b) test section 2 and (c) test section 3

Table E- 5 5E10-LEV air voids (%)- IDT samples I-475

5E10-LEV Air voids (%)	1	2	3
TS-1	7.4	6.8	6.3
TS-2	6.3	7.1	6.6
TS-3	6.1	7.3	6.7

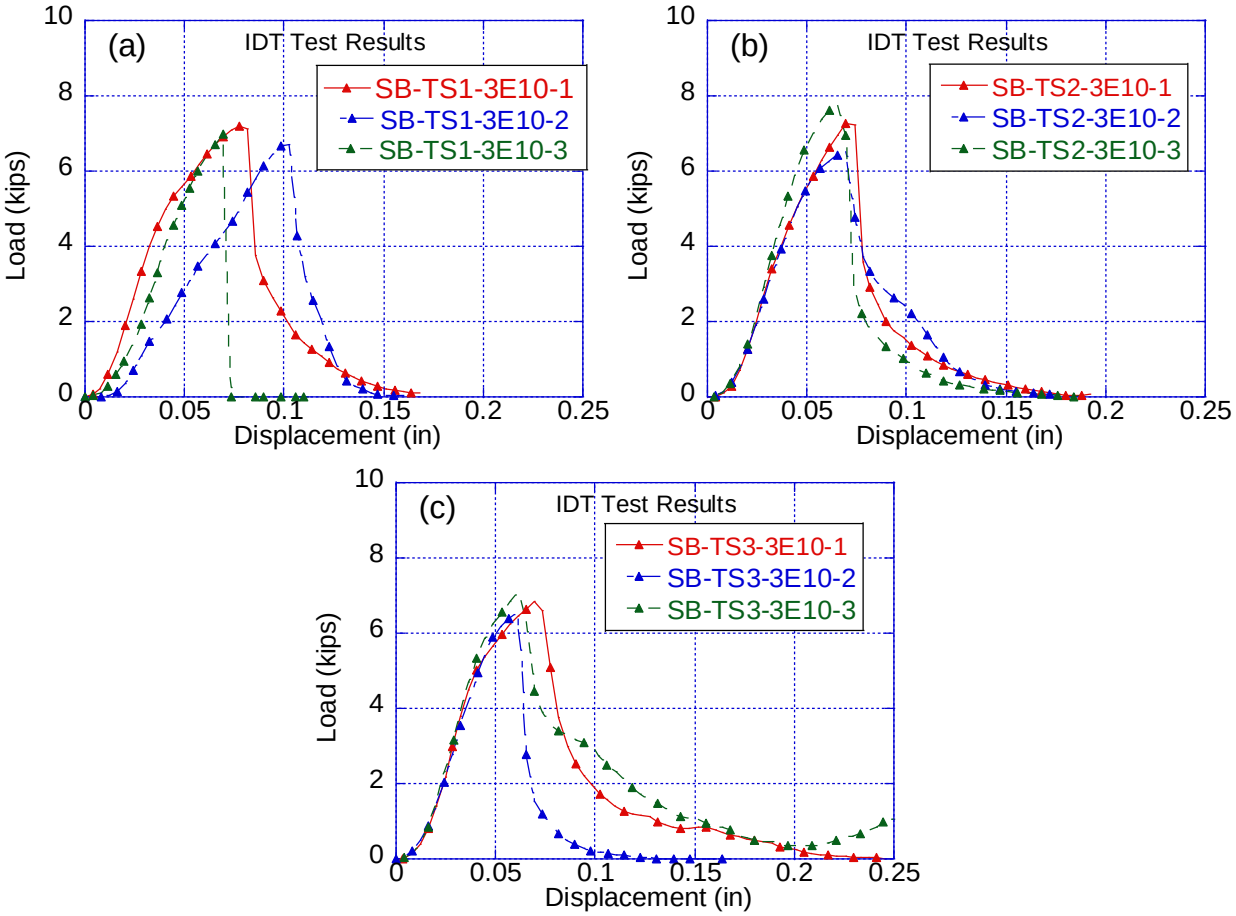

Figure E- 6 IDT test results 3E10 I-475-SB: (a) test section 1, (b) test section 2 and (c) test section 3

Table E- 6 3E10 air voids (%)- IDT samples I-475

3E10 Air voids (%)	1	2	3
TS-1	6.8	7.9	7.2
TS-2	6.9	8.0	7.1
TS-3	6.9	8.5	6.7

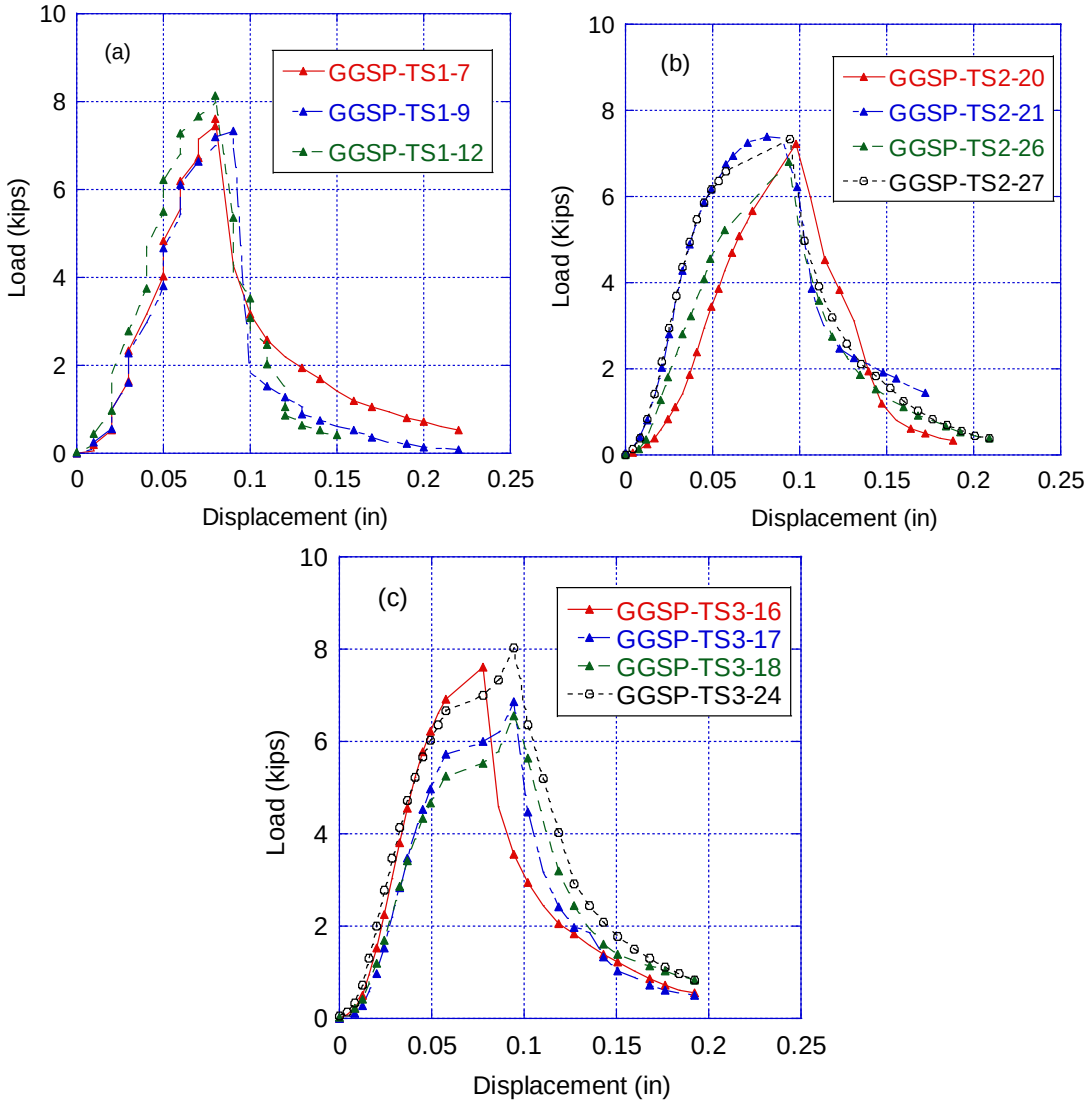

Figure E- 7 IDT test results GGSP US-131: (a) test section 1, (b) test section 2 and (c) test section 3

Table E- 7 GGSP air voids (%)- IDT samples US-131

GGSP Air voids (%)	1	2	3	4
TS-1	6.6	7.1	6.8	NA
TS-2	6.7	7.3	7.4	6.8
TS-3	6.7	8.9	6.9	7.4

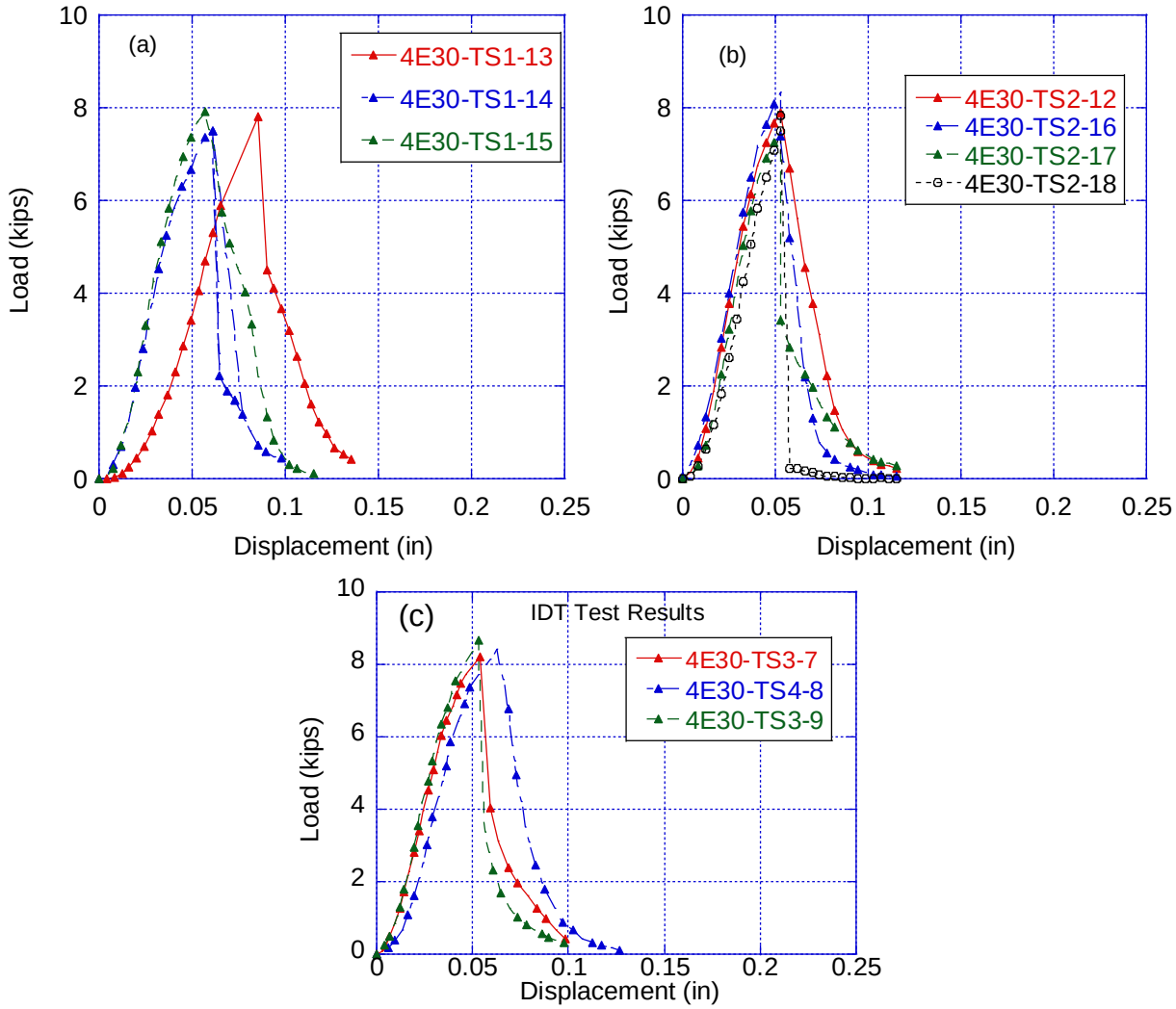

Figure E- 8 IDT test results 4E30 US-131: (a) test section 1, (b) test section 2 and (c) test section 3

Table E- 8 4E30 air voids (%)- IDT samples US-131

4E30 Air voids (%)	1	2	3	4
TS-1	6.6	7.4	7.2	NA
TS-2	7.2	6.8	7.5	7.1
TS-3	6.7	7.5	7.0	NA

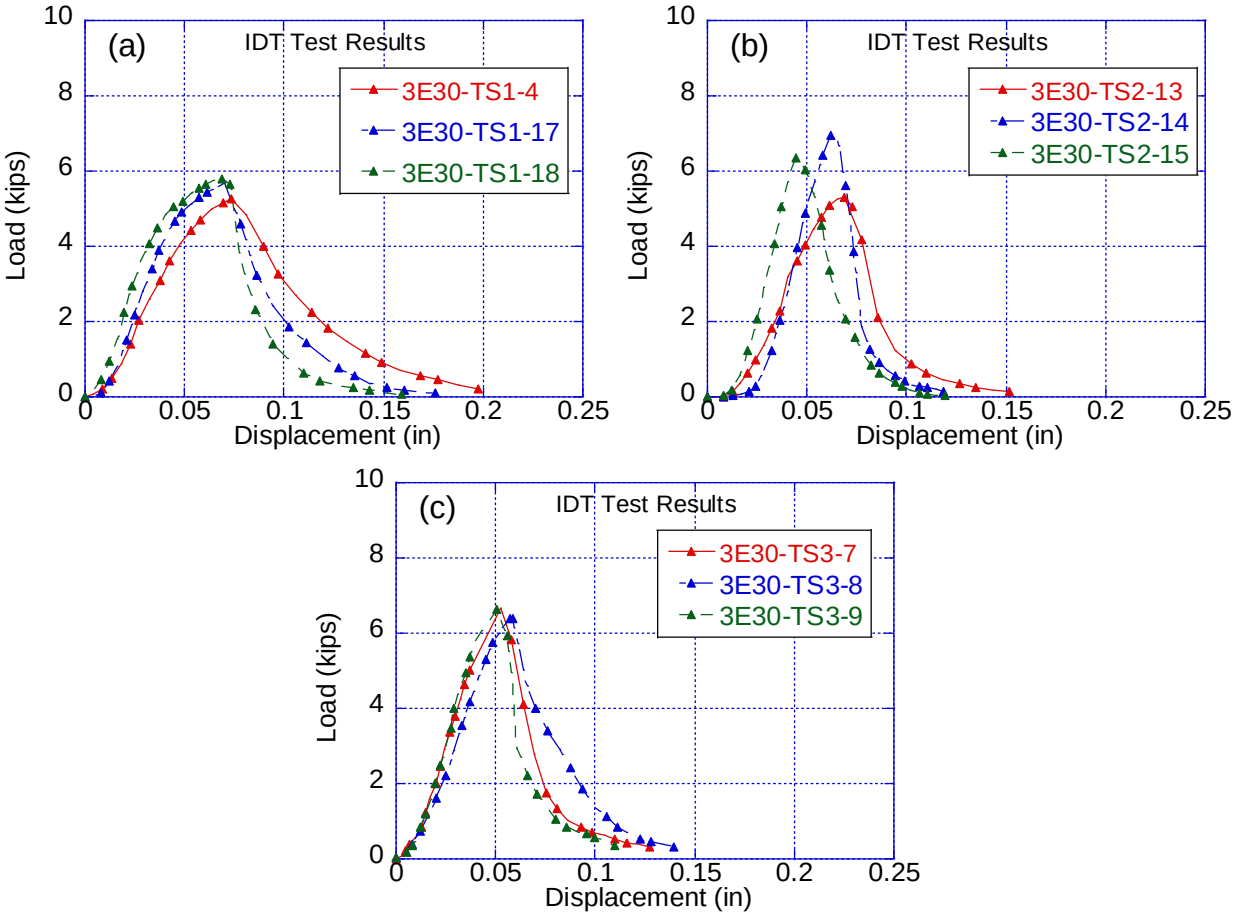

Figure E- 9 IDT test results 3E30 US-131: (a) test section 1, (b) test section 2 and (c) test section 3

Table E- 9 3E30 air voids (%)- IDT samples US-131

3E30 Air voids (%)	1	2	3
TS-1	7.3	8.5	7.5
TS-2	7.1	6.8	6.6
TS-3	7.0	7.3	7.4

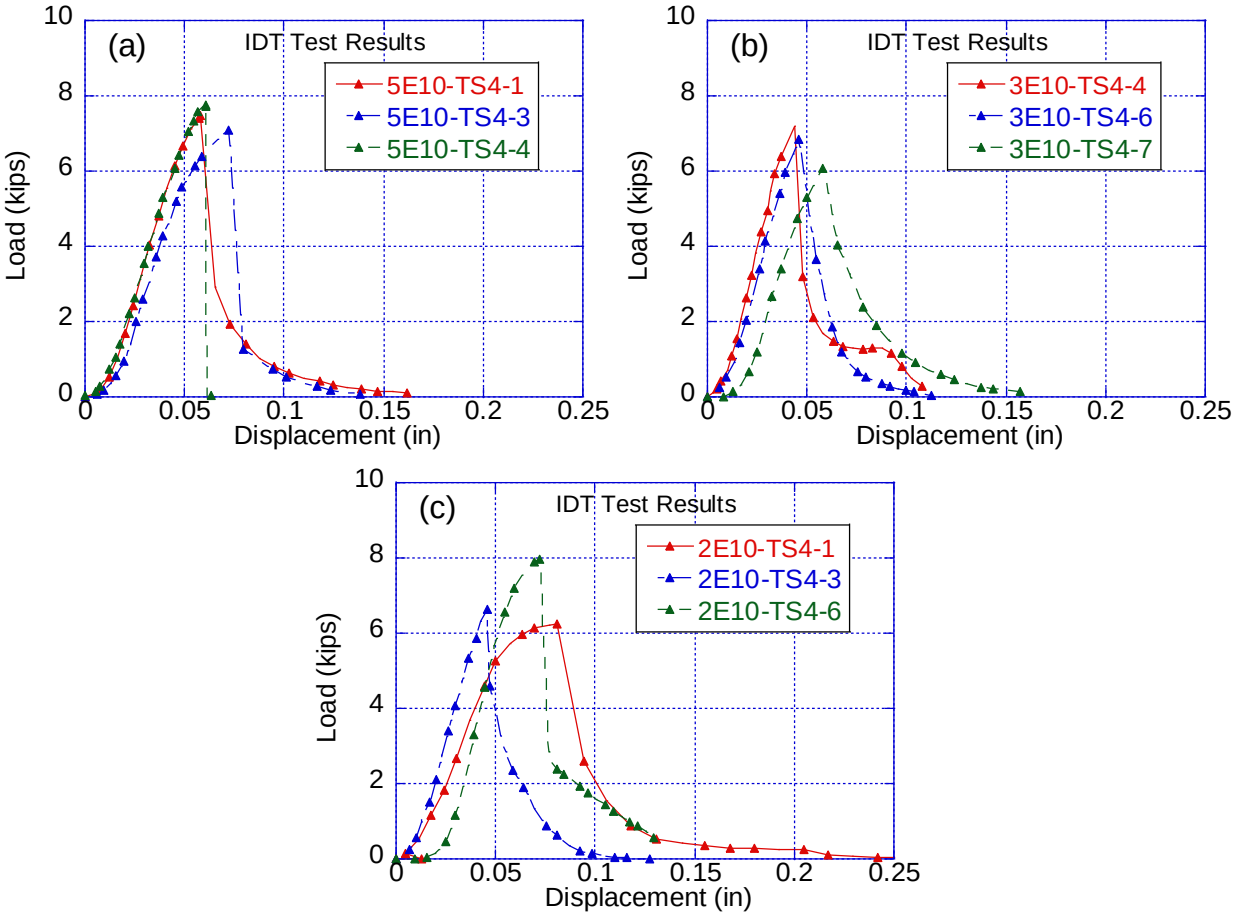

Figure E- 10 IDT test results US-131 test section 4: (a) 5E10, (b) 3E10 and (c) 2E10

Table E- 10 Air voids (%)- IDT samples US-131 test section 4

Air voids (%)	1	2	3
5E10 TS-4	7.1	7.5	7.3
3E10 TS-4	6.4	7.1	6.9
2E10 TS-4	7.1	7.0	7.5